



National Library
of Canada

Bibliothèque nationale
du Canada

Canadian Theses Service

Service des thèses canadiennes

Ottawa, Canada
K1A 0N4

NOTICE

The quality of this microform is heavily dependent upon the quality of the original thesis submitted for microfilming. Every effort has been made to ensure the highest quality of reproduction possible.

If pages are missing, contact the university which granted the degree.

Some pages may have indistinct print especially if the original pages were typed with a poor typewriter ribbon or if the university sent us an inferior photocopy.

Reproduction in full or in part of this microform is governed by the Canadian Copyright Act, R.S.C. 1970, c. C-30, and subsequent amendments.

AVIS

La qualité de cette microforme dépend grandement de la qualité de la thèse soumise au microfilmage. Nous avons tout fait pour assurer une qualité supérieure de reproduction.

S'il manque des pages, veuillez communiquer avec l'université qui a conféré le grade.

La qualité d'impression de certaines pages peut laisser à désirer, surtout si les pages originales ont été dactylographiées à l'aide d'un ruban usé ou si l'université nous a fait parvenir une photocopie de qualité inférieure.

La reproduction, même partielle, de cette microforme est soumise à la Loi canadienne sur le droit d'auteur, SRC 1970, c. C-30, et ses amendements subséquents.

The University of Alberta

Optimum Design of Gear Shaper Cutters

by



Debkumar Rakshit

A thesis
submitted to the Faculty of Graduate Studies and Research
in partial fulfilment of the requirements for the degree of

Master of Science

Department of Mechanical Engineering

Edmonton, Alberta

Fall 1989



National Library
of Canada

Bibliothèque nationale
du Canada

Canadian Theses Service

Service des thèses canadiennes

Ottawa, Canada
K1A 0N4

NOTICE

The quality of this microform is heavily dependent upon the quality of the original thesis submitted for microfilming. Every effort has been made to ensure the highest quality of reproduction possible.

If pages are missing, contact the university which granted the degree.

Some pages may have indistinct print especially if the original pages were typed with a poor typewriter ribbon or if the university sent us an inferior photocopy.

Reproduction in full or in part of this microform is governed by the Canadian Copyright Act, R.S.C. 1970, c. C-30, and subsequent amendments.

AVIS

La qualité de cette microforme dépend grandement de la qualité de la thèse soumise au microfilmage. Nous avons tout fait pour assurer une qualité supérieure de reproduction.

S'il manque des pages, veuillez communiquer avec l'université qui a conféré le grade.

La qualité d'impression de certaines pages peut laisser à désirer, surtout si les pages originales ont été dactylographiées à l'aide d'un ruban usé ou si l'université nous a fait parvenir une photocopie de qualité inférieure.

La reproduction, même partielle, de cette microforme est soumise à la Loi canadienne sur le droit d'auteur, SRC 1970, c. C-30, et ses amendements subséquents.

ISBN 0-315-60400-X

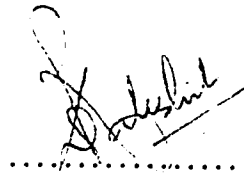
The University of Alberta

Release Form

Name of Author: **Debkumar Rakshit**
Title of Thesis: **Optimum Design of Gear Shaper Cutters**
Degree: **Master of Science**
Year this degree granted: **Fall 1989**

Permission is hereby granted to The University of Alberta Library to reproduce single copies of this thesis and to lend or sell such copies for private, scholarly, or scientific research purposes only.

The author reserves other publication rights, and neither the thesis nor extensive tracts from it may be printed or otherwise reproduced without the author's written consent.



.....

(Student's signature)

Debkumar Rakshit
D-11, Rohraband, Sindri
Dhanbad, Bihar
INDIA
828 122

Date : *24 July '89*

The University of Alberta
Faculty of Graduate Studies and Research

The undersigned certify that they have read, and recommend to the Faculty of
Graduate Studies and Research for acceptance, a thesis entitled


Optimum Design of Gear Shaper Cutters

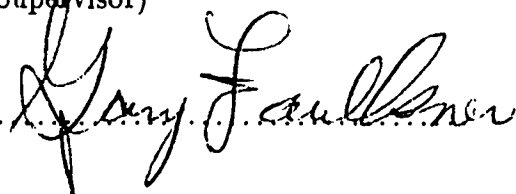
submitted by

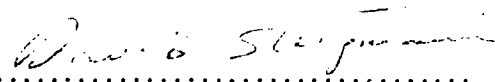
Debkumar Rakshit

in partial fulfilment of the requirements for the degree of

Master of Science.


.....
(Supervisor)


.....


.....

Date : 24 July 89

dedicated to my parents and sisters

Acknowledgement

The author wishes to express his sincere gratitude to Dr. J.R. Colbourne, for his guidance during the course of this work and for the careful and patient review of each of the chapters.

The author would like to thank Mr. E.W. Haug of Pfauter-Maag and Mr. N.C. Ainsworth of Fellows Corporation for supplying industrial publications and technical information pertinent to his research. A special thanks are extended to Mr. A.G. Taylor for proof-reading the first draft of the thesis.

Finally, the author would like to thank his parents for their overall support and encouragement throughout his academic career.

Abstract

Gear shaping is a versatile and accurate method of producing involute gears of varying sizes by a generating process. The presence of rake and relief angles, however, causes certain profile deviations in the cutter, and subsequently in the generated gear. Moreover, resharpening the conical rake face alters the tip profile of the cutter, which consequently does not generate a constant fillet radius in the gear blank throughout the cutter life.

Results obtained from the analysis of the profile deviations in the present shaper design are shown, and a new approach to the design is presented. The new design permits high rake and relief angles in the cutter, and thereby increases the cutting efficiency without any profile deviation in the generated gear. Investigations are carried out to determine the effects of multiple resharpenings on the active profiles of both the conventional and the new design of cutter, and on the profiles of the generated gear. Methods are also suggested for modifying the new cutter to generate gear tooth relief, if required.

Devices for practically manufacturing the new cutter shape are also suggested. A modification is outlined that will be required to the small and medium size grinding machine for incorporating the additional kinematic group that is necessary for generating the new cutter shape.

Changes in the cutter corner radius after multiple resharpening of the cutter are simulated, and their effects on the generated gear fillet are found. Finally, methods are suggested for minimizing the changes in the fillet of the generated gear.

Contents

Chapter 1

Introduction	1
1.1 Shaping machine	2
1.2 Advantages of Shaping	5
1.3 Limitation of shaping	7
1.4 Gear generation by shaper cutter	7
1.4.1 Evaluation of profile details	11
1.4.2 Evaluation of other profile parameters	15
1.5 Gear cutter grinding	20
1.5.1 Zero pressure angle grinding	20
1.5.2 Generating pressure angle grinding	20
1.6 Shaper cutter resharpening	22
1.7 The problem and its relevance	23
1.7.1 Inaccuracies in the active surface profile	24
1.7.2 Inaccuracies due to tip profile	25

1.8	Survey	26
1.9	Thesis Outline	26
 Chapter 2		
	Present design of pinion shaping cutters	28
2.1	Shape of cutter profile (conventional design)	28
2.2	Front and side relief angle	30
2.3	Rake angles	36
2.4	Deviation in profile due to rake angle	38
2.5	Profile deviation of effective profile	44
2.6	Measure of normal deviation in cutter profile	47
2.7	Variation in tooth thickness	49
2.8	Profile correction methods	55
2.9	Pressure angle correction	55
2.10	Tooth thickness correction	60
	2.10.1 Method I of tooth thickness correction	60
	2.10.2 Method II of tooth thickness correction	61
2.11	Determination of value of design distance	65
2.12	Graphical method	69
2.13	Approximate analytical method	72
 Chapter 3		
	New design of pinion shaping cutters	77

3.1	Shape of cutter (new design)	77
3.2	Front relief angles	80
3.3	Side relief angle	81
3.4	Amount of relief	82
3.5	Cutter coordinates	87
3.6	Tooth relief (Method I)	90
3.7	Tooth relief (Method II)	92
3.7.1	Grinding assembly height	95
3.8	Flexibility in relief	96
3.9	Design distance	97

Chapter 4

	Effect of resharpening of cutter	98
4.1	Conventional design	98
4.1.1	Depth of cut	98
4.1.2	Tooth thickness	100
4.1.3	Addendum	100
4.2	New design	104
4.2.1	Cutter addendum	104
4.2.2	Cutter tooth thickness	109
4.3	Comparison of conventional and new cutter	109

Chapter 5

Effect of Resharpener on tooth tip corners	115
5.1 Cutter tip corner surface	116
5.2 Oblique cylindrical cutter corner surface	117
5.2.1 Equation of axis of oblique corner cylinder	119
5.2.2 Fillet generated by oblique corner cylinder	121
5.3 Oblique conical cutter corner surface	123

Chapter 6

Devices for manufacturing the new cutter	133
6.1 The grinding machine	133
6.2 Formative machine motions required	134
6.3 Cutting motion group	135
6.4 Longitudinal feed motion group	136
6.5 Roll motion group	138
6.6 Advance motion group and roll motion group	139
6.7 Roll and Advance group for small grinding machine	141
6.7.1 Modification for rake advance group	143
6.8 Rake advance kinematic group: Method I	144
6.9 Working principle of advance mechanism	146
6.10 Alternative rake advance kinematic group: Method II	149
6.11 Setup of advance mechanism: Method I	151

6.12 Setup of advance mechanism: Method II	151
6.13 Medium size grinding machine	153
6.14 Grinding procedure changes for new cutter	156
Chapter 7	
Conclusion	158
References	161
Appendix A	
Definitions and Derivations	164
A.1 Relation between pinion tooth thickness and rack space width	164
A.2 Involute function and tooth thickness	168
A.3 Relation between the meshing gear and cutter positions	171
A.4 Standard cutting position	173
A.5 Machine motions and constraints	175
A.5.1 Surfaces and elements	175
A.5.2 Operative motions	175
A.5.3 Kinematic group	177
A.5.4 Kinematic structure	177
A.6 Span measurement	179
Appendix B	
Case Studies Data	181

Appendix C

Gear Shaping Simulator Program Listing

196

List of Figures

1.1	Gear shaping cutter	2
1.2	Gear shaping process	3
1.3	Relieving arrangement of shaper cutter	4
1.4	Common types of shaper cutters	6
1.5	Relation between tooth thickness of gear and cutter	9
1.6	Involute active side profile	12
1.7	Non-involute active side profile	14
1.8	Evaluation of other cutter profile parameters	16
1.9	Evaluation of gear parameters	17
1.10	Cutter and generated gear	19
1.11	Zero pressure angle grinding	21
1.12	Generating pressure angle grinding	21
1.13	Important dimensions of shaper cutter	22
1.14	Shaper cutter resharpening	24
2.1	Rake and relief angles of shaper cutter	29
2.2	Rack and pinion cutter	31
2.3	Orientation of the rack when generating the pinion cutter	32
2.4	Helicoid side surface of Pinion cutter	35
2.5	Cutting edge of a pinion cutter	37

2.6	Effective profile of a pinion cutter	39
2.7	Sweep surface of the effective profile	42
2.8	Relation of the family of involute profiles to the effective profile . . .	43
2.9	Theoretical profile and effective profile of cutter	45
2.10	Theoretical profile and effective profile on the generated gear	46
2.11	Measure of normal profile deviation of cutter.	48
2.12	Normal deviation of effective profiles of cutter	50
2.13	Normal deviation of generated gear profiles	51
2.14	Tooth thickness variation of effective profiles of cutter	53
2.15	Tooth thickness variation of generated gear profiles	54
2.16	Pressure angle correction method	57
2.17	Cutter profile thickness deviations on using correction method I . . .	62
2.19	Resultant cutter thickness deviations on using correction Method II .	66
2.21	Effect of pressure angle and tooth thickness corrections	68
2.22	Effect of different cutter tooth correction on generated gear profile . .	70
2.23	Plot of t_{tc}^T/m against χ	73
2.24	Determination of design distance	75
3.1	Design cone and section cones	78
3.2	Front relief angle in the new design	81
3.3	Determination of amount of relief	83
3.4	Profile of the cutter(new design)	88
3.5	Profile of the gear generated by the cutter (new design)	89
3.6	Profile relief (Method I)	90
3.7	Tooth relief (Method II)	93
3.8	Grinding wheel assembly lies directly above root of cutter teeth . . .	94
3.9	Grinding wheel assembly is rotated as well as translated	94
3.10	Grinding wheel height	95

4.1	Depth of cut and related parameters	99
4.2	Variation of addendum with rake angles for different modules	101
4.3	Variation of addendum with front relief angles for different modules	102
4.4	Variation of addendum with rake angles for different front relief angles	103
4.5	Overlaid profiles of cutter after resharpenings(conventional design)	105
4.6	Overlaid gear profiles generated by corresponding resharpened cutter profiles	106
4.7	Cutter profile normal deviation on resharpening	107
4.8	Generated gear profile normal deviations	108
4.9	Overlaid profiles of cutter after resharpenings(new design)	110
4.11	Overlaid normal deviation curves of cutter after resharpenings(new design)	112
5.1	Variation of radius of curvature of the gear fillet	118
5.2	Cylindrical cutter tooth corner surface	119
5.3	Axis of tooth tip corner oblique cylinder	120
5.4	Overlaid resharpened cutter tip profiles	124
5.5	Overlaid generated gear fillet profiles	125
5.6	Effect of resharpenings on radii of curvatures at the gear fillet profile	126
5.7	Oblique conical cutter corner surface	127
5.8	Overlaid resharpened cutter tip profiles (Conical cutter corner surface)	129
5.9	Overlaid generated gear fillet profiles (Conical cutter corner surface)	130
6.1	Formative motions of the grinding machine	134
6.2	Cutting motion group	136
6.3	Longitudinal feed motion group	137
6.4	Roll motion group	138
6.5	Advance motion group	139
6.6	Small size grinding machine	142

6.7	Section (diagrammatic) through generating head (conventional) . . .	143
6.8	Section(diagrammatic) through generating head (modified)	145
6.9	Sectional view of the advance mechanism	147
6.10	Alternative rake advance kinematic group: Method II	149
6.11	Setup of advance mechanism: Method I	150
6.12	Setup of advance mechanism: Method II using scale	152
6.13	Setup of advance mechanism: Method II using Y & Z encoders	153
6.14	Medium size grinding machine	154
6.15	Placement of the linear encoder	156
A.1	Pinion and rack positions at time t_0	165
A.2	Rack cutter position at t	166
A.3	Involute profile	169
A.4	Tooth thickness at radius R	169
A.5	Meshing position of gears with contact at the pitch point	171
A.6	Shift “ e ”, of the rack cutter, from standard cutting position	173
A.7	Span measurement over N'_c teeth	179

Nomenclature

Lower case symbols

a arbitrary distance from design section
b distance of tooth tip from design section
e profile shift
h_a addendum of cutter
h_d dedendum of cutter
m_g gear ratio
m profile shift
p pitch
r radius of circle not centred at gear axis
r_f minimum radius of curvature at fillet
t tip circle; tooth thickness
u position of rack
v velocity
w space width
x, y, z distance along X, Y, Z ; coordinates velocity

Uppercase symbols

<i>A</i>	arbitrary section; point in tooth profile
<i>B</i>	point where involute meets the base circle
<i>C</i>	centre distance, tangent to base circle
<i>D</i>	design section; diameter
<i>O</i>	center
<i>L</i>	lead
<i>N</i>	number of teeth
<i>P</i>	pitch point
<i>R</i>	Radius of circle at pinion axis
<i>X, Y, Z</i>	coordinates

Greek symbols

α	inclination of radius vector line of centres
β	angular position of pinion
γ	rake angle
γ_s	side rake angle
δ	relief angle
δ_s	side relief angle
ϵ	reduction in addendum; roll angle
ϵ_1	amount of stock removed
ϵ_2	reduction in usable width
χ, η	coordinates at pitch point
r, θ	polar coordinates

ρ	radius of curvature
ω	angular velocity
ϕ	profile angle; pressure angle
χ	profile shift coefficient

Subscripts

b	at base circle
c	for cutter
g	for gear
i	number of resharpenings
f	at fillet
n	normal
p	at pitch circle
r	for rack, at the root circle
s	at standard pitch circle
t	at the tip circle
x, y, z	in the x, y, z directions
ct	at circular tip

Superscripts

A	at an arbitrary section $A - A$
D	at the design section $D - D$
$corr$	correction

T at the tip section $T - T$
 c cutting

Other notations

$[]^c$ cutting
 $[]^o$ operating
 $\hat{i}, \hat{j}, \hat{k}$ unit vectors in x, y, z directions
 \hat{U} unit vector
 \vec{U} vector

Chapter 1

Introduction

This thesis is written assuming that the reader is familiar with the basic principles of gearing and gear cutting technology. However, much of the theory on the geometry of involute gearing that has been directly used in this thesis has been included in Appendix A. Fundamental gear terminology and background information can be found in the references [3, 4, 5, 7, 8, 12]

Gear shaping is a generating process for producing gears using a machine tool. The machine tool (gear shaper) generates the gear, from a blank, using a cutting tool known as gear shaping cutter, which is similar to another gear, except that the teeth are relieved to provide clearance as shown in figure 1.1. The cutting tool and the gear blank are rotated simultaneously, while the cutter makes successive passes through the blank, generating a series of closely spaced individual cuts. When the cutter reaches full depth, the desired tooth form is produced.

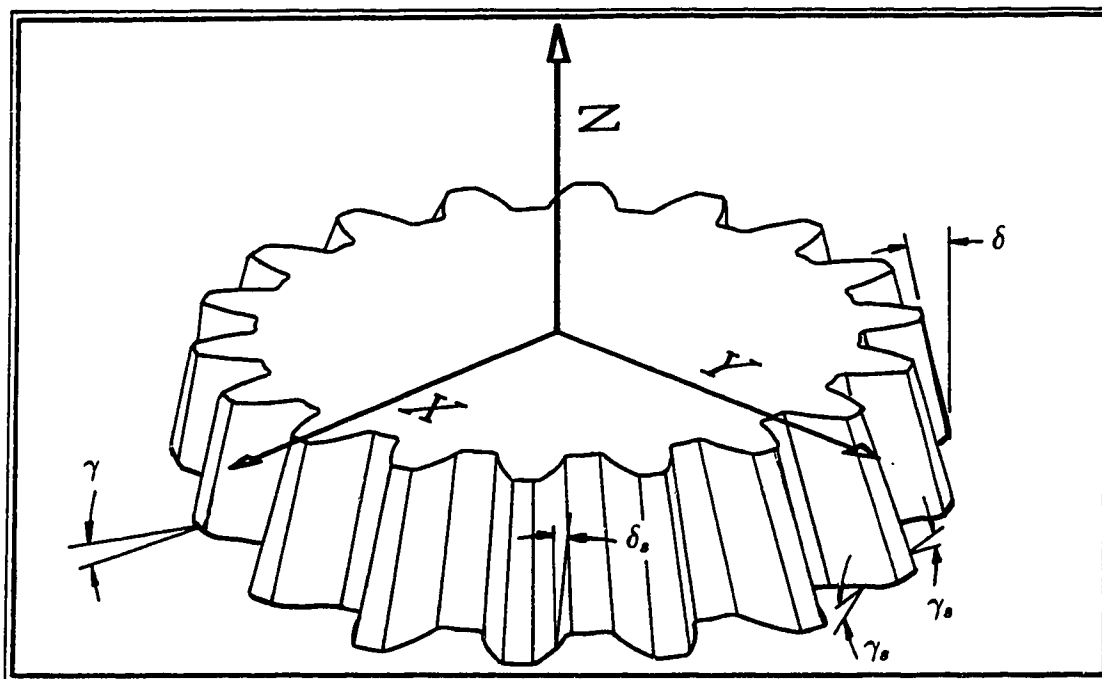


Figure 1.1: Gear shaping cutter

1.1 Shaping machine

There are a number of models of gear shapers, ranging from one which will cut a gear as small as 1/16" dia and as fine as 200 DP, to one which has a capacity of 23ft and courser than 1 diametral pitch. While most single spindle gear shaping machines are in a vertical configuration, this is not an essential principle and they can work equally well in the horizontal plane.

The pinion cutter is a gear with cutting edges, which can reciprocate along its own axis and at the same time rotate with the gear at the prescribed gear ratio (Figure 1.2).

The reciprocating motion, along the axis of the cutter, is usually performed by some form of crank and lever arrangement, or hydraulic stroking arrangement (presently, more common). The speed of stroking can be regulated, by control valves in the hydraulic system, and by pulleys or gearboxes in the crank and lever arrangements.

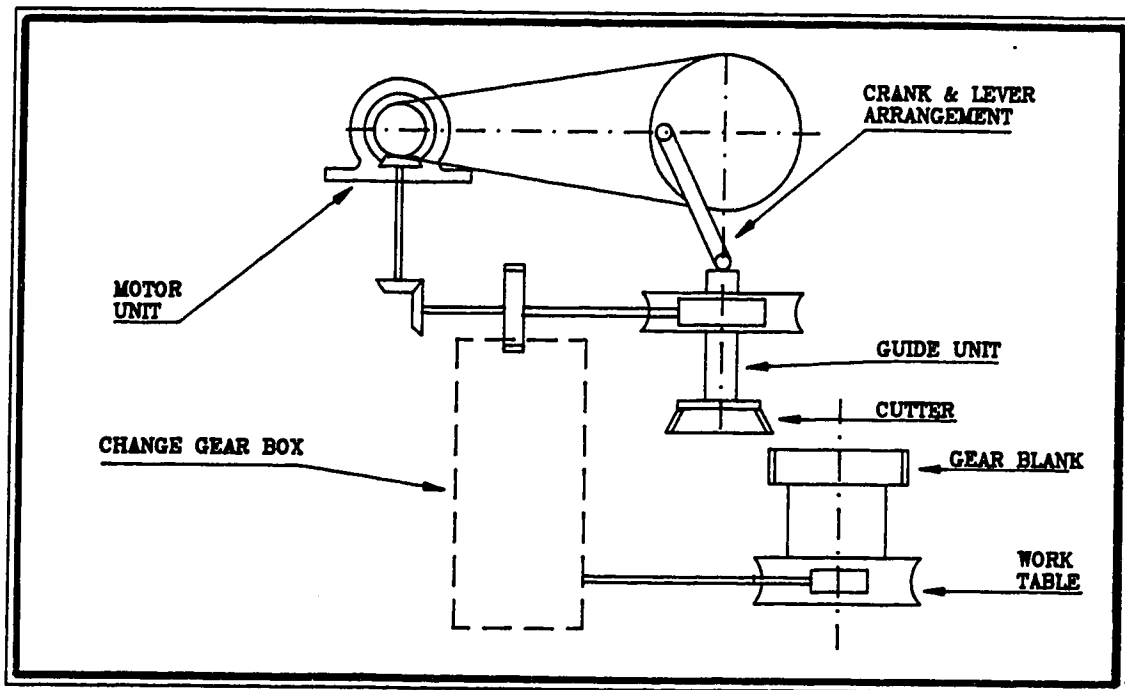


Figure 1.2: Gear shaping process

There is a guide unit attached to the cutter spindle, that has to be changed for each helix angle or hand of helix, when cutting helical gears. Since dragging back through the work destroys the cutting edge and affects tool life, the cutter spindle has to be relieved from the work on the non-cutting return stroke. Some manufacturers provide relief by moving the tool (Figure 1.3), while others move the gear. One advantage in relieving the cutting tool is that the weight of the mechanism is constant and therefore, the mass and the inertia forces are known to the designer beforehand. For relieving the work, the largest mass to be placed on the table has to be anticipated and then allowance has to be made for variations.

It is also necessary to provide a means for feeding the cutter into the work slowly, as the gear rotates. Thus, the table has to rotate by a certain angle before the full depth of cut has been reached and before infeed ceases. The number of cuts necessary for cutting a particular gear, therefore, depends on the size of the gear and

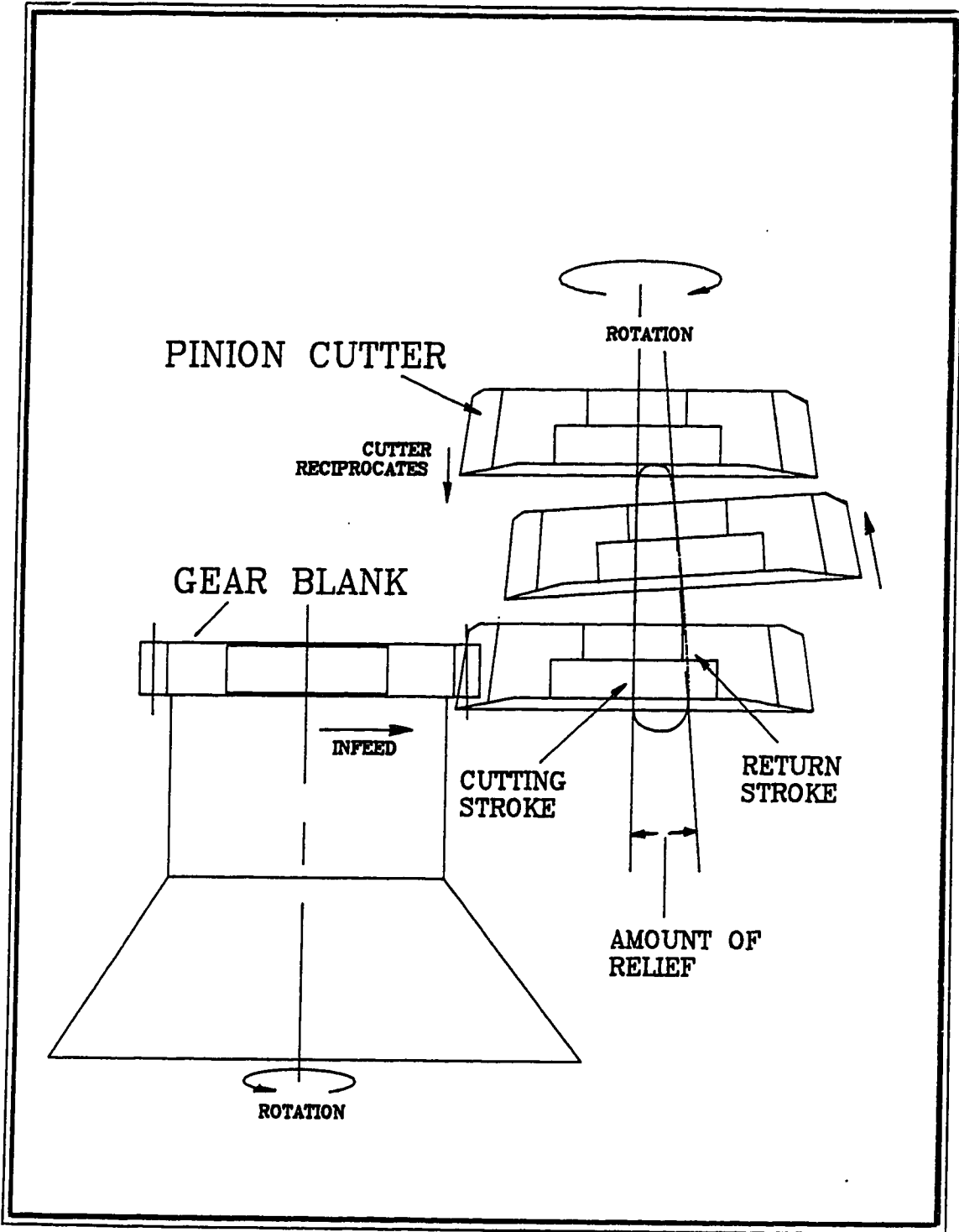


Figure 1.3: Relieving arrangement of shaper cutter

the machine tool.

Adjustments for the length of stroke and for the height of cutter above the work fixture are necessary. These adjustments must also be made after a number of resharpenings of the cutter.

Depending upon the nature and shape of work, various types of shaper cutters are available. Figure 1.4 shows some of the common types of cutters.

1.2 Advantages of Shaping

There are certain types of components, which can be produced only on a gear shaper and others which, although they can be produced on the hobber, are best produced by the shaping method. Racks cannot be generated by hobbing. They can be produced by an attachment to a form milling cutter, but this is not as accurate as a generating process. On the other hand, they are rapidly and accurately produced by shaping, though the maximum length of the rack is limited by the practical limitations of the machine table.

Gears with adjacent shoulders, which limit the runout of cutting tools, are easily generated by the shaping process. Although special attachments and hobs can be produced to allow internal gears to be hobbled, they are extremely limited in their application and far less versatile than the gear shapers.

Double helical gears of the gap and staggered type and continuous-tooth herring-bone gears can be produced only by shaping. Other applications of shaping include cutting of roller and silent chain sprockets, interrupted tooth gears, segmented gears, elliptical gears and face gears.

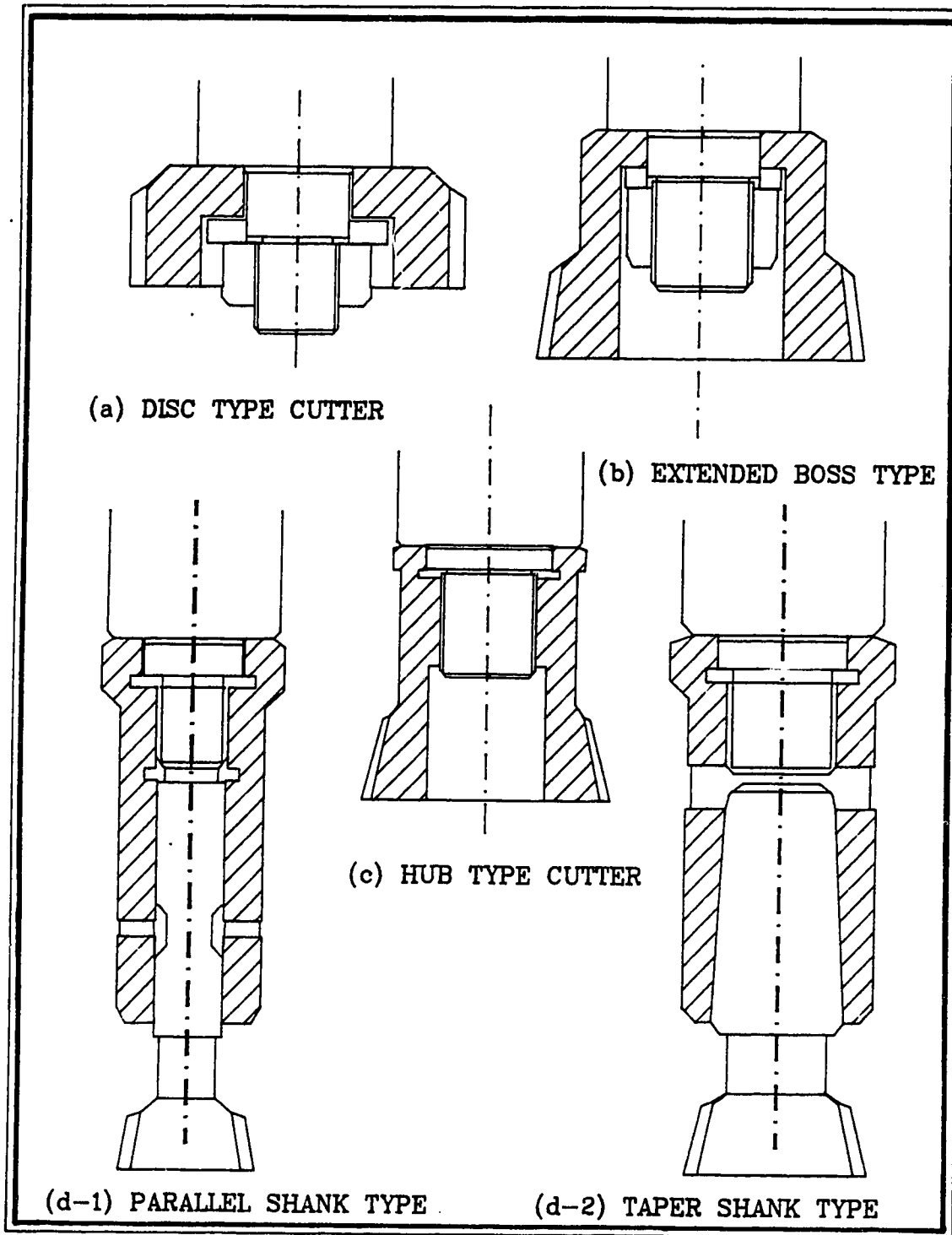


Figure 1.4: Common types of shaper cutters

1.3 Limitation of shaping

Worms and wormwheels cannot be made by the gear shaping process. Another limitation of gear shaping is the length of cut, which depends on the length of the shank or hub of the cutter. Also, gear parts which are integral with long shafts, are difficult to mount in the machine. In this respect, hobbing is advantageous. The requirement for a separate helical guide, for each lead and hand of gear to be cut, is also a disadvantage.

1.4 Gear generation by shaper cutter

In the process of gear generation by shaping, the gear blank and the cutter are driven with constant relative angular velocity, as if they were a meshing gear pair. In addition, the cutter is given a reciprocating motion, in the direction of its axis, to provide for the cutting action.

If we let the gear to be cut have N_g teeth, module m , pressure angle ϕ_s , tip circle diameter D_{tg} and tooth thickness t_{sg} , then the standard pitch circle of the gear is given by,

$$R_{sg} = \frac{1}{2}N_g m \quad (1.1)$$

Since the tip circle diameter of the gear has nothing to do with the cutting process, a cylindrical gear blank of diameter D_{tg} , and of blank length equal to the face width F of the gear, is normally obtained by turning before the shaping begins. Now, since the cutter and gear act like a meshing gear pair, the minimum condition for correct meshing applies in this case, which is that the base pitches of the cutter and gear

should be equal.

$$\begin{aligned}
 p_{bc} &= p_{bg} \\
 \Rightarrow p_{sc} \cos \phi_c &= p_{sg} \cos \phi_s \\
 \Rightarrow \pi m_c \cos \phi_c &= \pi m \cos \phi_s
 \end{aligned} \tag{1.2}$$

It follows from the above that the cutter can be conveniently chosen to have the same value of module m , and pressure angle ϕ_s , as those required by the gear.

To cut N_g number of teeth in a gear blank, the gear blank and the cutter must be rotated, during the cutting process, with definite relative angular velocity deduced from the condition that the pitch circle velocity of the gear and the cutter must be the same, for non-slip rolling of the pitch circles ($V_p = \omega r \propto \omega N$).

$$\begin{aligned}
 N_g \omega_g &= -N_c \omega_c \\
 \Rightarrow \frac{\omega_c}{\omega_g} &= -\frac{N_g}{N_c} = -m_g
 \end{aligned} \tag{1.3}$$

The required gear ratio m_g , is obtained by a number of change gears, in a gear train, connected to the work table and the cutter. In some of the most recent shapers, separate stepping motors are used to drive the cutter and gear, and are electrically controlled for the required angular velocity ratios.

The final quantity to be adjusted is the tooth thickness t_{sg} of the gear. This is done by radially feeding the cutter into the blank, to the exact cutting centre distance required for cutting the specified gear tooth thickness t_{sg} .

Referring to Figure 1.5, the tooth thickness of the gear and cutter, at the cutting pitch circle, will be equal to the space width, on either side, of the imaginary rack, along its cutting pitch line.

$$t_{pg} = w_{r1} \tag{1.4}$$

$$t_{pc} = w_{r2} \tag{1.5}$$

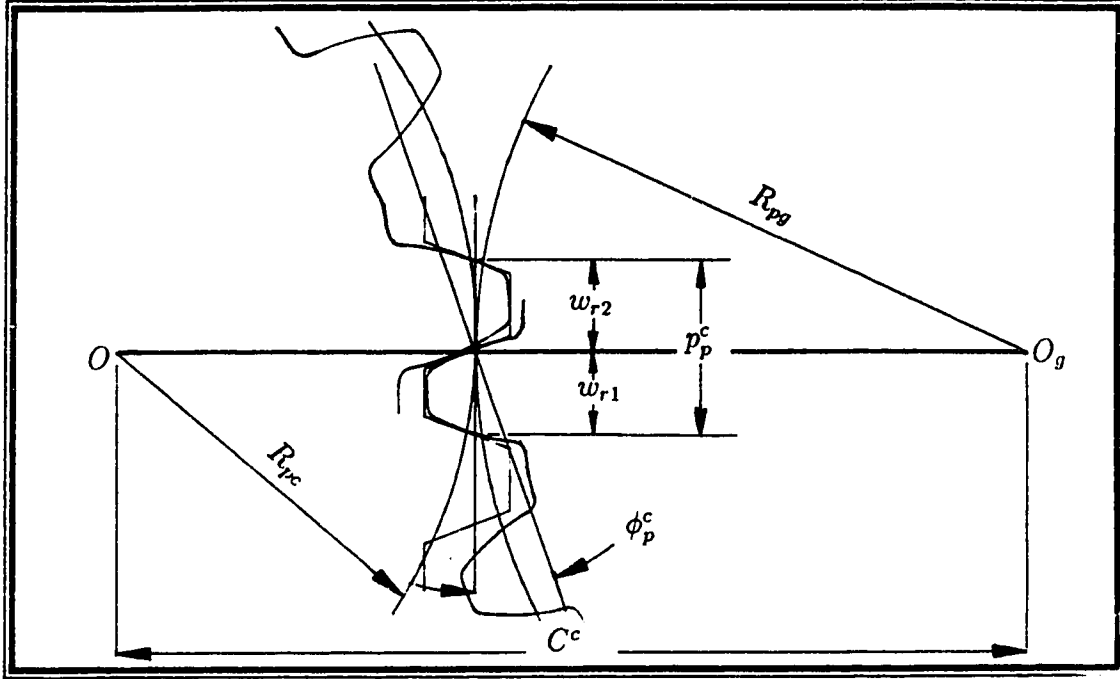


Figure 1.5: Relation between tooth thickness of gear and cutter

The sum of the adjacent tooth spaces, along the cutting pitch line, of the imaginary rack is equal to the pitch of the rack, which is also equal to the circular pitch of the gear and the cutter, and is given by,

$$w_{r1} + w_{r2} = p_p^c = \frac{2\pi C^c}{N_g + N_c} \quad (1.6)$$

For both the gear and the cutter, the tooth thickness at the cutting pitch circle and at the standard pitch circle are given by (Appendix A.2),

$$\begin{aligned} t_{pg} &= R_{pg} \left\{ \frac{t_{sg}}{R_{sg}} + 2(\text{inv}\phi_s - \text{inv}\phi_p^c) \right\} \\ t_{pc} &= R_{pc} \left\{ \frac{t_{sc}}{R_{sc}} + 2(\text{inv}\phi_s - \text{inv}\phi_p^c) \right\} \end{aligned} \quad (1.7)$$

From equation 1.4, 1.5 and 1.6 we get,

$$t_{pg} + t_{pc} = p_p^c \quad (1.8)$$

On substituting the value of the tooth thicknesses, from equation 1.7, in the above equation, we get,

$$R_{pg} \left\{ \frac{t_{sg}}{R_{sg}} + 2(\text{inv}\phi_s - \text{inv}\phi_p^c) \right\} + R_{pc} \left\{ \frac{t_{sc}}{R_{sc}} + 2(\text{inv}\phi_s - \text{inv}\phi_p^c) \right\} = p_p^c \quad (1.9)$$

The standard cutting centre distance C_s^c , is defined as the sum of standard pitch circle radii of gear and cutter,

$$C_s^c = R_{sg} + R_{sc} \quad (1.10)$$

and the standard circular pitch, p_s , is given by,

$$p_s = \frac{2\pi C_s^c}{N_g + N_c} \quad (1.11)$$

Multiplying equation 1.9 by $\frac{C_s^c}{C^c}$, we get,

$$\left(\frac{C_s^c}{C^c} \cdot \frac{R_{pg}}{R_{sg}} \right) t_{sg} = \frac{p_p^c \cdot C_s^c}{C^c} - \left(\frac{C_s^c}{C^c} \cdot \frac{R_{pc}}{R_{sc}} \right) t_{sc} - 2(\text{inv}\phi_s - \text{inv}\phi_p^c) \frac{C_s^c}{C^c} [R_{pc} + R_{pg}] \quad (1.12)$$

Now,

$$\begin{aligned} R_{pg} &= \frac{N_g C^c}{N_g + N_c} ; & R_{sg} &= \frac{N_g C_s^c}{N_g + N_c} \\ \frac{C_s^c}{C^c} \cdot \frac{R_{pg}}{R_{sg}} &= 1 ; & \frac{C_s^c}{C^c} \cdot \frac{R_{pc}}{R_{sc}} &= 1 \\ \frac{C_s^c}{C^c} [R_{pc} + R_{pg}] &= C_s^c ; & \frac{p_p^c \cdot C_s^c}{C^c} &= p_s \end{aligned}$$

Hence,

$$t_{sg} = p_s - t_{sc} - 2C_s^c \{ \text{inv}\phi_s - \text{inv}\phi_p^c \} \quad (1.13)$$

Rearranging the above equation, the involute function of the cutting pressure angle, ϕ_p^c , can be found in terms of the known values,

$$\text{inv}\phi_p^c = \text{inv}\phi_s - \frac{1}{2C_s^c} (p_s - t_{sg} - t_{sc}) \quad (1.14)$$

The cutting pressure angle ϕ_p^c is found from an equation given by Polder [16], and the value of the cutting distance can then be found.

$$q = (\text{inv}\phi_p^c)^{\frac{2}{3}}$$

$$\frac{1}{\cos \phi_p^c} = 1.0 + 1.04004q + 0.32451q^2 - 0.00321q^3 - 0.00894q^4 + 0.00319q^5 - 0.00048q^6 \quad (1.15)$$

$$C^c = \frac{R_{bg} + R_{bc}}{\cos \phi_p^c} \quad (1.16)$$

Therefore, knowing the required gear tooth thickness, the cutting centre distance can be evaluated.

1.4.1 Evaluation of profile details

The cutter profile normally consists of the following three parts:

1. The tip circular arc,
2. The corner radius,
3. The side active profile.

For different values of the x -coordinate from the tooth tip to the tooth root of the cutter, the values of the y -coordinate, r, θ (in polar coordinates), $\frac{dy}{dx}$ and $\frac{d^2y}{dx^2}$ can be obtained from the geometry of the cutter, as explained in the later chapters. The values of $\frac{dy}{dx}$ and $\frac{d^2y}{dx^2}$, at any point are used in finding the value of γ , the angle between the profile tangent at that point and the centre line, and for the value of curvature of profile at that point, using the following equations:

$$\gamma = -\tan^{-1} \left(\frac{dy}{dx} \right)$$

R_{tc} , at point A . The centre of the circular section lies at point C , and the coordinates of points A , B and C can be evaluated as follows:

The polar co-ordinates of point $B(R_B, \theta_B)$ are given by,

$$R_B = \frac{R_{bc}}{\cos \phi_B} \quad (1.18)$$

$$\theta_B = \frac{t_{sc}}{2R_{sc}} + inv\phi_s - inv\phi_B \quad (1.19)$$

where, ϕ_B can be obtained from the following relation:

$$\begin{aligned} \overline{OE} \tan \phi_B &= \overline{EC} + \overline{CB} \\ \text{or, } R_{bc} \tan \phi_B &= \sqrt{(R_A - r_{ct})^2 - R_{bc}^2} + r_{ct} \end{aligned} \quad (1.20)$$

Now, the rectangular co-ordinates of point C , can be found.

$$x_C = R_B \cos \theta_B - r_{ct} \sin(\phi_B - \theta_B) \quad (1.21)$$

$$y_C = R_B \sin \theta_B - r_{ct} \cos(\phi_B - \theta_B) \quad (1.22)$$

$$\theta_C = \tan^{-1} \left(\frac{y_C}{x_C} \right) \quad (1.23)$$

Hence, the polar coordinates of point A , clearly, are:

$$R_A = R_{tc} \quad (1.24)$$

$$\theta_A = \theta_C \quad (1.25)$$

Case II : Non-involute active side profile

As shown in the Figure 1.7, the location of point C would be such that the magnitude of the radius vector of point C equals the difference between the radius of the tip circle and that of the circular section, while its orientation is such that the

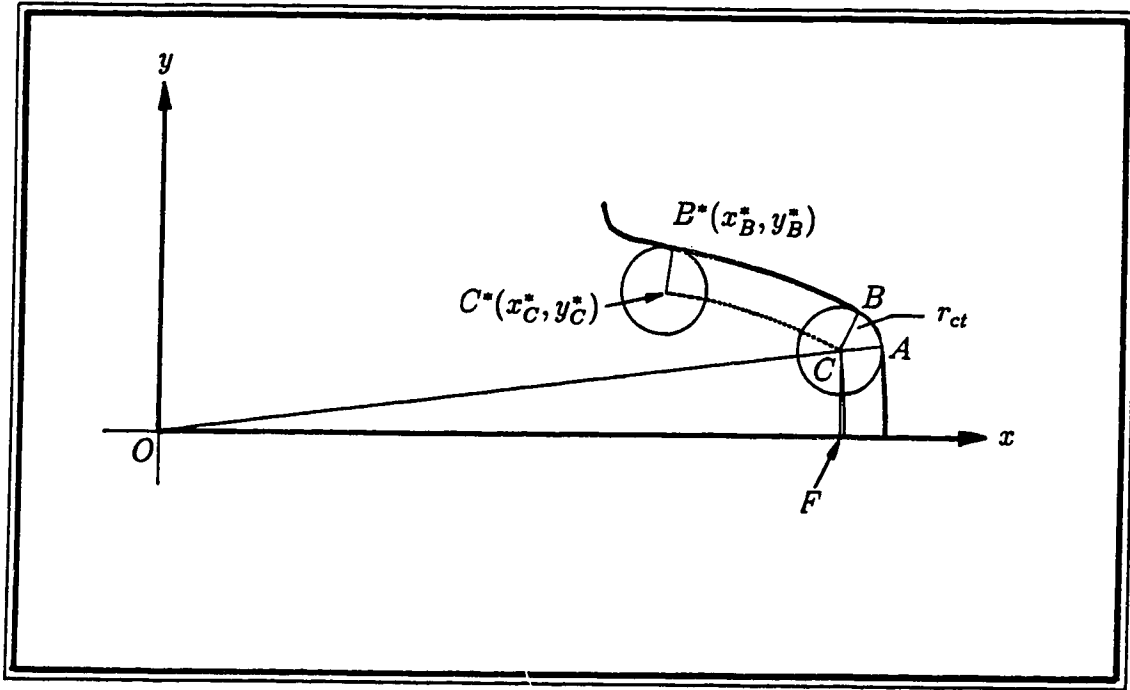


Figure 1.7: Non-involute active side profile

tip corner circle is tangent to both the active side profile and the tip circle.

$$\begin{aligned}\overline{CF}^2 + \overline{FO}^2 &= \overline{CO}^2 \\ x_C^2 + y_C^2 &= (R_{tc} - r_{ct})^2\end{aligned}\quad (1.26)$$

Since the value of $\frac{dy}{dx}$ is known for all points on the active side profile, from geometry, then the coordinates of the centre of a circle, (x_C^*, y_C^*) touching the active profile at the point (x_B^*, y_B^*) is given by,

$$\begin{aligned}x_C^* &= x_B^* - r_{ct} \sin \gamma \\ &= x_B^* - r_{ct} \sqrt{\frac{\left(\frac{dy}{dx}\right)^2}{1 + \left(\frac{dy}{dx}\right)^2}}\end{aligned}\quad (1.27)$$

$$\begin{aligned}y_C^* &= y_B^* - r_{ct} \cos \gamma \\ &= y_B^* - \frac{r_{ct}}{\sqrt{1 + \left(\frac{dy}{dx}\right)^2}}\end{aligned}\quad (1.28)$$

When x_B^*, y_B^* approaches the value of x_B, y_B , the values of x_C^*, y_C^* and x_C, y_C become equal and therefore equation 1.26 will be satisfied. Hence, the value of x_B and y_B can be evaluated from an iterative solution (Gauss Seidel) of the following equations:

$$y_B = f(x_B) \quad (1.29)$$

$$\frac{dy}{dx} = F(x_B) \quad (1.30)$$

$$x_B = \sqrt{(R_{tc} - r_{ct})^2 - \left\{ y_B^* - \frac{r_{ct}}{\sqrt{1 + \left(\frac{dy}{dx}\right)^2}} \right\}^2} + r_{ct} \sqrt{\frac{\left(\frac{dy}{dx}\right)^2}{1 + \left(\frac{dy}{dx}\right)^2}} \quad (1.31)$$

Once point B(x_B, y_B) is evaluated, coordinates of point C are found by substituting the values of x_B, y_B in equation 1.21 and 1.22. Coordinates of point A are found from equations 1.24 and 1.25, since the co-ordinates of B and C are now known.

1.4.2 Evaluation of other profile parameters

Knowing the coordinates of any point $P_c(x_c, y_c)$ or $P_c(R_c, \theta_c)$ on the cutter profile, the tooth thickness t_c at that point of the profile can be found.

$$t_c = 2\sqrt{x_c^2 + y_c^2} \tan^{-1} \left(\frac{y_c}{x_c} \right) \quad \dots(\text{for non-involutes}) \quad (1.32)$$

$$= 2R_c \left\{ \frac{t_s}{2R_s} + \text{inv} \phi_s - \text{inv} \cos^{-1} \left(\frac{R_b}{R_c} \right) \right\} \quad \dots(\text{for involutes}) \quad (1.33)$$

When this point $P_c(R_c, \theta_c)$ is the point of contact with a mating conjugate gear, the orientation of the tooth should be such that the normal at this point $P_c(R_c, \theta_c)$ passes through the pitch point.

As shown in the Figure 1.8 the value of the profile angle (Appendix A-2) at the point $P_c(R_c, \theta_c)$ is,

$$\phi_c = \gamma_c + \theta_c \quad (1.34)$$

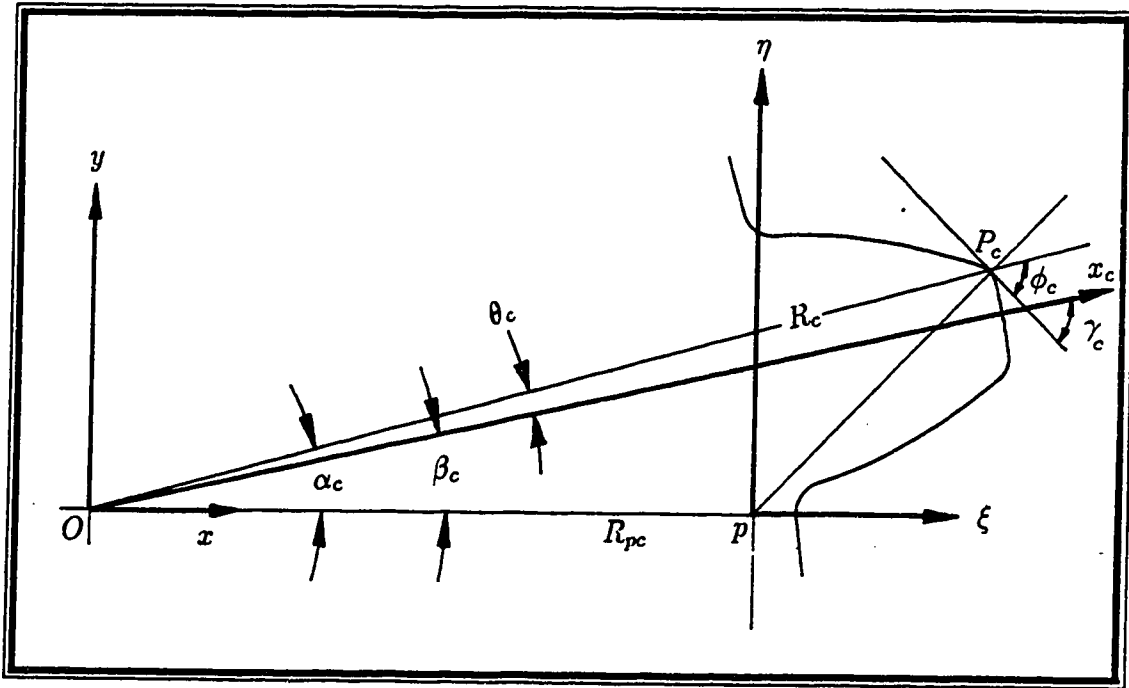


Figure 1.8: Evaluation of other cutter profile parameters

where γ_c is found from equation 1.17. In this orientation the angle α_c that the radius vector R_c of point $P_c(R_c, \theta_c)$ on the cutter makes with the line of centres, can be found using the sine law, from triangle P_cOp (Figure 1.8),

$$\frac{R_{pc}}{\sin(90 - \phi_c)} = \frac{R_c}{\sin(90 + \phi_c - \alpha_c)}$$

or

$$\alpha_c = \cos^{-1} \left(\frac{R_c}{R_{pc}} \cos \phi_c \right) + \phi_c \quad (1.35)$$

Knowing α_c , the coordinates of the path of contact $P_c(\xi, \eta)$, for different values of $P_c(R_c, \theta_c)$, with reference to pitch point can be easily found.

$$\xi = R_c \cos \alpha_c - R_{pc} \quad (1.36)$$

$$\eta = R_c \sin \alpha_c \quad (1.37)$$

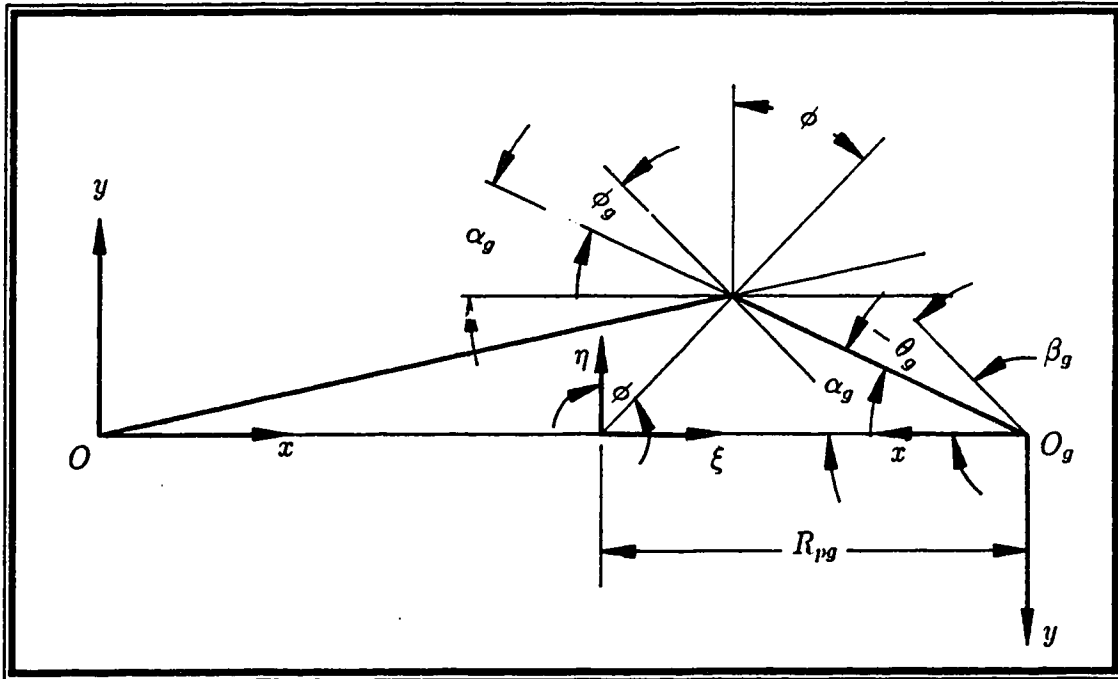


Figure 1.9: Evaluation of gear parameters

The relation between the cutter and gear positions is given by (Appendix A.3),

$$R_{pc}\beta_c + R_{pg}\beta_g + \frac{1}{2}(t_{pc} + t_{pg}) = 0 \quad (1.38)$$

The inclination of the cutter tooth centre-line, with respect to the line of centres, when $P_c(R_c, \theta_c)$ is the point of contact, is then (Figure 1.8),

$$\beta_c = \alpha_c - \theta_c \quad (1.39)$$

Using equation 1.8 and 1.38, the inclination of the conjugate gear tooth centre line, with respect to the line of centres is,

$$\beta_g = -\frac{1}{R_{pg}} \left(R_{pc}\beta_c + \frac{1}{2}t_{pc} \right) \quad (1.40)$$

Now it is possible to evaluate the coordinates of the corresponding contact point in the gear. Referring to Figure 1.9, the values R_g and θ_g , the profile angle and the inclination of the contact with respect to line of centres are,

$$R_g = \sqrt{(R_{pg} - \xi)^2 + \eta^2} \quad (1.41)$$

$$\alpha_g = \tan^{-1} \left(\frac{\eta}{R_{pg} - \xi} \right) \quad (1.42)$$

$$\theta_g = \alpha_g - \beta_g \quad (1.43)$$

$$\text{then, } \tan \phi = \frac{\xi}{\eta} \quad (1.44)$$

To evaluate the radius of curvature of gear at this contact point, the Euler Savary Equation can be used [4, pages 229–238].

$$\text{Let, } s = \sqrt{\xi^2 + \eta^2} \quad (1.45)$$

$$\text{and } \frac{1}{R_0} = \frac{1}{R_{pg}} + \frac{1}{R_{pc}} \quad (1.46)$$

$$\text{then, } \rho_g = -\rho_c - \frac{(\rho_c + s)^2}{R_0 \sin \phi - (\rho_c + s)} \quad (1.47)$$

On repeating the calculations, for different points of the cutter profile, all profile parameters in the generated gear can be evaluated.

A computer program (Appendix C) has been written, which is based on the above approach, that evaluates the profile coordinates, tooth thicknesses, profile angle, centre angle, radius of curvature of various incremental points in the tip, corner and side profiles of the cutter and those in the generated gear. The operating pressure angles and coordinates of the path of contact are also evaluated. A sample program output is attached in Appendix B and a sample plot of a cutter and the generated gear is shown in Figure 1.10.

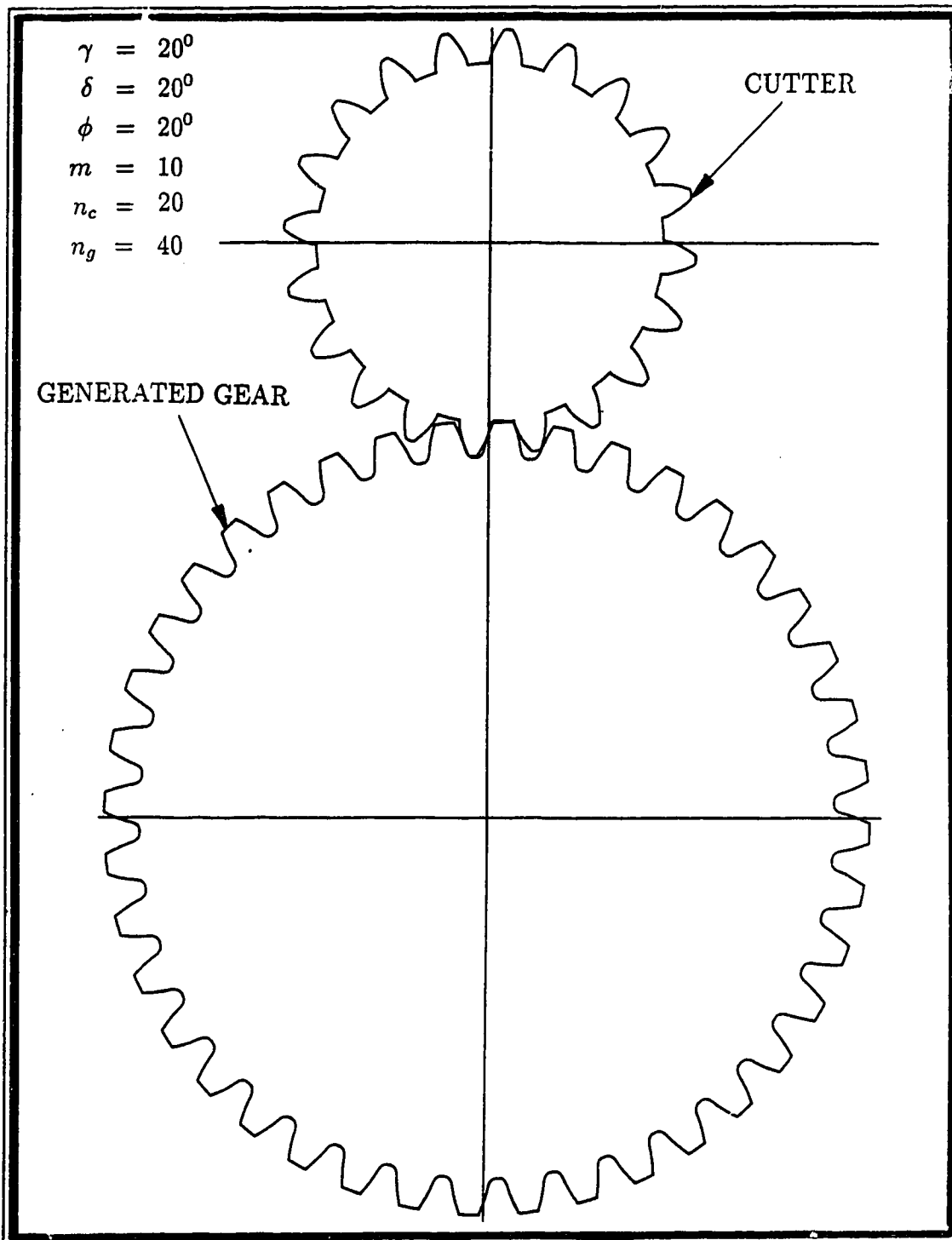


Figure 1.10: Cutter and generated gear

1.5 Gear cutter grinding

The teeth of the cutters are ground on a generating grinding machine where the flank of the grinding wheel represents one or both sides of the basic rack depending upon the method employed.

1.5.1 Zero pressure angle grinding

The most common generating process employed in the past was stationary grinding. For the single position wheel arrangement (Figure 1.11), the wheel represents one flank of a rack tooth with zero pressure angle. The cutter is rocked on its base circle against the working side of a single position grinding wheel. The grinding wheel remains stationary, at midway through the cutter, and the teeth are ground on one flank all the way round before the cutter is removed from the grinding machine, reversed, and then replaced on the machine to grind the other flank.

In some grinding machines the grinding cycle time is substantially reduced by a second grinding wheel which is positioned on the other side to simultaneously grind the opposite side of another tooth. As is evident from the Figure 1.11, if a modification is introduced to the straight side of the wheel then this modification varies from front to back, which means modifications can not be reproduced accurately, on the cutter throughout the cutter life (or usable width). To overcome this handicap, in some grinding machines, the grinding wheel is also reciprocated along the cutter teeth.

1.5.2 Generating pressure angle grinding

In this case the wheel dresses both flanks, at the generating pressure angle, by rocking the cutter on the pitch circle (Figure 1.12). At the same time, the wheel

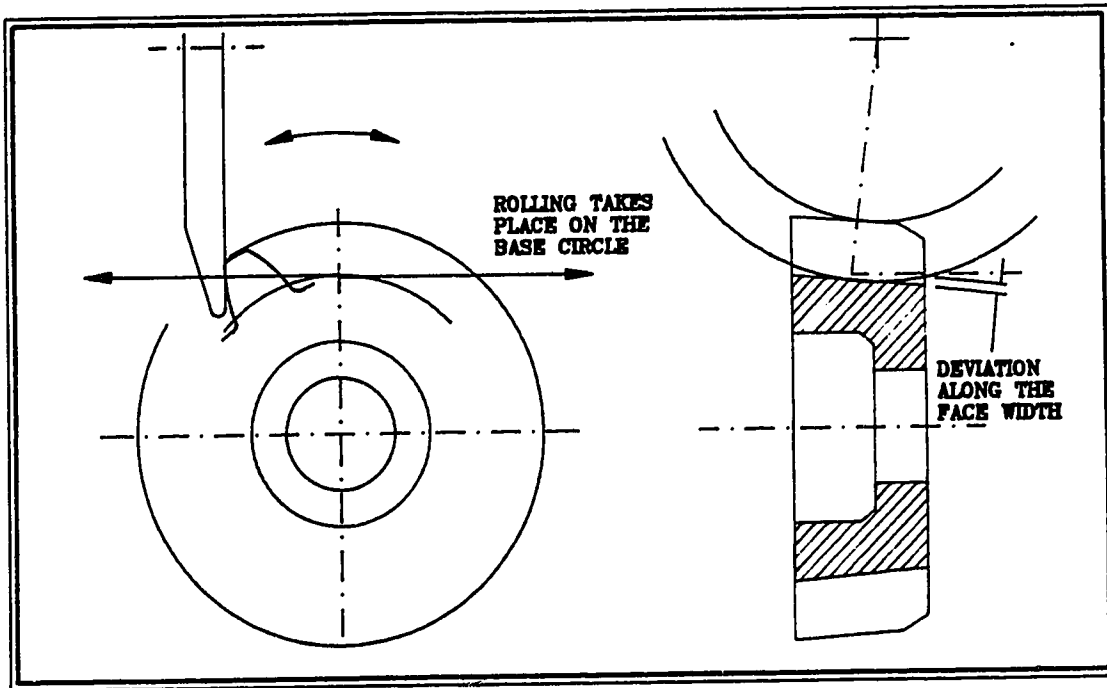


Figure 1.11: Zero pressure angle grinding

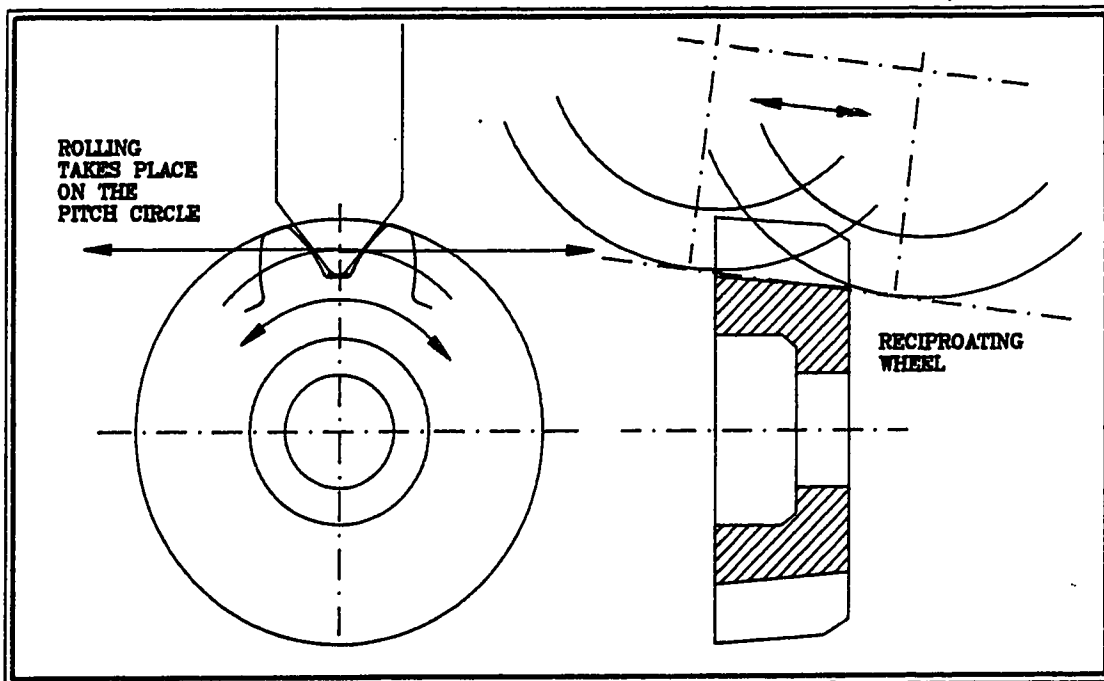


Figure 1.12: Generating pressure angle grinding

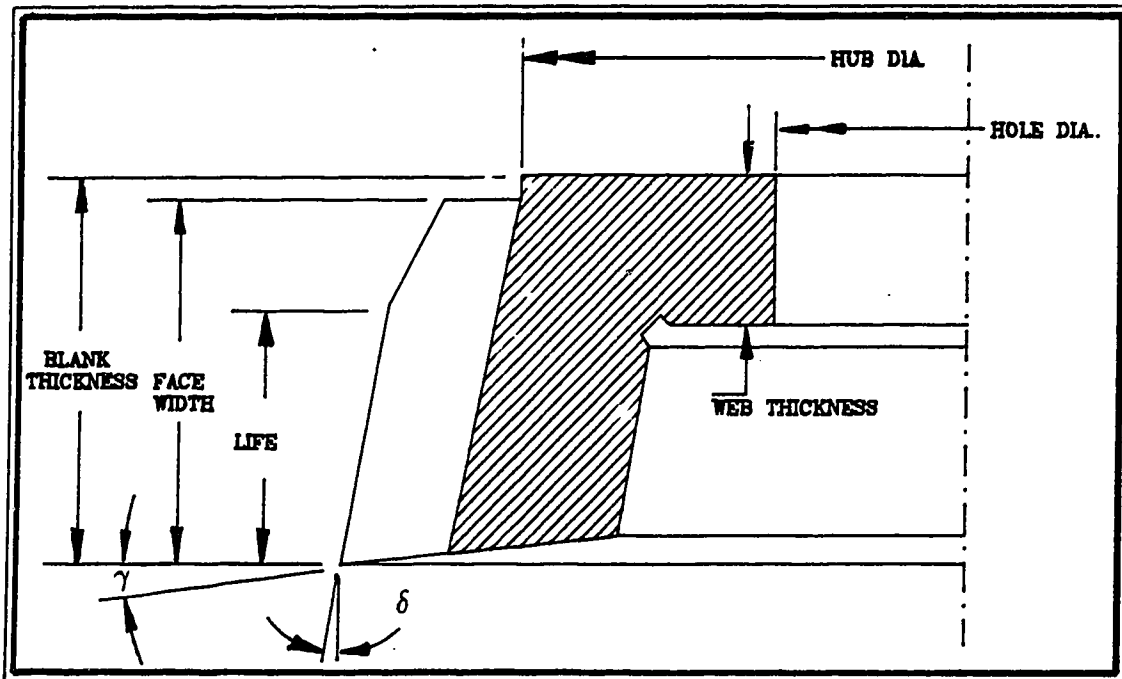


Figure 1.13: Important dimensions of shaper cutter

reciprocates back and forth so that, if profile modifications are imparted, they will be transferred accurately from the back to front owing to its reciprocating action, producing a constant basic rack throughout the usable cutter width. In this method, each cutter tooth is symmetrical and all the teeth are of uniform thickness and spacing. Some manufacturers also call this method “isoform grinding”.

1.6 Shaper cutter resharpening

After the new cutter has been used for a number of times, it becomes blunt and has to be resharpened before it can be used again. A cutter can be resharpened by grinding the conical rake surface and this can be done repetitively, until all the usable width (Figure 1.13) of the cutter is exhausted.

The most common method of regrinding a shaper cutter is by cylindrical grinding wheel, whose axis forms an angle $\beta_w (= 90 - \gamma_c)$, where γ_c is the rake angle of the cutter. Normally, the wheel is operated at around 1800 m/min and the work rotated at 160 rpm and a cut of 0.0064 mm is taken, at a feed rate of around 0.5 m/sec. The inner edge of the grinding wheel is traversed to the root diameter of the cutter and the vertical feed is made when the wheel is in the position indicated by the dotted line (Figure 1.14). The number of gears generated before resharpening is usually so regulated that no more than 0.4mm of stock is removed from the cutter, at each resharpening. With small fine pitch cutters, no more than 0.25 mm should be removed at each resharpening.

Normally, the rake angle is kept at 5° , when the cutter is designed. While grinding, if the rake angle γ is increased the cutter efficiency may be increased, but the pressure angle will be incorrect (as will be evident from chapter 2). On decreasing the rake angle, cutting efficiency decreases and the pressure angle also changes. To ensure the correct pressure angle, grinding is done at the rake angle specified by the manufacturer. Normally a soft wheel with medium grain is used and the wheel is cleaned periodically, as a glazed wheel may crack the cutter teeth. Grinding too much metal at a time, may also cause heat cracks in the cutter and is generally avoided.

1.7 The problem and its relevance

The needs of high speed transmission systems, precision mechanisms and machines, have placed stringent demands on the quality of gears. Good quality gears, having high profile accuracy, are needed for gear drives, that should be free of noise and chatter, have high load carrying capacity and long life.

Shaping is a very popular method of cutting various types of gears, especially

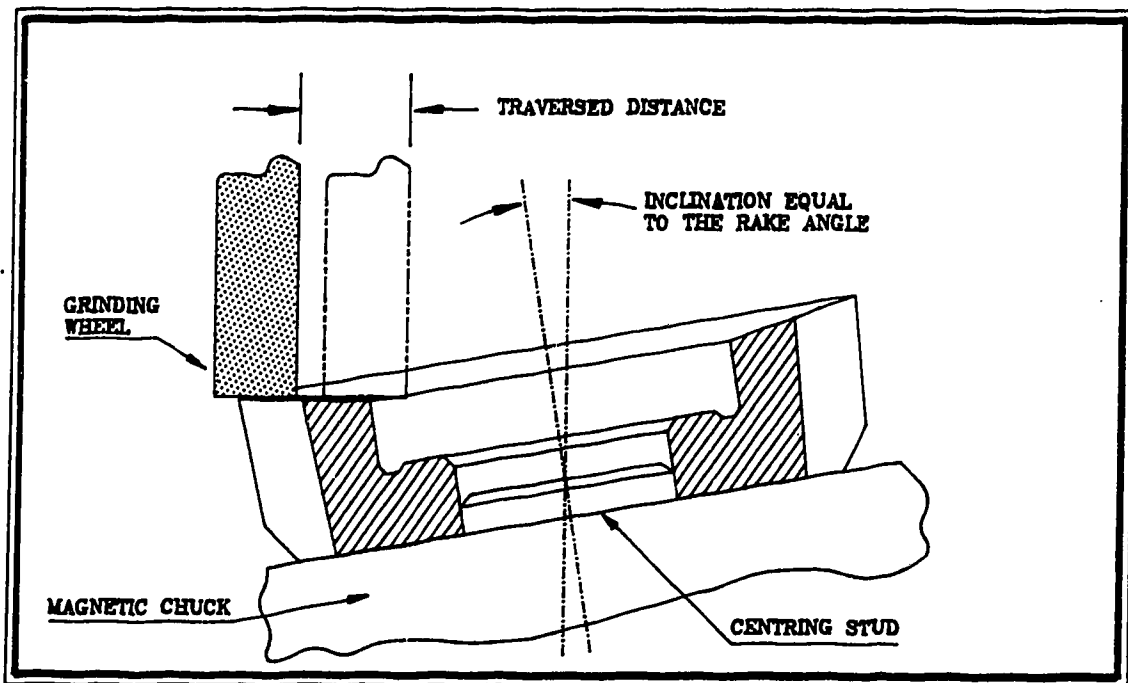


Figure 1.14: Shaper cutter resharpening

herringbone, double helical, cluster gears and gears with adjacent shoulders, that are virtually impossible to cut with any other method. In some of these cases, subsequent grinding is also not possible and therefore accurate generated shaping is important. However, the present design of cutter has some profile deficiencies, as mentioned below.

1.7.1 Inaccuracies in the active surface profile

With the existing gear shaping cutter geometries and calculation methods, it is impossible to make full use of all the advantages of the gear shaping process. Presently, analysis of the gear shaping method is usually done considering the design section (having a standard tooth form at constant height, z) and neglecting the direct effect of top relief and rake angles. To compensate for the the change in pressure and

tooth thickness, caused by the presence of rake angle and front relief angles, certain corrections are subsequently made, in the choice of theoretical base diameter and tooth thickness. However, the effective profile (projected profile of cutter on plane perpendicular to cutter axis) still deviates from the theoretical involute profile, and consequently, does not generate an exact involute in the gear.

In many applications, like shaping of small internal gears, further finishing operations, like gear grinding, may not always be possible. Gears with adjacent shoulders, which limit the runout of gear grinding tools, cannot be accurately finished after shaping operations. The same sort of restrictions apply where accurate double-helical and herring-bone gears are needed. In many of these cases shaping happens to be the last operation, and there is a need to design cutters, that can generate gears with high accuracy.

In the present study, an attempt has been made to find a method of obtaining a cutter capable of generating an exact involute in the gear even after multiple resharpenings of the cutter. This approach also allows for incorporating higher rake angles and top relief angle without any profile deviation; there have been reports that higher front-relief angles of 9° and higher rake angles of $12^\circ - 17^\circ$ prolong cutter life [2].

1.7.2 Inaccuracies due to tip profile

A different tip radius of the cutter produces a different fillet in the root of the gear during gear shaping. The fillet size generated also depends also upon the size of gear blank and that of the cutter, at the rake face. This causes a variation of the fillet radius of the gear after multiple resharpenings of cutter. An attempt has been made to find a suitable tip profile that produces minimum variation in the gear fillet

profile.

1.8 Survey

Most of the research work done on the optimization of the gear cutter profile is based on the traditional approach of the cutter design. Research done by V.F. Romanov [18, 19] is on the modification of the cutter geometry, for avoiding excessive point thinning and undercutting by determining the optimum cutter width. He has also suggested an optimum design distance of the cutter. Extensive research has also been done [13, 20, 21] on interference by the shaper cutter when internal gears are generated. N. Srinivasan and M.S.Shunmugam [22] have investigated deviations of the shaper cutter profile due to the presence of rake and relief angles and have suggested some correction methods to reduce them.

However, the basis of cutter design still remains the same, and thus, some amount of profile error is inevitable, as explained in the later chapters. In this study, an attempt has been made to design the cutter from a different approach, so that the rake and relief angles provided in the cutter teeth do not affect the effective profile.

1.9 Thesis Outline

A thorough investigation of the process of the generation and the geometry of pinion type gear shaping cutters is carried out. Deviations in the profile form of gear shapers are analyzed, and the commonly applied profile correction methods are investigated. The above results are compared with the suggested method of gear cutter profile design. A computer program to simulate the gear cutting process

is prepared, based on calculations explained in section 1.6, so that the effect of resharpener the cutter (throughout life) on the generated gear profiles can be analyzed, for both conventional and suggested methods, and compared with each other.

A modification is suggested to the present set-up of gear cutter generating grinding machines, whereby it becomes possible to generate the required surface profile in the new design of cutter. Other alternative designs are also suggested.

The gear shaping simulator program also incorporates multiple resharpenerings of the cutter and allows for the analysis of the variation of fillet radius of a gear cut by different tooth tip radii in the cutter. Various tooth tip configurations are tried out by this program, in an attempt to find out the most suitable as well as practical cutter tooth tip shape, that will give a minimum number of variations in the gear fillet, even after multiple resharpenerings of the cutter.

For the present study all computer programs to try out different designs of cutter profiles, and to simulate the gear shaping process for multiple resharpenerings, to find out the corresponding gear profile shapes, were written in FORTRAN-VS and run on an Amdahl 5870 mainframe, using a MTS (Michigan Terminal System) as the operating system. These simulator programs were linked to profile graphics programs, using the DISSPLA graphics package. Other line drawings were obtained using AUTOCAD.

Chapter 2

Present design of pinion shaping cutters

2.1 Shape of cutter profile (conventional design)

A spur gear shaping cutter is essentially a spur gear, that has been converted into a cutting tool, by providing proper rake and relief angles.

As shown in Figure 2.1, two vertical planes can be drawn through any point on the cutting edge, one of them passing through the cutter axis, and the other perpendicular to the tooth centre line. When these set of planes pass through a point on the cutter tip, then the angle between the line of intersection of the two planes, and the line of intersection of the axial plane with the cutter tip surface, is called the front relief angle. The angle between the line of intersection of the axial plane and the conical rake face, and the base plane, is defined as the front rake angle. The perpendicular plane intersects the conical rake face in a hyperbolic curve of intersection. When the set of vertical planes pass through a point on the cutter side edge, then the angle

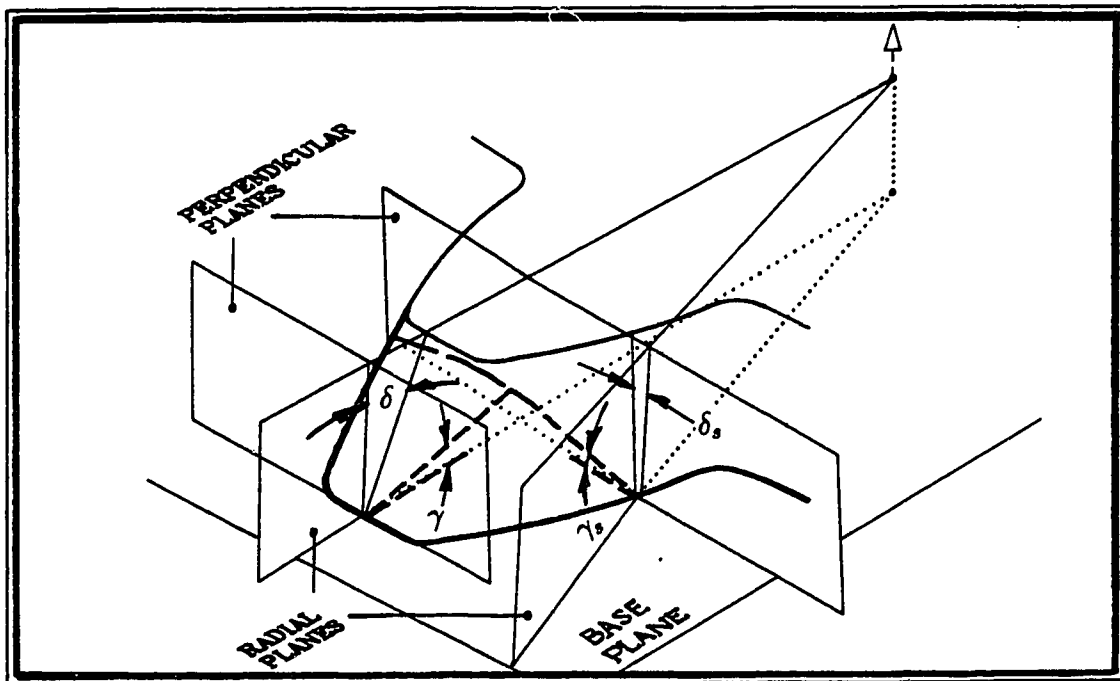


Figure 2.1: Rake and relief angles of shaper cutter

between the tangent to this hyperbolic curve at the cutting edge, and the line of intersection of the perpendicular plane and the base plane, is called the side rake angle. The angle between the line of intersection of the two planes, and the tangent to the curve of intersection of the perpendicular plane and the cutter side surface is called the side relief angle. The front rake angle γ , and the side rake angle γ_s , are provided for ease of metal deformation during cutting. The front relief angle δ , and the side relief angle δ_s , are required for providing clearance on the cutter tooth flank and to avoid rubbing with the gear blank. A rack can be considered the most fundamental and simple of all gear teeth forms, and the tooth profiles of spur and helical gears can be conveniently defined in terms of a basic rack. The same can be done for pinion gear cutters by analyzing them as being generated, by rack cutters.

2.2 Front and side relief angle

For the purpose of mathematical analysis, therefore, a pinion type gear cutter is considered to be generated from a right cylindrical blank, by a rack cutter. In the theoretical analysis, it is assumed that the rack type cutter has zero rake angle and a cutting edge identical to a basic rack (Figure 2.2). A right handed co-ordinate system is assumed with the z-axis pointing out of the paper, in the plan views. For the pinion, the origin lies at the centre of the base circle, with the x-axis pointing radially outwards through the tooth centreline. For the rack, the x-axis lies along the tooth centre line, while the y axis coincides with the rack reference line.

The rack cutter reciprocates at an angle δ to the cutter blank axis, where δ is the front relief angle of the pinion cutter. At the same time, the rack cutter moves forward and the pinion blank rotates with a prescribed velocity ratio, exactly as if the two were running in a tight mesh action. Such a cutting action will generate pinion cutter teeth which will be tapered, both to the cutter tooth tip and to the cutter side, by an angles δ (front relief angle), and δ_s (side relief angle) respectively, as shown in Figure 2.3.

A section $D - D$ is considered, where the reference line of the rack type cutter profile is tangent to the standard pitch circle of the pinion cutter. At this section, the configuration of rack and pinion is similar to the standard cutting position (Appendix A-4), and therefore, will produce an unmodified tooth profile in the cutter blank. At any other arbitrary sections such as $A - A$, the rack will cut a modified tooth profile in the pinion cutter which will be a have a profile shift e^A , given by,

$$e^A = a \tan \delta \quad (2.1)$$

since the offset of the rack varies linearly with distance "a" of the section $A - A$, from design section $D - D$.

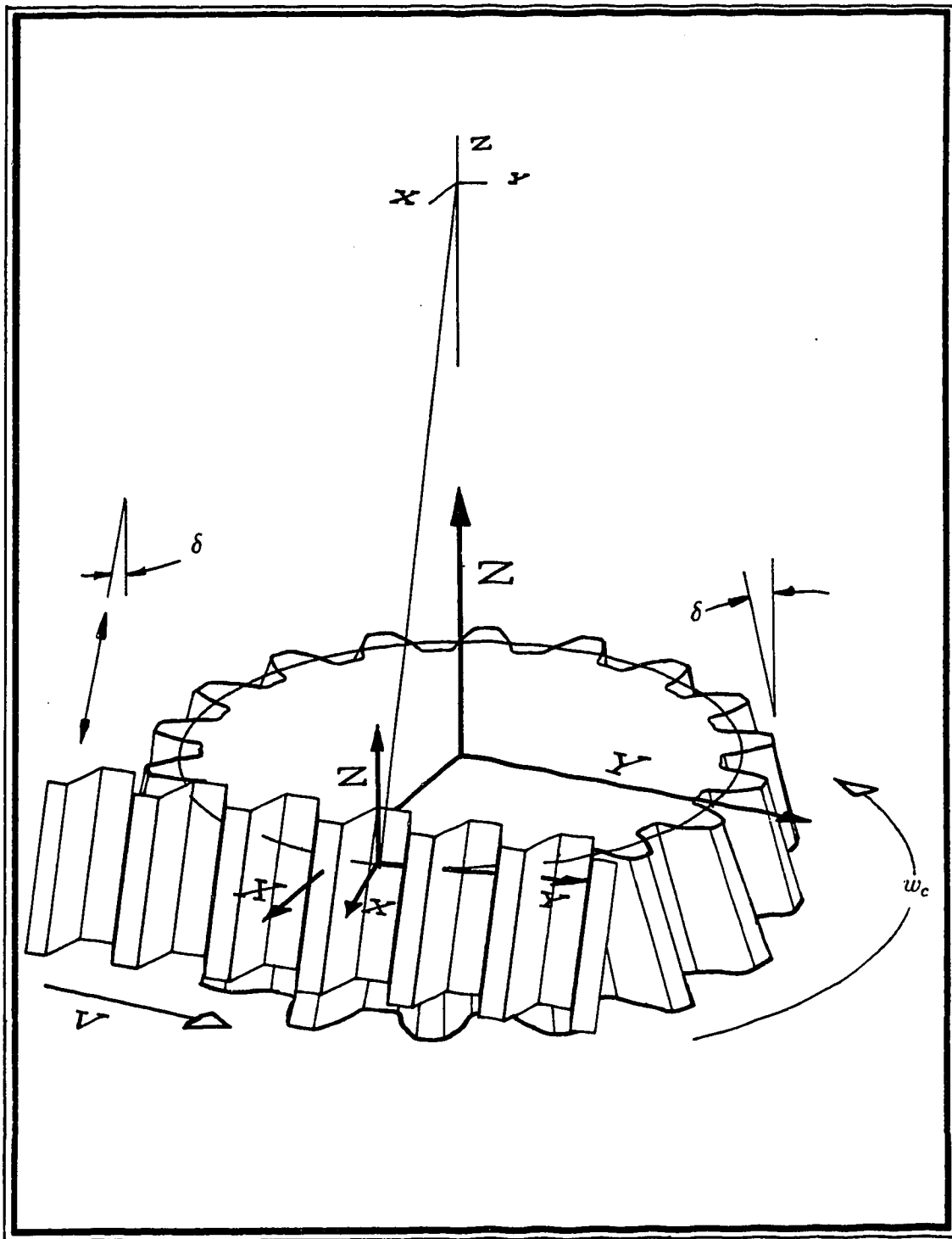


Figure 2.2: Rack and pinion cutter

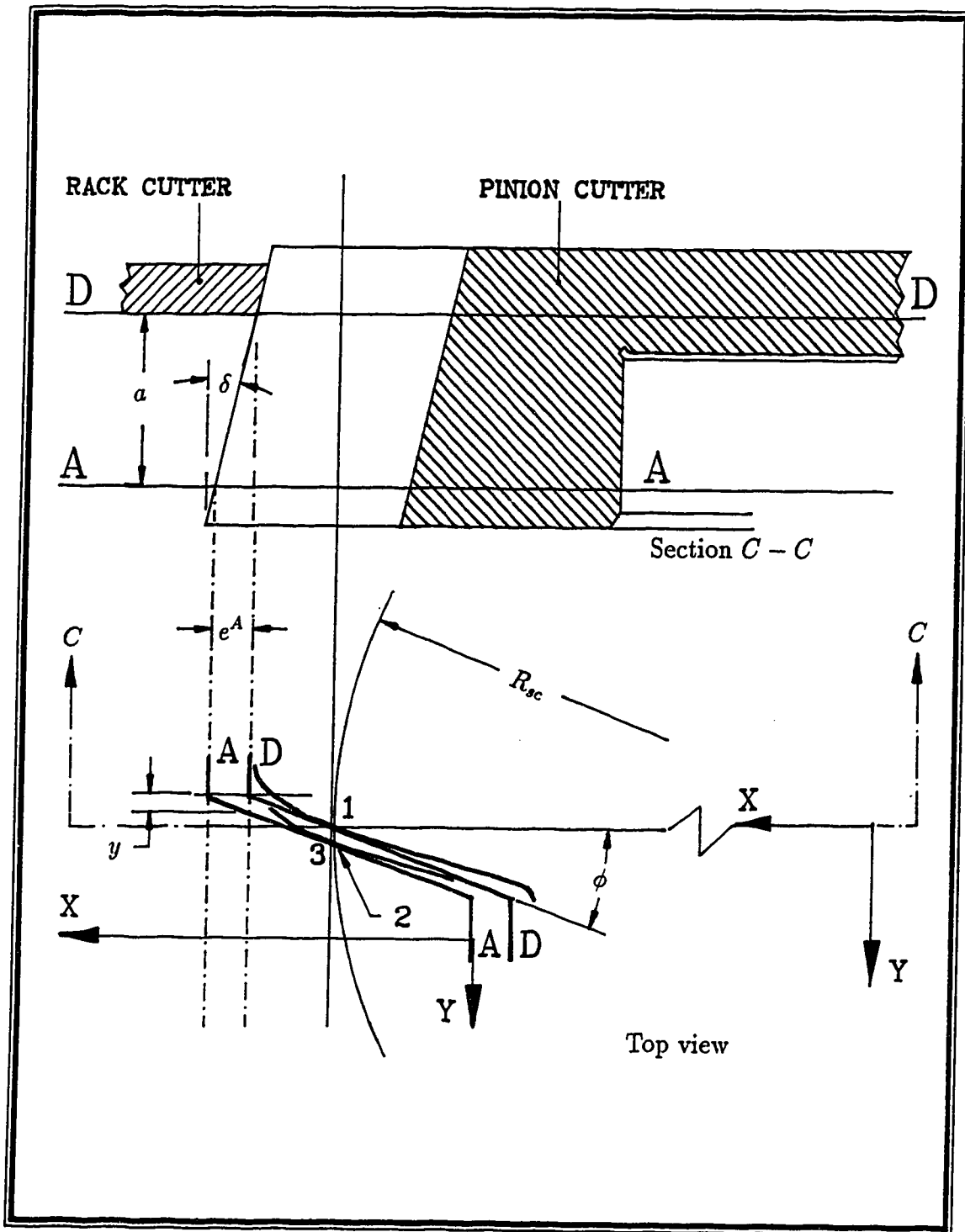


Figure 2.3: Orientation of the rack when generating the pinion cutter

The section $D - D$, where the cutter has an unmodified tooth profile, is called the design section. Thus, the pinion cutter can be considered to be a toothed gear with a variable amount of profile shift, on progressive sections from the design section. The sections, located between the design section and the cutting face, have positive tooth profile shift, and those between the design section and the mounting face, have a negative tooth profile shift.

Since the design section has no profile shift the tooth thickness at this section is,

$$t_{sc}^D = \frac{\pi m}{2} \quad (2.2)$$

In many cases, corrected gear cutters are used that have an initial profile shift in the design section itself, and the tooth thickness at design section, in such cases is,

$$t_{sc}^D = \pi m - t_{pr}^D \quad (2.3)$$

where t_{pr}^D is the tooth thickness of the rack cutter at its cutting pitch line in the design section, $D - D$.

Since the generating motion is not changed during the reciprocating motion of the rack cutter, the cutting pressure angle ϕ^c , is always equal to the rack pressure angle ϕ , and does not depend on the offset of the rack cutter along the blank axis. Since the rack pitch is independent of the profile shift, the cutting pitch circle of the pinion remains the same for all sections and always coincides with the standard pitch circle.

$$[R_{pc}]^c = R_{sc} = \frac{1}{2} N_c m \quad (2.4)$$

Moreover, no change takes place in the base circle in going from one section to another, since its radius is equal to:

$$\begin{aligned} R_{bc} &= R_{sc} \cos \phi \\ &= R_{sc} \cos \phi_s \end{aligned} \quad (2.5)$$

where, R_{sc} is the standard pitch circle of the pinion cutter machined by a rack cutter, and ϕ_s is the standard pressure angle of the pinion cutter. It is important to note that since the rack moves at an angle δ with respect to the pinion blank axis, ϕ is actually the transverse pressure of the rack. The normal pressure angle of the rack cutter will be $\tan \phi_n$ where

$$\tan \phi_n = \frac{\tan \phi}{\cos \delta}$$

This is the normal pressure angle to which the rack cutter (or the grinding wheel¹) has to be made in order to achieve the required standard pressure angle of ϕ_s and the required relief angle δ on the pinion cutter.

It can be easily seen that tooth profiles, at various sections, are constructed from the same base circle of radius R_{bc} . From the figure therefore, it is evident that the family of involutes, lying in sections $D - D$ to $A - A$, are generated by a family of shifted rack profiles at various cutting centre distances, which occurs during the reciprocating action of the cutter. This causes the successive sets of conjugate profiles of the rack and pinion cutters to be radially shifted outwards, as sections go from $D - D$ to $A - A$. Similarly, for sections lying above $D - D$, the profiles would get shifted radially inwards. The top view (Figure 2.3) suggests that if a rack and pinion ran in tight mesh assembly, where successive incremental movement of the rack profile along its pitch line would cause the pinion to rotate on its axis, the same family of conjugate curves would be traversed by the rack and pinion, as were formed by taper cutting. Therefore, if the rack moved by a distance “ y ” along its pitch line causing the pinion to rotate on its axis from point 1 to 2, the length of arc $1\widehat{-}2$ will be:

$$\text{arc } 1\widehat{-}2 = y = a \tan \delta \tan \phi_s \quad (2.6)$$

¹In practice the side surfaces of the cutter are generated by grinding. If isoform grinding method is used (Section 1.5.2), the section of the grinding wheel should conform to a basic rack with a pressure angle of “ ϕ_n ”

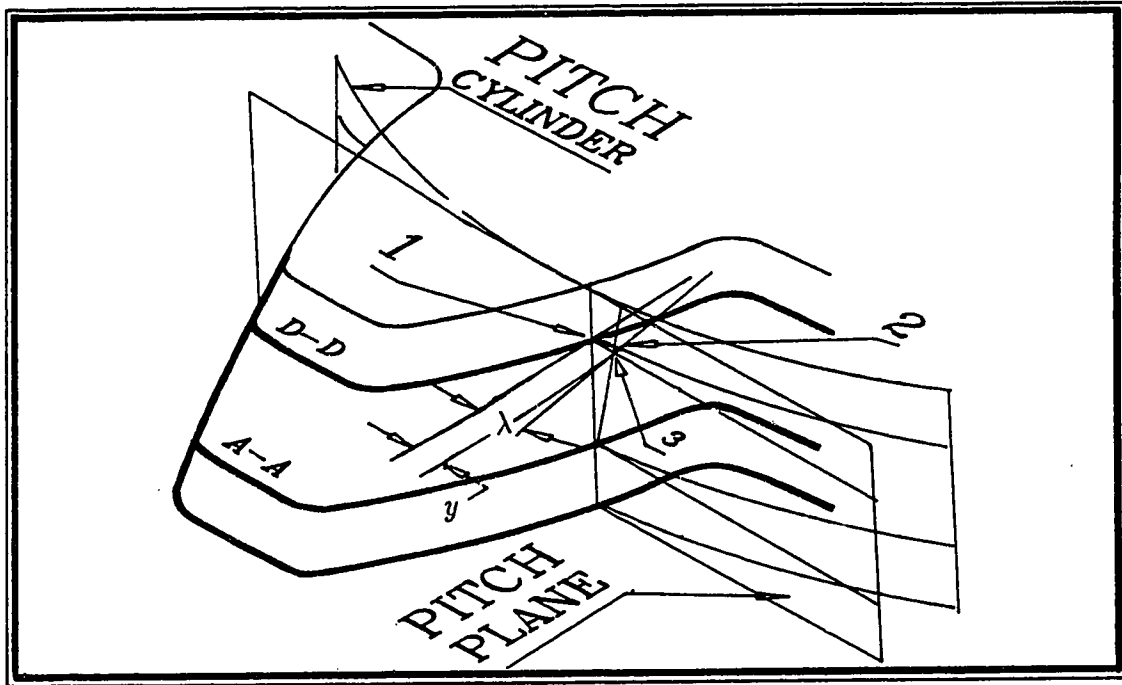


Figure 2.4: Helicoid side surface of Pinion cutter

and the angle of rotation of involute curves with respect to one another corresponding to arc $1-2$ is

$$\lambda = \frac{\text{arc } 1-2}{R_{sc}} \quad (2.7)$$

or,

$$\lambda = \frac{a \tan \delta \tan \phi_s}{R_{sc}} \quad (2.8)$$

From the above equation, it can be inferred that the side surface of the pinion cutter is an involute helicoid surface of constant lead, because the angle of rotation of the involute curves, in going over from section $D - D$ to section $A - A$, is proportional to the distance "a" between the sections. The lead "L" (corresponding distance "a", when $\lambda = 2\pi$) will be,

$$L = \frac{2\pi R_{sc}}{\tan \delta \tan \phi_s} \quad (2.9)$$

and, the side relief angle, from Figure 2.4, is,

$$\begin{aligned}\delta_s &= \tan^{-1} \left(\frac{y}{a} \right) \\ &= \tan^{-1} (\tan \delta \tan \phi_s)\end{aligned}\tag{2.10}$$

2.3 Rake angles

Apart from the front and side relief angles, as discussed in the last section, cutting rake angles (front and side rake angles) are also required at the cutting face of the pinion cutter for the ease of metal removal. These rake angles are produced by grinding the cutting face in the shape of a cone, by the method explained in Chapter 1.

As shown in Figure 2.5, cutter teeth are essentially made up the following surfaces:

1. The conical tooth tip surface
2. The side involute helicoid surface
3. The bottom conical rake surface
4. The top mounting surface
5. The tooth tip corner surface

The cutting edges are produced by the intersection of the conical rake surface and the surrounding surfaces forming the cutter teeth. The projection of these cutting edges, on a plane perpendicular to the axis of the cutter (called the projection plane), forms the effective (or resultant) tooth profile, which actually determines the shape of the generated gear profile during shaping.

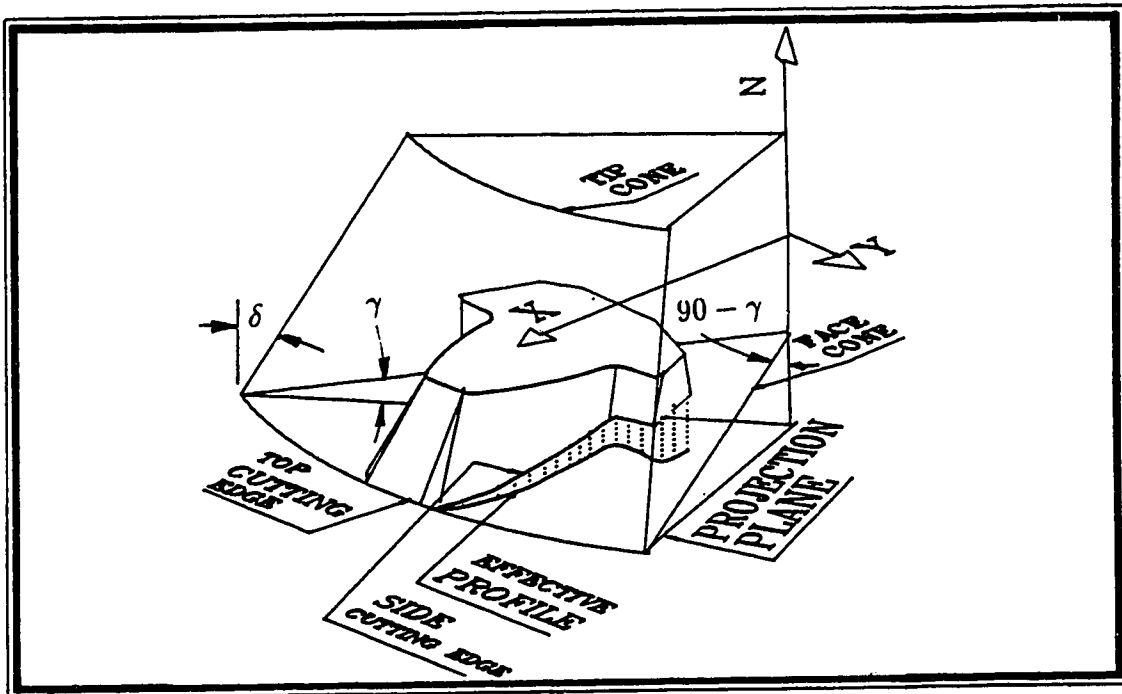


Figure 2.5: Cutting edge of a pinion cutter

It can be seen that the intersection of the conical rake surface of the cutter and the involute helicoid side surface produces side cutting edges, while the intersection of the conical rake surface and a much steeper conical tooth tip surface of the cutter produces the tip cutting edge. The intersection of the conical rake surface and the tooth tip corner surface produces the corner cutting edge, whose projection (on the projection plane) is the effective tooth corner profile, which is responsible for generating the fillet radii in the gear teeth. The side cutting edge will be a 3D curve lying on the rake face cone, whose projection on the projection plane will form the effective side profile of cutter. The effective side profile will not be an involute curve, in the current cutter design. The front cutting edge is an arc of a horizontal circle of intersection of two cones and it will, obviously, remain unchanged when projected onto the projection plane. As will be explained in the following section, the side cutting edge of such a cutter, when it reciprocates along the axis of the gear blank, will not describe a

cylindrical involute surface. Hence, gears will be produced with a certain inevitable profile error.

The remaining parts of this chapter comprise three sections. The next section explains the cause of profile deviation and investigates the amount of profile deviations, due to the presence of rake angles. A computer program (Appendix C) is written to simulate the cutting process. The profile errors in the cutter and those generated, subsequently in the gear are plotted for a typical case.

The following section deals with the correction methods used for reducing the profile errors. Effects of the corrections are simulated in a computer program and the results plotted. The effectiveness of the corrections are then discussed.

The last section discusses methods of evaluation of the optimum distance of cutting face from the design section of a new cutter.

2.4 Deviation in profile due to rake angle

Figure 3.6 shows a rack cutter generating a pinion type cutter which has a front rake angle γ , and a relief angle δ . Various sections in the pinion cutter are taken and the involute profiles at those section are shown to mesh with the same ribbon rack (i.e. the horizontal sectional outline of the rack cutter) at various offset positions.

Design section $D-D$, in the elevation, corresponds to the standard tooth form for an uncorrected gear cutter ($e^D = 0$) and is marked in the plan as $D'-D'$. At this section the addendum, dedendum, and standard tooth thickness at R_{sc} are denoted by h_a^D , h_b^D , and t_{sc}^D respectively. Any arbitrary section $A-A$, at a vertical distance "a", from the design section, has the profile (marked $A'-A'$ in the plan), which is

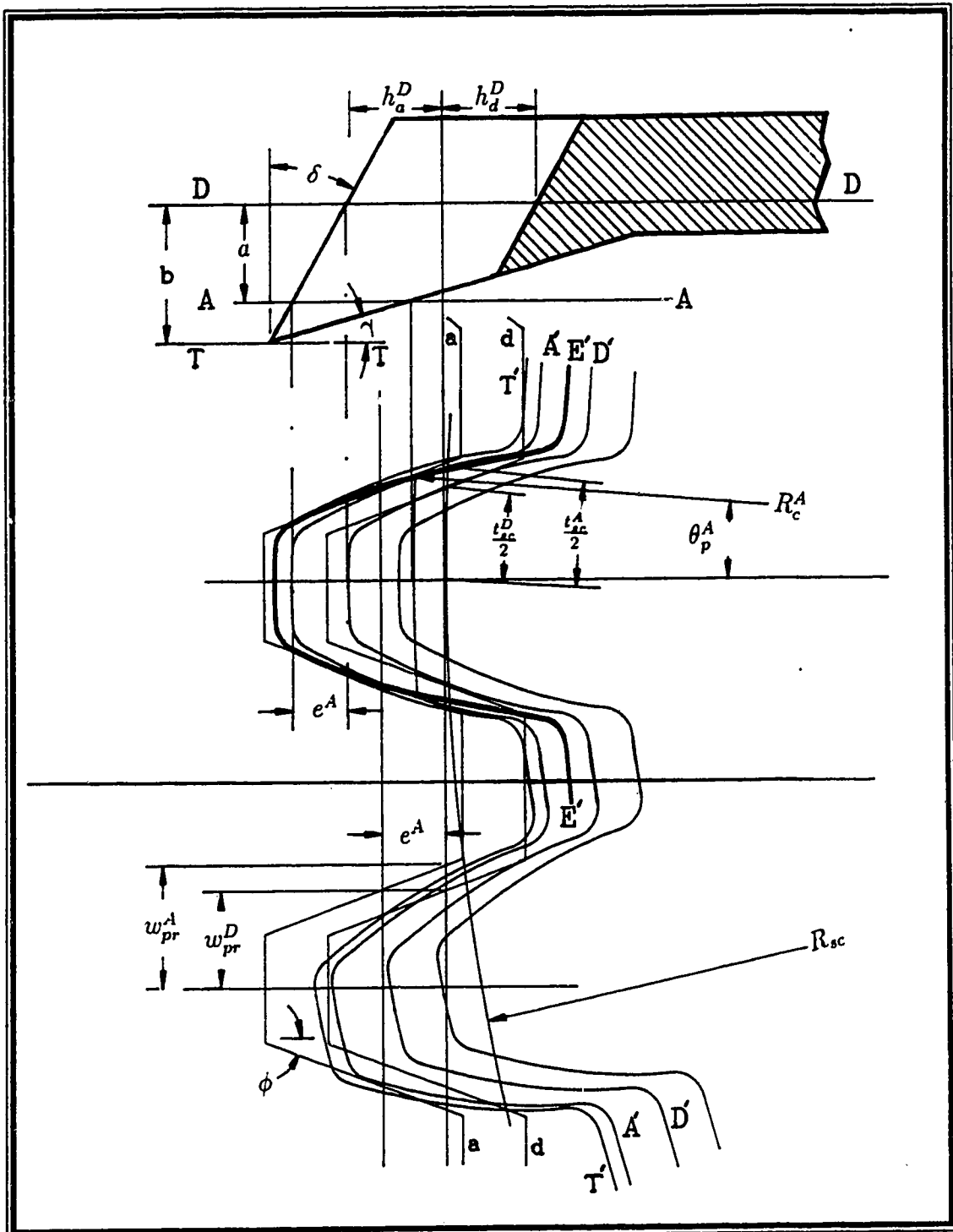


Figure 2.6: Effective profile of a pinion cutter

shifted from the design section an amount e^A where,

$$e^A = a \tan \delta \quad (2.11)$$

The circular tooth thickness, t_{sc}^D and t_{sc}^A , at these two sections are equal to the tooth space widths of the ribbon racks at the corresponding positions, measured on the cutting pitch line (Appendix A-1). Therefore,

$$t_{sc}^D = w_{pr}^D \quad (2.12)$$

also,

$$\begin{aligned} t_{sc}^A = w_{pr}^A &= w_{pr}^D + 2e^A \tan \phi \\ &= t_{sc}^D + 2e^A \tan \phi_s \\ &= t_{sc}^D + 2a \tan \delta \tan \phi_s \end{aligned} \quad (2.13)$$

The value of t_{sc}^D will depend upon the initial profile shift of the design section, if any. For a non-corrected cutter, the design section is taken to be such that the rack at that section meshes at the standard cutting position, and therefore, there is no initial profile shift. The standard tooth thickness of the design section in such a case is,

$$t_{sc}^D = \frac{1}{2} \pi m \quad (2.14)$$

For corrected gear cutters, the rack has an initial offset e_0 , resulting in an initial profile shift of the pinion cutter profile of an amount e_0 in the design section itself. In this case the tooth thickness in design section will be,

$$t_{sc}^D = \frac{1}{2} \pi m + 2e_0 \tan \phi_s \quad (2.15)$$

Let “ b ” be the distance of the tip section $T - T$ from the design section $D - D$. It can be seen that section plane $A - A$ cuts the conical rake face surface in a circle

of intersection, having a radius R_c^A where,

$$R_c^A = R_{tc}^T - \frac{(b-a)}{\tan \gamma} \quad (2.16)$$

where R_{tc}^T is the radius of the tip circle of the cutter at the tip section $T - T$ and is given by,

$$R_{tc}^T = R_{sc} + h_a^D + b \tan \delta \quad (2.17)$$

where $R_{sc} (= \frac{mN_c}{2})$ remains constant irrespective of the cutter profile shift at various sections, since it is only dependent on the module and on the number of cutter teeth. The addendum h_a^D , at the design section is often taken to be 1.25m.

The circle of intersection cuts the involute profile, corresponding to the plane section A-A, at point P^A . The coordinates of P^A can be found with respect to a right handed coordinate system, situated at the cutter centre, with the x-axis aligned with the tooth centre line and the z axis lying along the cutter axis as shown in the Figure 2.6. Noting that the profile angle at radius R_{sc} on the profile is equal to the pressure angle of the cutter ϕ_s , which is equal to the rack pressure angle ϕ , the angle θ_c^A of point P^A on section A - A of the cutter, with respect to the x-axis is given by equation 1.19.

$$\theta_c^A = \frac{t_{sc}^A}{2R_{sc}} + \text{inv} \phi_s - \text{inv} \phi_c^A \quad (2.18)$$

where ϕ_c^A is the pressure angle of point P^A , which is on the shifted involute profile at section A - A. Since the shifted profile is also generated from the same design base circle of the cutter,

$$\cos \phi_c^A = \frac{R_{bc}}{R_c^A} \quad (2.19)$$

where R_{bc} is the radius of the design base circle.

$$R_{bc} = R_{sc} \cos \phi_s \quad (2.20)$$

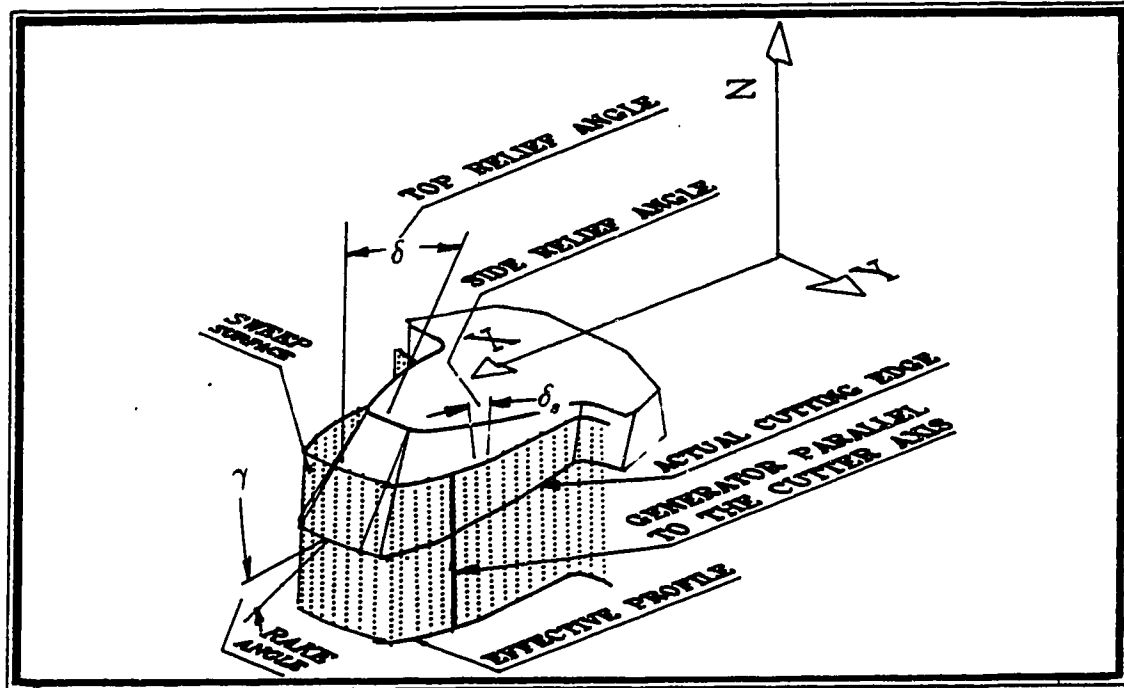


Figure 2.7: Sweep surface of the effective profile

The effective profile (or resultant profile) of the cutter is the projected profile of the cutting face of the cutter, on a plane perpendicular to the axis of the cutter. The cutting edge, reciprocating along the axis of the gear, will describe a cylindrical sweep surface, whose generator moves in contact with the effective profile and always remains parallel to the gear axis, as shown in Figure 2.7. The coordinates of point P^A on the cutter, can be expressed in terms of R_c^A and θ_c^A as,

$$\begin{aligned} X_c^A &= R_c^A \cos \theta_c^A \\ Y_c^A &= R_c^A \sin \theta_c^A \\ Z_c^A &= -a \end{aligned} \quad (2.21)$$

Combining equations 2.13, 2.16, 2.17, 2.18, 2.19, 2.20 and 2.21, the corresponding points on the effective profile can be obtained by moving through a successive arbitrary section $A - A$ from the tip to root as shown in Figure 2.8.

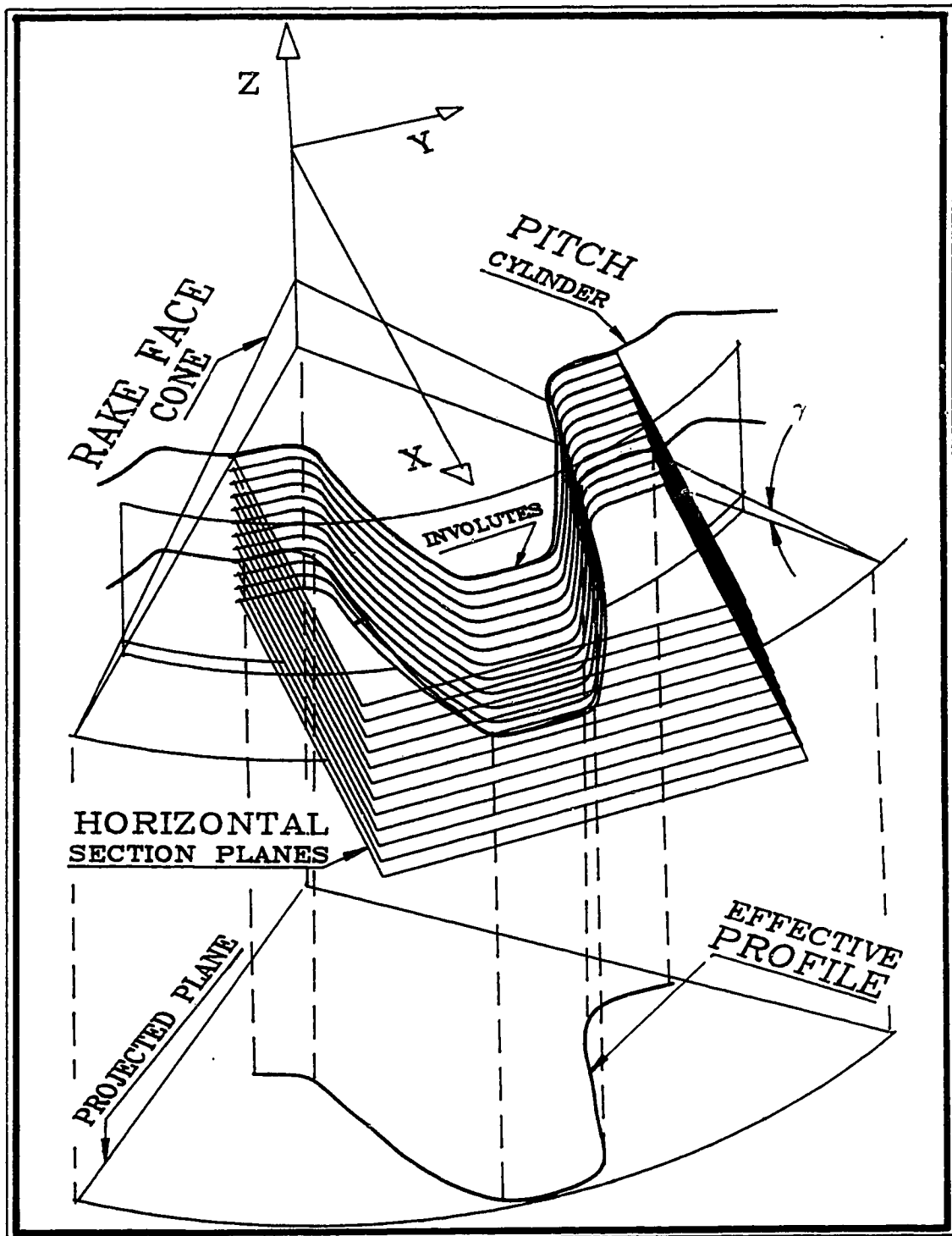


Figure 2.8: Relation of the family of involute profiles to the effective profile

For a fixed tool geometry and a certain design distance, “ b ”, the coordinates of the cutting edge is a function of variable, “ a ”, (section distance), as shown below:

$$X_c^A = \left(R_{sc} + h_a^D + b \tan \delta - \frac{b-a}{\tan \gamma} \right) \cos \left[\frac{t_{sc}^D + 2a \tan \delta \tan \phi_s}{R_{sc}} + \text{inv} \phi_s - \text{inv} \cos \left(\frac{R_{sc} \cos \phi_s}{R_{sc} + h_a^D + b \tan \delta - \frac{b-a}{\tan \gamma}} \right) \right] \quad (2.22)$$

$$Y_c^A = \left(R_{sc} + h_a^D + b \tan \delta - \frac{b-a}{\tan \gamma} \right) \sin \left[\frac{t_{sc}^D + 2a \tan \delta \tan \phi_s}{R_{sc}} + \text{inv} \phi_s - \text{inv} \cos^{-1} \left(\frac{R_{sc} \cos \phi_s}{R_{sc} + h_a^D + b \tan \delta - \frac{b-a}{\tan \gamma}} \right) \right] \quad (2.23)$$

$$Z_c^A = -a \quad (2.24)$$

The Figure 2.9 shows a theoretical profile shape and the effective profile shape of the cutter for $\gamma = 20^\circ$, $\delta = 20^\circ$, $\phi_s = 20^\circ$ and $m = 10$. The profiles generated on the gear blank, by the theoretical and effective profiles of cutter are shown in Figure 2.10. In Figure 2.9, γ and δ are unusually large to show that the current design restricts the choice of γ and δ to small values. As would be expected, the figure shows that the effective profile deviates from the theoretical profile, and the deviation varies from tip to root in the range of 0-1000 microns, in this particular case. The tooth thinning of the cutter causes extra material to be left in generated gear teeth. The profile deviation of the gear also varies from the tip to the root in the of range of 900-0 microns, as shown in Figure 2.10. Appendix B gives a table of various parameters of the cutter and generated gear.

2.5 Profile deviation of effective profile

Deviation of the effective profile is ascertained by comparing the effective profile with respect to the theoretical profile. The theoretical profile can be considered to be

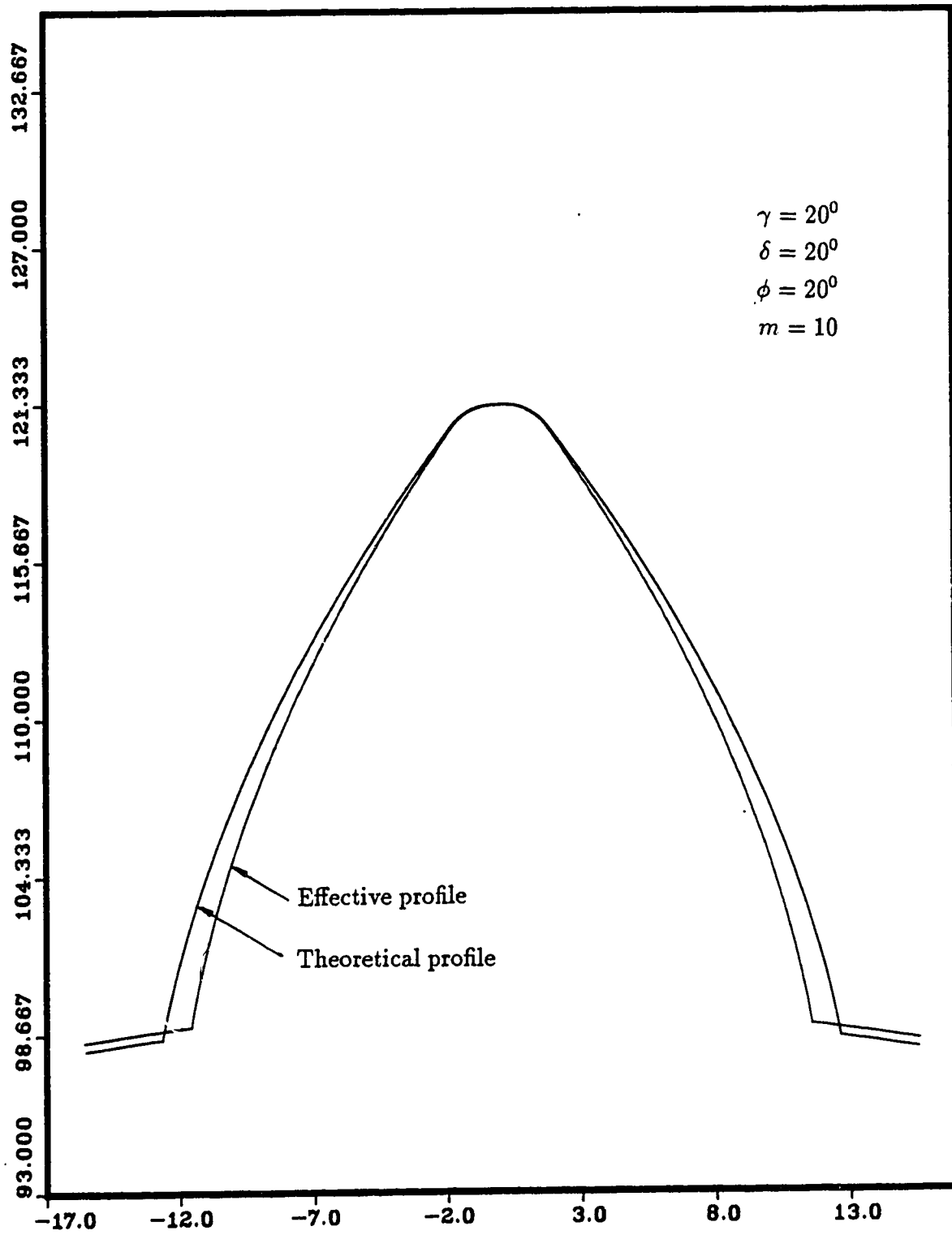


Figure 2.9: Theoretical profile and effective profile of cutter

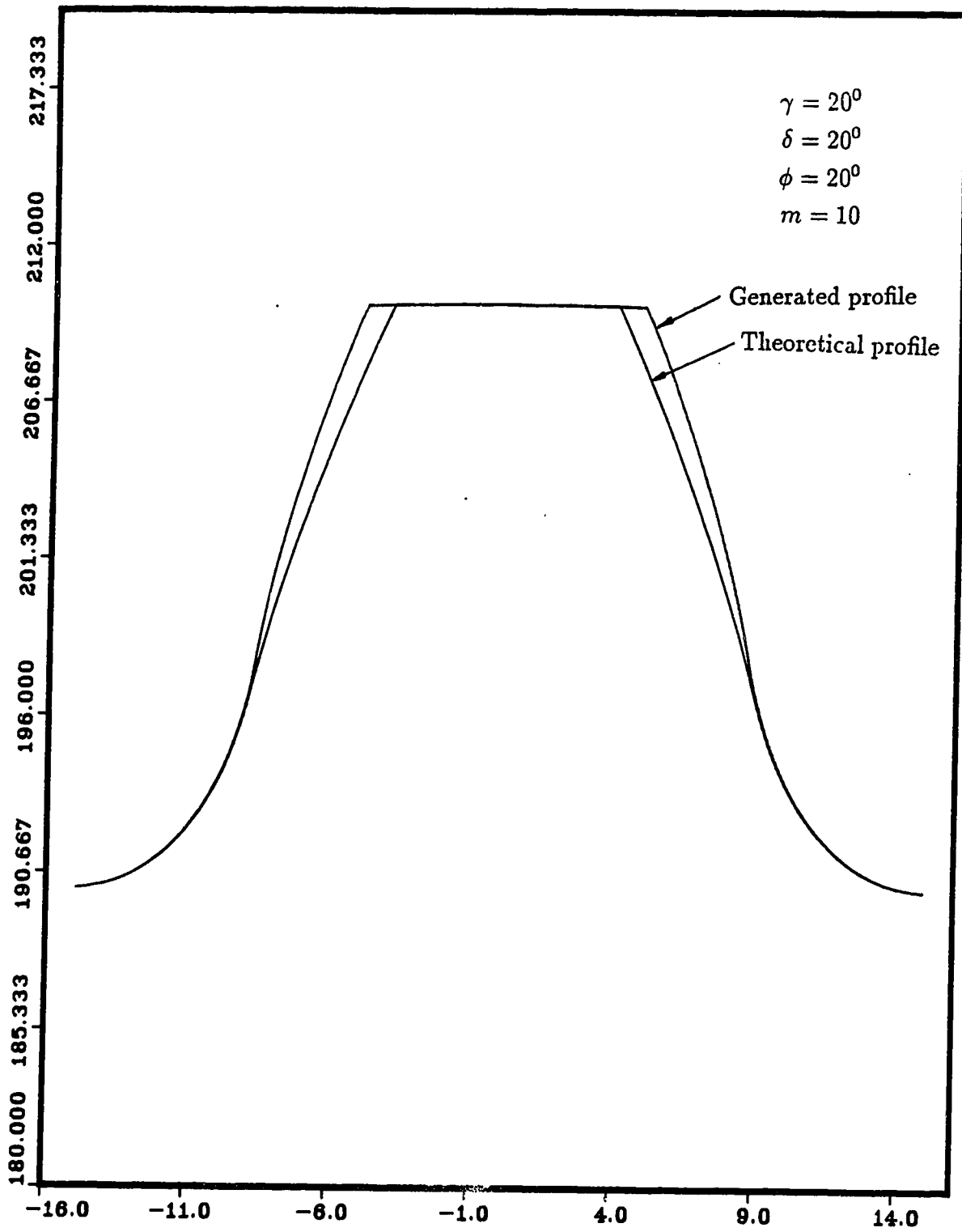


Figure 2.10: Theoretical profile and effective profile on the generated gear

the effective profile of a zero rake angle cutter². The quantitative amount of profile deviation of the cutter, with respect to the theoretical profile, can be conveniently determined, in the following two ways:

1. Measuring the deviation of each point on the theoretical profile, in the direction normal to the profile at that point,
2. Measuring the change in tooth thickness, at each point of the profile, due to the deviation.

2.6 Measure of normal deviation in cutter profile

The deviation in the involute profile can be measured as the distance of the effective profile from the theoretical profile, in a direction normal to the theoretical involute profile [22]. The theoretical involute profile is the shifted involute profile at section T-T, passing through the tooth tip of the cutter. As shown in the Figure 2.11, the point $P^A(R_c^A, \theta_c^A)$, on the effective profile, deviates from the theoretical involute profile, by the distance $\overline{P^A P^T}$. Since the involutes on sections A - A and T - T are generated due to the rolling of the line containing points P^T and P^A on the same base circle, the deviation $\overline{P^A P^T}$ can be written as:

$$\begin{aligned} \overline{P^A P^T} &= \overline{P^T C} - \overline{P^A C} \\ &= \text{arc } \widehat{B^T C} - \text{arc } \widehat{B^A C} \end{aligned} \quad (2.25)$$

$$= \Delta\theta R_{bc} \quad (2.26)$$

²If either the rake or the relief angle is zero, the effective profile would be the same as the theoretical profile. From a practical point of view, with the use of carbide or ceramic tool materials, it might be possible to do away with the rake angle but a certain amount of relief angle will always be needed.

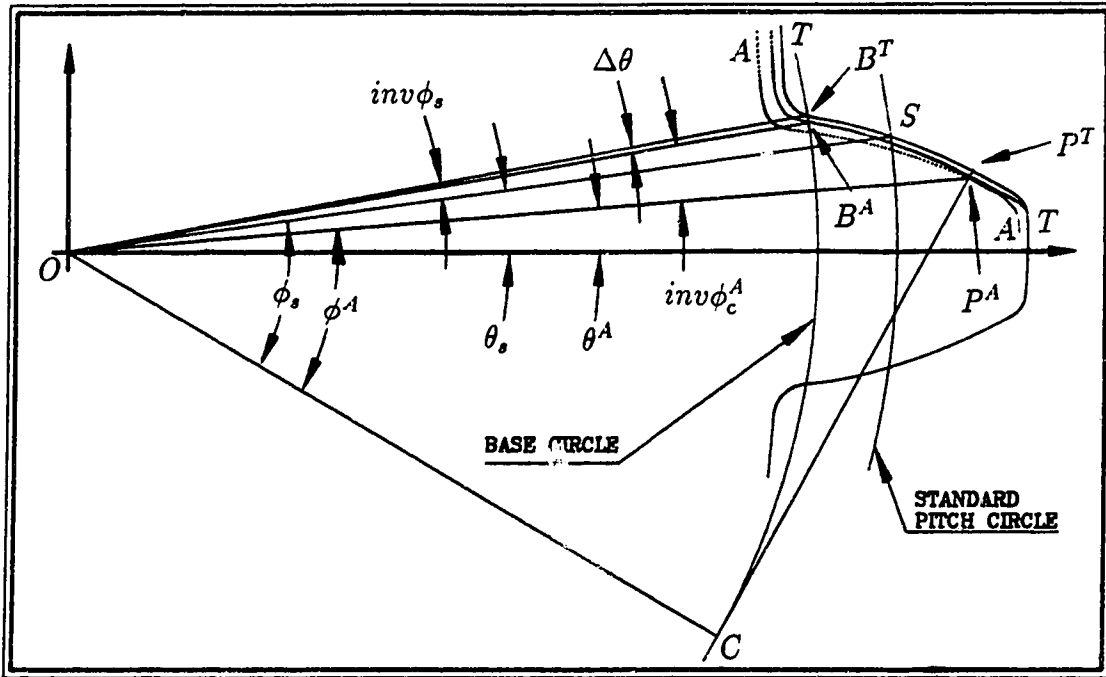


Figure 2.11: Measure of normal profile deviation of cutter.

Hence the normal deviation at any point on the profile is equal to half the difference of the tooth thicknesses at the base circle between the theoretical profile and the shifted involute profile passing through that point. The angle subtended by arc $B^T B^A$ at the centre of the cutter is given by,

$$\Delta\theta = \theta_s + \text{inv}\phi_s - (\theta_c^A + \text{inv}\phi_c^A) \quad (2.27)$$

where,

$$\theta_s = \frac{t_{sc}^T}{2R_{sc}} = \frac{t_{sc}^D + 2e^T \tan \phi_s}{2R_{sc}} \quad (2.28)$$

where e^T is the profile shift of the tooth tip,

$$e^T = b \tan \delta \quad (2.29)$$

$$\text{and} \quad \cos \phi_c^A = \frac{R_{bc}}{R_c^A} \quad (2.30)$$

Combining equation 2.27, 2.28, 2.29 and 2.30, the deviation of point P^A can be written as a function of section distance "a",

$$\Delta P_c(R_c^A, \theta_c^A) = \left\{ \frac{t_{tc}^D + 2b \tan \delta \tan \phi_s}{2R_{sc}} + inv \phi_s - \theta_c^A - inv \cos^{-1} \left(\frac{R_{bc}}{R_c^A} \right) \right\} R_{bc} \quad (2.31)$$

Normal deviation of the generated gear is obtained by inserting corresponding values in equation 2.27,

$$\Delta P_g(R_g, \theta_g) = \left\{ \frac{t_{tg}}{2R_{sg}} + inv \phi_s - \theta_g - inv \cos^{-1} \left(\frac{R_{bg}}{R_g} \right) \right\} R_{bc} \quad (2.32)$$

Taking various points along the tooth profile the corresponding deviations can be found as illustrated in the Figure 2.12. The amount of normal deviation depends upon the rake and relief angles, and as well as on the tooth size (m). The normal deviations in the generated gear are plotted in figure 2.13.

2.7 Variation in tooth thickness

To estimate the amount of deviation in the generated gear profile, it is convenient to determine the change in tooth thickness at various points on the effective profile, with respect to the theoretical tooth thickness at that point. The deviation in tooth thickness of the effective profile, from the theoretical profile (zero rake angle) is evaluated for various radii as follows:

At any radius R_c^A , the tooth thickness of the effective profile, from equation 2.18, will be,

$$\begin{aligned} t_c^A &= 2R_c^A \theta_c^A \\ &= 2R_c^A \left\{ \frac{t_{sc}^A}{2R_{sc}} + inv \phi_s - inv \phi_c^A \right\} \end{aligned} \quad (2.33)$$

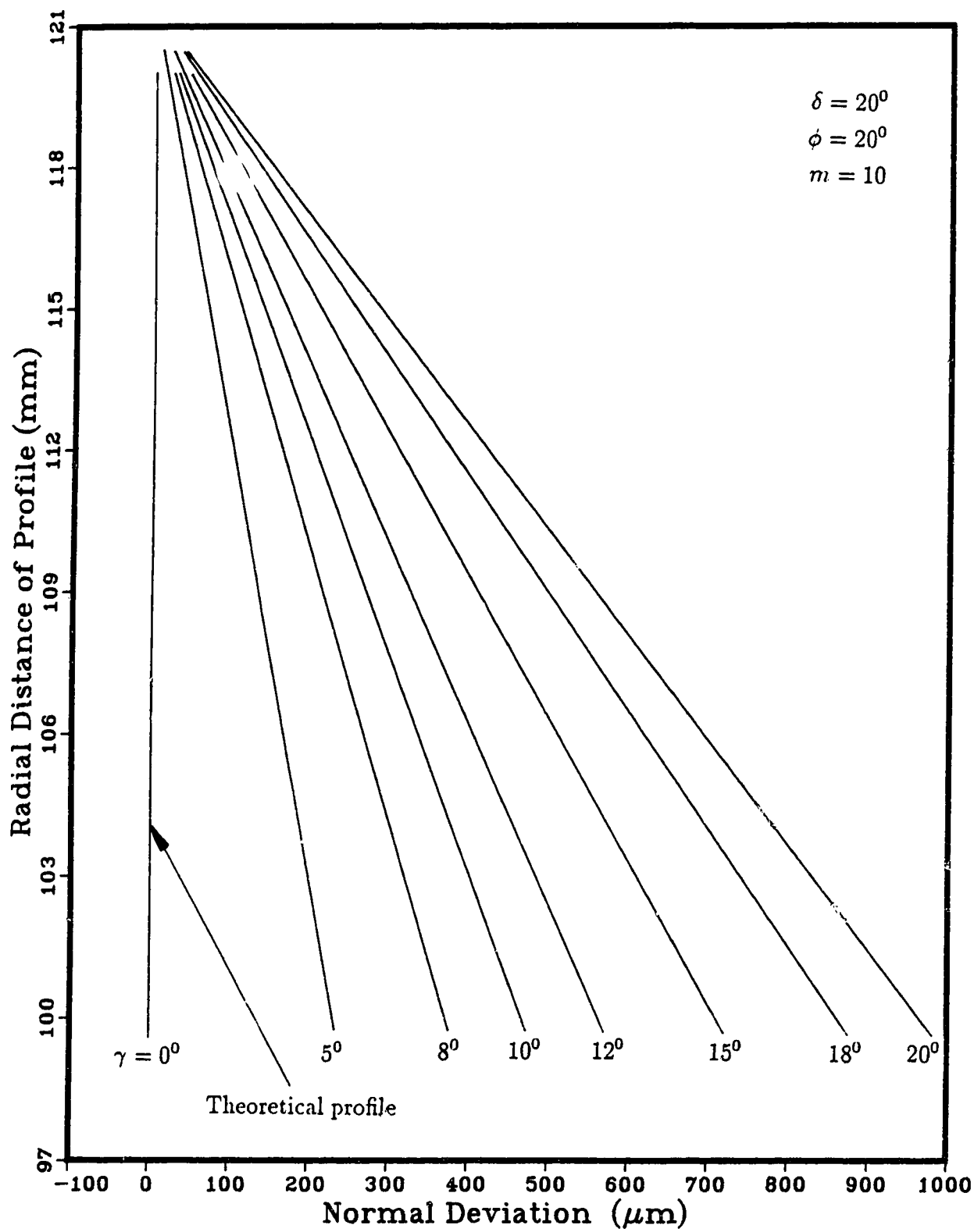


Figure 2.12: Normal deviation of effective profiles of cutter

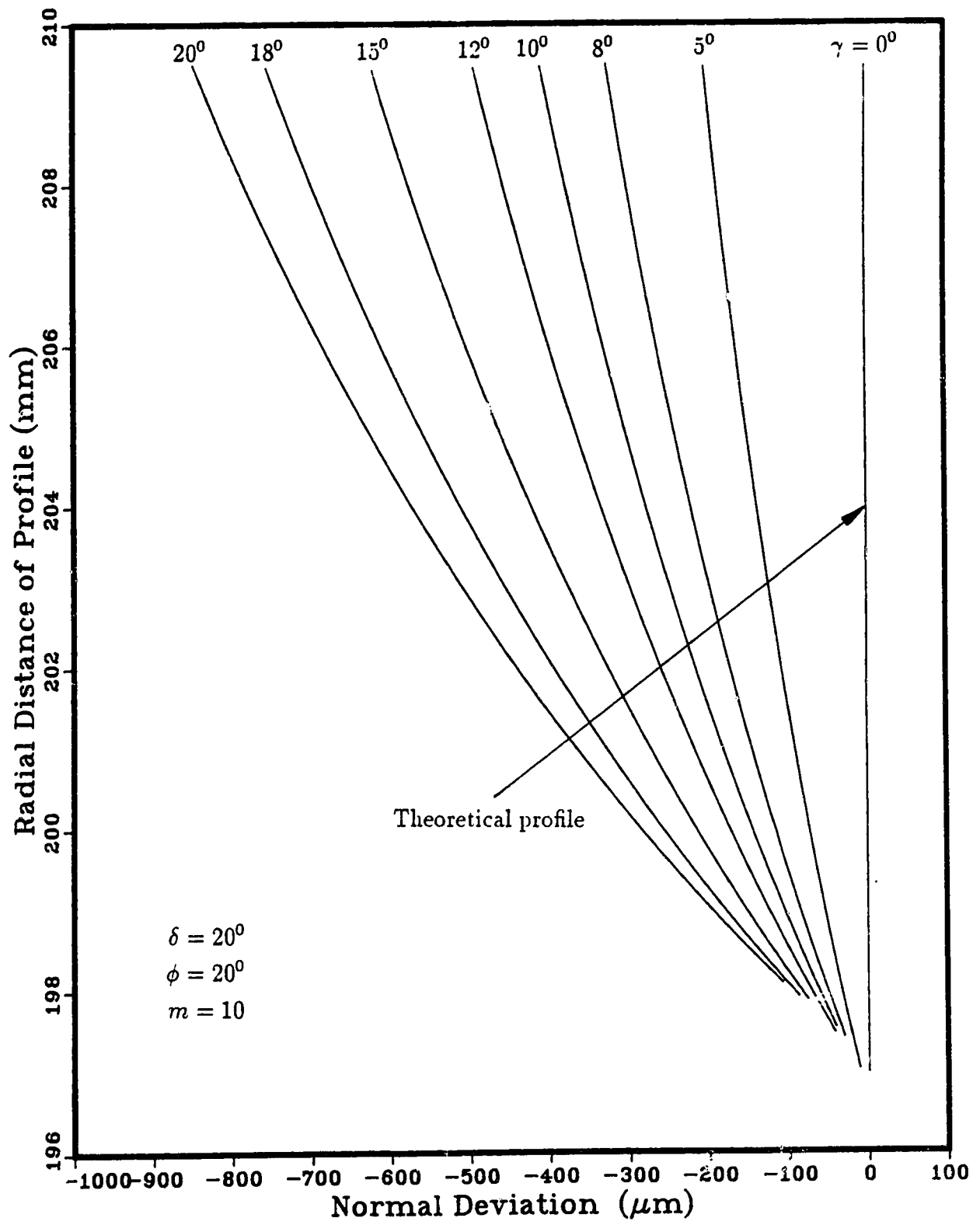


Figure 2.13: Normal deviation of generated gear profiles

At a radius R_c^A , the theoretical profile which is the involute profile at section T-T, when $a = b$, the cutter will have a tooth thickness of (Appendix A-2):

$$\begin{aligned} [t_c^A]^{th} &= 2R_c^A \theta_c^T \\ &= 2R_c^A \left\{ \frac{t_{sc}^T}{2R_{sc}} + \text{inv}\phi_s - \text{inv}\phi_c^T \right\} \end{aligned} \quad (2.34)$$

But, ϕ_c^A , the profile angle on the shifted profile corresponding to profile A-A and ϕ_c^T , the profile angle on the theoretical involute profile, are equal, because they are profile angles at the same radius vector R_c^A , and are given by,

$$\phi_c^T = \phi_c^A = \cos^{-1} \left(\frac{R_{bc}}{R_c^A} \right) \quad (2.35)$$

Hence combining (2.13), (2.33), (2.34), and (2.35), the deviation in tooth thickness, at a radius R_c^A , for the effective profile is obtained.

$$\begin{aligned} \Delta t_c(R_c^A) &= [t_c^A]^{th} - t_c^A \\ &= 2R_c^A \left(\frac{t_{sc}^T - t_{sc}^A}{2R_{sc}} \right) \\ &= 2R_c^A \left(\frac{2(b-a) \tan \delta \tan \phi_s}{2R_{sc}} \right) \\ &= 2R_c^A \left(\frac{R_{tc}^T - R_c^A}{R_{sc}} \right) \tan \gamma \tan \delta \tan \phi_s \end{aligned} \quad (2.36)$$

Thus, the variation of tooth thickness is a quadratic in the radius vector, R_c^A for a fixed tool geometry ($\gamma, \delta, \phi_s = \text{constant}$). Similarly, for the generated gear, the tooth thickness variation at a point $P(R_g, \theta_g)$ is given by,

$$\begin{aligned} \Delta t_g(R_g, \theta_g) &= [t_g(R_g, \theta_g)]^{th} - t_g(R_g, \theta_g) \\ &= 2R_g \left\{ \frac{t_{sg}}{2R_{sg}} + \text{inv}\phi_s - \text{inv} \cos^{-1} \left(\frac{R_{bg}}{R_g} \right) \right\} - 2R_g \theta_g \end{aligned} \quad (2.37)$$

The variation of tooth thickness of the effective profile, compared to the theoretical involute profile, and the variation of tooth thickness of the generated gear profile, with respect to theoretical gear profile are plotted in Figure 2.14 and 2.15.

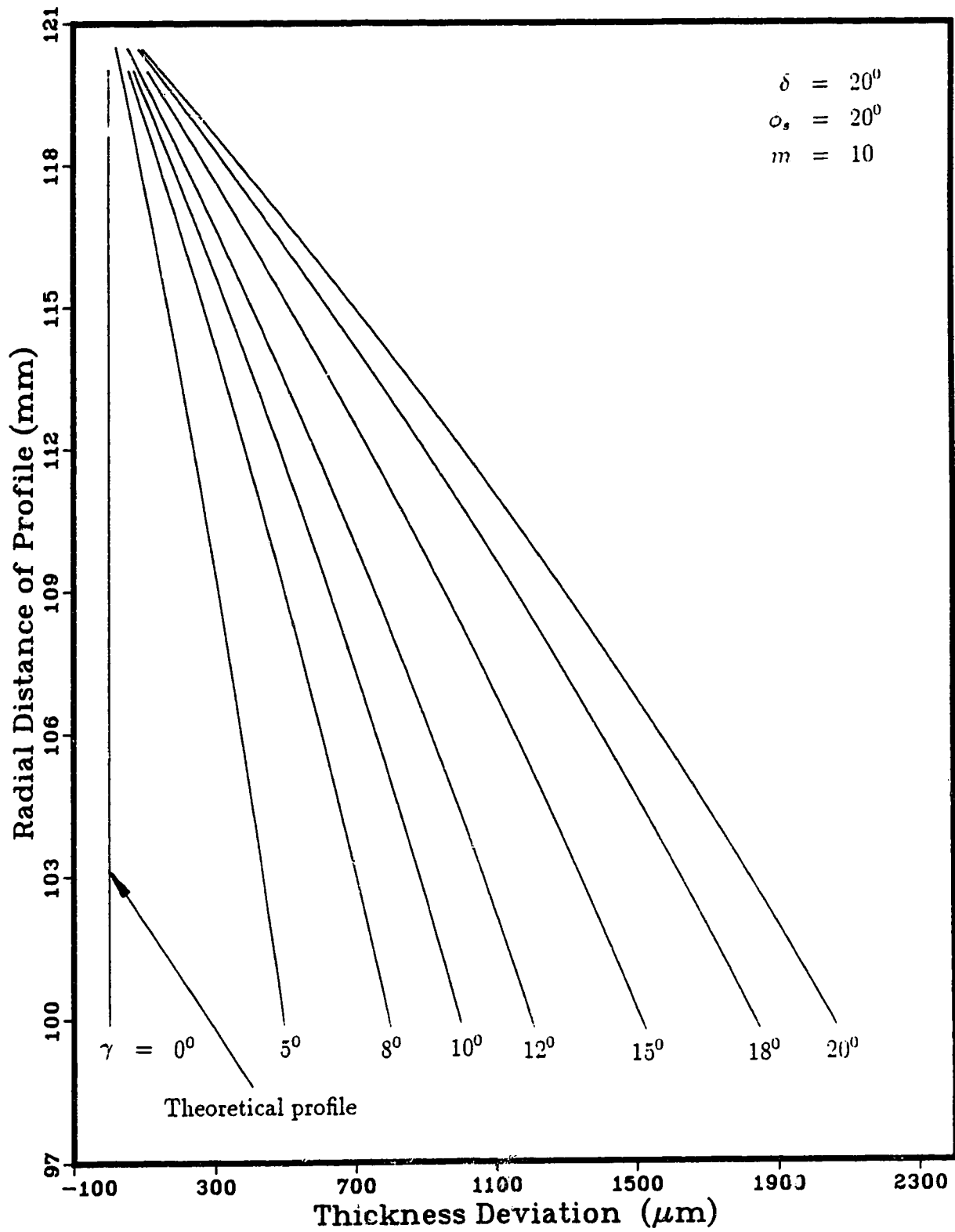


Figure 2.14: Tooth thickness variation of effective profiles of cutter

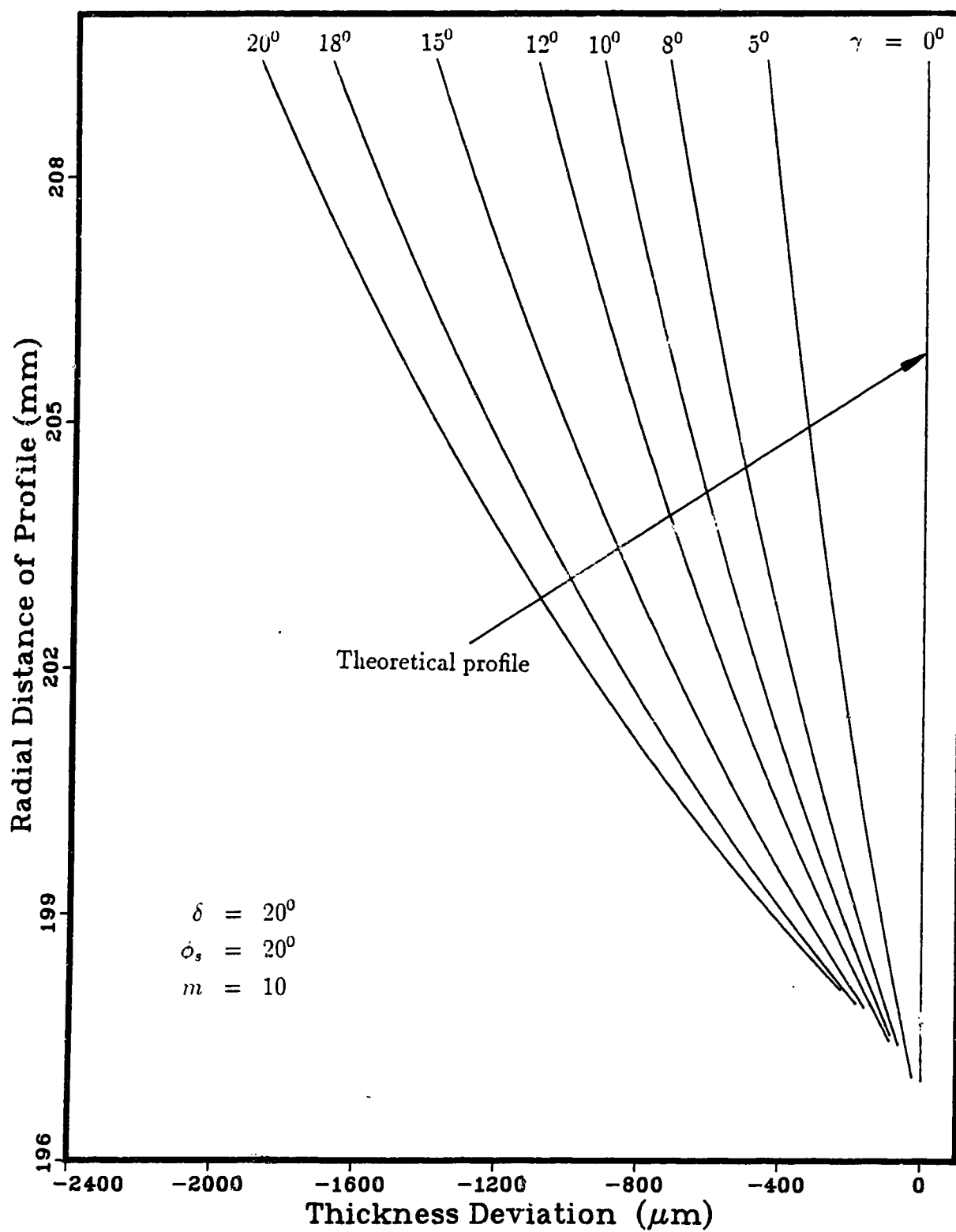


Figure 2.15: Tooth thickness variation of generated gear profiles

2.8 Profile correction methods

Present design practice of pinion cutters gives rise to an inherent profile error as described in the last section. As explained earlier, the side cutting edge of a pinion cutter will not describe a cylindrical involute sweep surface, and this will give rise to a profile deviation in the generated gear. In fact tooth thinning, that occurs in the cutter (Figure 2.8), results in lower tooth thickness and pressure angle when compared to the theoretical profile. The profile error, which increases with the increase in rake and relief angles, can be reduced to some extent, by certain correction methods.

The correction used for the present cutter designs is based on an evaluation of corrected base circle and pressure angle so that after the cutter is generated, with a corrected pressure angle ϕ^{corr} , by a modified basic rack (or grinding wheel), the subsequent grinding of the rake face will lead to the correct pressure angle. Tooth thickness can be corrected by manufacturing the cutter to a corrected tooth thickness so that the subsequent tooth thinning, that occurs on grinding the rake surface of the gear, would give the required tooth thickness.

It must be pointed out that these corrections can fully eliminate profile deviation only at one selected point, usually the pitch point, since the effective profile does not exactly correspond to an involute profile. At all other points on the profile there will still be varying amounts of profile deviations.

2.9 Pressure angle correction

Let it be assumed that the helicoid surface of the cutter teeth is generated, in the manner explained in section 2.2, with a rack having a pressure angle ϕ^{corr} , so selected that the effective profile (projection of the side cutting edge on projection

plane) of the cutter is tangent to the theoretical profile at the pitch point P, on the standard pitch circle of the cutter. Then this corrected pressure angle ϕ^{corr} , to which the pinion cutter is generated, will give the required pressure angle ϕ_s , at the pitch point, after grinding the conical rake surface.

Figure 2.16 (a) shows the cutter teeth generated by the rack, whose cutting edge is projected on the projection plane, and Figure 2.16 (b) shows the three orthogonal views of the same. A right handed co-ordinate system is selected such that the origin lies at point P (pitch point), on the standard pitch circle of the cutter and the z axis is parallel to the cutter z-axis, while the y-axis passes through the point P, and intersects the axis of the cutter (Figure 2.15 (a)). The unit vectors \hat{i} , \hat{j} , \hat{k} lie along the x, y, and z directions, respectively.

Since the pressure angle of the cutter is the profile angle at the pitch radius (which is the inclination of the tangent at that point to the radius vector), a relation can be found between:

1. the unit vector \widehat{U}_H tangent to the involute at section xy , which accounts for the corrected theoretical pressure angle ϕ^{corr} , and
2. the unit vector \widehat{U}_R , tangent to the resultant curve on the projected plane, which accounts for the effective pressure angle ϕ_s .

To relate the above two angles, we also have to consider the relation of the above two vectors with the following:

1. the helicoid form of the side surface, accounted for by a unit vector tangent to this surface \widehat{U}_S , and
2. the rake angle by which the cutting edge is inclined, accounted for by selecting

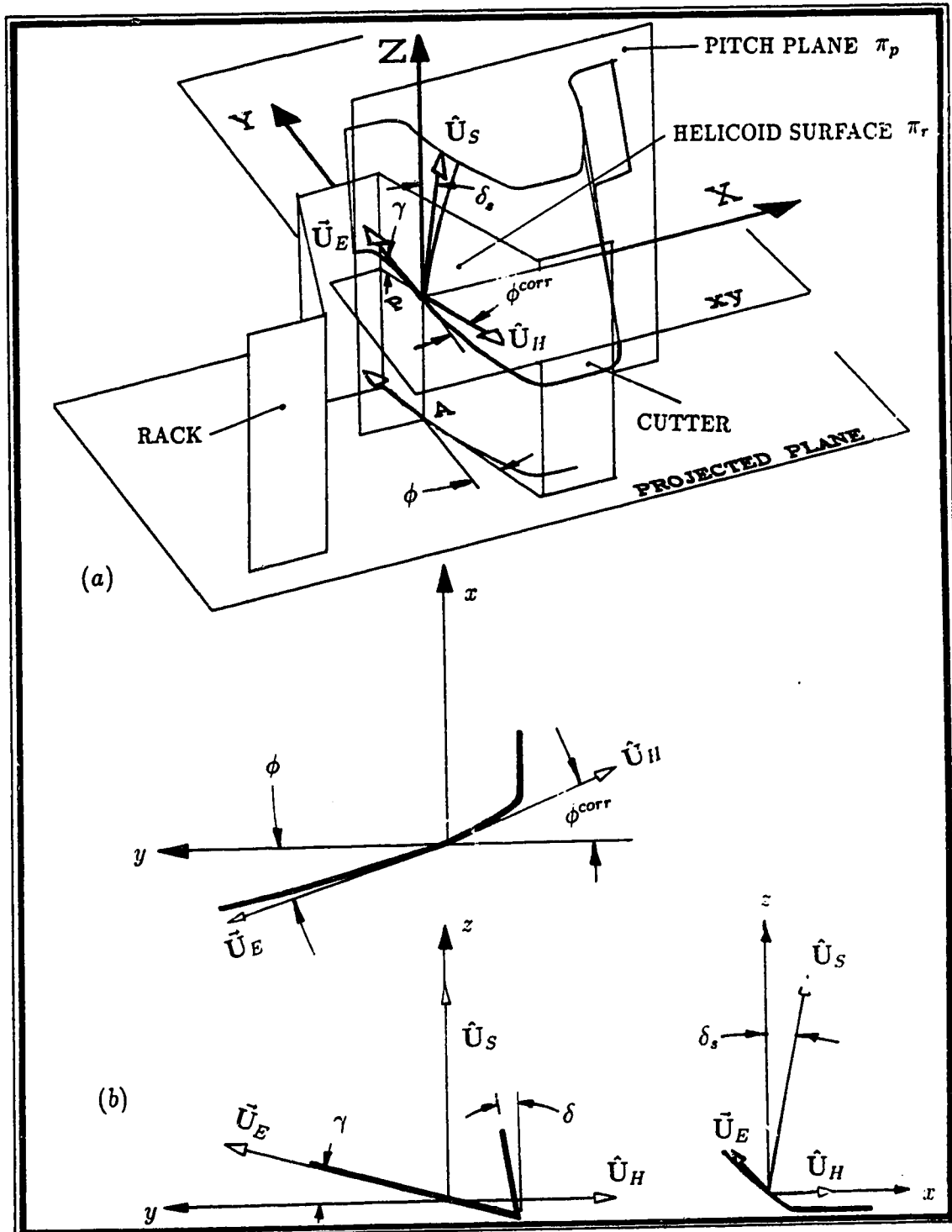


Figure 2.16: Pressure angle correction method

a vector \vec{U}_E , lying on the cutting edge, so that its projection on the projection plane is parallel to vector \widehat{U}_R .

In Figure 2.16 (a) The surface π_r forms the side helicoid surface of the pinion cutter. The pitch plane π_p , which passes through the pitch point P, cuts the pinion cutter surface π_r in a curve, tangent to which lies the unit vector \widehat{U}_S , at the pitch point. Therefore, U_S contacts the helicoid surface π_r at an angle δ , as shown in the elevation in Figure 2.16 (b). Also from equation 2.10,

$$\tan \delta_s = \tan \delta \tan \phi^{corr} \quad (2.38)$$

From the side view, Figure 2.16 (b), the orthogonal components of \widehat{U}_S can be found.

$$\widehat{U}_S = \sin \delta_s \hat{i} + \cos \delta_s \hat{k} \quad (2.39)$$

The horizontal plane “xy” cuts the cutter teeth surface π_r in a curve, tangent to which lies unit vector \widehat{U}_H , at the pitch point. Referring to the plan view, in Figure 2.16 (b), the unit vector \widehat{U}_H can be written as,

$$\widehat{U}_H = \sin \phi^{corr} \hat{i} - \cos \phi^{corr} \hat{j} \quad (2.40)$$

A third vector \vec{U}_E , is tangent to the cutting edge through point P, and can be written as [fig 2-16 (b), elevation],

$$\widehat{U}_E = -\sin \phi_s \hat{i} + \cos \phi_s \hat{j} + \cos \phi_s \tan \gamma \hat{k} \quad (2.41)$$

All the three vectors \widehat{U}_S , \widehat{U}_H and \vec{U}_E are drawn through the same point, and are tangent to curves lying on same helicoid surface, π_r . Therefore, they are co-planer and their mixed vector product will be equal to zero.

$$\widehat{U}_S \cdot \widehat{U}_H \times \vec{U}_E = 0 \quad (2.42)$$

or,

$$\begin{vmatrix} \sin \delta_s & 0 & \cos \delta_s \\ \sin \phi^{corr} & -\cos \delta^{corr} & 0 \\ -\sin \phi_s & \cos \phi_s & \cos \phi_s \tan \gamma \end{vmatrix} = 0 \quad (2.43)$$

Dividing the 1st, 2nd and 3rd rows by $\cos \delta_s$, $\cos \phi^{corr}$, and $\cos \phi_s$ respectively,

$$\begin{vmatrix} \tan \delta_s & 0 & 1 \\ \tan \phi^{corr} & -1 & 0 \\ -\tan \phi_s & 1 & \tan \gamma \end{vmatrix} = 0 \quad (2.44)$$

$$\text{or,} \quad \tan \phi^{corr} = \frac{\tan \phi_s}{1 - \tan \delta \tan \gamma} \quad (2.45)$$

Hence a cutter that has to have a pressure angle ϕ_s should be manufactured to a corrected pressure angle $\left(\tan^{-1} \frac{\tan \phi_s}{1 - \tan \delta \tan \gamma}\right)$ before the rake angle is ground. However, this ensures that correct pressure angle is obtained only at the pitch point. At all other points on the effective profile, the profile angle deviates from that required by the theoretical value, at that point.

In case of corrected cutters, the standard pitch circle is sometimes very close to the root circle which makes it necessary to choose a corrected pressure angle such that the effective profile is tangent to the theoretical profile at a point lying at an optimal radius ($R_{opt} > R_{sc}$). A suitable value of R_{opt} may be the average radius of the tip and root circles:

$$R_{opt} = \frac{R_{tc} + R_{rc}}{2} \quad (2.46)$$

When the effective profile is tangent to the theoretical profile at the optimal radius then the profile angle and the corrected profile angle at this radius will be,

$$\phi_{R_{opt}} = \cos^{-1} \frac{R_{bc}}{R_{opt}} \quad (2.47)$$

$$\phi_{R_{opt}}^{corr} = \tan^{-1} \frac{\tan \cos^{-1} \left(\frac{R_{bc}}{R_{opt}} \right)}{1 - \tan \delta \tan \gamma} \quad (2.48)$$

Therefore, in such cases, the corrected pressure angle ϕ^{corr} will be,

$$\phi^{corr} = \cos^{-1} \left\{ \frac{R_{opt}}{R_{sc}} \cdot \cos \tan^{-1} \frac{\tan \cos^{-1} \left(\frac{R_{bc}}{R_{opt}} \right)}{1 - \tan \delta \tan \gamma} \right\} \quad (2.49)$$

2.10 Tooth thickness correction

In addition to ϕ^{corr} , a corresponding corrected tooth thickness t^{corr} , can be selected to give the required tooth thickness, at the pitch point, after grinding the rake face. Srinivasan and Shunmugam [22] suggest that the same corrections, as applied to a rack cutter, can be applied to the pinion cutter. Unlike the pressure angle correction, the effect of tooth thickness correction on the shape of generated gear profile is only marginal, as will be evident from this section.

2.10.1 Method I of tooth thickness correction

In this method the value of t^{corr} is unchanged and equal to t_{sc}^D but since a modified pressure angle ϕ^{corr} , is chosen the cutter tooth thickness t_{sc} before grinding the rake face ($= t_{sc}^T$) will be greater.

$$t^{corr} = t_{sc}^D \quad (2.50)$$

$$t_{sc} = t_{sc}^D + 2e^T \tan \phi^{corr} = t_{sc}^D + 2\chi m \tan \phi^{corr} \quad (2.51)$$

where, $e^T =$ profile shift of the tip section $T - T$, and
 $\chi = e^T/m =$ profile shift coefficient.

Here we obtain an effective profile which deviates from the theoretical profile depending upon the number of teeth and the profile shift coefficient $\chi(\chi = e^T/m)$, which indicates that not only is there a certain amount of profile deviation, but also that the deviation varies throughout the cutter life. Cutter life depends on the total usable width of the cutter, which governs the maximum possible number of resharpenings before disposing of the cutter. (Chapter 4 discusses more on the effect of resharpening on cutters.) The resultant profile after applying this correction value is shown in Figure 2.17 and Figure 2.18.

2.10.2 Method II of tooth thickness correction

Let the modified cutter be manufactured with the standard tooth thickness at the design section of t_{sc}^{corr} , and modified pressure angle ϕ^{corr} , so that the tooth thickness of the effective profile at a radius R_{sc} is equal to required tooth thickness t_{sc} . Then to find the value of the section distance "a", for which the radius of intersecting circle (of sectional plane with rake cone) R_c^A is equal to R_{sc} , we use equation 2.16 and 2.17.

$$R_c^A = R_{sc} + h_a^D + b \tan \delta - \frac{(b - a)}{\tan \gamma} \quad (2.52)$$

When $R_c^A = R_{sc}$, the value of "a" will be,

$$a = (1 - \tan \delta \tan \gamma) b - h_a^D \tan \gamma \quad (2.53)$$

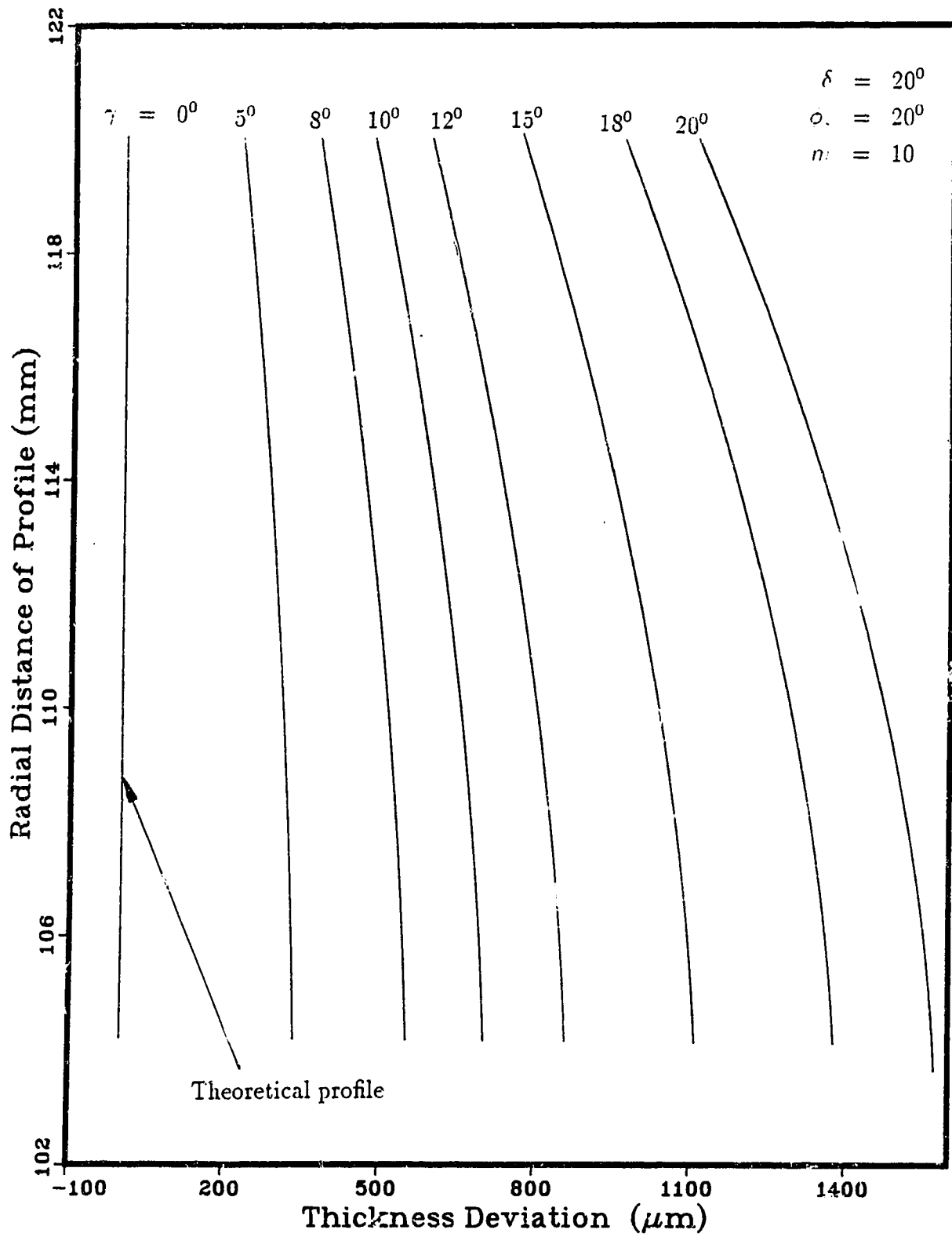


Figure 2.17: Cutter profile thickness deviations on using correction method I

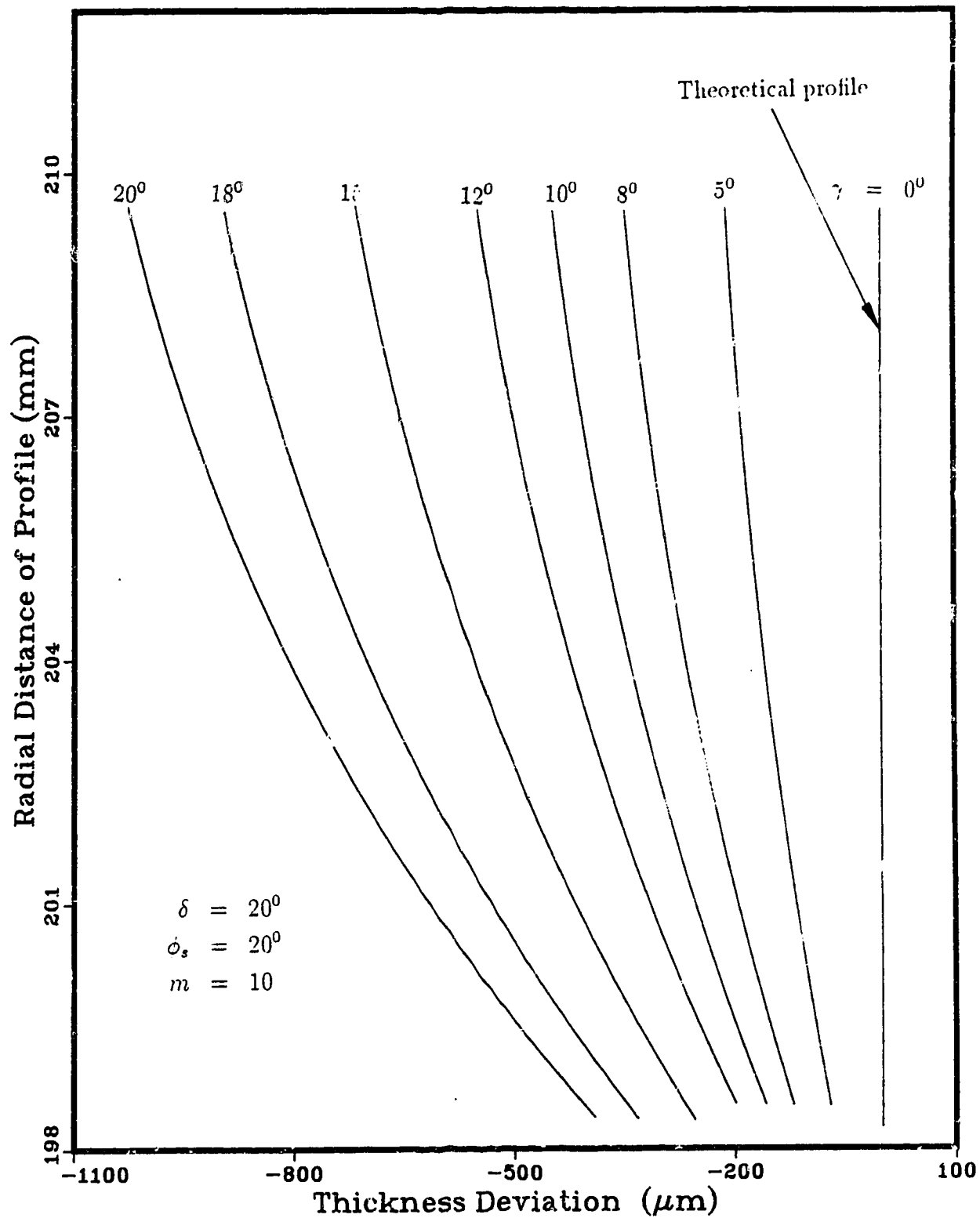


Figure 2.18: Generated gear profile thickness deviations on using cutter correction method I

where “ b ” is the design distance when the cutter is new. If the tooth thickness, at this value of “ a ”, is the required tooth thickness, then

$$t_{sc}^T = t_{sc}^{corr} + 2a \tan \delta \tan \phi^{corr} \quad (2.54)$$

where,

$$t_{sc}^T = t_{sc}^D + 2b \tan \delta \tan \phi_s$$

Hence, the corrected tooth thickness at the design section should be,

$$\begin{aligned} t_{sc}^{corr} &= t_{sc}^T - 2(1 - \tan \delta \tan \gamma) b \tan \delta \tan \phi^{corr} + 2h_a^D \tan \gamma \tan \delta \tan \phi^{corr} \\ &= t_{sc}^D - 2\chi m (\tan \phi^{corr} - \tan \phi_s) + 2(\chi m - h_a^D) \tan \gamma \tan \delta \tan \phi^{corr} \quad (2.55) \end{aligned}$$

where b is the design distance and χ is the profile coefficient when the cutter is new.

The cutter tooth thickness before grinding the rake face cone is,

$$\begin{aligned} t_{sc} &= t_{sc}^{corr} + 2\chi m \tan \phi^{corr} \\ &= t_{sc}^D + 2\chi m \tan \phi_s + 2(\chi m + h_a^D) \tan \gamma \tan \delta \tan \phi^{corr} \quad (2.56) \end{aligned}$$

The correction values are tabulated in Appendix B and the cutter and gear profile deviation after applying this correction is shown in Figures 2.19 and 2.20 respectively. Figure 1.21 shows the effect of pressure correction and tooth thickness correction (both methods) for a single case for comparison.

The above choice of t_{sc}^{corr} at the design section will give an effective tooth thickness near to the correct tooth thickness of t_{sc} , when the cutter is new. After regrinding the cutter, the tooth thickness will continue reducing until it becomes t_{sc}^{corr} when,

$$b = \frac{h_a^D \tan \gamma}{1 - \tan \gamma \tan \delta} \quad [\text{put } a=0 \text{ in 2.47}]$$

which is the design distance when the rake surface cuts the design section plane at the circle of intersection of R_{sc} . Below $b = \frac{h_a^D \tan \gamma}{1 - \tan \gamma \tan \delta}$, the tooth thickness will reduce still further until it reaches the end of the cutter life.

However, since the cutter can always be fed further into the gear blank, (by reducing the cutter centre distance), when the tooth thickness reduces on resharping, the choice of tooth thickness correction is not very important. Different tooth thickness corrections will, therefore, generate almost the same gear tooth profile as can also be seen from the effect of different cutter tooth corrections (Figure 2.21) on the generated gear shape (Figure 2.22). If the cutter tooth thickness is left uncorrected the only eventuality is that for the value of $b = \frac{h_a^D \tan \gamma}{1 - \tan \gamma \tan \delta}$, the tooth thickness will be exactly as specified at the design section, but for:

$$b > \frac{h_a^D \tan \gamma}{1 - \tan \gamma \tan \delta}, \text{ the tooth thickness will be greater than } t_{sc}, \text{ and}$$

$$b < \frac{h_a^D \tan \gamma}{1 - \tan \gamma \tan \delta}, \text{ the tooth thickness will be less than } t_{sc}.$$

2.11 Determination of value of design distance

The choice of the value of the design distance “ b ”, is very important because it affects the following factors:

1. The increase in distance “ b ” raises the possible number of resharpings, and hence the total life of the cutter.
2. The increase in distance “ b ”, however, leads to sharper tooth tips and increases the possibility of interference of the profile with the corner transitional curves.
3. As “ b ” increases, the tooth thickness of the tooth tip decreases which increasingly weakens it.

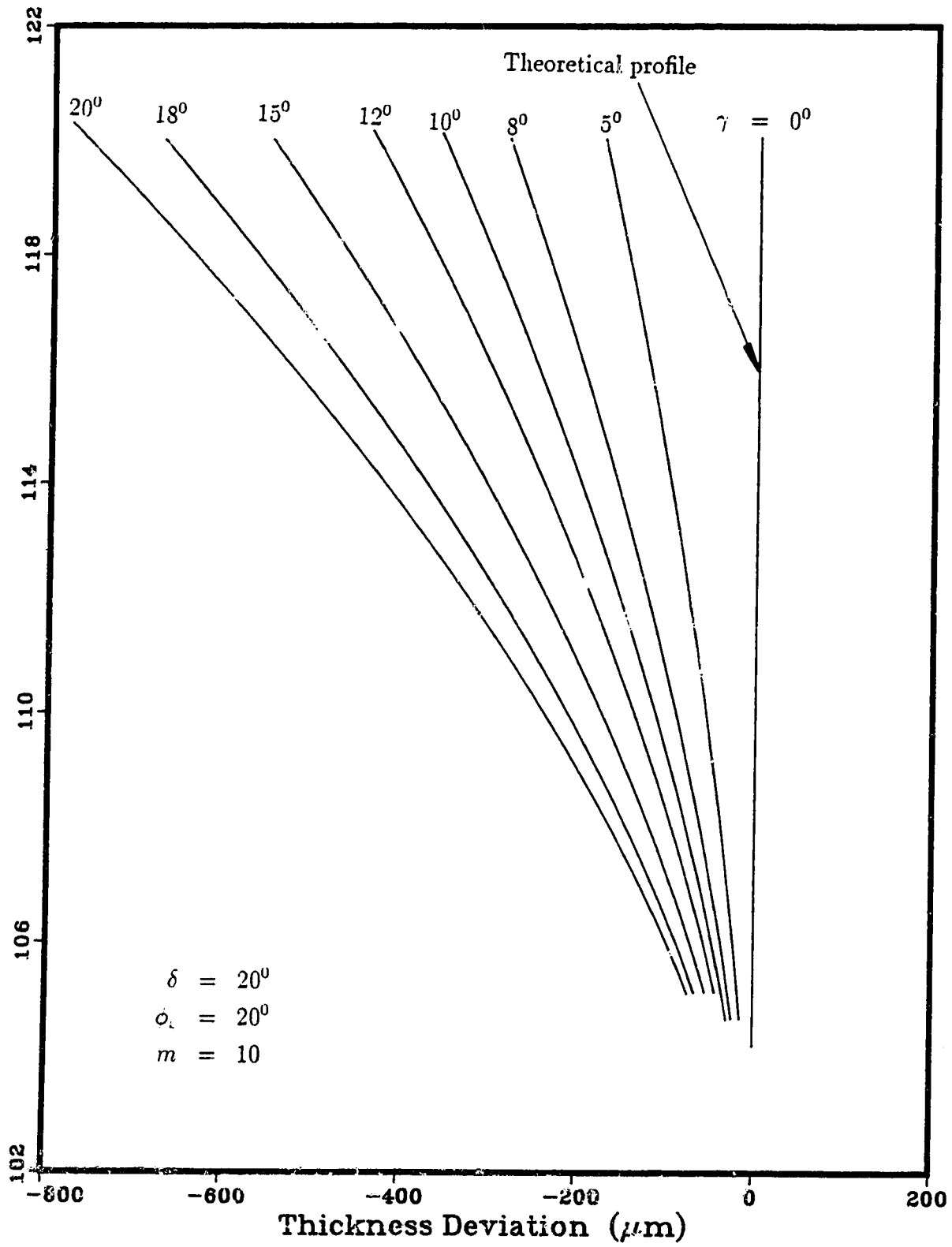


Figure 2.19: Resultant cutter thickness deviations on using correction Method II

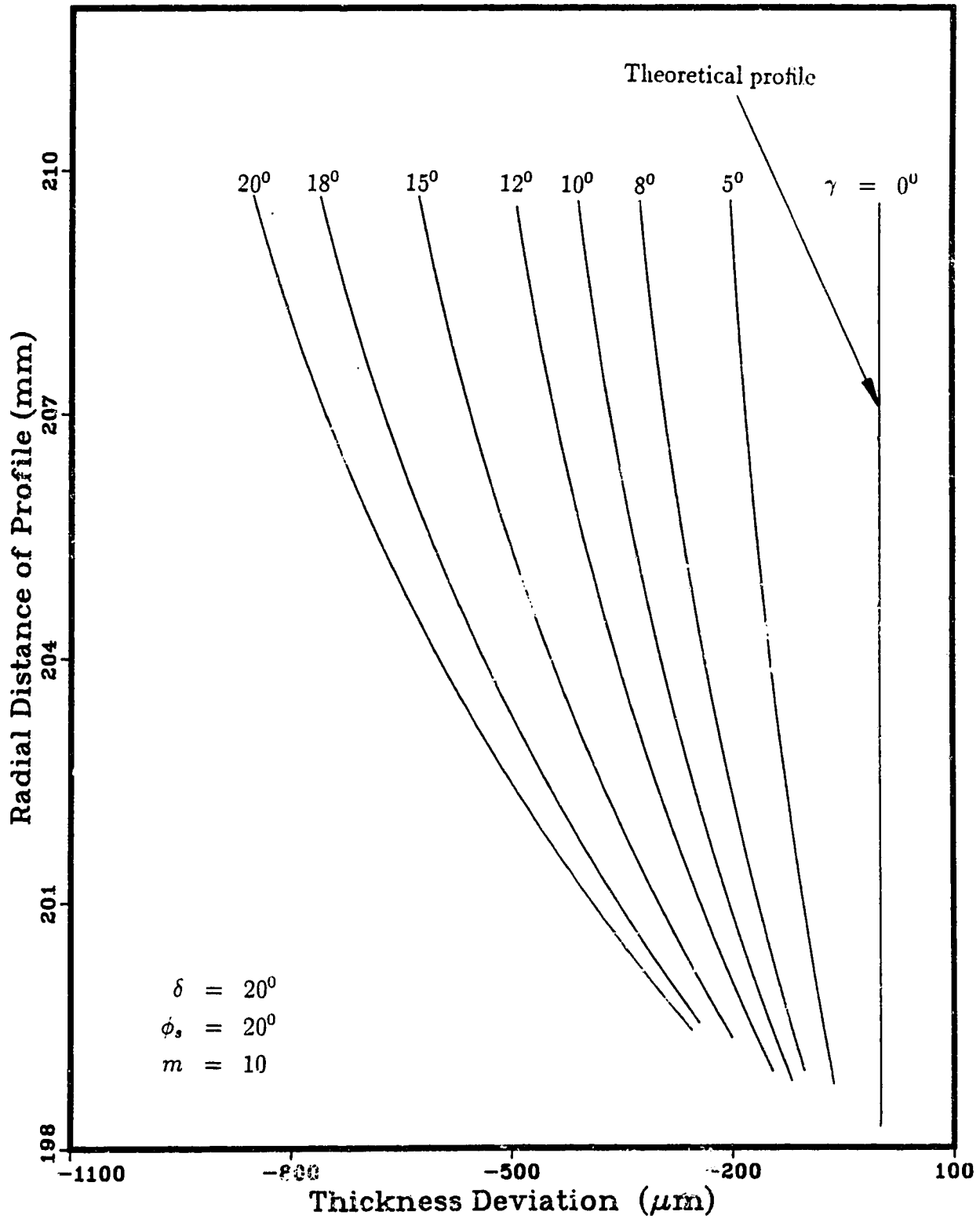


Figure 2.20: Generated gear profile thickness deviations on using cutter correction method II

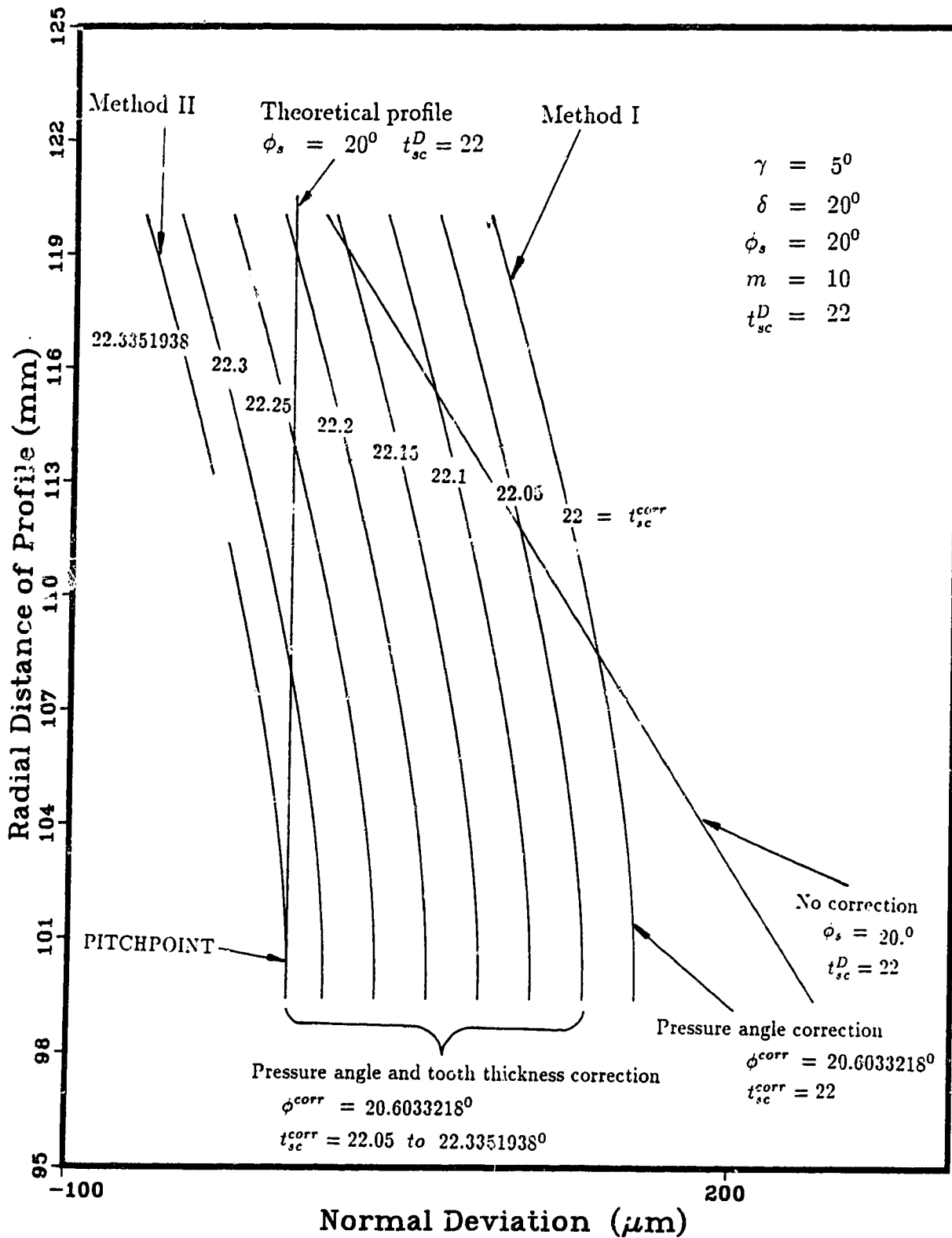


Figure 2.21: Effect of pressure angle and tooth thickness corrections

Since the front tip cutting edge is subject to the highest loads during gear cutting, and consequently the most intense wear, the criterion for determining “ b ” is to obtain sufficient tooth thickness at the tooth tip, while attempting, on the other hand, to increase the total tool life by increasing “ b ”. Normally, this permissible value of tooth thickness at the tooth tip varies from 0.5 to 1.5mm for standard shaping cutters with a module of 1 to 8mm [18]. It must be noted that, while the value of “ b ” is limited by a number of factors, the usual recommendation is to determine “ b ” based on the tooth tip thickness.

2.12 Graphical method

The value of “ b ” cannot be determined by purely analytical procedures, and therefore, a graphical method is usually employed. From equation 2.13, the standard tooth thickness of the cutter, on any arbitrary section A-A, at a section distance of “ a ”, is given by (Figure 2.6),

$$t_{sc}^A = t_{sc}^D + 2a \tan \delta \tan \phi_s \quad (2.57)$$

Hence the standard tooth thickness, t_{sc}^T , at the tooth tip section T-T (which is at a section distance of “ b ” = the design distance), will be, for uncorrected cutters,

$$t_{sc}^T = t_{sc}^D + 2b \tan \delta \tan \phi_s \quad (2.58)$$

The angle θ_{tc}^T , for the tooth tip, of cutter at section T-T can be obtained from equation (2.18),

$$\theta_{tc}^T = \frac{t_{sc}^T}{2R_{sc}} + \text{inv} \phi_s - \text{inv} \phi_{tc}^T \quad (2.59)$$

where,

$$\cos \phi_{tc}^T = \frac{R_{sc} \cos \phi_s}{R_{tc}^T} \quad (2.60)$$

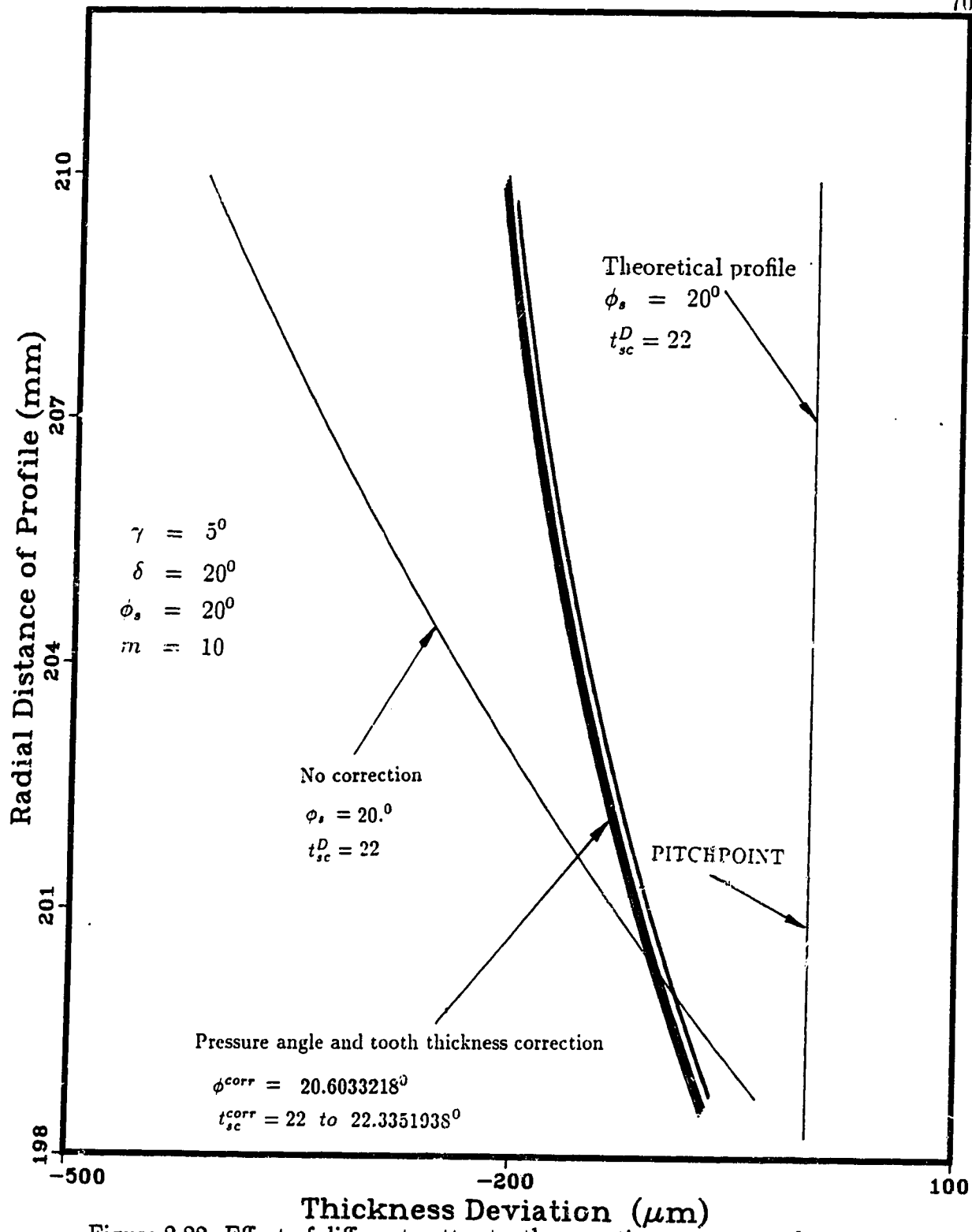


Figure 2.22: Effect of different cutter tooth correction on generated gear profile

From equation 2.17, the radius R_{tc}^T of the tip circle at section $T - T$ is equal to,

$$R_{tc}^T = R_{sc} + h_a^D + b \tan \delta \quad (2.61)$$

where h_a^T , the addendum with respect to standard pitch circle, is given by,

$$h_a^T = h_a^D + b \tan \delta \quad (2.62)$$

The tooth thickness at the tooth tip is,

$$\begin{aligned} t_{tc}^T &= 2R_{tc}^T \theta_{tc}^T \\ &= 2R_{tc}^T \left(\frac{t_{sc}^T}{2R_{sc}} + \text{inv} \phi_s - \text{inv} \phi_{tc} \right) \end{aligned} \quad (2.63)$$

Substituting from equations 2.57, 2.58, 2.59, 2.60 and 2.53 into equation 2.55, the expression for t_{tc}^T as a function of “ b ”, for non-corrected cutters, will be,

$$\begin{aligned} t_{tc}^T &= 2(R_{sc} + h_a^D + b \tan \delta) \left\{ \frac{t_{sc}^D + 2b \tan \delta \tan \phi_s}{2R_{sc}} \right. \\ &\quad \left. + \text{inv} \phi_s - \text{inv} \cos^{-1} \left(\frac{R_{sc} \cos \phi_s}{R_{sc} + h_a^D + b \tan \delta} \right) \right\} \end{aligned} \quad (2.64)$$

This formidable equation proves rather difficult to solve for “ b ” because of the term containing “ $\text{inv} \cos^{-1}$ ”, and therefore a graphical solution is resorted to, in which, $t_{tc}^T = f(b)$ can be plotted, for a series of values of “ b ”.

For the design distance “ b ”, the profile shift “ e ”, from the design profile (which itself may have an additional profile shift “ e_0 ”) and the profile shift coefficient “ e/m ” are,

$$e = b \tan \delta \quad (2.65)$$

$$\chi = e/m = \frac{b \tan \delta}{m} \quad (2.66)$$

Then the equations 2.60 and 2.64 can be written in terms of “ e ” and “ χ ” as,

$$t_{sc}^T = t_{sc}^D + 2\chi m \tan \phi_s \quad (2.67)$$

$$h_a^T = h_a^D + \chi m \quad (2.68)$$

which clearly indicates that the shape of the cutter teeth is largely influenced by the profile shift coefficient, $\chi (= e/m)$. Therefore, it is more relevant to construct a family of curves relating to parameters t_{ic}^T/m and χ , as shown in Figure 2.23.

For a selected value of t_{ic}^T , the profile shift coefficient is determined from the pertinent curve and then the value of “ b ” is determined by,

$$b = \frac{\chi m}{\tan \delta} \quad (2.69)$$

2.13 Approximate analytical method

The basis of the analytical method [18] is that the reduction in tooth thickness t_{ic}^T , given by Δt_{ic}^T , and the corresponding increase in radius R_{ic}^T , denoted by ΔR_{ic}^T , caused by the increase in design distance “ b ”, can be replaced by dt_{ic}^T and dR_{ic}^T . The substitution of these increments by differentials or vice-versa, is permissible because:

1. Increments are small compared to t_{ic}^T and R_{ic}^T , and the substitution gives small magnitude of error.
2. The value of “ b ” is, in fact, an approximate value varying up to 0.3mm, and therefore the magnitude of error in (1) can be overlooked.

Differentiating the unsuperscripted form of the equation 2.63, to get an expression for the change in parameters between sections,

$$dt_{ic} = 2 dR_{ic} \left(\frac{t_{sc}}{2R_{sc}} + \text{inv}\phi_s - \text{inv}\phi_{ic} \right) + 2R_{ic} \left(\frac{dt_{sc}}{2R_{sc}} - d \tan \phi_{ic} + d\phi_{ic} \right). \quad (2.70)$$

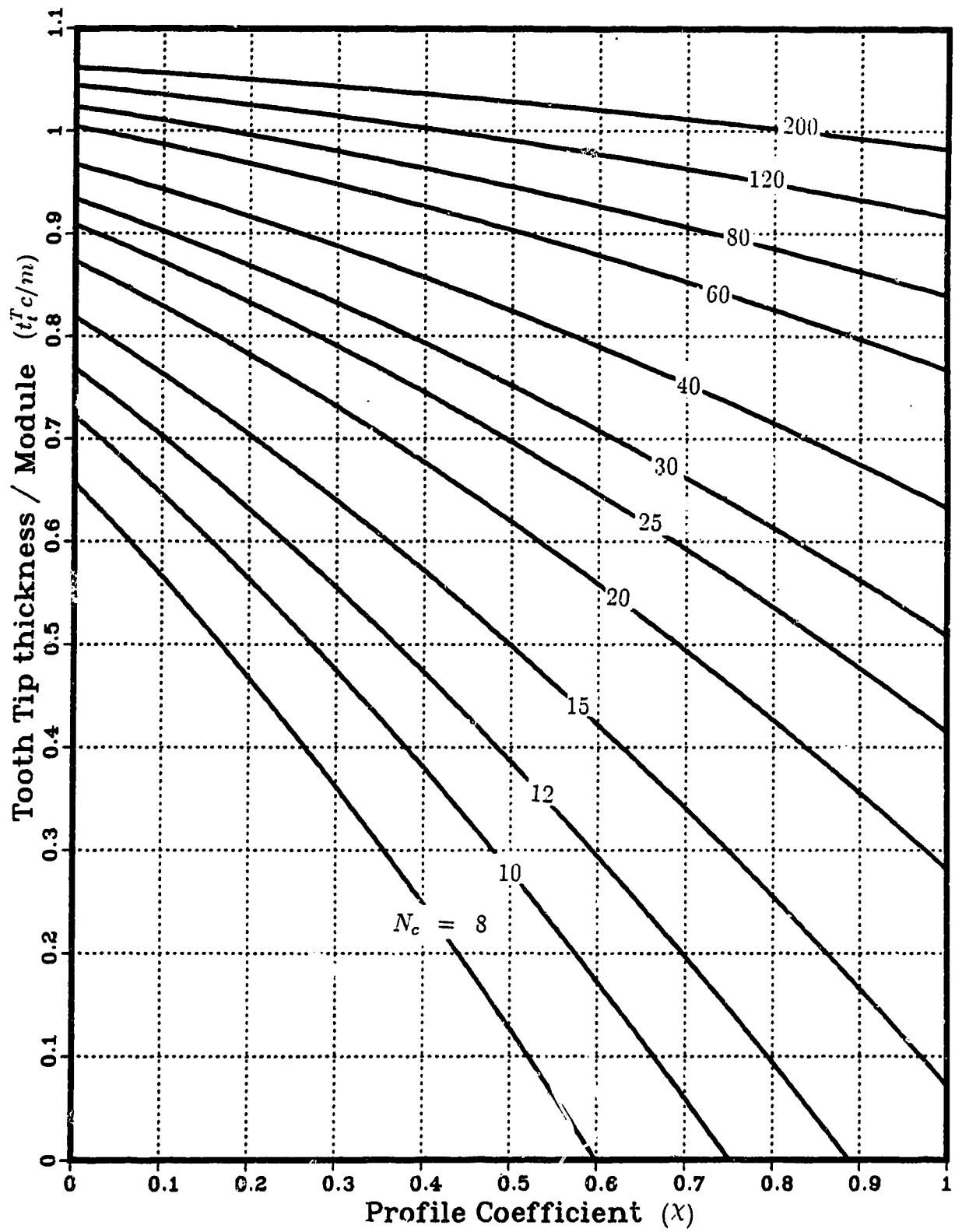


Figure 2.23: Plot of t_{tc}^T/m against χ

Similarly, differentiating the unsuperscripted form of equation 2.60 we get,

$$\begin{aligned}
 -\sin \phi_{tc} d\phi_{tc} &= -\frac{dR_{tc}}{R_{tc}^2} R_{sc} \cos \phi_s \\
 &= -\frac{dR_{tc}}{R_{tc}} \cos \phi_{tc} \quad [\text{from 2.60}] \\
 \text{or, } d\phi_{tc} &= \frac{dR_{tc}}{R_{tc} \tan \phi_{tc}} \quad (2.71)
 \end{aligned}$$

Now replacing the differentials by the corresponding increments (shown in Figure 2.24) we get,

$$\begin{aligned}
 dR_{tc} &= \Delta R_{tc} \\
 &= R_{tc}^T - R_{tc}^D \\
 &= e^T = b \tan \delta
 \end{aligned}$$

$$\begin{aligned}
 dt_{sc} &= \Delta t_{sc} \\
 &= t_{sc}^T - t_{sc}^D \\
 &= 2b \tan \delta_s
 \end{aligned}$$

$$\begin{aligned}
 dt_{tc} &= \Delta t_{tc} \\
 &= t_{tc}^T - t_{tc}^D \\
 &= -(t_{tc}^D - t_{tc}^T) \quad [t_{tc}^D > t_{tc}^T]
 \end{aligned}$$

Substituting the values of the differentials into equation 2.70,

$$-(t_{tc}^D - t_{tc}^T) = 2b \tan \delta \theta_{tc}^D + 2R_{tc}^D \left\{ \frac{2b \tan \delta_s}{2R_{sc}} - \tan^2 \phi_{tc} d\phi_{tc} \right\}^D \quad (2.72)$$

Combining the above we get,

$$-(t_{tc}^D - t_{tc}^T) = \frac{b \tan \delta}{R_{tc}^D} t_{tc}^D + \frac{2b R_{tc}^D \tan \delta_s}{2R_{sc}} - 2b \tan \delta \tan \phi_{tc}^D$$

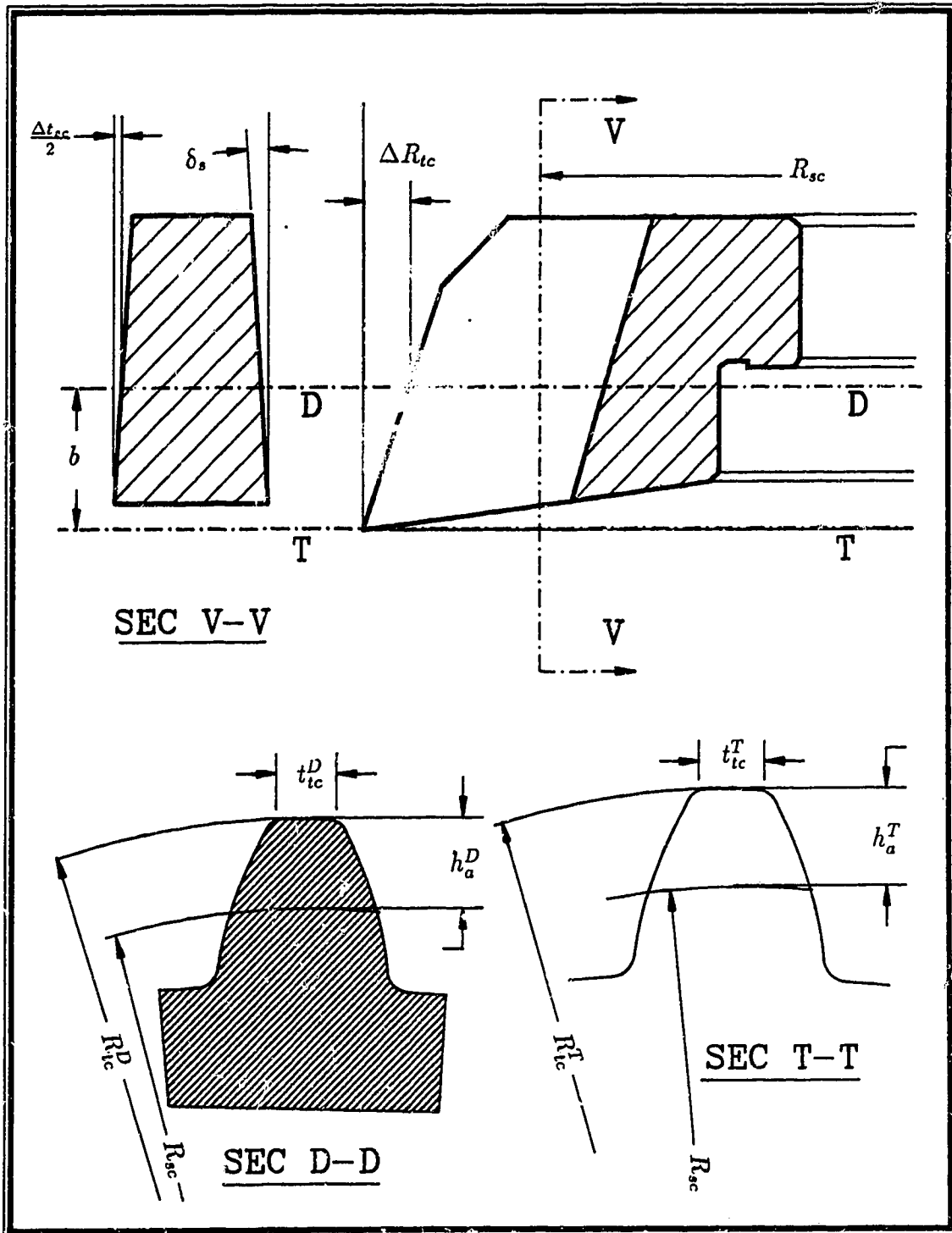


Figure 2.24: Determination of design distance

$$= -\frac{2b}{R_{tc}^D} \left\{ \tan \delta \left(R_{tc}^D \tan \phi_{tc}^D - \frac{t_{tc}^D}{2} \right) - \frac{[R_{tc}^D]^2 \tan \delta_s}{R_{sc}} \right\} \quad (2.73)$$

whence,

$$b = \frac{(t_{tc}^D - t_{tc}^T) R_{tc}^D}{2 \tan \delta \left(R_{tc}^D \tan \phi_{tc}^D - \frac{t_{tc}^D}{2} \right) - \frac{2[R_{tc}^D]^2 \tan \delta_s}{R_{sc}}} \quad (2.74)$$

where,

$$t_{tc}^D = 2R_{tc}^D \left\{ \frac{t_{sc}^D}{2R_{sc}} + \text{inv} \phi_s - \text{inv} \phi_{tc}^D \right\} \quad (2.75)$$

$$\phi_p^D = \cos^{-1} \left(\frac{R_{sc} \cos \phi_s}{R_{tc}^D} \right) \quad (2.76)$$

$$R_{tc}^D = R_{sc} + h_a^D \quad (2.77)$$

While selecting δ_s , consideration may be given to aspects described in section 3.5, but usually the value of δ_s is chosen so that $\tan \delta_s$ is equal to $(\tan \delta \tan \phi_s)$ as discussed in section 2.2, and on substituting this value equation 2.74 can be simplified to:

$$b = \frac{(t_{tc}^D - t_{tc}^T) R_{tc}^D}{2 \tan \delta \left\{ R_{tc}^D \tan \phi_{tc}^D - \frac{t_{tc}^D}{2} - \frac{[R_{tc}^D]^2 \tan \phi_s}{R_{sc}} \right\}} \quad (2.78)$$

Thus the value of design distance "b" can be estimated for a specified for value of tooth tip thickness t_{tc}^T .

The next chapter describes a new approach to the design of cutter which gives no profile deviation, in spite of relief and rake angles. This, then, allows the liberty of increasing rake and relief angles without restriction, by way of profile accuracy, and thereby increasing the cutting efficiency of the cutter and total life of the cutter. Also, for the new design, there are no profile deviations, even after multiple sharpening of the cutter, which is an added advantage when compared to the present design, where the profile deviation varies throughout cutter life, as will be explained in Chapter 4.

Chapter 3

New design of pinion shaping cutters

The objective of this chapter is to present a new design of the pinion cutter whose modified active profile surface gives no profile deviation, even after multiple resharpenings. This chapter explains the theoretical basis of the new design, while chapter 6 gives guidelines for practically obtaining such a cutter surface.

3.1 Shape of cutter (new design)

In the conventional design, the successive shifted cutter profiles lie in various planes displaced successively from the design section. In this new design, the profiles lie on shifted cones instead, and the profiles themselves are such that their projection on the projection plane are exact involutes.

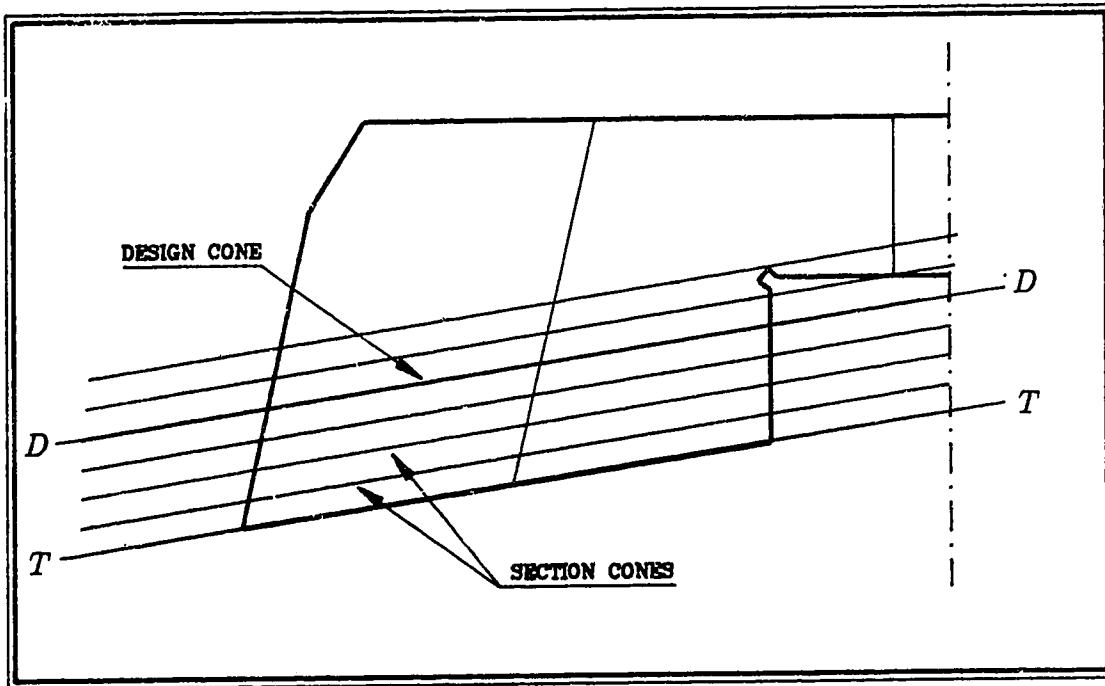


Figure 3.1: Design cone and section cones

As shown in Figure 3.1, instead of the design sectional plane, a design cone $D - D$ is chosen, whose projection on the projection plane is an involute with tooth thickness of,

$$\begin{aligned}
 t_{sc}^D &= \frac{\pi m}{2} && \dots \text{ for corrected cutters} \\
 &= \frac{\pi m}{2} + 2e_0 \tan \phi_s && \dots \text{ for non- corrected cutters} \quad (3.1)
 \end{aligned}$$

where e_0 is the initial profile shift.

When we take any arbitrary section cone $A - A$, anywhere between the design cone and the rake face cone, the projection of the curve of intersection of the cutter tooth side surface with the section cone, on the projection plane, will be an involute with a positive profile shift. For sectional cones above the design cone, the corresponding profiles of intersection will produce an involute with negative profile shift, when projected on the projection plane. In other words, the new design of cutter will

have such a side relief surface, that its intersection with any section cone produces a profile whose projection on the projection plane is always an involute. The amount of profile shift of the involute depends upon the position of the section cone.

If the rake face has the same semi-cone angle as that of the section cones, designated by ψ where,

$$\psi = 90 - \gamma \quad (3.2)$$

then, the projected profile, on the projection plane, will always be an involute, even after multiple resharpenings of the cutter, and such a cutter will never produce any theoretical profile deviation throughout the cutter life, even for high rake and relief angles. However, if a slight amount of relief is required on the profile, this can still be achieved by slightly lowering the semi-cone angle of the rake face cone with respect to the section cones and then taking a smaller base circle for pressure angle correction.

The geometry of the surface required to provide the above features, can be determined by simply projecting a family of involute profiles from the projection plane to corresponding displaced concentric section cones. This process can be simplified by theoretically generating the required surface in the following way:

Step I Let the pinion cutter be assumed to be generated from a right cylindrical blank, by a rack cutter. The rack cutter reciprocates at angle δ (relief angle) to the pinion blank axis and at the same time runs in tight mesh action with the pinion blank, as explained in section 2.2, to produce a family of shifted involute profiles on successive parallel planes perpendicular to the axis. This provides the necessary side and front relief angles.

Step II To provide the necessary rake angle each point of the pinion cutter is displaced by an amount proportional to its radial distance from the cutter tip circle. This displacement field is a function of the radius vector and the rake angle and is given by,

$$z = (R_{tc}^T - R) \tan \gamma \quad (3.3)$$

This displacement field will cause all plane sections to be deformed into a cone. Hence, the cutter can be imagined to be press-forged to this shape by a concave conical upper die and a convex conical lower die, with $(90 - \gamma)$ as semi-cone angles. When manufacturing the cutter practically, it would not be convenient to carry out step II physically. Instead the cutter rake surface is ground as a cone as usual, while a modified method of generated grinding (dealt with further in chapter 6) can be imparted to the side surface to incorporate the feature required by step II.

3.2 Front relief angles

If the rack cutter, while generating the pinion cutter (step I), reciprocates at an angle δ to the cutter blank axis, it will produce a front relief angle of δ and a side relief angle of δ_s , as explained in section 2.2. However, in step II, because the cutter is subjected to the displacement field, the relief angle δ will change to a new angle, which can be seen from Figure 3.2, to be:

$$\tan \delta^* = \frac{\tan \delta}{1 + \tan \delta \tan \gamma} \quad (3.4)$$

which indicates that the front relief angle reduces from the value of δ in step I. In practice, since the front relief and side relief surfaces can be generated separately

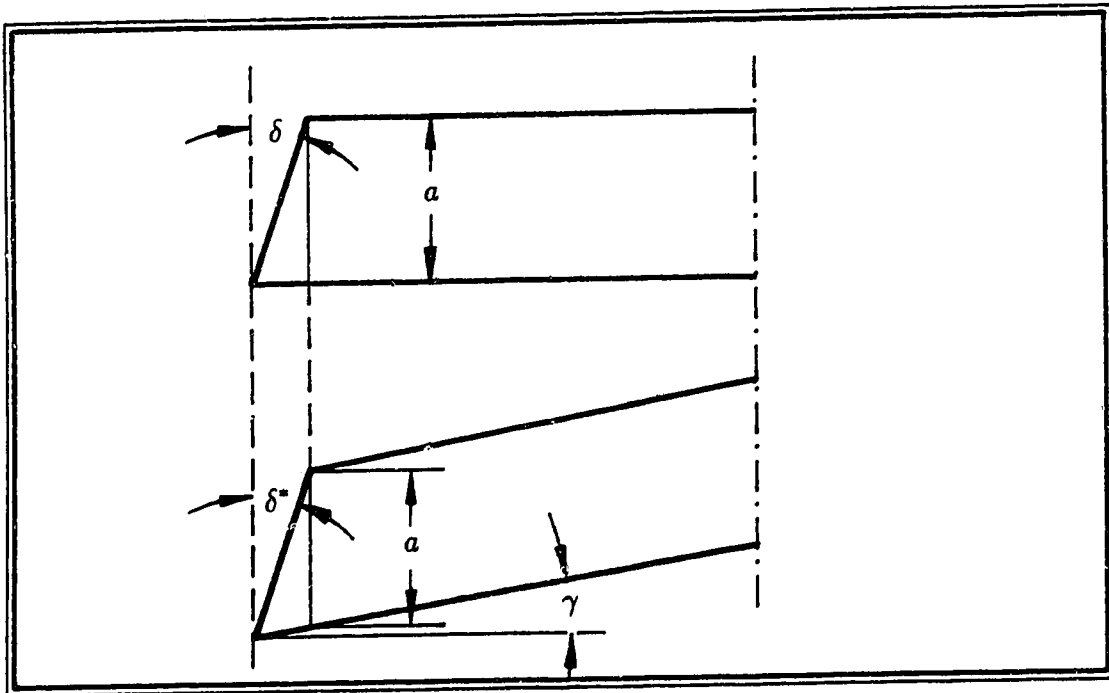


Figure 3.2: Front relief angle in the new design

by grinding, the front and side relief angles can be made independent of each other. An important consideration while manufacturing the front relief angle is the effect of resharpener of the cutter. The front and side relief angles should be chosen, such that, as far as possible, on feeding the cutter further into the blank after resharpener, the same amount of dedendum should be produced, on the gear blank. This aspect is dealt with further, later in this chapter.

3.3 Side relief angle

Using the same reasoning as in section 2.1, it can be inferred that the side surface is a non-involute helicoidal surface. Since the vertical distances between the section cones $A - A$ and $D - D$ are unchanged, when the curve rotates from point 1 to 2 (Figure 2.4), the side relief angle also remains unchanged. Also the displacements

“ y ” and “ a ” remains the same as in Figure 2.3 because the displacement field shears the cutter in the z - direction only. Therefore, the lead of the helicoid will be (from equation 2.9),

$$L = \frac{2\pi R_{sc}}{\tan \delta^* \tan \phi_s} \quad (3.5)$$

and the side relief angle, δ_s^* , will be (from equation 2.10),

$$\delta_s^* = \tan^{-1}(\tan \delta^* \tan \phi_s) \quad (3.6)$$

3.4 Amount of relief

Thus in the new approach, the cutter side profile is the envelope of successive shifted profiles lying on consecutive cones as shown in Figure 3.3. The choice of the value of “ e ” for the profile shift that should occur for a certain depth of cut given while regrinding the cutter rake face, is important. On having chosen a side relief angle, the front relief angle should be so chosen that after resharpener the cutter the amount by which the cutter has to be fed in for obtaining the required gear tooth thickness, should be as close as possible to the amount by which the addendum of the cutter reduces on regrinding, due to the presence of the front relief angle. This will ensure that after successive regrindings of the cutter, the whole depth of the generated gear does not change significantly.

Let the profile shift be “ e ”, at a distance “ a ” from the design section, so that the tooth thickness of the cutter there becomes,

$$t_{sc}^A = t_{sc}^D + 2e \tan \phi_s \quad (3.7)$$

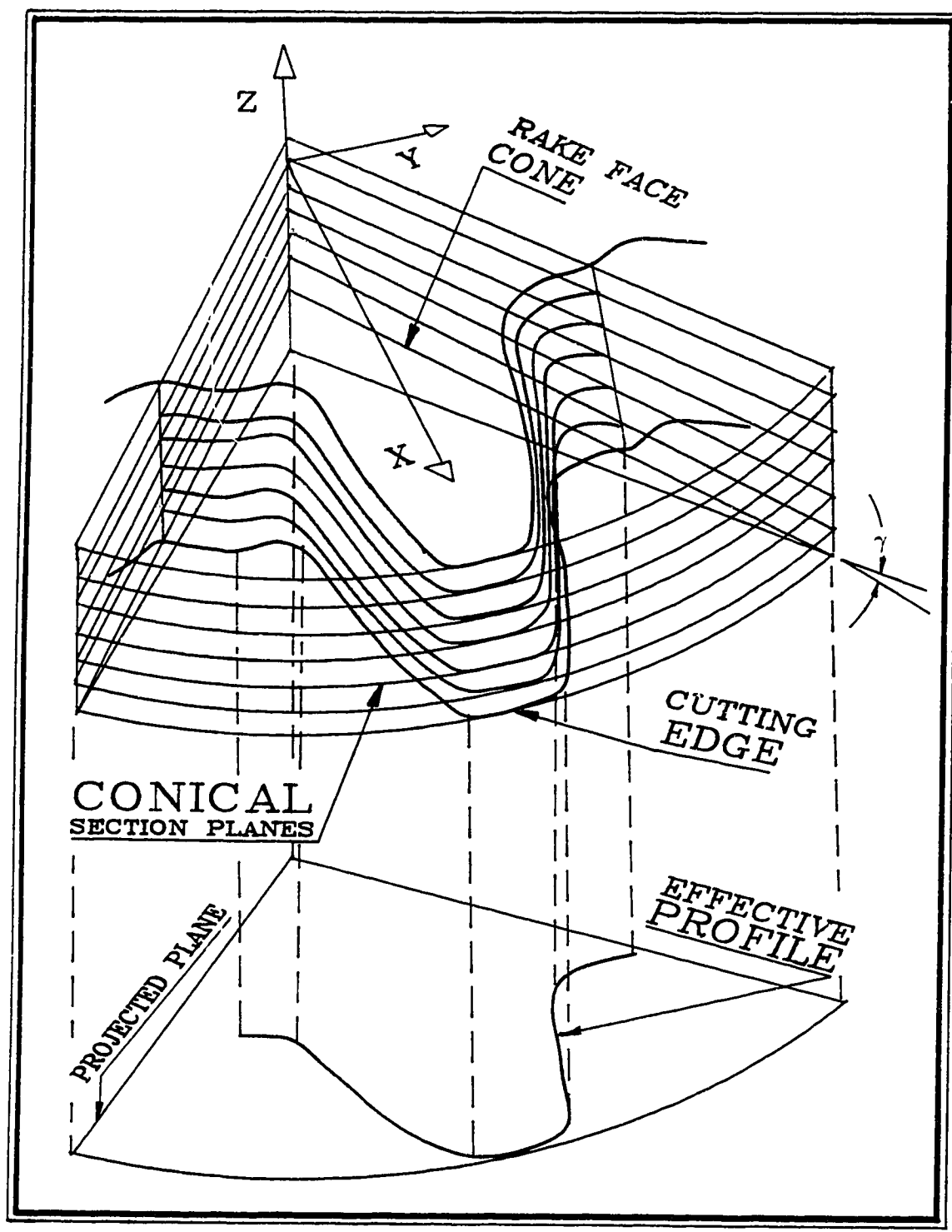


Figure 3.3: Determination of amount of relief

Then, while carrying out step I, the addendum of the cutter also decreases by a value of “ e ” since the root of the rack cutter generating the pinion cutter addendum moves towards the centre by a distance “ e ”, while generating the profile at section $A - A$. The required decrease in the cutter addendum should be however, slightly lower than “ e ”, if constant working depth is to be maintained in the generated gear, apart from the requirement of constant gear tooth thickness.

To obtain this required decrease in cutter tooth addendum, to satisfy the condition of constant whole depth and tooth thickness in the generated gear, a relation has to be found between the change in cutting centre distance and the change in cutter tooth thickness, as different shifted profiles become the effective cutting edge after resharpenering of the cutter. For a constant gear tooth thickness of t_{sg} the required cutting centre distance C^c can be found from equation 1.14,

$$\text{inv}\phi_p^c = \text{inv}\phi_s - \frac{1}{2C_s}(p_s - t_{sg} - t_{sc}) \quad (3.8)$$

The relation between the change of cutter centre distance required for different profile shifts in the cutter, cannot be evaluated analytically. Hence an approximate relationship is found by taking differentials of the variables in question.

The cutter centre distance can be written (from equation 1.16) in terms of the cutter pressure angle as,

$$C^c = \frac{R_{bg} + R_{bc}}{\cos \phi^c} \quad (3.9)$$

Using only the first term from Polder’s relation (equation 1.15), C^c can be rewritten as,

$$C^c = (R_{bg} + R_{bc}) \left\{ 1 + 1.04004(\text{inv}\phi^c)^{\frac{2}{3}} \right\} \quad (3.10)$$

Differentiating the above equation we get,

$$dC^c = \frac{0.69336(R_{bg} + R_{bc})d(\text{inv}\phi^c)}{(\text{inv}\phi^c)^{\frac{1}{3}}} \quad (3.11)$$

Differentiating equation 3.8 we get,

$$d(inv\phi^c) = \frac{dt_{sc}}{2C_s^c} \quad (3.12)$$

Substituting the value of $d(inv\phi^c)$ from the above equation in equation 3.11 we get,

$$\frac{dC^c(inv\phi_p^c)^{\frac{1}{2}}}{.69336(R_{bg} + R_{bc})} = \frac{dt_{sc}}{2C_s^c} \quad (3.13)$$

The differentials dC^c and dt_{sc} can be replaced by increments ΔC^c and Δt_{sc} where,

$$\Delta C^c = [C^c]^A - [C^c]^D \quad (3.14)$$

$$\begin{aligned} \Delta t_{sc} &= [t_{sc}]^A - [t_{sc}]^D \\ &= 2e \tan\phi_s \end{aligned} \quad (3.15)$$

The equation 3.13 can be simplified to,

$$[C^c]^D - [C^c]^A = \frac{0.69336 \sin \phi_s}{(inv\phi_p^c)^{\frac{1}{2}}} e \quad (3.16)$$

$$= ke \quad (3.17)$$

Since ϕ_p^c will decrease less than ϕ_s for the profiles below the design section and increase more than ϕ_s for profiles above the design section, when $t_{sc}^D + t_{sg} = p_s$, the average value of ϕ_s^c can be taken equal to ϕ_s when evaluating the value of "k". Consequently, the value of "k" is,

$$\begin{aligned} k &= 0.9636 & \text{for } \phi_s &= 20^\circ \\ k &= 0.9977 & \text{for } \phi_s &= 5^\circ \end{aligned} \quad (3.18)$$

Hence the cutter profile addendum at section $A - A$ should be shifted in or out, depending upon its relative position to section $D - D$, by an amount equal to " $k \cdot e$ ", if the profile shift coefficient of the section $A - A$ is " e ". Therefore, " k " can be called the

"Relief Correction Factor¹", and having chosen a suitable value for "k" the corrected side relief angle δ_s , or the corrected profile shift for front relief can be evaluated as a function of γ , δ , ϕ_s and k so that a constant whole depth is generated in the gear, as far as possible. If the front relief angle of the cutter is δ^* , then the profile shift of the profile at a distance "a" from the design section should be,

$$\begin{aligned} e &= \frac{a \tan \delta}{k} && \dots \text{ for conventional cutters}^1 \\ &= \frac{a \tan \delta^*}{(1 - \tan \delta^* \tan \gamma)k} && \dots \text{ for new cutters} \end{aligned} \quad (3.19)$$

The cutter manufactured with a rake angle γ and a front relief angle of δ^* will have a side relief angle of (from equation 3.4, 3.6, 3.19):

$$\begin{aligned} \delta_s^* &= \tan^{-1} \left\{ \frac{\tan \delta \tan \phi}{k} \right\} && \dots \text{ for conventional cutters}^1 \\ &= \tan^{-1} \left\{ \frac{1}{k} \cdot \frac{\tan \delta^* \tan \phi_s}{(1 - \tan \delta^* \tan \gamma)} \right\} && \dots \text{ for new cutters} \end{aligned} \quad (3.20)$$

For greater accuracy, it might be worthwhile to form grind the tip surface of the cutter in the shape of a modified cone whose generator has a slight curvature (calculated from equation 3.16), as opposed to a straight line generator, so that the whole depth imparted to the gear, throughout the cutter life, remains practically constant. However, for small rake angles, even if the addenda of shifted profiles are decreased by an amount equal to their profile shift coefficients, the radius of the root circle of the gear (or the whole depth) would not change significantly after multiple resharpenings of the cutter.

¹The "Relief Correction factor" can be applied to conventional cutters also.

3.5 Cutter coordinates

Let the cutter be designed to have a module “ m ”, pressure angle “ ϕ_s ” and a tooth thickness of t_{sc}^D at the design cone. Then the tooth thickness of the effective profile, which is the profile lying on cone $T - T$, will be,

$$t_{sc}^T = t_{sc}^D + 2e \tan \phi_s \quad (3.21)$$

On the effective profile, for any point P_c having a radius vector of R_c , the inclination of P_c to the tooth centreline will be,

$$\theta_c = \frac{t_{sc}^T}{2R_{sc}} + \text{inv} \phi_s - \text{inv} \cos^{-1} \left(\frac{R_{sc} \cos \phi_s}{R_c} \right) \quad (3.22)$$

Hence the coordinates of any point P_c on the effective profile will be,

$$X_c = R_c \cos \theta_c \quad (3.23)$$

$$Y_c = R_c \sin \theta_c \quad (3.24)$$

$$Z_c = b - (R_{tc}^T - R_c) \tan \gamma \quad (3.25)$$

For a rake and relief angle of 20° and a pressure angle of 20° , the effective profile of the new cutter is plotted in Figure 3.4. The gear generated by this cutter is plotted in Figure 3.5. Both for the cutter and the generated gear, the active side profiles are involutes. Thus, the advantages of greater tool life and of better cutting efficiency due to high rake and relief angles can be achieved without compromising the accuracy of the profile of the cutter and consequently those generated in the gear.

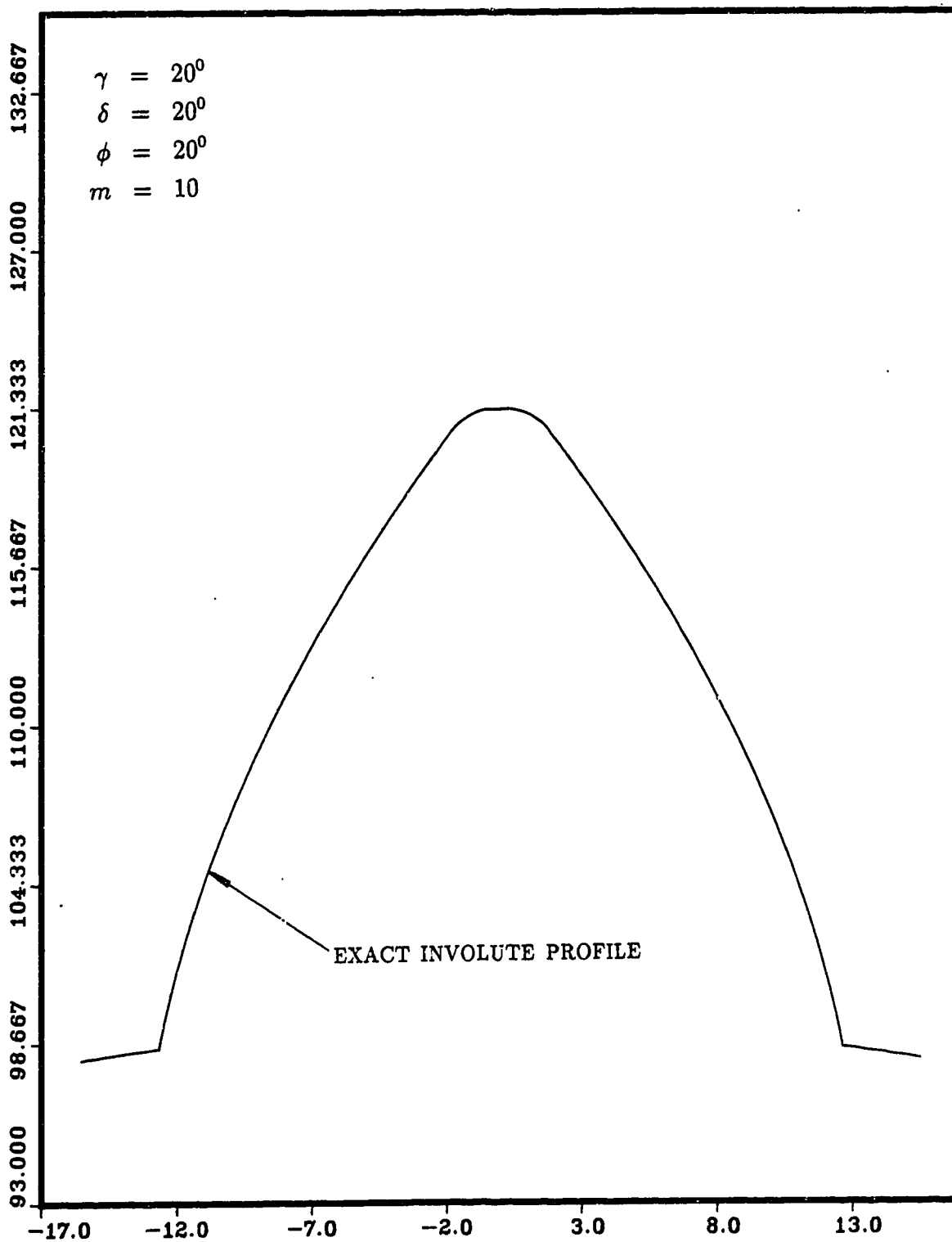


Figure 3.4: Profile of the cutter(new design)

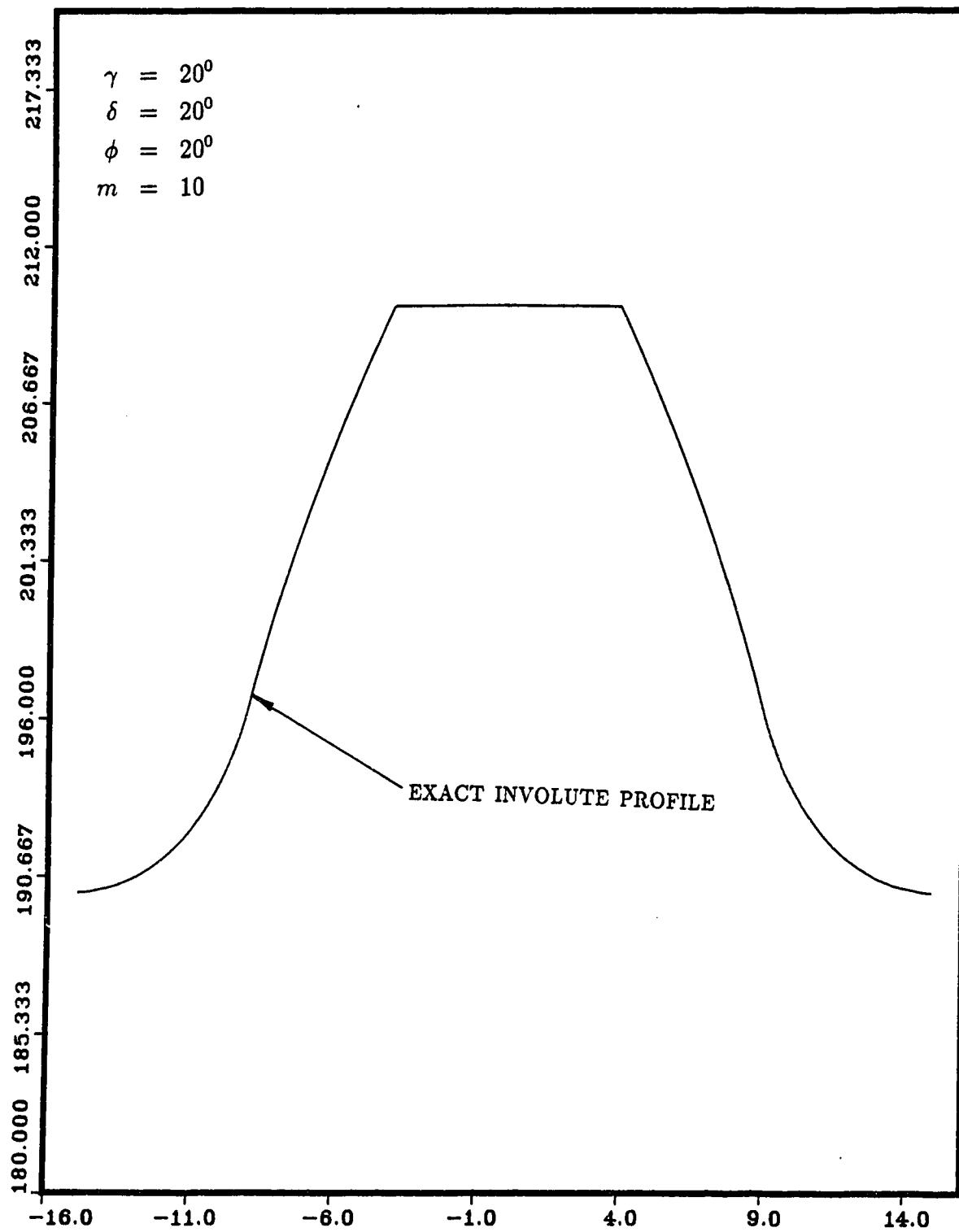


Figure 3.5: Profile of the gear generated by the cutter (new design)

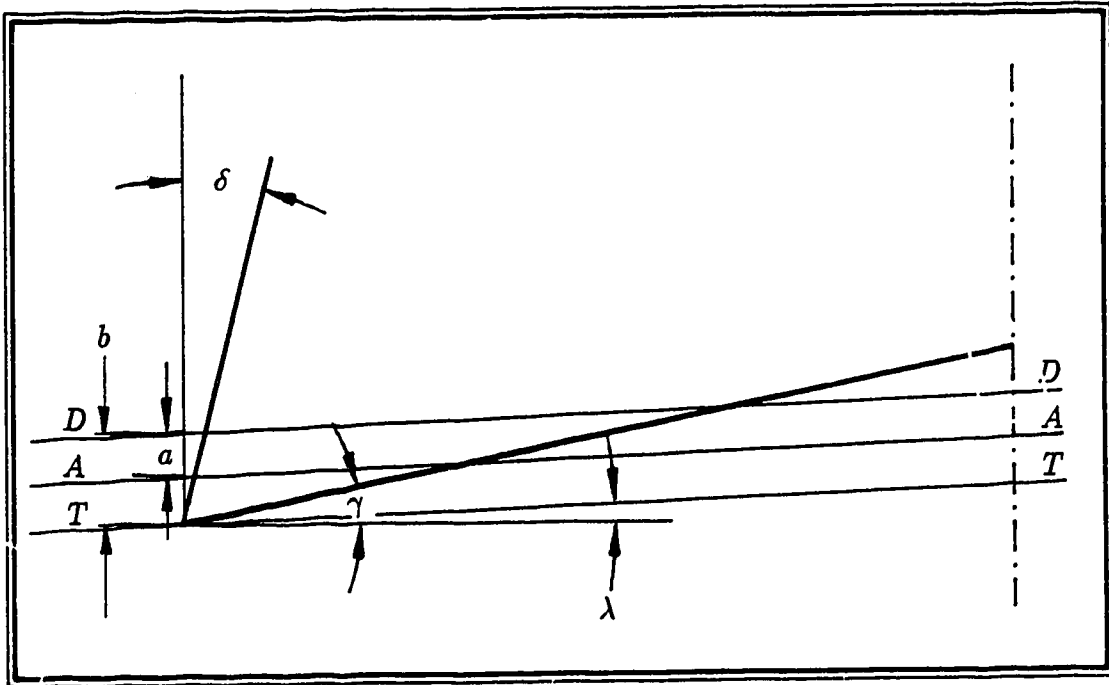


Figure 3.6: Profile relief (Method I)

3.6 Tooth relief (Method I)

It might sometimes be required for the cutter to provide a slight amount of profile relief at the tooth tip and the root of the generated gear. Even for high rake and relief angles, this can be achieved by designing the cutter with a greater semi-cone angle, of the sectional cones on which lie the family of cutter profiles, compared to that of the rake cone, as shown in Figure 3.6. Let the origin of the cutter axes lie at the vertex of the design section cone. Also, as shown in the figure, let the inclination of the generator of the sectional cones with respect to the base plane be λ and that of the rake cone be γ , where

$$\lambda < \gamma$$

The sectional cone $A - A$ cuts the rake cone in a circle of intersection having a

radius R_c^A , where,

$$R_c^A = R_{tc}^T - \frac{b - a}{\tan \gamma - \tan \lambda} \quad (3.26)$$

where R_{tc}^T , the radius of the tip circle $T - T$, is,

$$R_{tc}^T = R_{sc}^D + h_a^D + b \tan \delta \quad (3.27)$$

where,

$$\tan \delta = \frac{\tan \delta^*}{(1 - \tan \delta^* \tan \gamma)k}$$

The tooth thickness at section $A - A$ then is,

$$\begin{aligned} t_{sc}^A &= t_{sc}^D + 2 a \tan \delta \tan \phi_s \\ &= t_{sc}^D + \frac{2 a \tan \delta^* \tan \phi_s}{(1 - \tan \delta^* \tan \gamma)k} \end{aligned} \quad (3.28)$$

The circle of intersection of radius R_c^A cuts the involute profile lying on the section cone $A - A$ at P^A and therefore the inclination of point P_p^A with respect to the tooth centre line will be,

$$\theta_p^A = \frac{t_{sc}^A}{2R_{sc}} + \text{inv} \phi_s - \text{inv} \phi_p^A \quad (3.29)$$

where

$$\phi_p^A = \cos^{-1} \frac{R_{bc}}{R_c^A} = \cos^{-1} \frac{R_{sc} \cos \phi_s}{R_c^A} \quad (3.30)$$

Hence the coordinate of R_c^A and θ_p^A can be expressed as

$$X_p^A = R_c^A \cos \theta_p^A \quad (3.31)$$

$$Y_p^A = R_c^A \sin \theta_p^A \quad (3.32)$$

$$Z_p^A = -a - R_c^A \tan \lambda \quad (3.33)$$

For a fixed value of “ b ” and “ λ ”, the coordinates of the cutting edge of the cutter will be a function of variable “ a ”,

$$X_p^A = \left(R_{sc} + h_a^D + \frac{b \tan \delta^*}{(1 - \tan \delta^* \tan \gamma)k} - \frac{b - a}{\tan \gamma - \tan \lambda} \right) \cos \left[\frac{\frac{\pi m}{2} + \frac{2a \tan \delta^* \tan \phi}{(1 - \tan \delta^* \tan \gamma)k}}{R_{sc}} + \right. \\ \left. \text{inv} \phi_s - \text{inv} \cos^{-1} \left(\frac{R_{sc} \cos \phi_s}{\left(R_{sc} + h_a^D + \frac{b \tan \delta^*}{(1 - \tan \delta^* \tan \gamma)k} - \frac{b - a}{\tan \gamma - \tan \lambda} \right)} \right) \right] \quad (3.34)$$

$$Y_p^A = \left(R_{sc} + h_a^D + \frac{b \tan \delta^*}{(1 - \tan \delta^* \tan \gamma)k} - \frac{b - a}{\tan \gamma - \tan \lambda} \right) \sin \left[\frac{\frac{\pi m}{2} + \frac{2a \tan \delta^* \tan \phi}{(1 - \tan \delta^* \tan \gamma)k}}{R_{sc}} + \right. \\ \left. \text{inv} \phi_s - \text{inv} \cos^{-1} \left(\frac{R_{sc} \cos \phi_s}{\left(R_{sc} + h_a^D + \frac{b \tan \delta^*}{(1 - \tan \delta^* \tan \gamma)k} - \frac{b - a}{\tan \gamma - \tan \lambda} \right)} \right) \right] \quad (3.35)$$

$$Z_p^A = -a - R_c^A \tan \lambda \quad (3.36)$$

Now we can choose a corrected value of pressure angle ϕ^{corr} , and a corrected value of tooth thickness t_{sc}^{corr} using methods similar to those described in sections 2.9 to 2.10.3, so that the deviation in profile increases towards the tip and root of the cutter. Thus by choosing a proper value of λ (which should differ slightly from γ) the required amount of relief on the tooth tip and root can be generated on the gear by the cutter.

3.7 Tooth relief (Method II)

For the new design of the shaper cutter it is possible to generate the tooth relief in a much simpler way. In this method, instead of grinding the rake face in the shape of a straight cone, it is ground in the shape of a modified cone whose generator is an arc of a circle.

As shown in Figure 3.7, the cutter lies inclined at an angle γ to the horizontal, and the grinding wheel assembly rotates about a fixed fixed centre whose position is at a

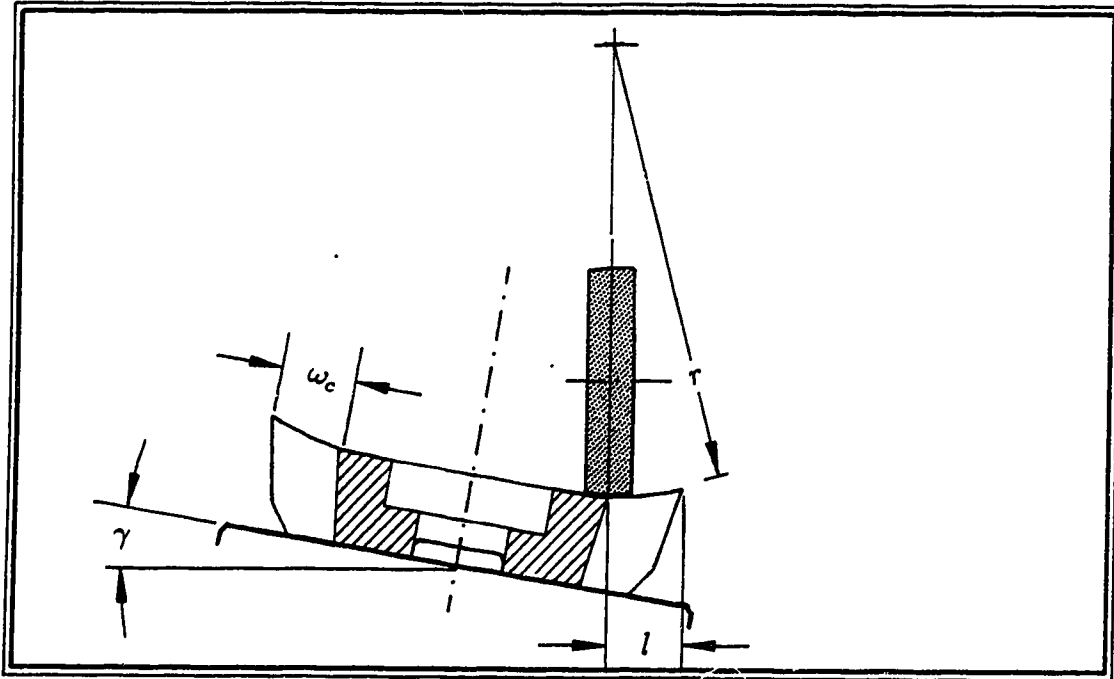


Figure 3.7: Tooth relief (Method II)

height of “ r ” over the rake face, and a distance “ l ” from the cutter tip. The working face of the wheel itself is dressed in the shape of an arc of a circle of radius “ r ”. Grinding the rake surface with such an arrangement will produce a certain amount of deviation both in the tip and the root of the cutter, which will provide the necessary tip and root relief in the generated gear.

If only a tip relief is required this can be achieved by:

1. positioning the centre of rotation of the grinding wheel assembly over the root of the cutter teeth, as shown in Figure 3.8,
2. or by modifying the rake face in the shape described above only up to a distance l from the cutter tip, while grinding the rest of the length flat by moving the grinding wheel assembly in translation, as shown in Figure 3.9.

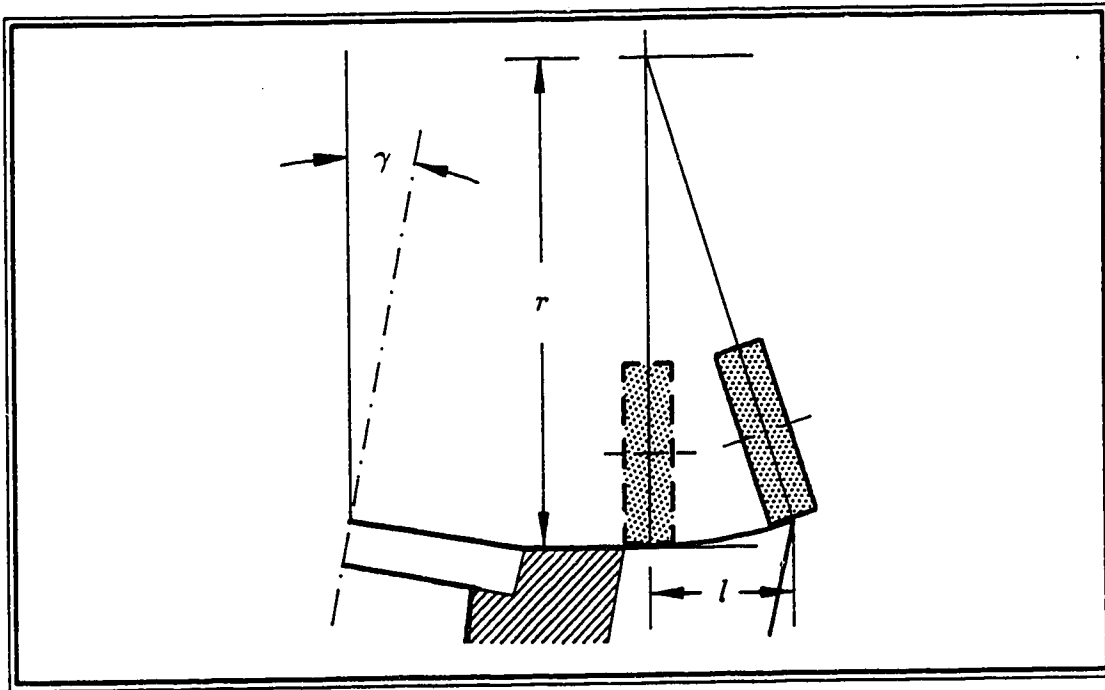


Figure 3.8: Grinding wheel assembly lies directly above root of cutter teeth

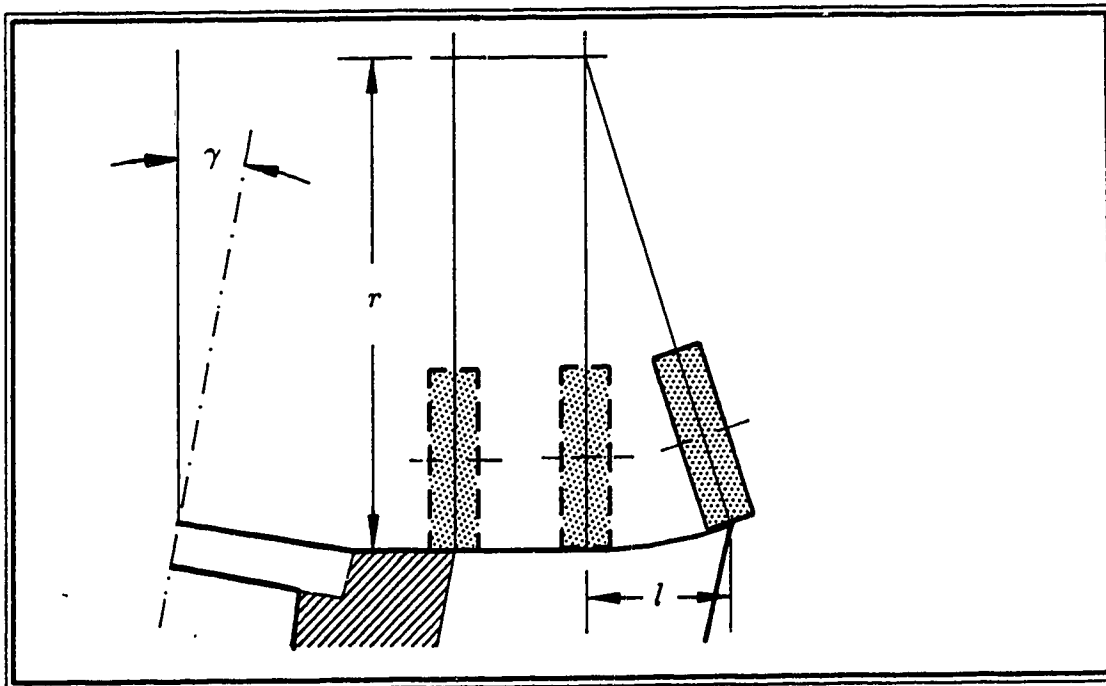


Figure 3.9: Grinding wheel assembly is rotated as well as translated

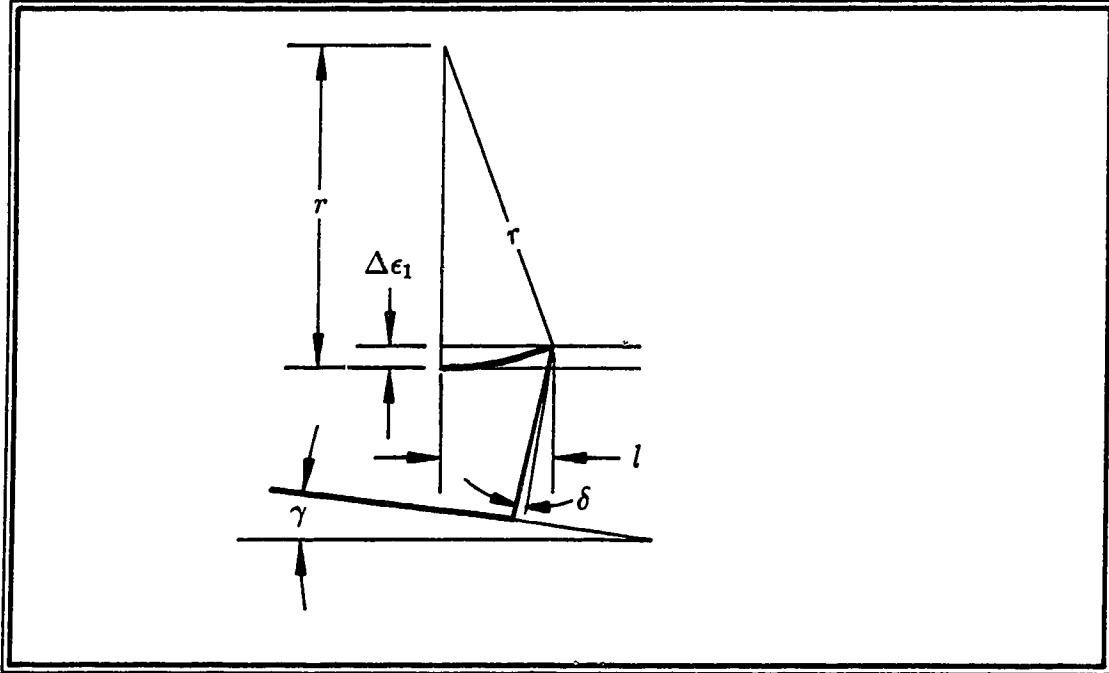


Figure 3.10: Grinding wheel height

3.7.1 Grinding assembly height

In this arrangement, the difference between the amount of material removed at the tooth centre and the tooth tip (ϵ_1) can be read from Figure 3.10.

$$\Delta\epsilon_1 = r - \sqrt{r^2 - l^2} \quad (3.37)$$

The difference in addendum (ϵ) between the profile exposed at the centre and that at the tip is also equal to the difference in profile shifts between the two. From equation 4.1 we can write:

$$\Delta\epsilon \approx \Delta e = \frac{\Delta\epsilon_1 \sin \delta^*}{\cos(\delta^* + \gamma)} \quad (3.38)$$

If the tooth thickness of the profile at the centre be,

$$t_{sc}^{cen} = t_{sc}^D + 2e \tan \phi_s \quad (3.39)$$

then that of the profile at the tooth tip will be,

$$t_{sc}^{tip} = t_{sc}^D + 2(e + \Delta e) \tan \phi_s \quad (3.40)$$

Hence the difference between the tooth thickness, which is also the amount of normal deviation of the tip with respect to the centre will be,

$$\Delta n_{tip} = t_{sc}^{tip} - t_{sc}^{cen} \quad (3.41)$$

$$= 2 \Delta e \tan \phi_s \quad (3.42)$$

$$= \frac{2r - \sqrt{r^2 - l^2}}{\cos(\delta^* - \gamma)} \sin \delta^* \tan \phi_s \quad (3.43)$$

Thus the required setting of the grinding wheel, for a required relief, can be found. For instance, if the required normal deviation Δn_{tip} at the tip is known, and if l is set equal to the addendum of the cutter h_a , then the required height of the grinding wheel assembly from the rake surface will be,

$$r = \left\{ \frac{h_a^2}{a} + \sqrt{\frac{h_a^4}{4} + \left(\frac{\Delta n_{tip} \cos(\delta^* + \gamma)}{2 \sin \delta^* \tan \phi_s} \right)^2} \right\}^{\frac{1}{2}} \quad (3.44)$$

3.8 Flexibility in relief

A particular advantage of this new design compared to the conventional design is the fact that the amount of tooth relief required in the gear, if it is required at all, can be regulated by the user, by altering the shape of the rake face or the angle at which the rake face of the cutter is ground. If the user grinds the rake face at the same angle as λ to which the manufacturer has designed and manufactured the cutter, then he would obtain a cutter whose effective profile is an exact involute. On grinding the same cutter at a calculated angle greater than λ he can achieve the required amount

of tooth relief in the gear but with a slightly smaller pressure angle. Grinding the same cutter in a arc of a circle (Figure 3.7), one can obtain a gear with the required tip relief or root relief or both and still maintain the same pressure angle as that of the cutter. In fact the new design provides greater control on the generated gear profile shape by permitting an exact involute shape in the active gear tooth section and a required relief in the tip section.

3.9 Design distance

The choice of design distance can be evaluated in a manner similar to that described in section 2.12 and 2.13,

$$b = \frac{(t_{tc}^D - t_{tc}^T) \cdot (1 - \tan \delta^* \tan \gamma) R_{tc}^D k}{2 \tan \delta^* \left\{ R_{tc}^D \tan \phi_p^D - t_{tc}^D - \frac{[R_{tc}^D]^2 \tan \phi_p^D}{R_{sc}} \right\}} \quad (3.45)$$

where

$$t_{tc}^D = \left\{ \frac{t_{sc}^D}{2 R_{sc}} + 2 (\text{inv} \phi - \text{inv} \phi_p^D) \right\} \quad (3.46)$$

$$\phi_p^D = \cos^{-1} \left(\frac{R_{sc} \cos \phi}{R_{tc}^D} \right) \quad (3.47)$$

$$R_{tc}^D = R_{sc} + h_a^D \quad (3.48)$$

The effects of resharpening the cutter for new and old designs are dealt with in the next chapter. The effects on the generated gear cut by a conventional and a new cutter are also investigated.

Chapter 4

Effect of resharpening of cutter

This chapter investigates the effect of resharpening on the active profile of the pinion shaper cutter. The changes in the generated gear are then observed with the help of the simulator program. Both the conventional and the new design of shaper cutter are compared with respect to profile deviations on resharpening.

4.1 Conventional design

In the conventional design of the cutter, the deviation of active profile varies throughout the life of the cutter. The computer program (Appendix C) also evaluates the profile shape and the deviation from the theoretical profile after different numbers of resharpening.

4.1.1 Depth of cut

A relation has to be found between the depth of cut ϵ_1 , given to the rake face at each resharpening and the consequent profile shape of the new cutting edge exposed.

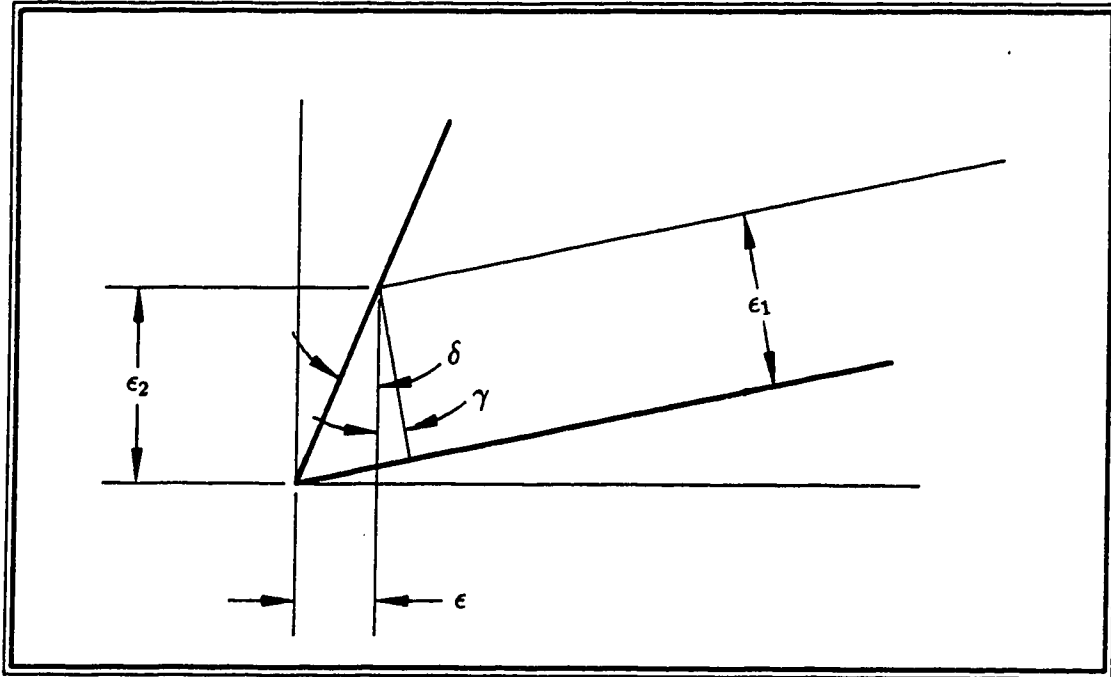


Figure 4.1: Depth of cut and related parameters

When ϵ_1 amount of stock is removed from the conical rake face, the value of ϵ and ϵ_2 can be read from figure 4.1

$$\epsilon = \frac{\epsilon_1 \sin \delta}{\cos(\delta + \gamma)} \quad (4.1)$$

$$\text{and} \quad \epsilon_2 = \frac{\epsilon_1 \cos \delta}{\cos(\delta + \gamma)} \quad (4.2)$$

$$(4.3)$$

Then after a number of resharpenings of the cutter, the new cutting edge will have a design distance of:

$$b_i = b - i\epsilon_2 \quad (4.4)$$

where b_i is the design distance after i resharpenings of the cutter, ϵ_2 is the reduction in the design distance, and ϵ_1 is the amount of material removed at each of the i resharpenings of the cutter.

4.1.2 Tooth thickness

After i resharpenings, the effective standard tooth thickness (i.e. the tooth thickness of the effective profile at the standard pitch circle of the cutter) will be at a value of "a" for which $R_c^A = R_{sc}^D$ (from equation 2.46),

$$a = (1 - \tan \delta \tan \gamma)(b - i\epsilon_2) - h_a^D \tan \gamma \quad (4.5)$$

Hence the tooth thickness of the effective profile of the cutter after i resharpenings will be (substituting the above value of a in equation 2.13),

$$t_{sc}]_i = t_{sc}^D + 2(1 - \tan \delta \tan \gamma)(b - i\epsilon_2) \tan \delta \tan \phi_s - 2h_a^D \tan \gamma \tan \delta \tan \phi_s \quad (4.6)$$

4.1.3 Addendum

The addendum of the cutter reduces at each resharpening of the cutter. From figure 4.1 it can be deduced that after i resharpenings, the addendum of the effective profile will be ,

$$h_a]_i = h_a^D + b \tan \delta - i\epsilon \quad (4.7)$$

where h_a^D is the addendum of the cutter at the design section. The change in the cutter addendum with rake angle and front relief angle, for different cutter teeth sizes (m) after regrinding the cutter are shown in figure 4.2 and 4.3. The variation of the cutter addendum with front relief angle for different modules is also shown in figure 4.4.

Figure 4.5 shows a number of overlaid effective profiles after different numbers of resharpenings of the shaper cutter. Figure 4.6 shows the overlaid profiles of the gear generated by the corresponding cutter profiles in figure 4.5. As can be seen from these plots the cutter profiles deviate throughout the life of the cutter, and the amount of

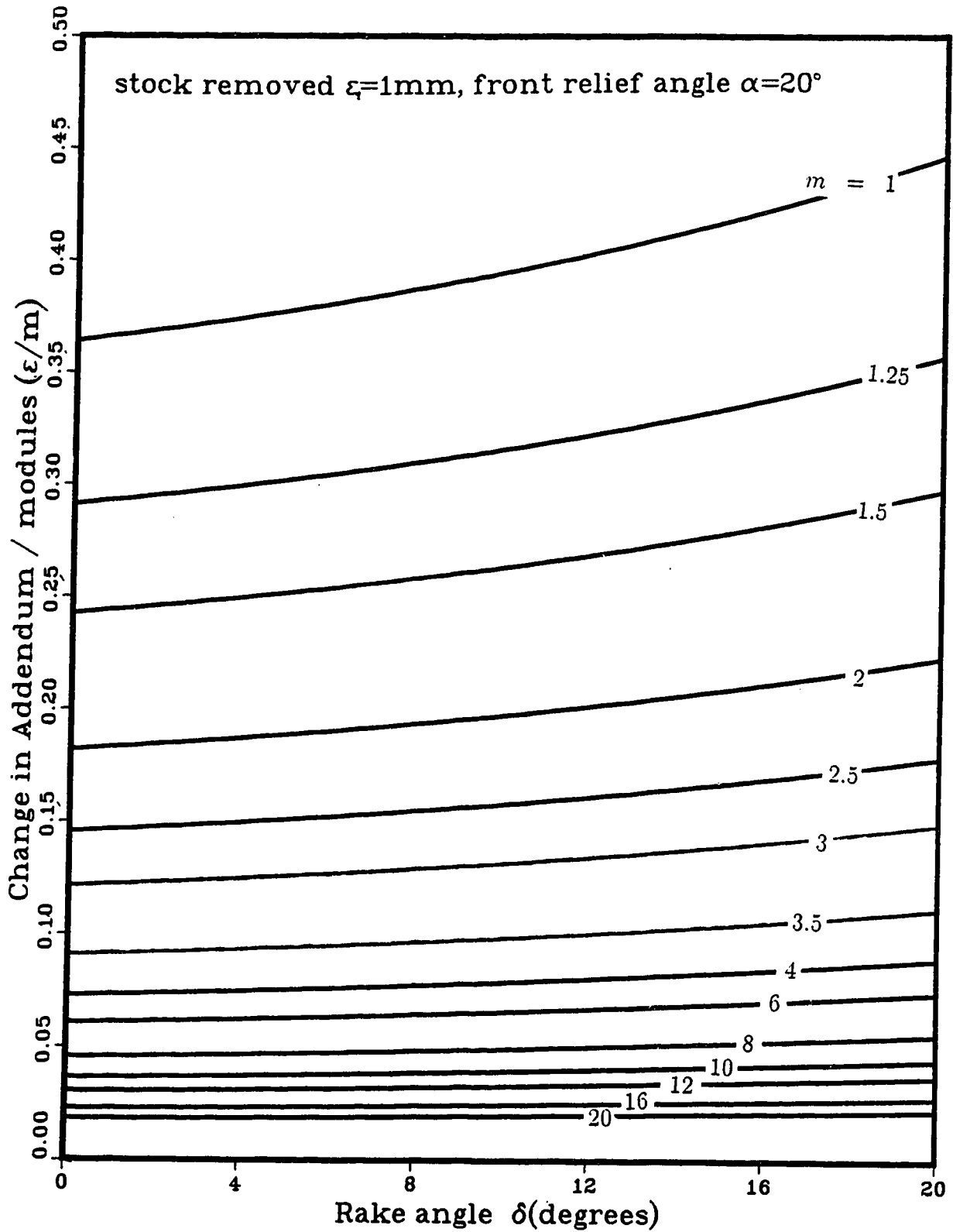


Figure 4.2: Variation of addendum with rake angles for different modules

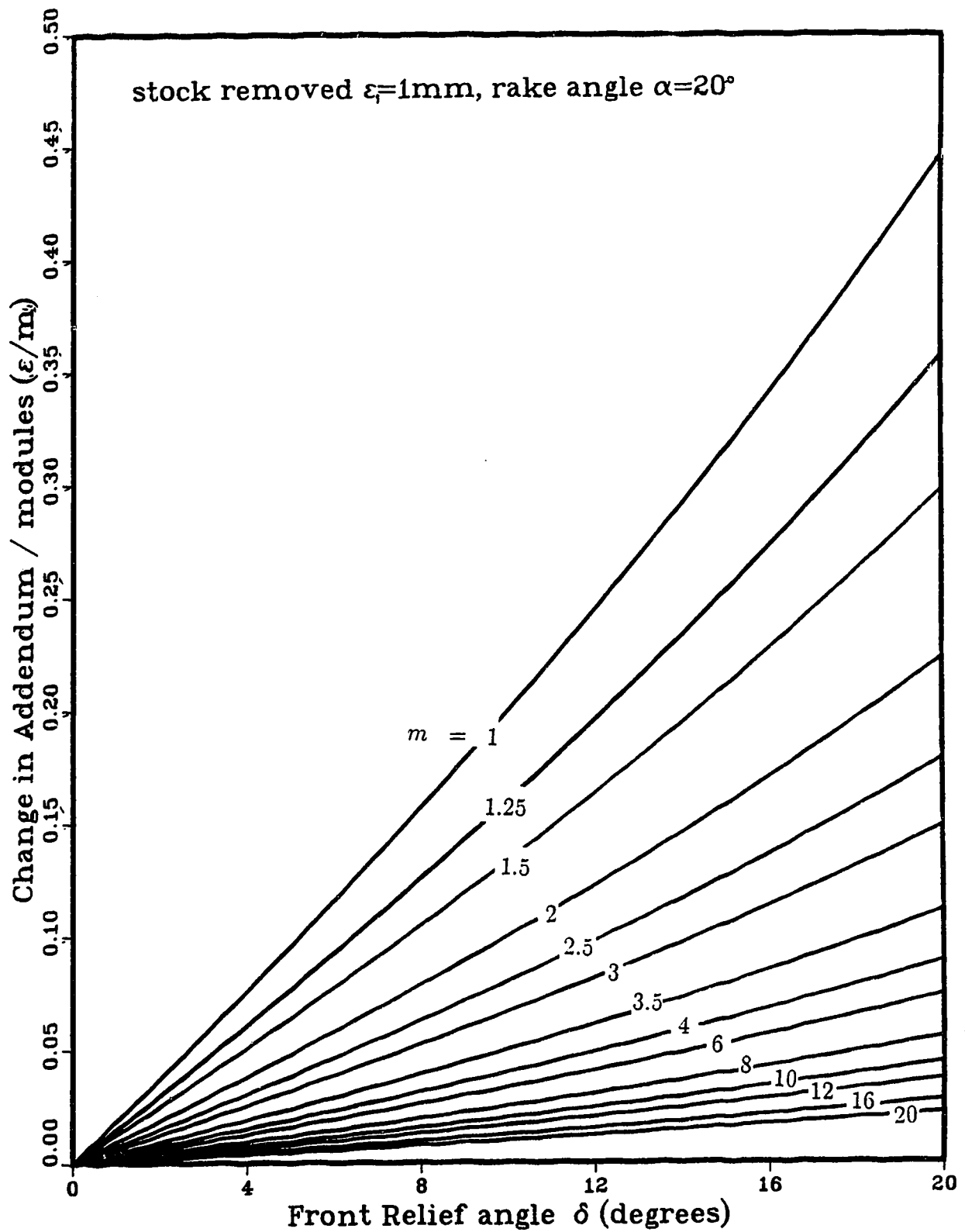


Figure 4.3: Variation of addendum with front relief angles for different modules

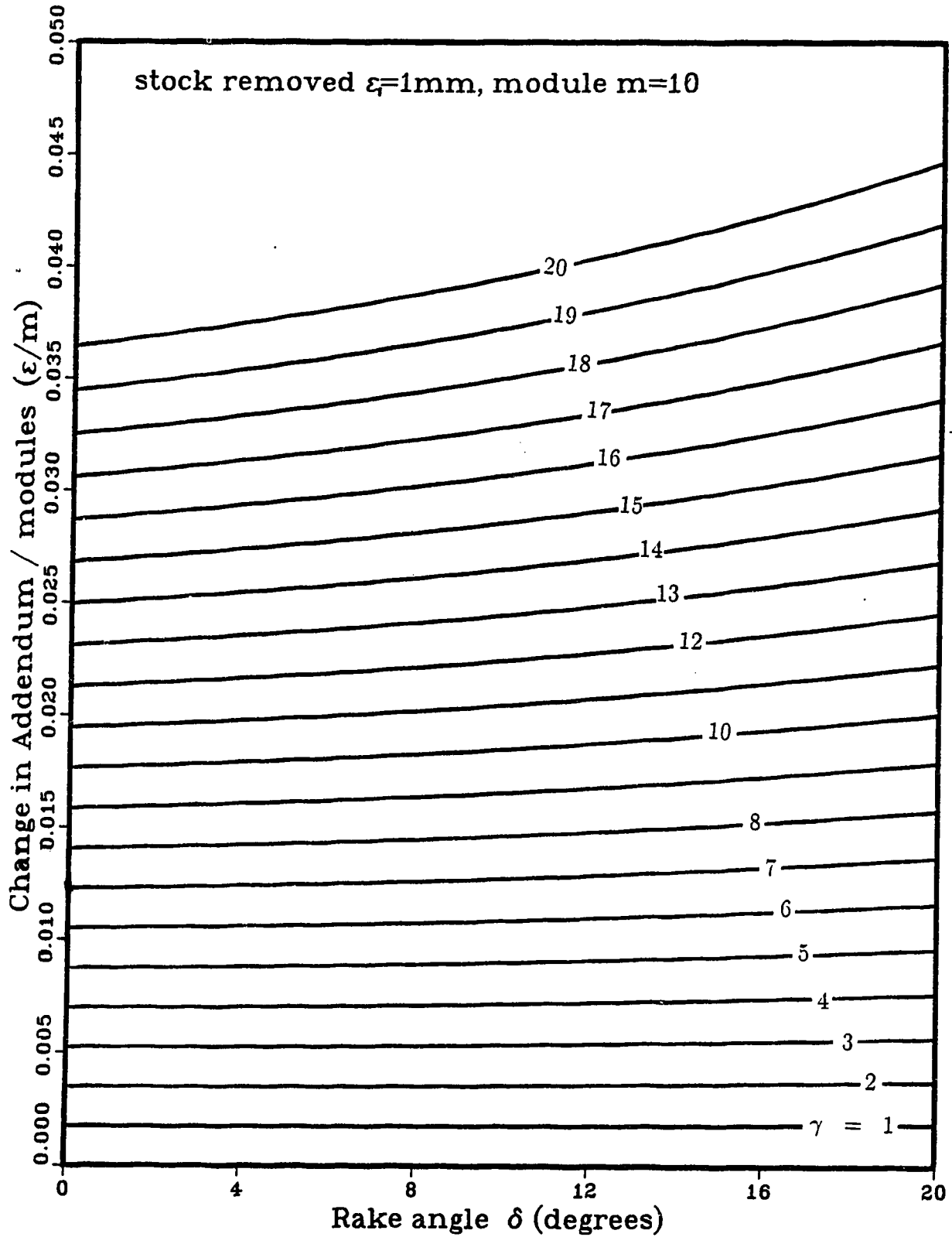


Figure 4.4: Variation of addendum with rake angles for different front relief angles

variation (normal deviation) of the profiles from the theoretical, can be clearly seen in figure 4.7. Figure 4.8 shows the normal deviation in the generated gear profile throughout the life of the cutter. The horizontal break in the normal deviation plots marks the location of the start of the non-involute tip section of the cutter. Since the profiles are drawn with reference to the theoretical profile at the initial design distance, a lateral displacement in the plot corresponds to the profile shift of the newly exposed cutting edge when the cutter is resharpened.

4.2 New design

For the new design, the change in the tooth thickness and addendum of the cutter on resharpening and its effect on the generated gear can be investigated and the effects compared with those of the conventional design.

When ϵ_1 amount of stock is removed from the conical rake face, the amount of change in addendum ϵ ($\simeq e$), change in design distance, and the design distance itself are given as before by,

$$\epsilon = \frac{\epsilon_1 \sin \delta^*}{\cos(\delta^* + \gamma)} \quad (4.8)$$

$$\epsilon_2 = \frac{\epsilon_1 \cos \delta^*}{\cos(\delta^* + \gamma)} \quad (4.9)$$

$$b]_i = b - i\epsilon_2 \quad (4.10)$$

4.2.1 Cutter addendum

The changes in the cutter addendum on resharpening are the same as in the old design. Hence the plots drawn in the figures 4.2, 4.3, and 4.4 also hold for the new design.

$$h_a]_i = h_a^D - b \tan \delta - i\epsilon \quad (4.11)$$

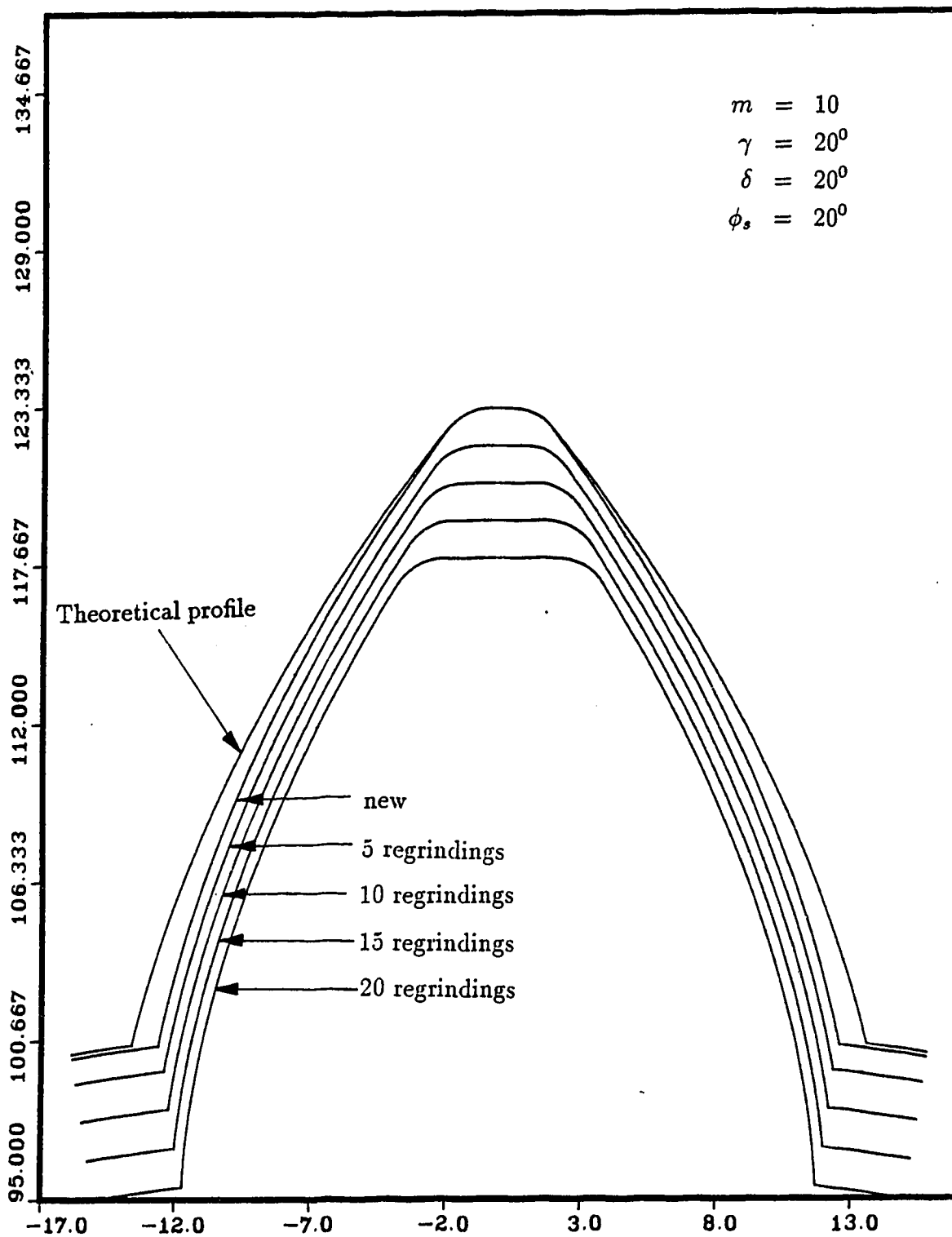


Figure 4.5: Overlaid profiles of cutter after resharpenings(conventional design)

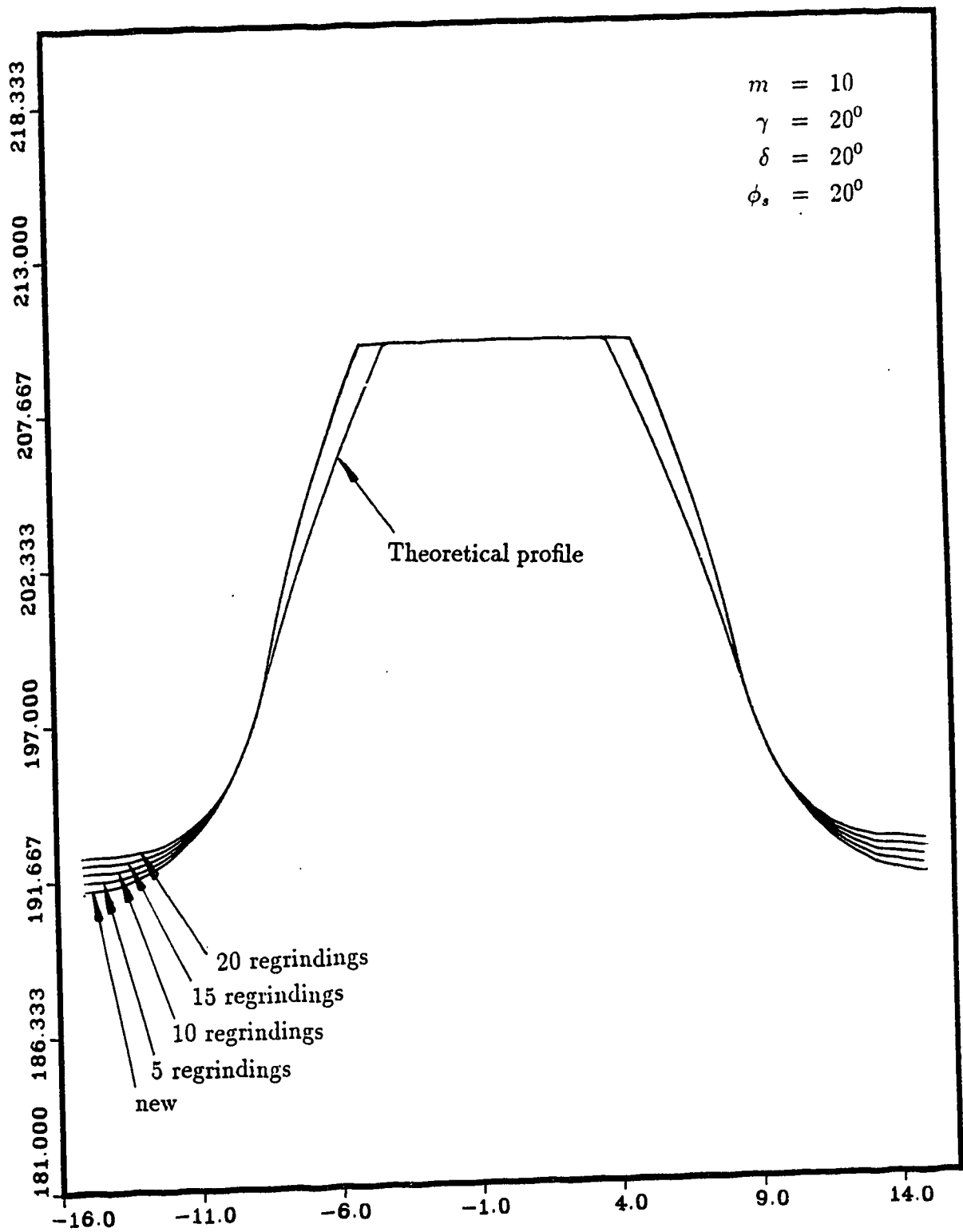


Figure 4.6: Overlaid gear profiles generated by corresponding resharpened cutter profiles

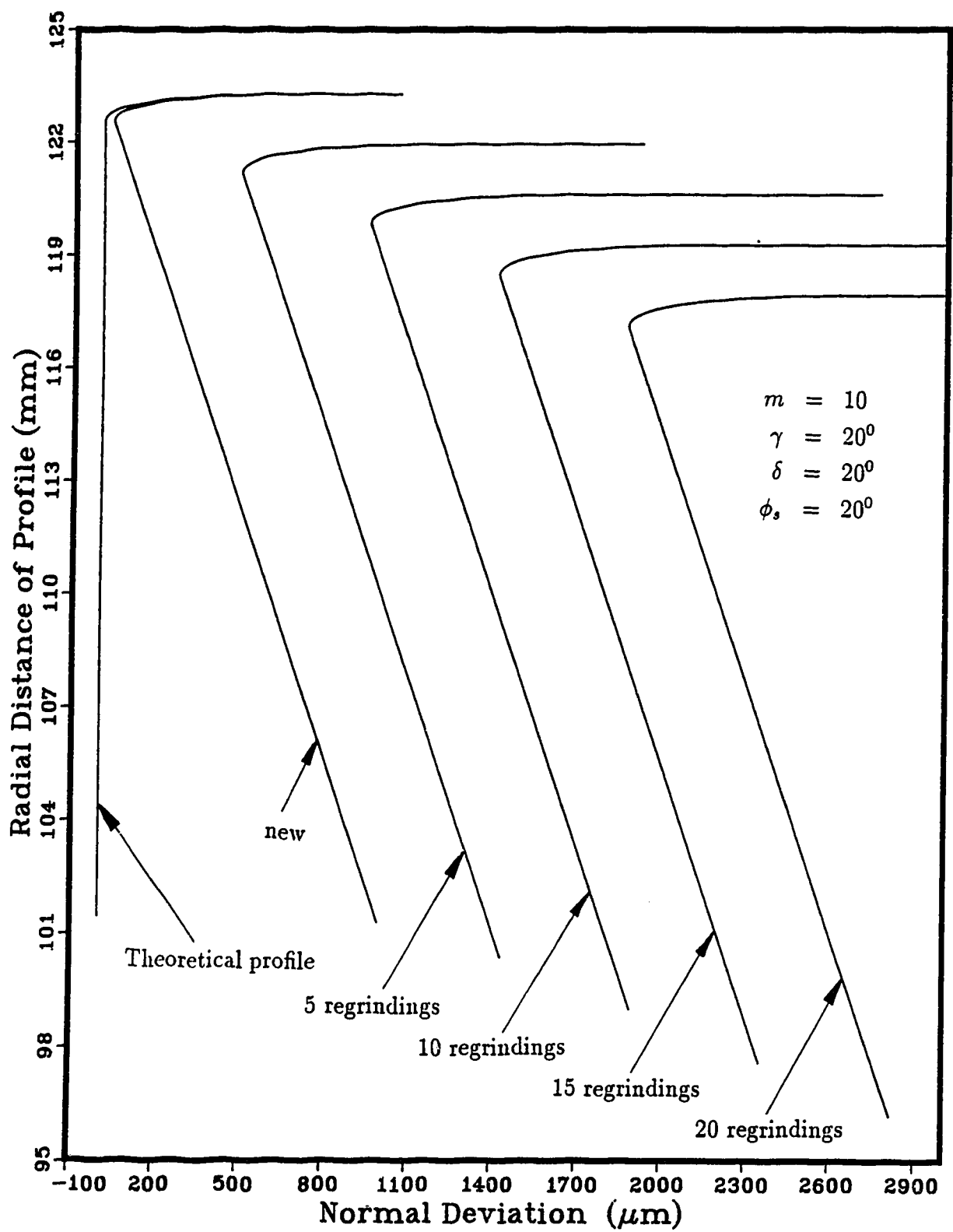


Figure 4.7: Cutter profile normal deviation on resharpener

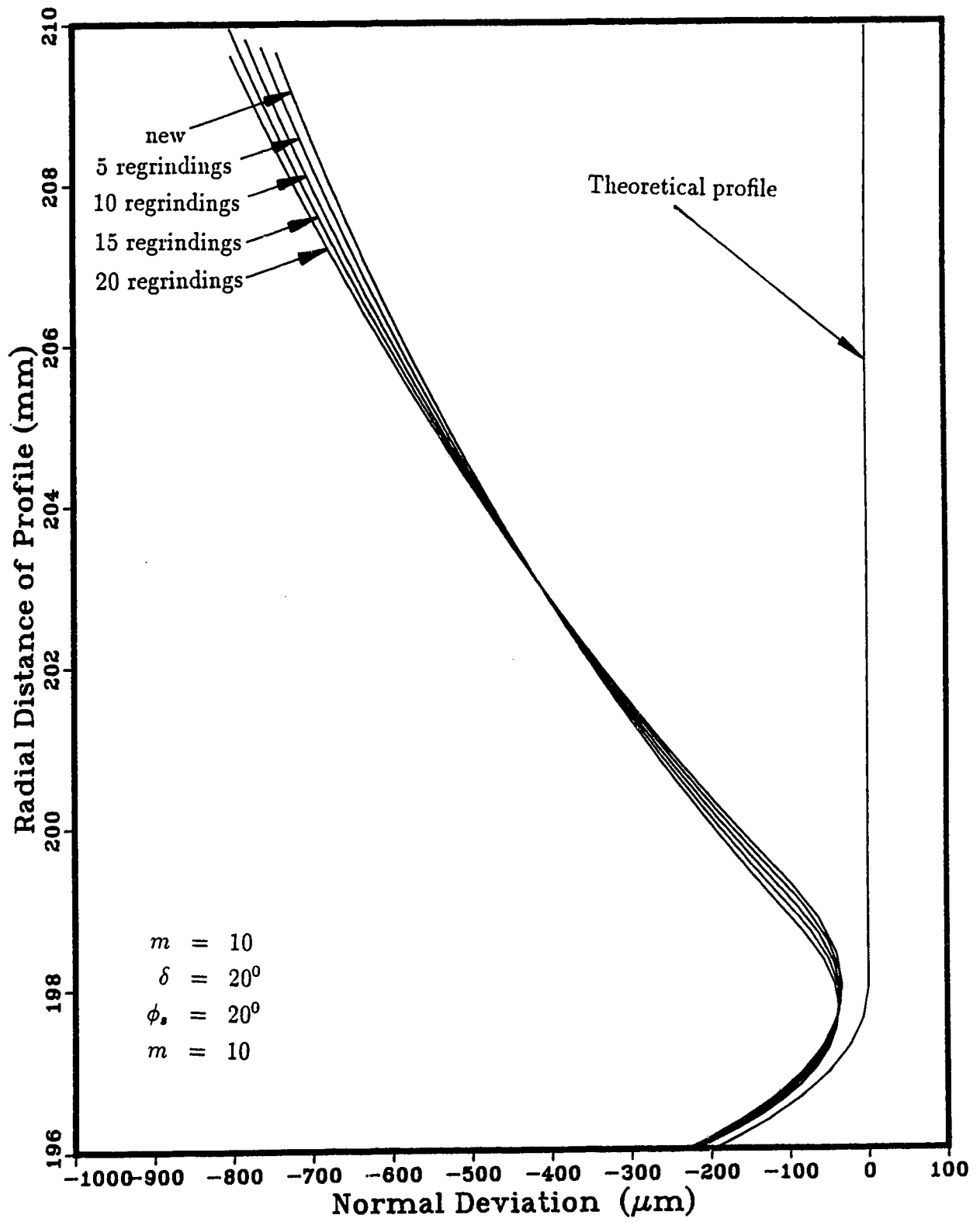


Figure 4.8: Generated gear profile normal deviations

where δ is the front rake angle at step I (Figure 3.2) and is given by re-arranging equation 3.4:

$$\tan \delta = \frac{\tan \delta^*}{(1 - \tan \delta^* \tan \gamma)k} \quad (4.12)$$

where δ^* is the front rake angle of the cutter and k is the relief correction factor mentioned in Section 3.4.

4.2.2 Cutter tooth thickness

The tooth thickness of the cutter after i resharpenings can be written as,

$$t_{sc}^D]_i = t_{sc}^D + 2b \tan \delta \tan \phi_s - 2i \epsilon_2 \tan \delta \tan \phi_s \quad (4.13)$$

where t_{sc}^D is the tooth thickness of the design section .

Figure 4.9 shows a number of overlaid effective profiles of the new cutter after different number of resharpenings of the shaper cutter. It must be pointed out that all the effective profiles belong to a family of shifted involute profiles having the same base circle. Figure 4.10 shows the overlaid profiles of a gear generated by the cutter at corresponding stages of resharpenings. To investigate the deviation in the new cutter, if any, in the cutter and the gear, the normal deviation plots are also drawn (Figure 4.11 and 4.12). Both the profiles (cutter and gear) are vertical indicating no profile deviations. The breaks in the profiles correspond to the start of the tip section in the cutter and the fillet section in the generated gear.

4.3 Comparison of conventional and new cutter

It is clear from figure 4.7 that the effective profile of the cutter in the conventional design changes throughout the cutter life. Hence the shape of the gear, cut by

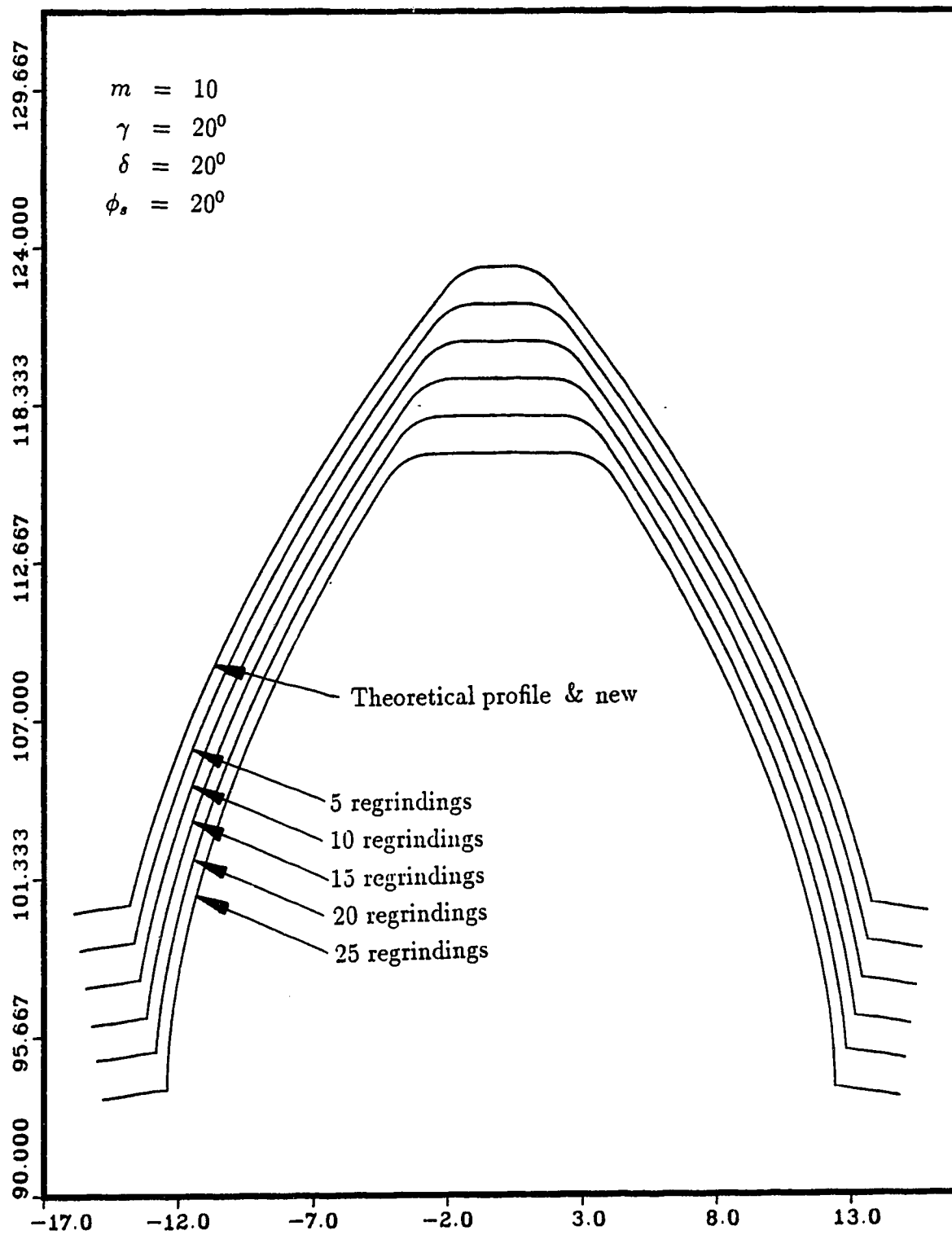


Figure 4.9: Overlaid profiles of cutter after resharpenings(new design)

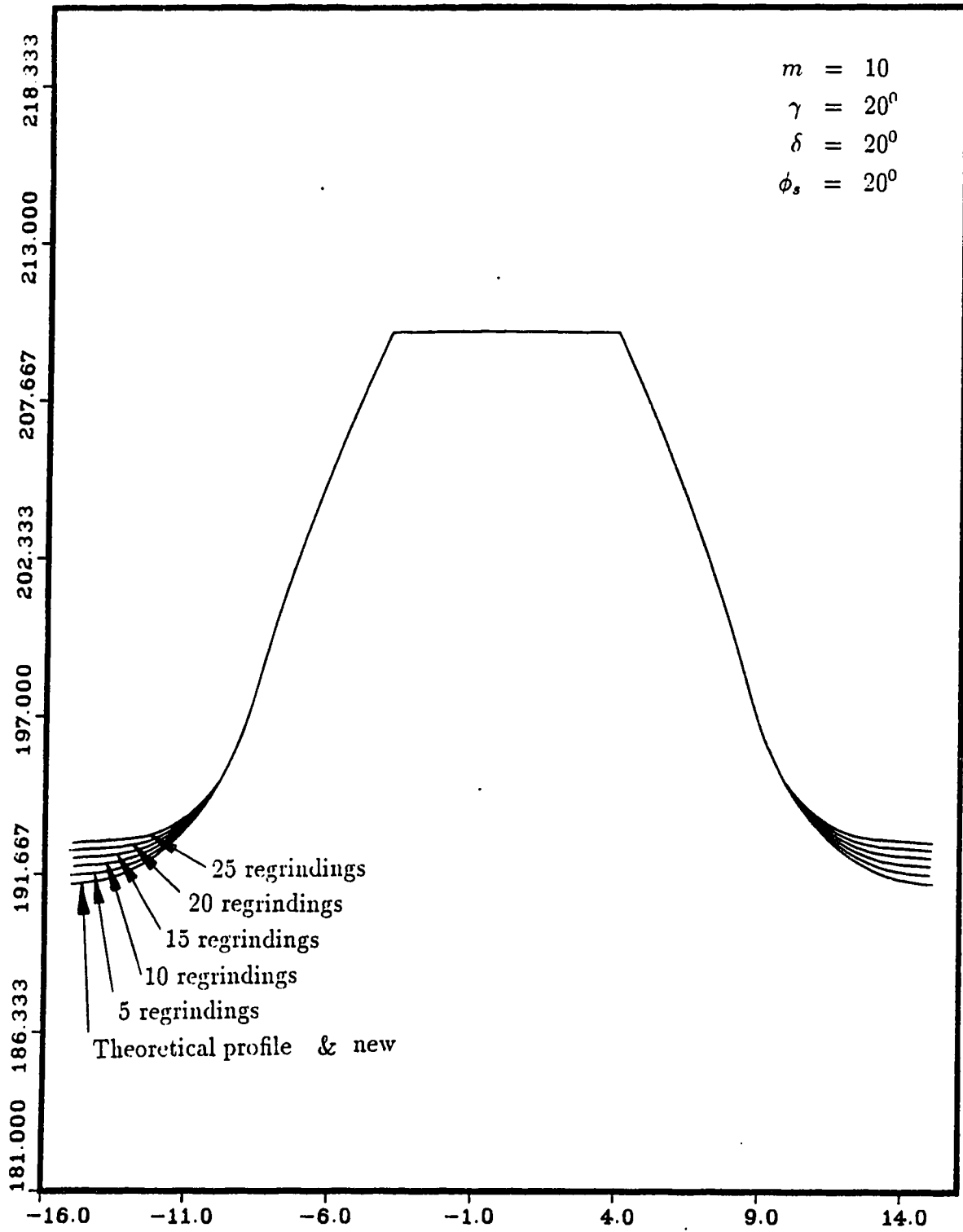


Figure 4.10: Overlaid gear profiles generated by corresponding resharpened cutter profiles

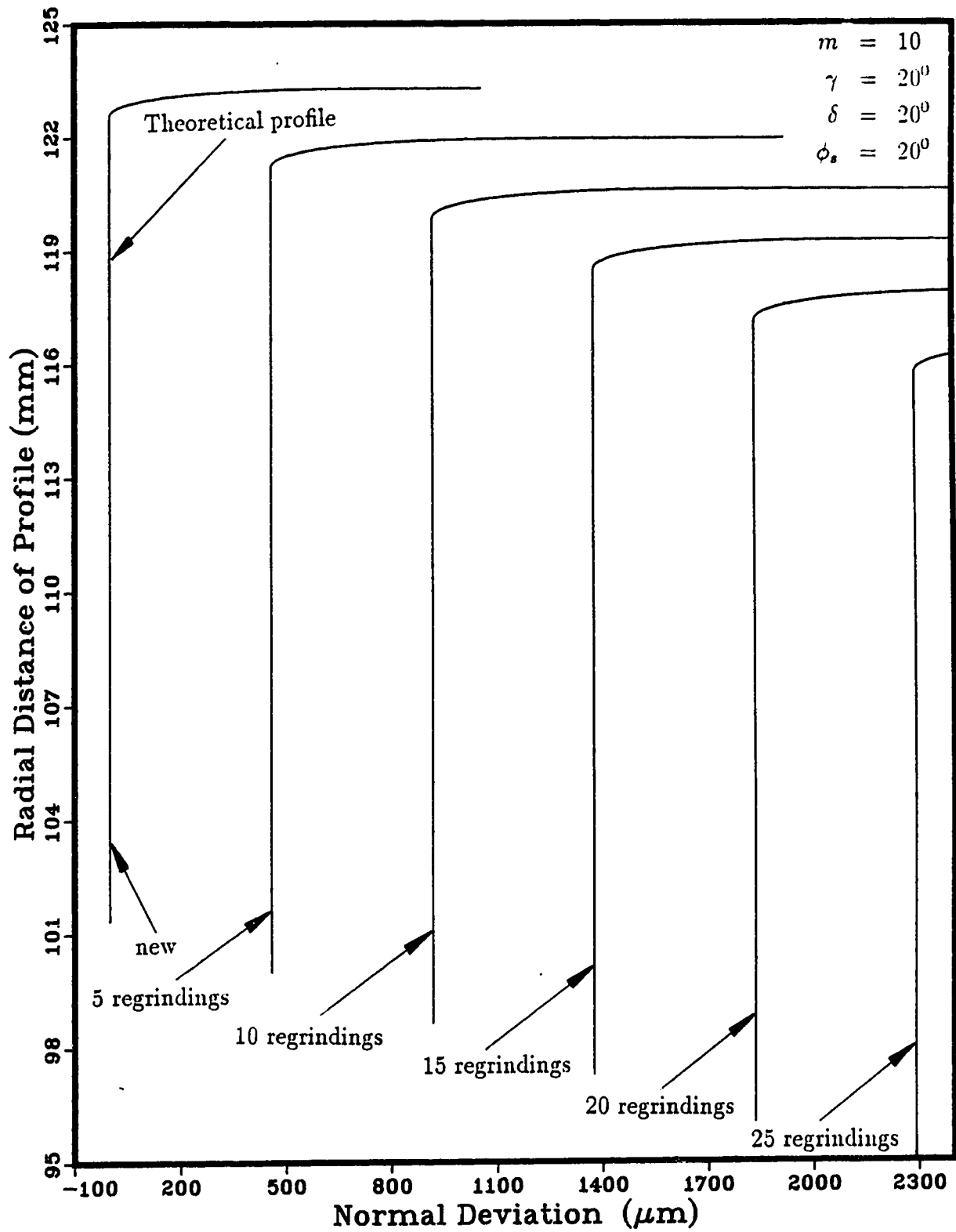


Figure 4.11: Overlaid normal deviation curves of cutter after resharpenings(new design)

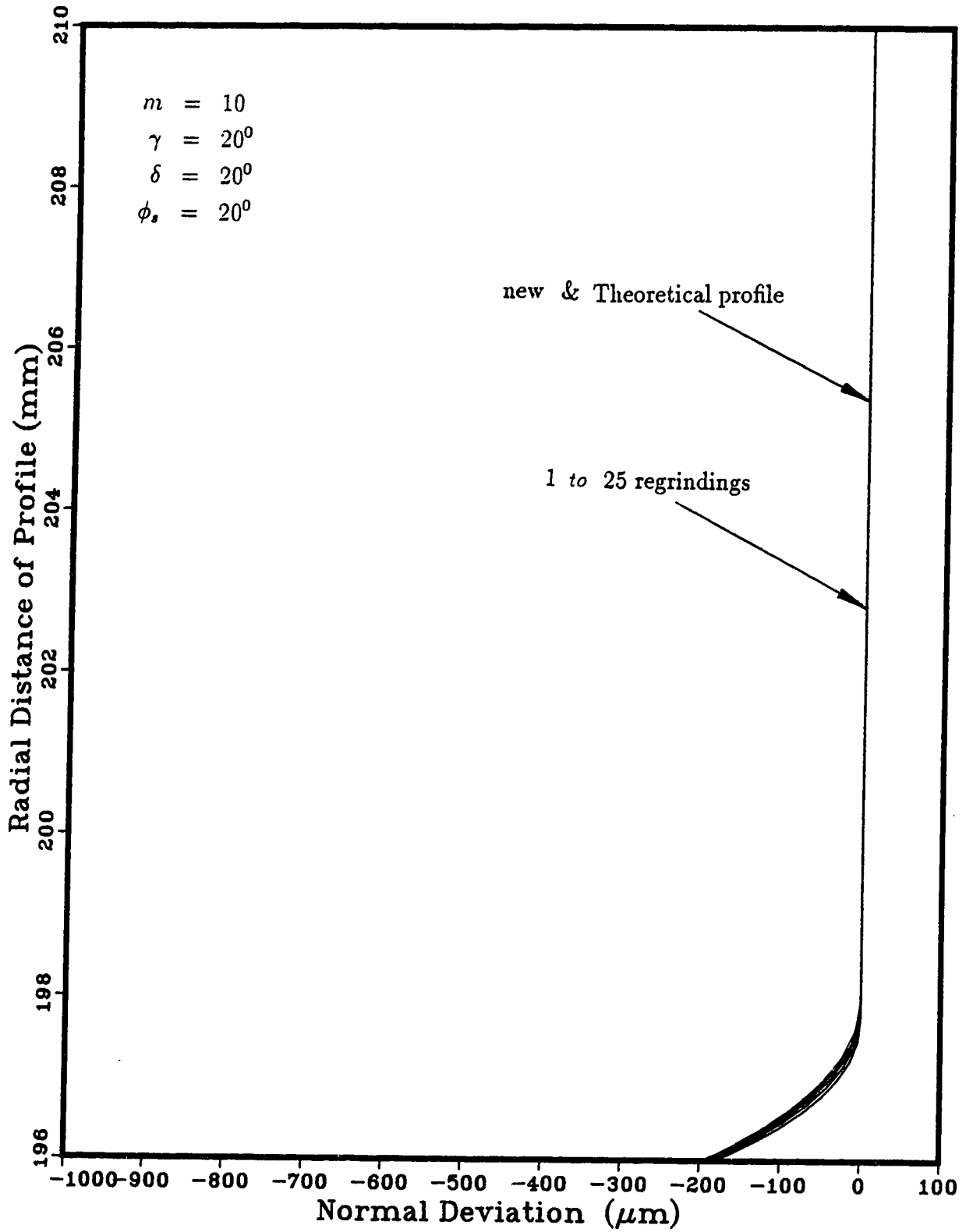


Figure 4.12: Overlaid normal deviation curves of gear profiles generated by corresponding resharpended cutter profiles

the cutter after any number of resharpenings, does not remain the same but varies depending upon the number of resharpenings, tooth size (m) and the cutting angles (γ, δ).

The new design permits higher rake and relief angles without any profile deviations and always presents a new shifted involute effective profile on resharpening, throughout cutter life. Thus there is no deviation in the generated gear active profile, throughout the life of the cutter.

Chapter 5

Effect of Resharpener on tooth tip corners

The fillet shape and size in a gear is important since the AGMA (American Gear Manufacturers Association) geometry factor J , which is required for calculating the fillet stress, depends on it. Also, in certain situations, the need to pass more power through existing transmissions without major re-designs has led to increased attention on the fillet shape.

The form of the tooth tip in the cutter determines " r_f " (the fillet radius of curvature at the point where it meets the root circle) in the generated gear. If other parameters are held constant, a larger cutter radius and a larger tip circle radius produce a larger r_f , which tends to increase the magnitude of J , which in turn results in reduction of fillet stress. However, the tip corner radius of the cutter and the position of its centre does not remain constant throughout the cutter life because of resharpener. The effects of these changes on the cutter tip radius and on the generated gear fillet are investigated in this chapter.

5.1 Cutter tip corner surface

As mentioned in section 2.3 the cutter is primarily made up of five surfaces. Of these five surfaces, the tooth tip corner surface is the most difficult to design theoretically and to generate practically. For a smooth transition between the conical tooth tip surface and the side involute helicoid surface, the tooth tip corner surface has to be tangent to both the former two surfaces throughout the entire usable cutter depth. For ease of analysis, on each horizontal section through the cutter, the transition curve between the circular tip profile and the involute side profile is usually taken to be an arc of a circle. Thus, we shall have a tip corner surface which is the envelope of a series of circles at different sections on the cutter, such that they are tangent to the corresponding involutes and tip circles. To define the surface of the corner profile the following two cases can be considered:

1. The transition corner surface is a part of an oblique cylinder touching both the tip conical surface and the side helicoid surface.
2. The transition corner surface is a part of an oblique frustum of a cone touching both the tip conical surface and the side helicoid surface.

In both cases, if the corner surface has to touch both the tip conical surface and the side helicoid surface, then the axis of the cylinder or the conical frustum will not, in general, be a straight line. The equation of the axis can be found and may be used as a guide for the path of the grinding tool during manufacturing (in guide templates or CNC part programs).

The radius of curvature of the gear fillet is not in the form of a true circle but varies, having minimum (r_f) at the root surface and maximum at the flank, as can be seen from the sample data in Appendix B. Figure 5.1 shows the variation of the

radius of curvature for a specific case. This minimum radius of curvature r_f at the point where the fillet meets the gear root is important because this is used for the calculation of the AGMA geometry factor J and the fillet stress.

Another important point that should be mentioned is the presence of the rake face cone which will slightly alter the effective shape (on projecting on projection plane) of the cutter corner radius slightly. Hence, the effective tooth corner profile will not truly be an arc of a circle, but since the gear fillet generated is only a supporting profile and not a working profile, this slight deviation does not matter. Moreover, the variation due to the rake angle is negligible compared to the overall cutter corner shape and since the corner tooth shape, at the cutter tooth tip is almost undisturbed by the presence of rake angle, the generated fillet radius r_f at the gear tooth root remains essentially unchanged. Therefore, for all subsequent calculations and analyses, the effect of rake angle on the cutter corner tip is neglected.

5.2 Oblique cylindrical cutter corner surface

In the case of an oblique cylindrical corner surface, it is assumed that the tooth corner radius remains unaltered at all sections of the cutter, as shown in Figure 5.2.

The axis of this cylinder would be the curve of intersection of a cone, parallel to the tooth tip cone of the cutter and a helicoid surface parallel to the side helicoid involute surface of the cutter, both the parallel surfaces being separated in the horizontal plane by a distance equal to the radius of the tip corner circle. This is because in any horizontal plane, if the tip corner circle rolls on the root tip circular arc and on the side involute profile, then its centre will also describe a parallel circular arc and a parallel involute, whose intersection will be the centre of the cutter tip corner arc. Hence, in effect the axis of the corner oblique cylinder of the cutter (C_u) can

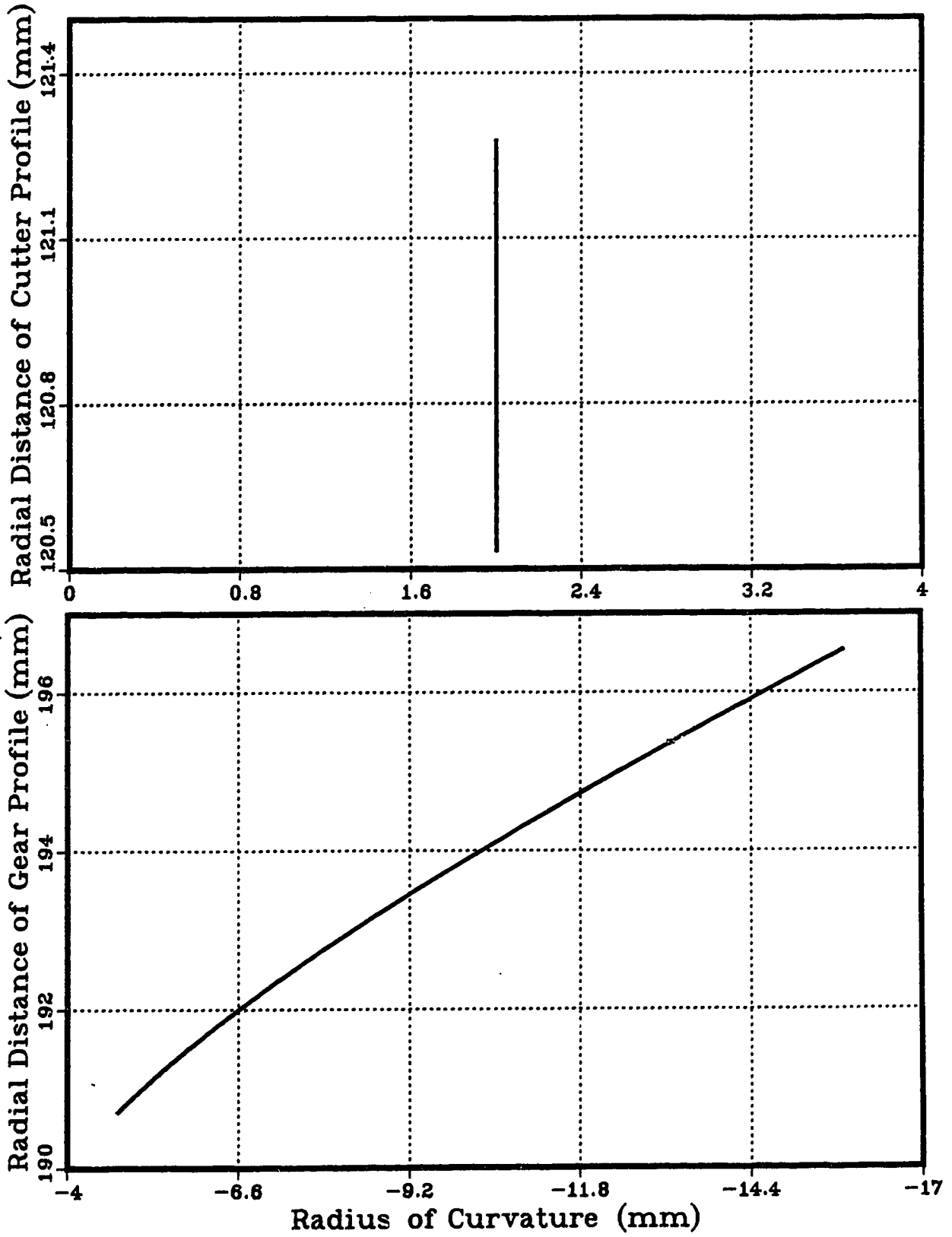


Figure 5.1: Variation of radius of curvature of the gear fillet

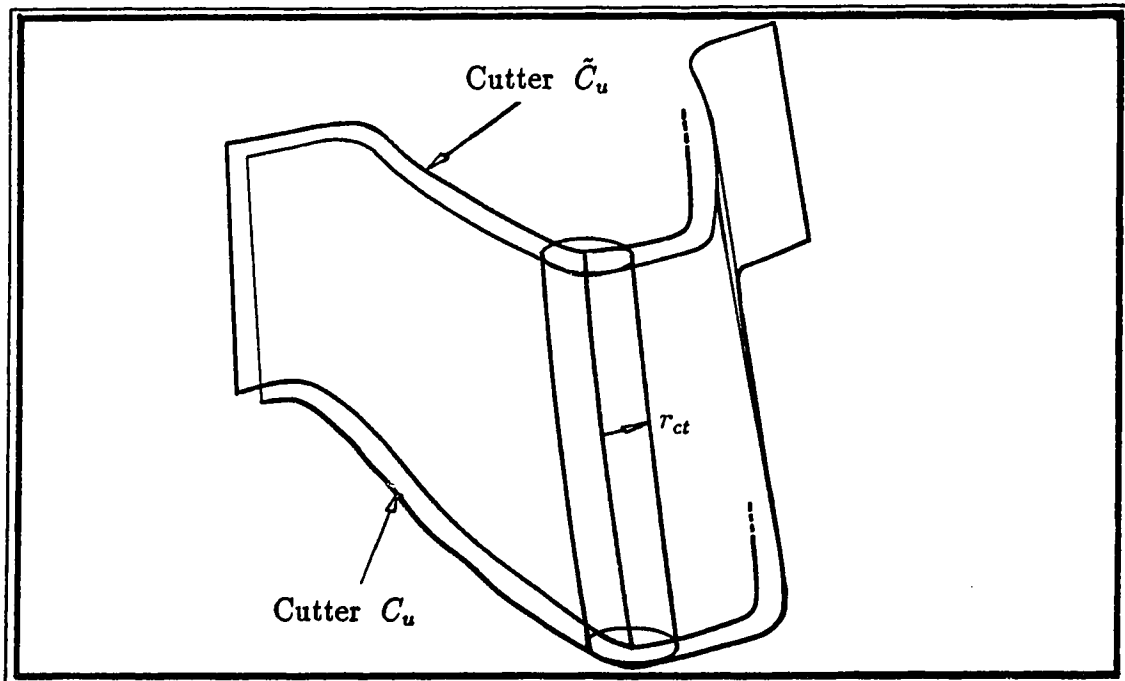


Figure 5.2: Cylindrical cutter tooth corner surface

be obtained by evaluating the curve of intersection of the tooth side helicoid edge and the tip circular cone of a smaller imaginary concentric cutter (\tilde{C}_u), having no rounding at the tooth tips.

5.2.1 Equation of axis of oblique corner cylinder

At any section $A - A$ (Figure 5.3), where the tooth thickness is t_{sc}^A and the radius of the tip is R_{tc}^A for the cutter C_u , the corresponding values for the parallel surfaces, of cutter \tilde{C}_u , shifted horizontally by r_{ct} are denoted by a tilde over the symbols and are given by:

$$\tilde{R}_{tc}^A = R_{tc}^A - r_{ct} \quad (5.1)$$

Since the difference in the tooth thickness of cutters C_u and \tilde{C}_u at the base circle

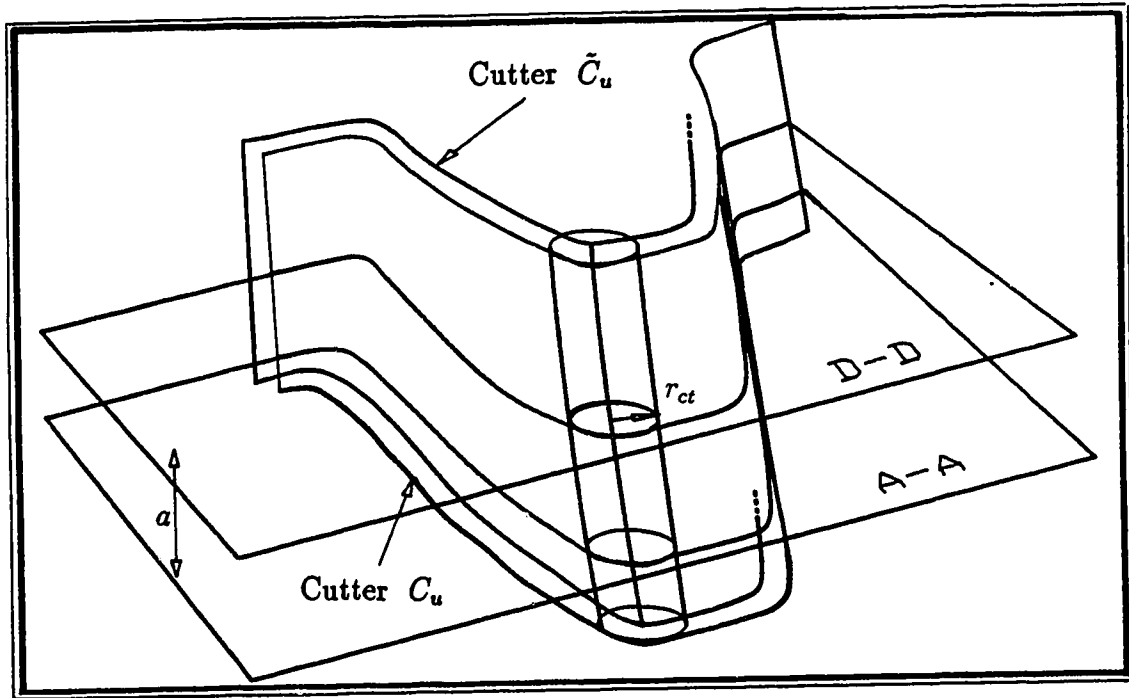


Figure 5.3: Axis of tooth tip corner oblique cylinder

is given by,

$$\tilde{t}_{bc}^A = t_{bc}^A - 2r_{ct} \quad (5.2)$$

$$\text{therefore, } \tilde{t}_{sc}^A = t_{sc}^A - 2r_{ct} \cdot \frac{R_{sc}}{R_{bc}} \quad (5.3)$$

Hence, the co-ordinates of the centre of the tooth tip circle at section $A - A$ can be evaluated.

$$R_C^A = R_{tc}^A - r_{ct} \quad (5.4)$$

$$\theta_C^A = \frac{t_{sc}^A}{2R_{sc}} - \frac{r_{rt}}{R_{bc}} + inv\phi_s - inv\cos^{-1}\left(\frac{R_{bc}}{R_C^A}\right) \quad (5.5)$$

$$z_C = -a \quad (5.6)$$

The equation of the axis can be written in the parametric form, where the function

parameter is the section distance “ a ”.

$$R_C^A = R_{sc} + h_a^D + a \tan \delta - r_{ct} \quad (5.7)$$

$$\theta_C^A = \frac{t_{sc}^D + a \tan \delta \tan \phi_s}{2R_{sc}} - \frac{r_{ct}}{R_{bc}} + \quad (5.8)$$

$$\text{inv} \phi_s - \text{inv} \cos^{-1} \left(\frac{R_{bc}}{R_{sc} + h_a^D + a \tan \delta - r_{ct}} \right) \quad (5.9)$$

$$z_C = -a \quad (5.10)$$

The above equation of the axis of the oblique corner cylinder is a part of a helical spiral of form: $x = f(t) \cos(t)$, $y = f(t) \sin(t)$, $z = bt$. However, the length of the axis between the usable width of the cutter is approximately linear, and can be replaced by a straight line joining the corner circle centre at the tip section to that at the design section. This makes the corner surface an oblique cylinder with straight axis which eases analysis and manufacturing, without substantial error.

5.2.2 Fillet generated by oblique corner cylinder

The magnitude (neglecting the sign) of the radius of curvature of the gear fillet generated is found by an expression derived from the Euler–Savary equation,

$$\rho_f = r_{ct} + \frac{(r_{ct} + s)^2}{R_0 \sin \phi - (r_{ct} + s)} \quad (5.11)$$

where R_0 is,

$$R_0 = \frac{N_g N_c}{(N_g + N_c)^2} \cdot C^C \quad (5.12)$$

Since the fillet stress depends on the radius of curvature of the fillet where it touches the root circle ([4], pages 250-254) it is important to be aware of the change of the this radius of curvature “ r_f ” during resharping of the cutter. As explained

in section 1.4.2, the angle α_c that the radius vector at any point of the cutter makes with the line of centres (Figure 1.7) is given by equation 1.35 as

$$\alpha_c = \cos^{-1} \left(\frac{R_c}{R_{pc}} \cos \phi_c \right) - \phi_c \quad (5.13)$$

The upper end of fillet is cut by the end point "B" of the involute of the cutter profile (Figure 1.5) while the lower end of the fillet is cut by the end point "A" of the corner radius of the cutter. The cutter inclination when cutting the upper end of the fillet is:

$$\alpha_c = \cos^{-1} \left(\frac{R_{bc}}{R_{pc}} \right) - \phi_c \quad [R_c \cos \phi_c = R_{bc}] \quad (5.14)$$

while the cutter inclination when cutting the lower end of the fillet is:

$$\alpha_c = 0 \quad [\text{since } \phi_c = 0] \quad (5.15)$$

At this position, when the cutter generates the lower end of the fillet, the coordinates (ξ, η) and s are equal to:

$$\xi = R_{pc} - R_{tc} \quad (5.16)$$

$$\eta = 0 \quad (5.17)$$

$$s = R_{pc} - R_{tc} \quad (5.18)$$

Inserting these values into the Euler-Savery equation ([4], eq 1.47) we get the radius r_f of the fillet at point where it meets the root circle,

$$r_f = r_{ct} + \frac{(R_{tc} - R_{pc} - r_{ct})^2}{R_0 + (R_{tc} - R_{pc} - r_{ct})} \quad (5.19)$$

where R_0 is given by equation 5.12.

Inspecting the above equation it can be found that a reduction in R_{tc} , R_{pc} and R_{pg} caused by the successive resharpening of the cutter, will result in a reduction in the value of r_f .

The effect of resharpening a cutter with an oblique cylindrical corner tip profile has been simulated through a computer program. Figure 5.4 shows the effect of successive resharpening of the cutter tip while Figure 5.5 shows the effect of these resharpened cutter tip profiles on the generated gear profiles. Figure 5.6 shows the effect of resharpenings on the radius of curvature of the fillet region.

5.3 Oblique conical cutter corner surface

As verified in the last section, an oblique corner cylinder profile produces a successively smaller fillet radius on resharpening the cutter. This effect can be compensated for by replacing the oblique cylindrical surface by a conical oblique frustum.

On inspecting equation 5.17 we find that a larger value of r_{ct} will result in a larger fillet radius r_f in the generated gear. Hence if the decrease in the generated gear fillet radius due to reduction of the cutter tip circular radius " R_{tc} " on resharpening, is compensated for by provided a larger cutter corner tip radius " r_{ct} " at upper section planes in the cutter as shown in figure 5.7, then better results could be obtained in our attempt to achieve constant gear fillet radius " r_f " throughout cutter life.

For the sake of simplicity, the increase in cutter corner tip radius can be made linear, which however, does not ensure that the axis of the cutter oblique corner conical frustum will be an exact straight line, though it will be an approximate one. Letting the cutter tooth corner radius at the design section be r_{ct}^D , this generates a gear fillet radius " r_f " where,

$$r_f = r_{ct}^D + \frac{(R_{tc}^D - R_{pc}^D - r_{ct}^D)^2}{R_0^D + (R_{tc}^D - R_{pc}^D - r_{ct}^D)} \quad (5.20)$$

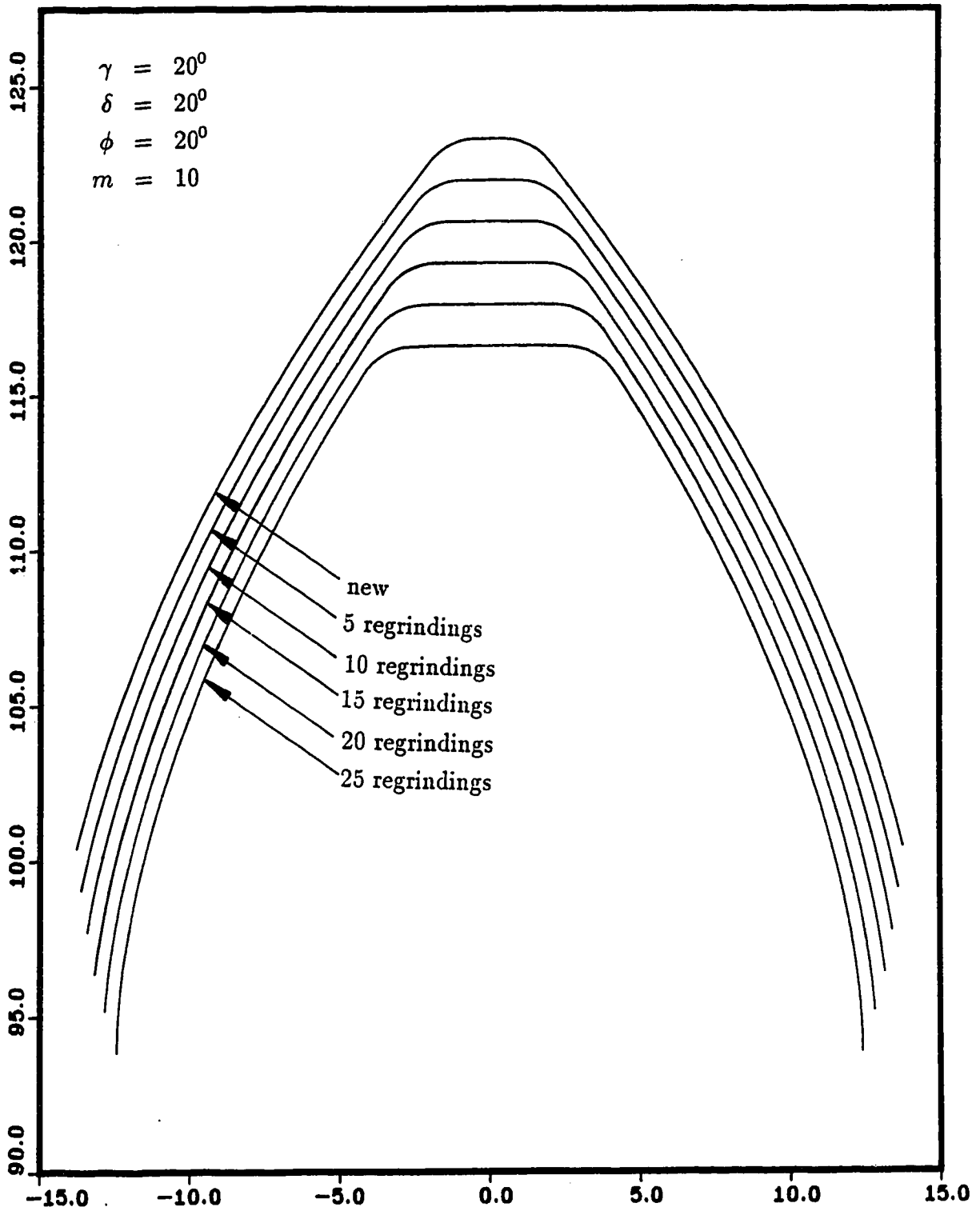


Figure 5.4: Overlaid resharpened cutter tip profiles

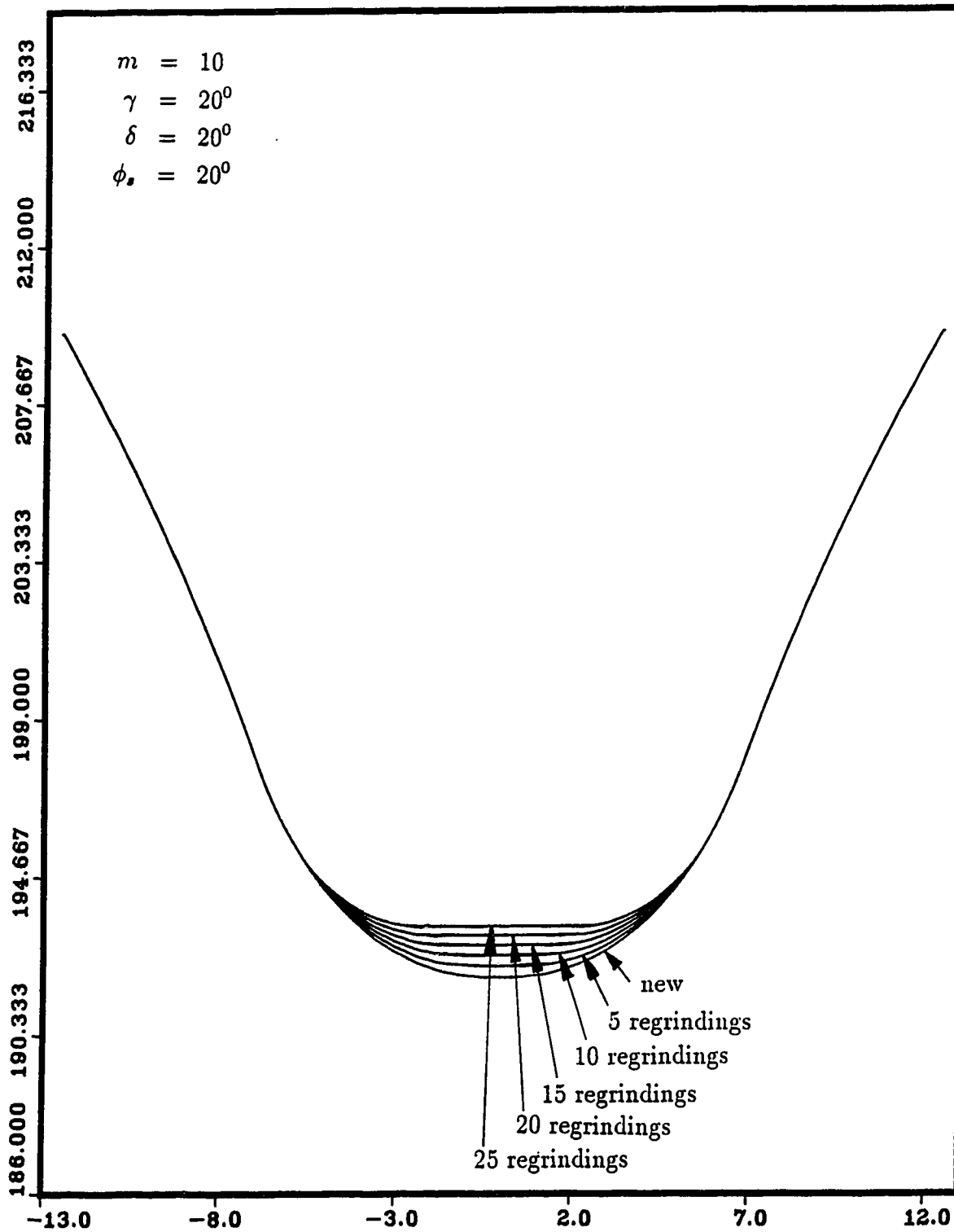


Figure 5.5: Overlaid generated gear fillet profiles

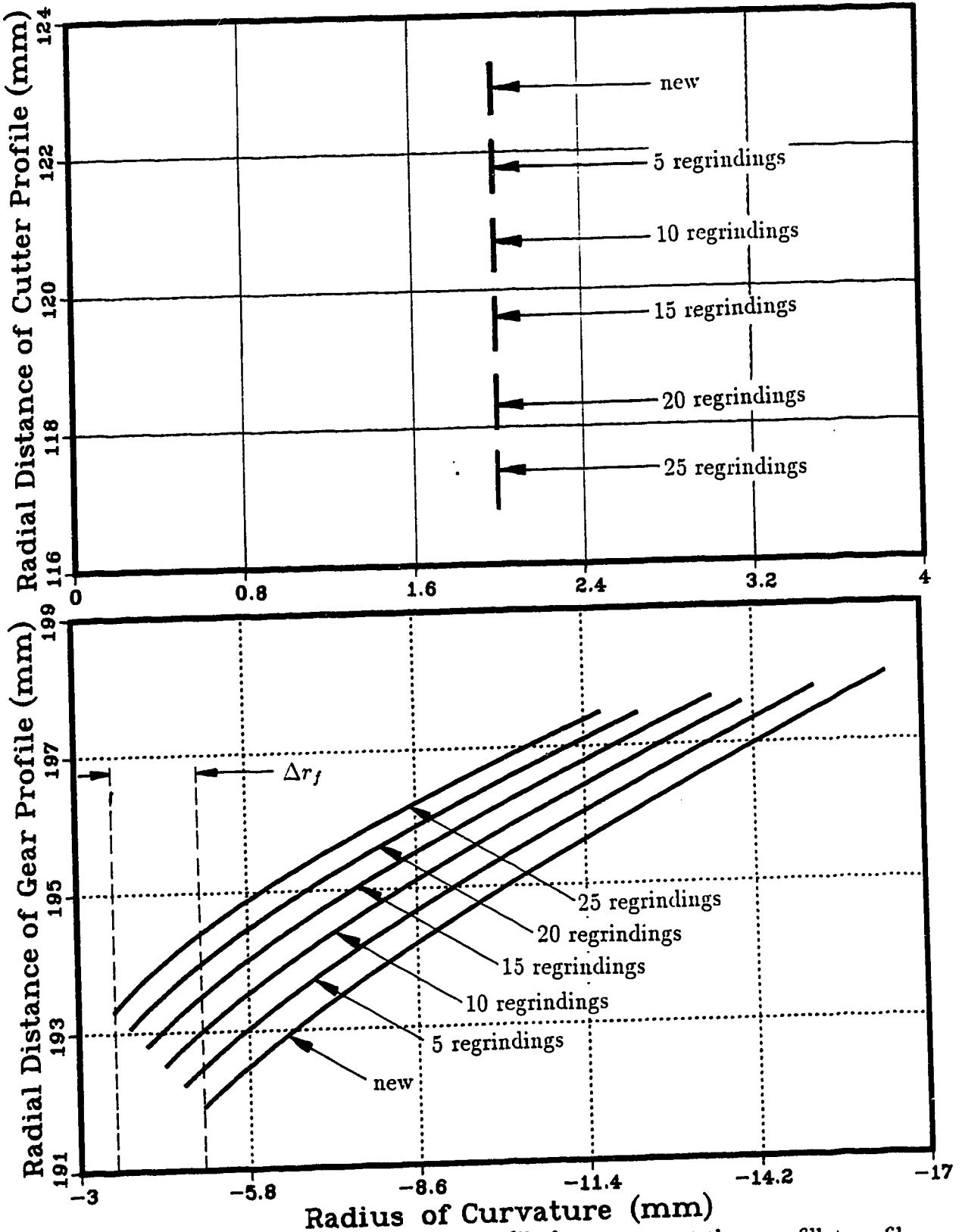


Figure 5.6: Effect of resharpenings on radii of curvatures at the gear fillet profile

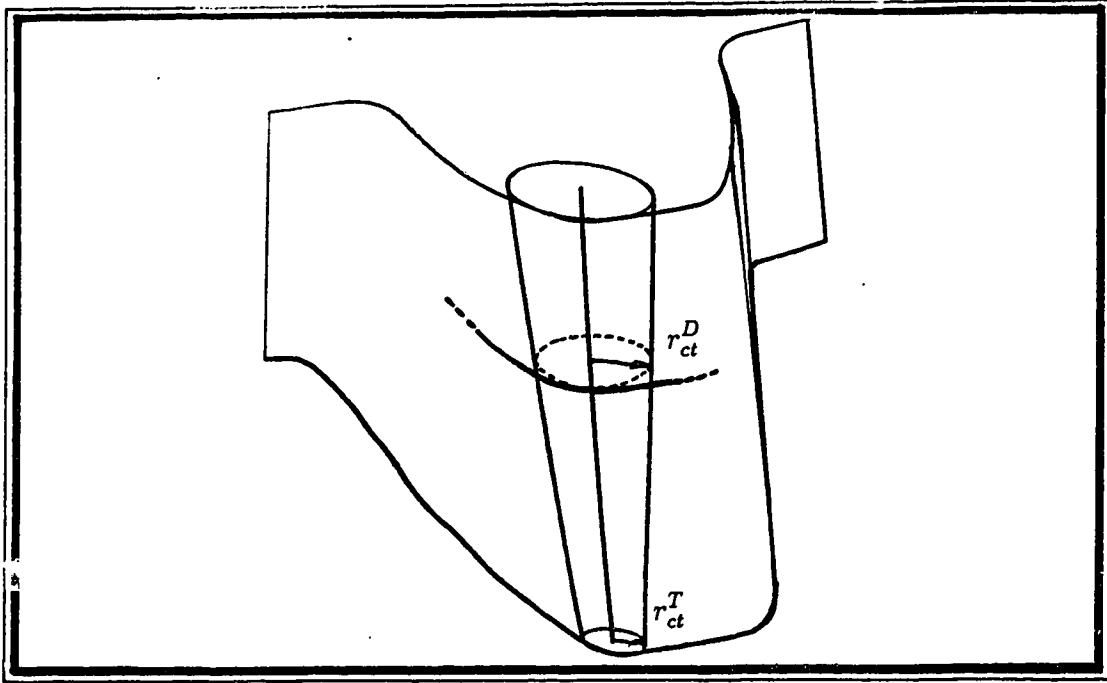


Figure 5.7: Oblique conical cutter corner surface

where,

$$\frac{1}{R_0^D} = \frac{1}{R_{pg}^D} + \frac{1}{R_{pc}^D} \quad (5.21)$$

The radius of the gear fillet, generated by the cutter profile at the tip section $T - T$, will be,

$$r_f^T = r_{ct}^T + \frac{(R_{tc}^T - R_{pc}^T - r_{ct}^T)^2}{R_0^T + (R_{tc}^T - R_{pc}^T - r_{ct}^T)} \quad (5.22)$$

where,

$$\frac{1}{R_0^T} = \frac{1}{R_{pg}^T} + \frac{1}{R_{pc}^T} \quad (5.23)$$

If the radius of curvature of the gear fillet r_f^T , generated by the cutter profile at section $T - T$, is equal to the radius of curvature of the gear fillet r_f , generated by the cutter profile at the design section, then the value of the cutter tip corner radius

r_{ic}^T , at section $T - T$, has to be,

$$r_{ic}^T = R_{ic}^T - R_{pc}^T + R_0^T + \frac{(R_0^T)^2}{R_{ic}^T - R_{pc}^T - r_f - R_0^T} \quad (5.24)$$

where,

$$R_{ic}^T = R_{ic}^D + b \tan \delta \quad (5.25)$$

$$R_{pc}^T = R_{pc}^D + \frac{2b \tan \delta \tan \phi_s}{m_g + 1} \quad (5.26)$$

$$R_{pg}^T = R_{pc}^D + \frac{2b \tan \delta \tan \phi_s m_g}{m_g + 1} \quad (5.27)$$

$$\frac{1}{R_0^T} = \frac{1}{R_{pc}^T} + \frac{1}{R_{pg}^T} \quad (5.28)$$

Here the change in centre distance from the meshing position at section distance $D - D$ to that at section $T - T$ is approximately taken to be $(2b \tan \delta \tan \phi_s)$ while the gear ratio " m_g " is taken to be equal to 2 in the present case. While choosing the value of m_g it must be born in mind that when this cutter is used for cutting larger gears ($m_g > 1$) the generated gear fillet will be smaller than that generated when m_g is 1 [11].

If the radius of the cutter corner arc at all sections between $T - T$ and $D - D$ increases linearly from r_{ct}^T to r_{ct}^D , then the radius at any section at a section distance of a can be given by,

$$r_{ct}^A = r_{ct}^D - \frac{a (r_{ct}^D - r_{ct}^T)}{b} \quad (5.29)$$

Using this modification, for the same specification of gear blank as in section 5.2.2, the effects of resharpener on the cutter tip and on the generated gear fillet, is simulated (calculated parameters are shown in Appendix B). The changes in the cutter tip and the gear root are plotted in Figures 5.8 and 5.9. Clearly the conical frustum modification of the cutter corner surface generates less deviation in the gear

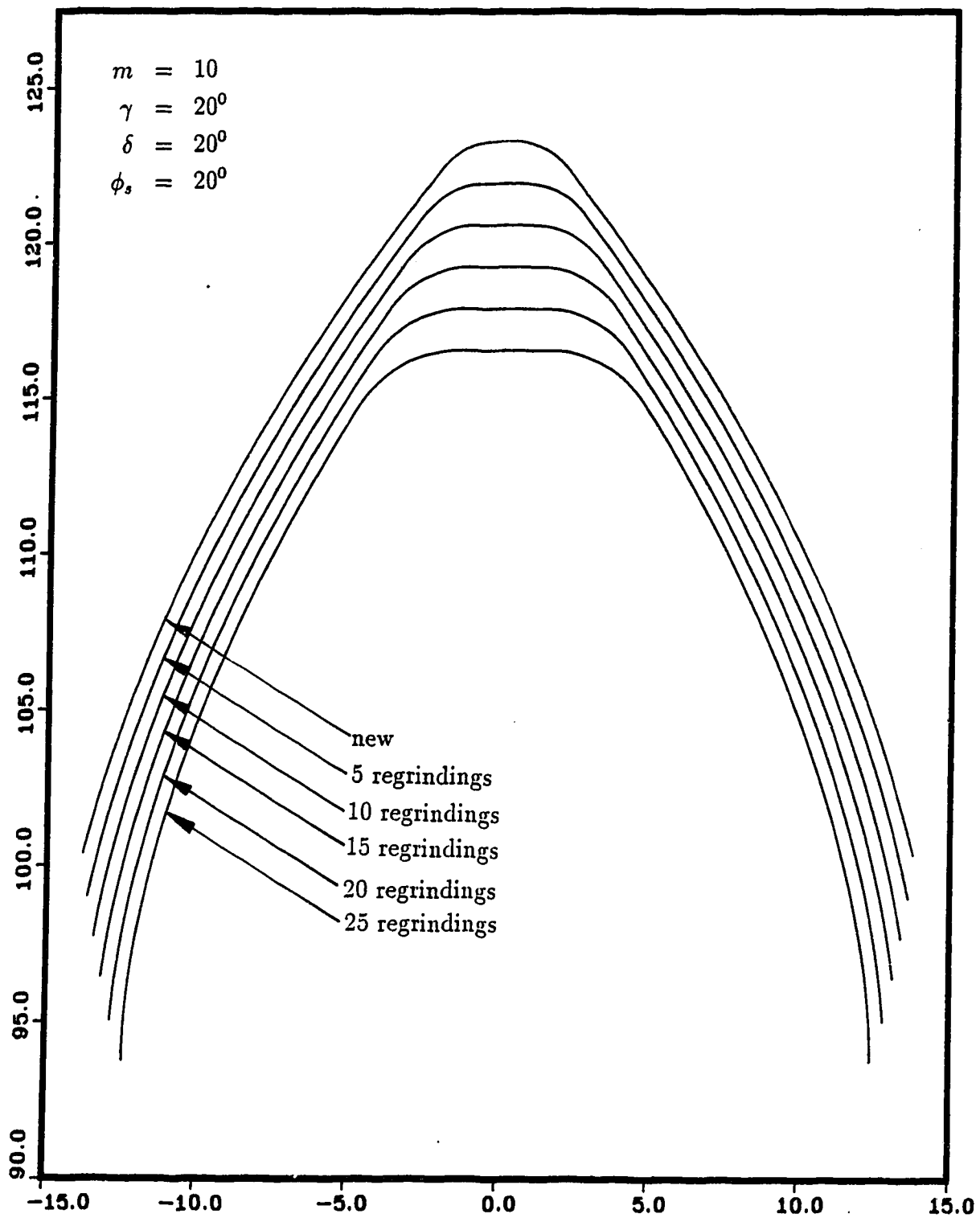


Figure 5.8: Overlaid resharpened cutter tip profiles (Conical cutter corner surface)

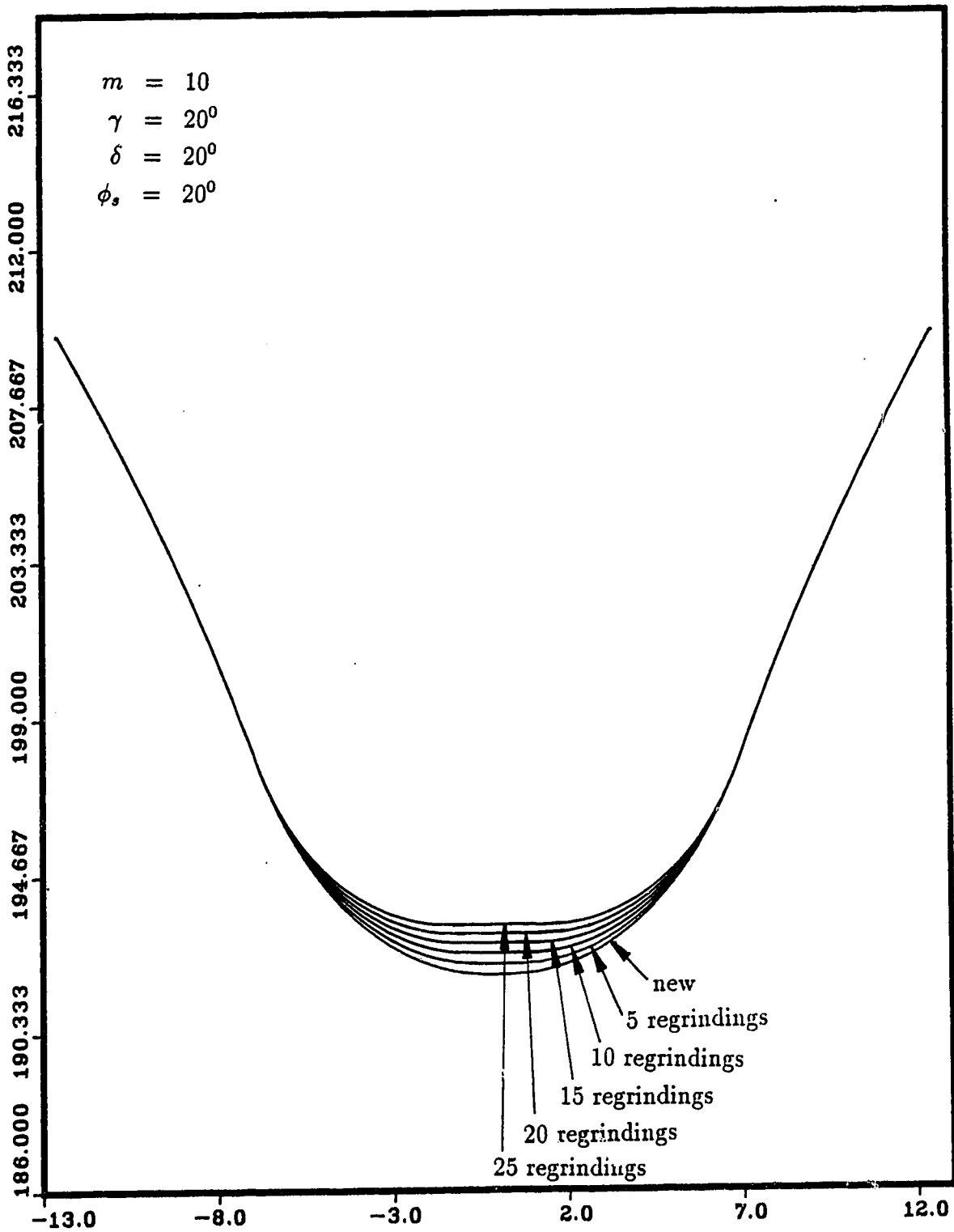


Figure 5.9: Overlaid generated gear fillet profiles (Conical cutter corner surface)

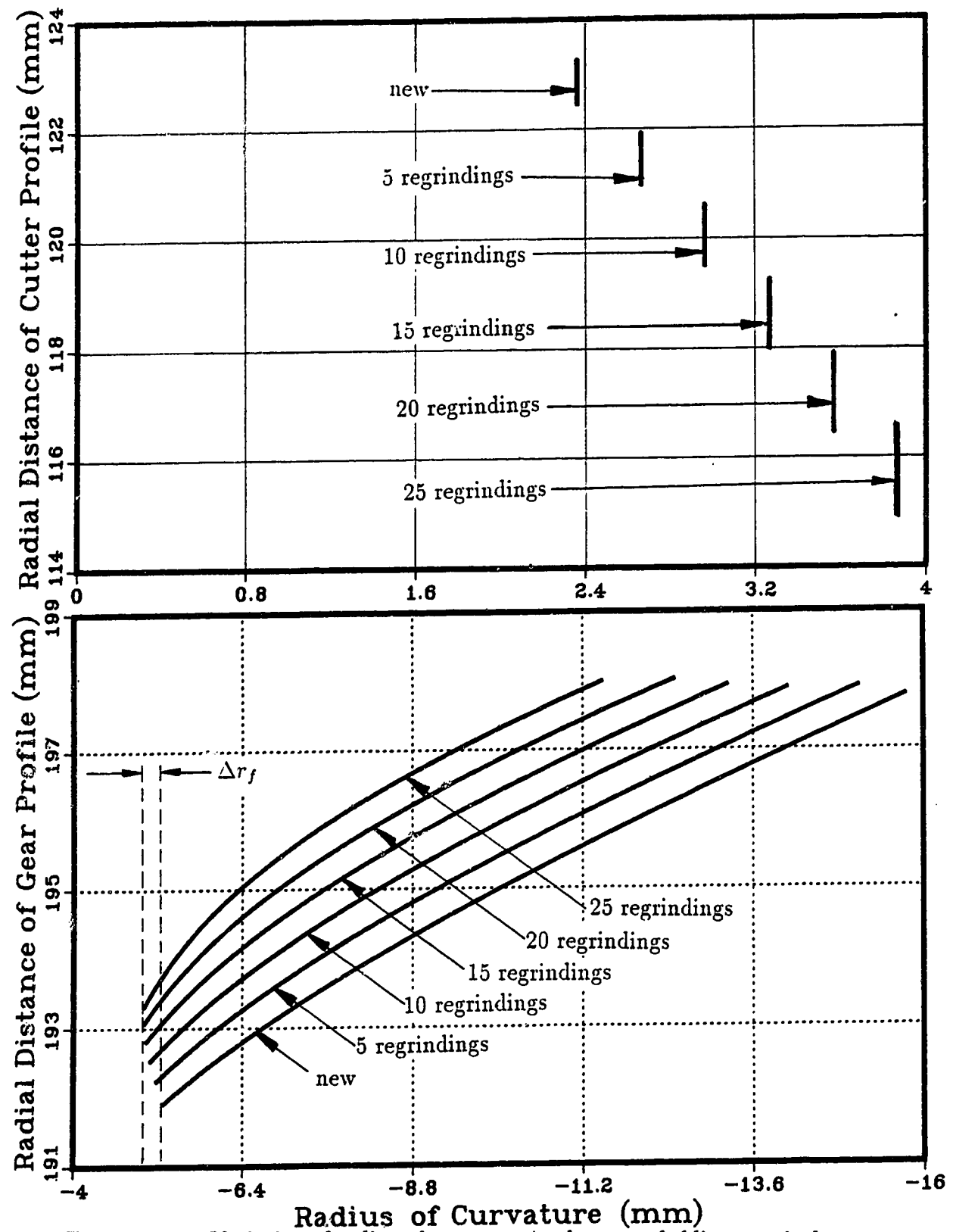


Figure 5.10: Variation of radius of curvature in the case of oblique conical corner cylinder

fillet minimum radius of curvature (r_f) on multiple resharpening, as shown in figure 5.10.

Obviously the fillet changes will be much higher when the gear ratio and the required tooth thickness in the gear blank are quite different from those considered for the cutter corner surface during the cutter design, but in general, this method would provide a better solution to the problem compared to a constant corner radius at all sections.

Chapter 6

Devices for manufacturing the new cutter

The manufacture of the pinion cutter usually involves the shaping of the pinion cutter from stock, its subsequent heat treatment, and the final grinding of the involute form. The shape of the side surface required for the new cutter design can be obtained during the grinding stage of the cutter manufacture by modifying the method of generated grinding of the cutter profile.

6.1 The grinding machine

As described in Section 1.5, the gear shaping cutter is ground by a rotating grinding wheel that travels rectilinearly along the cutter tooth being ground, with an inclination of δ (front relief angle) with respect to the cutter axis. At the same time the cutter oscillates on its pitch circle until it rolls out of mesh with the reciprocating grinding wheel. After this, the wheel is retracted from the tooth space and the cutter

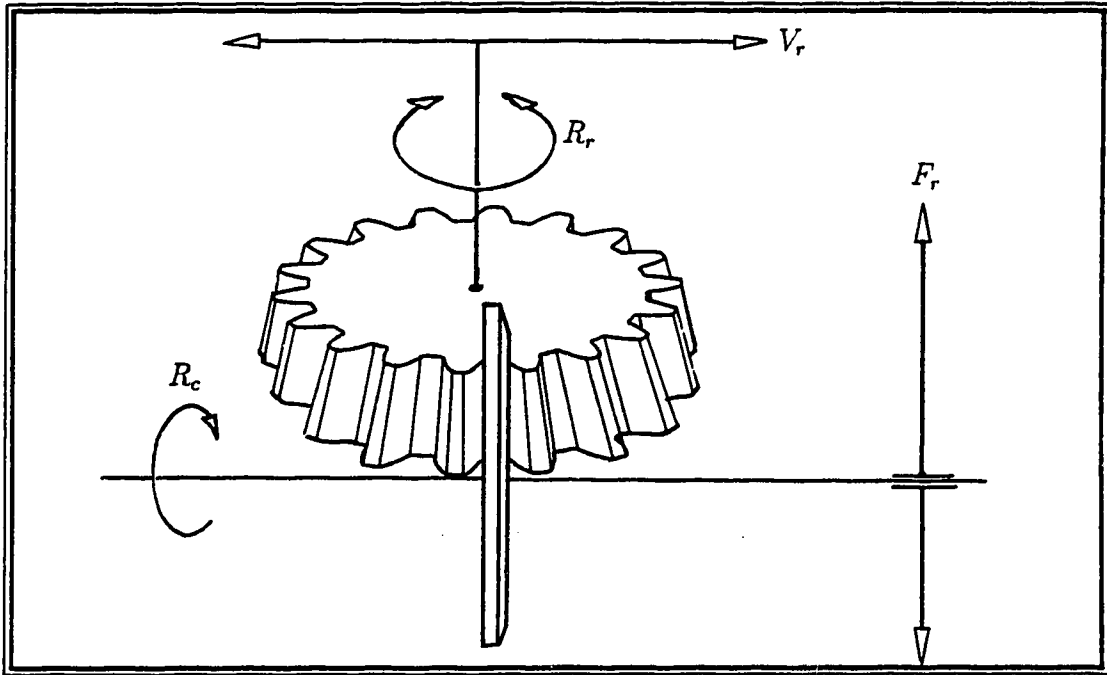


Figure 6.1: Formative motions of the grinding machine

indexed to the next tooth before the whole operation is repeated.

6.2 Formative machine motions required

For the conventional cutter design the following three formative motions (Appendix A.5) are required.

1. Cutting motion kinematic group, $F_c(R_c)$,
2. Longitudinal feed motion kinematic group, $F_f(V_f)$,
3. The roll motion kinematic group, $F_r(R_r, V_r)$.

For grinding a helical cutter, the grinding wheel has only to be set at the helix angle β , and no rotating component of motion is required to be superimposed on the

roll motion group since any helix can be developed on a pitch plane giving a straight line inclined at the helix angle. Consequently a longitudinal feed motion F_f at an inclined angle β and the roll motion F_r is sufficient to grind the helicoid surface in a helical cutter.

Other essential motions required are the following

1. Indexing motion kinematic group $I_d(R_d)$,
2. Radial in-feed motion kinematic group $I_i(V_i)$.

Therefore the main part of the grinder requires the above five essential kinematic groups, besides the handling motions. The grinders also have an additional formative group for trueing and dressing the grinding wheel and also a control group for grinding wheel wear compensation. Figure 6.1 shows the formative motions required for grinding the conventional pinion cutter.

In a small size grinding machine the whole cutter assembly, which is usually horizontal, is moved for the longitudinal feed, while the grinding wheel stays stationary, as shown in Figure 6.1. In a medium size machine, the cutter assembly is normally vertical, and the longitudinal feed is usually given by moving the grinding wheel instead, as shown in Figure 6.2. To illustrate the motion of the kinematic groups, the role of each group is explained schematically for the case of a medium size grinding machine.

6.3 Cutting motion group

The cutting motion group is of the simple type (Appendix A.5). Its internal constraint ($R_c \rightarrow 2 \rightarrow 3$) is a rotating kinematic pair which is made up of the grinding

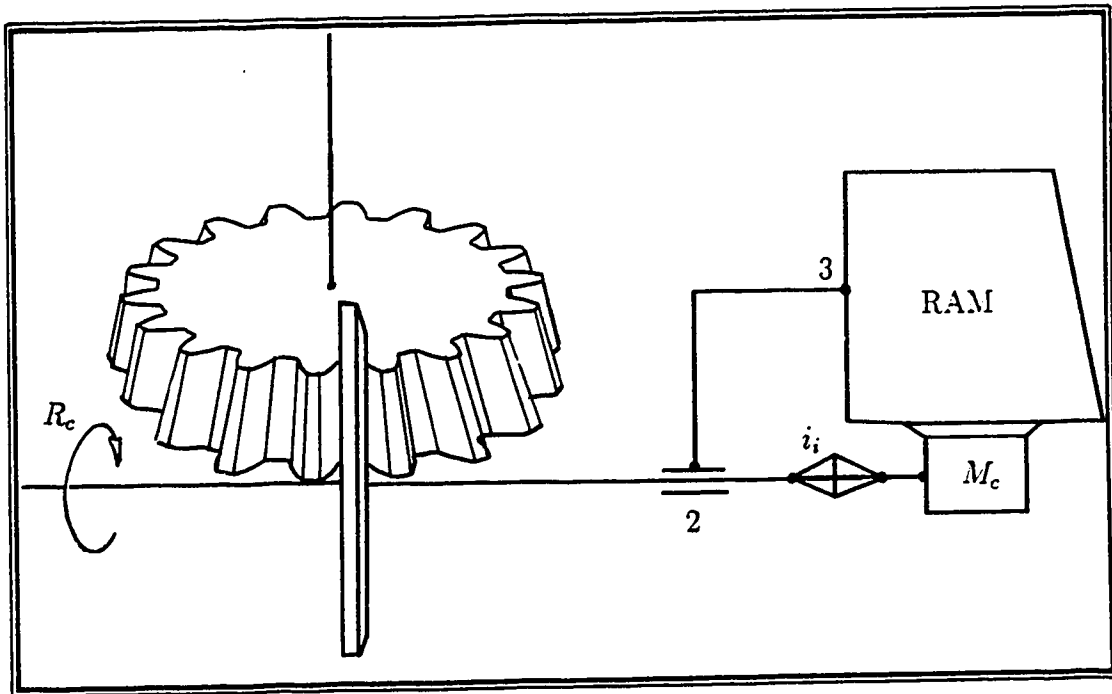


Figure 6.2: Cutting motion group

wheel spindle and the ram, while the external constraint ($M_c \rightarrow i_c \rightarrow 2$) is normally a belt drive (i_c) between the wheel and the motor M_c mounted on the ram, as shown in Figure 6.2.

6.4 Longitudinal feed motion group

The longitudinal feed motion $F_f(V_f)$ is also of a simple type consisting of a translatory kinematic internal pair ($V_f \rightarrow 3 \rightarrow 4 \rightarrow 5$) in the form of the rectilinear guide ways of ram and stanchion (for a medium size grinding machine).

The guide ways are set to the inclination δ equal to the front relief angle of the cutter ¹. The external constraint ($M_f \rightarrow i_f \rightarrow 4$) is housed in the stanchion and

¹Instead of inclining the ram at an angle δ , the longitudinal feed motion $F_f(V_f)$ can be replaced by

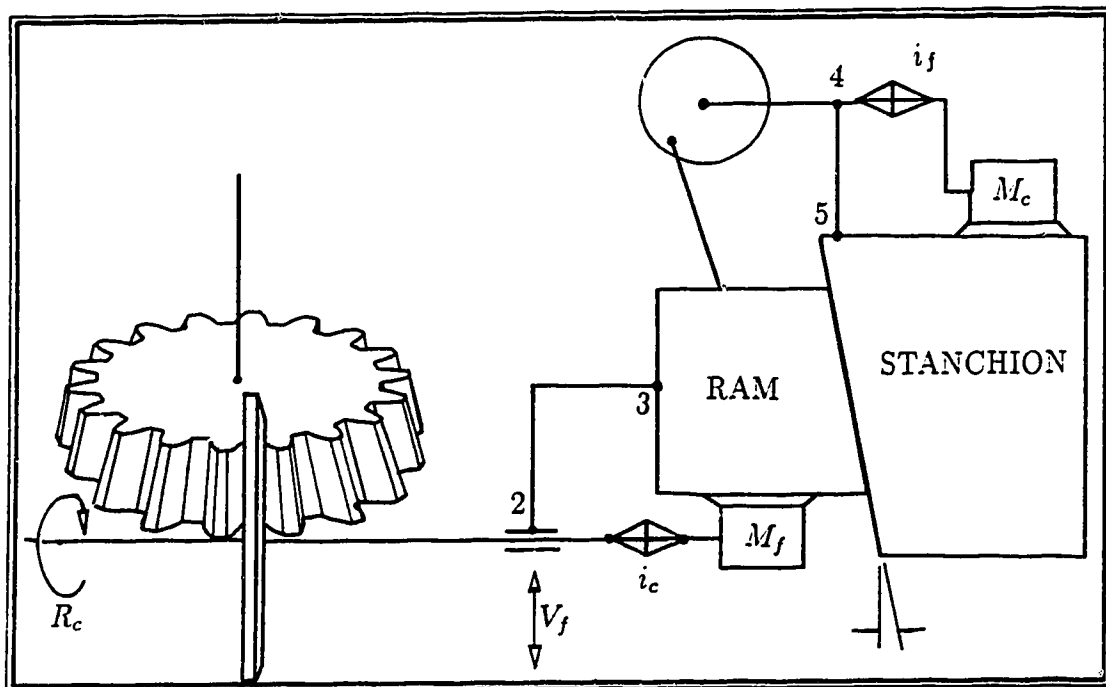


Figure 6.3: Longitudinal feed motion group

transmits motion from motor M_f to a crank drive through a ram speed gear box (i_f) and eventually to the ram and grinding wheel assembly, as shown in Figure 6.3. In the case of grinding a helical cutter, the simple longitudinal feed motion $f_f(v_f)$ is inclined at the helix angle β by setting the ram at the same angle with relation to the cutter axis. No co-ordination is required between the longitudinal motion of the ram and the cutter rotation, unlike the case of hobbing or shaping of a helical gear, since the ram itself is swivelled to the required helix angle.

a complex motion $F_f(V_{f1}, V_{f2})$ composed of two simultaneous elementary motions: (a) The vertical oscillation of the ram parallel to the cutter axis V_{f1} , and (b) The inclined or perpendicular motion of the grinding wheel on the ram itself V_{f2} so that the resultant motion is directed along the front relief of the cutter.

external constraint of this group is also the same as the roll group, as shown in Figure 6.5.

For the rake advance motion, the internal constraint should have a kinematic pair that advances the cutter by an amount proportional to the radial distance from the cutter tip to the grinding contact point.

$$d = (R_{tc} - R_c) \tan \gamma \quad (6.1)$$

$$\text{or} \quad \Delta d = -\Delta R_c \tan \gamma \quad (6.2)$$

The displacement Δs of the contact point corresponding to a rotation $\Delta\beta$ of the pinion is (equation A.11 in Appendix A.1),

$$\Delta s = R_{bc} \Delta\beta \quad (6.3)$$

The radius of the grinding contact point in terms of s is,

$$R_c = \sqrt{(R_{sc} + s \sin \phi_s)^2 + (s \cos \phi_s)^2} \quad (6.4)$$

Differentiating the above, ΔR_c is found to be,

$$\Delta R_c = \frac{R_{sc} \sin \phi_s + s}{R_c} \cdot \Delta s \quad (6.5)$$

From equation 6.2, 6.3, and 6.5 the advance Δd of the cutter for a rotation $\Delta\beta$ of the cutter spindle is,

$$\begin{aligned} \Delta d &= -\frac{R_{sc} \sin \phi_s + s}{R_c} \cdot \tan \gamma \cdot R_{bc} \Delta\beta \\ &= -R_{bc} \sin \phi_{R_c} \tan \gamma \Delta\beta \end{aligned} \quad (6.6)$$

Thus the advance Δd is not proportional to the rotational change of the cutter but depends also on the profile angle ϕ_{R_c} of the contact point of the cutter centre

and as a result is higher when the radius vector is at the root of the cutter than at the tip for the same change in cutter rotation $\Delta\beta$. Consequently a simple gear train connecting the advance to the rotation of the cutter spindle would not suffice. However the change ΔR_c can be recorded directly by a rack and pinion or a linear encoder scale which then can be converted to the required cutter advance as suggested in the following sections.

6.7 Roll and Advance group for small grinding machine

Figure 6.6 shows the sketch of a small sized grinding machine in which the axis is horizontal. The column (C) is pivoted on the semicircular rear part of the bed (B) and can be set at an angle equal to the helix angle when grinding a helical gear, while the cross-beams (CB) and its two grinding supports (S) carrying the grinding wheel (GW) can be adjusted vertically according to the diameter of the cutter.

The feed carriage (FC) has the facility to be inclined at the required front relief angle δ with respect to the horizontal bed (B). The cutter (CT) on arbour (A) is mounted between centres and the extension shaft of the arbour carries the pitch block (PB) which can be either a segment or a full cylinder.

One end of each pitch block tape is passed round and fastened to the pitch-block itself while the other end is connected to the tape stand (TS) that is mounted on the feed carriage (FC), while the pitch block arbor, cutter and the generating head (GH) are connected to the generating slide (GS). The generating head is imparted a transverse oscillatory motion by the crank disk (not shown), thereby causing the pitch block to roll on the tapes. Grinding across the entire face-width is achieved by

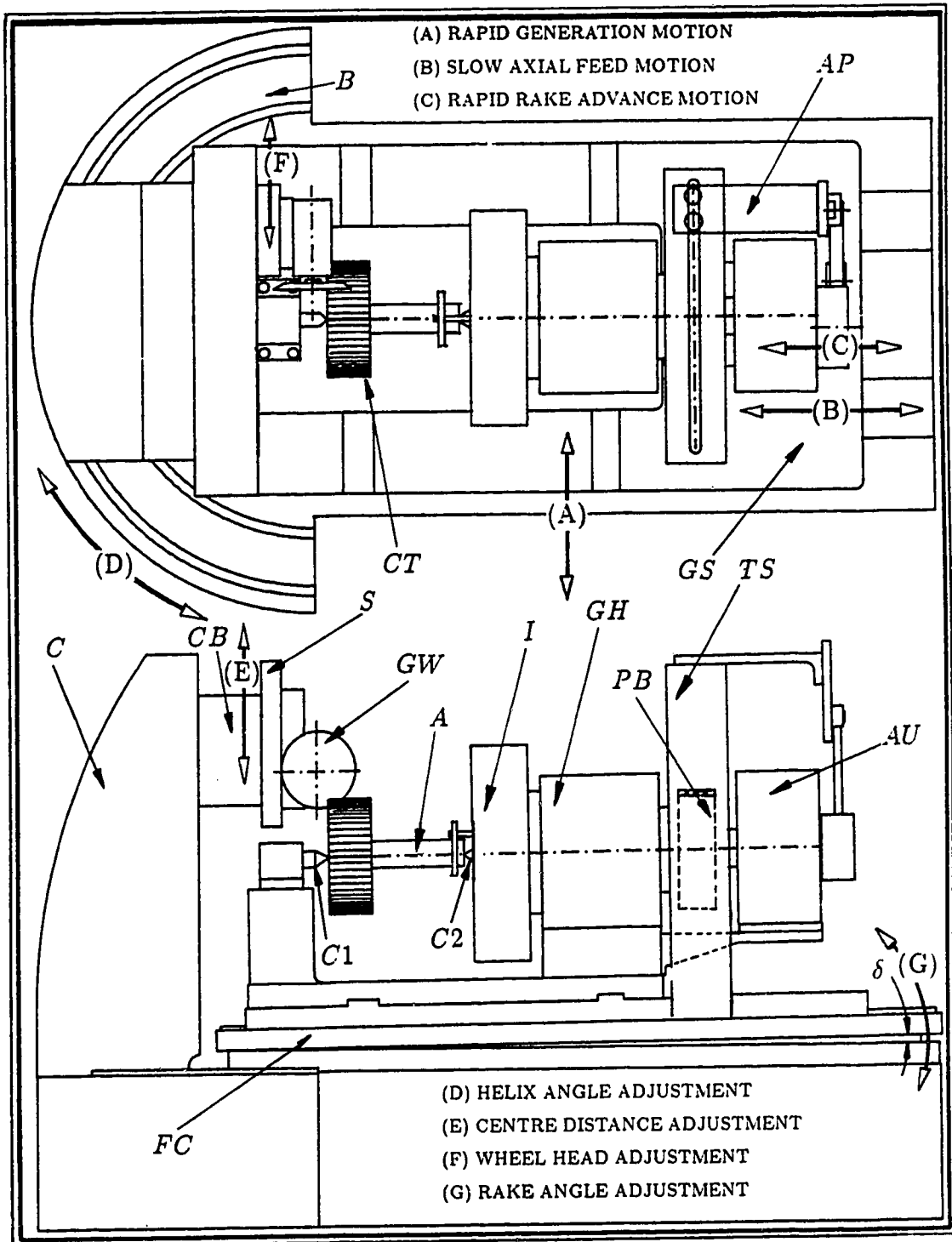


Figure 6.6: Small size grinding machine

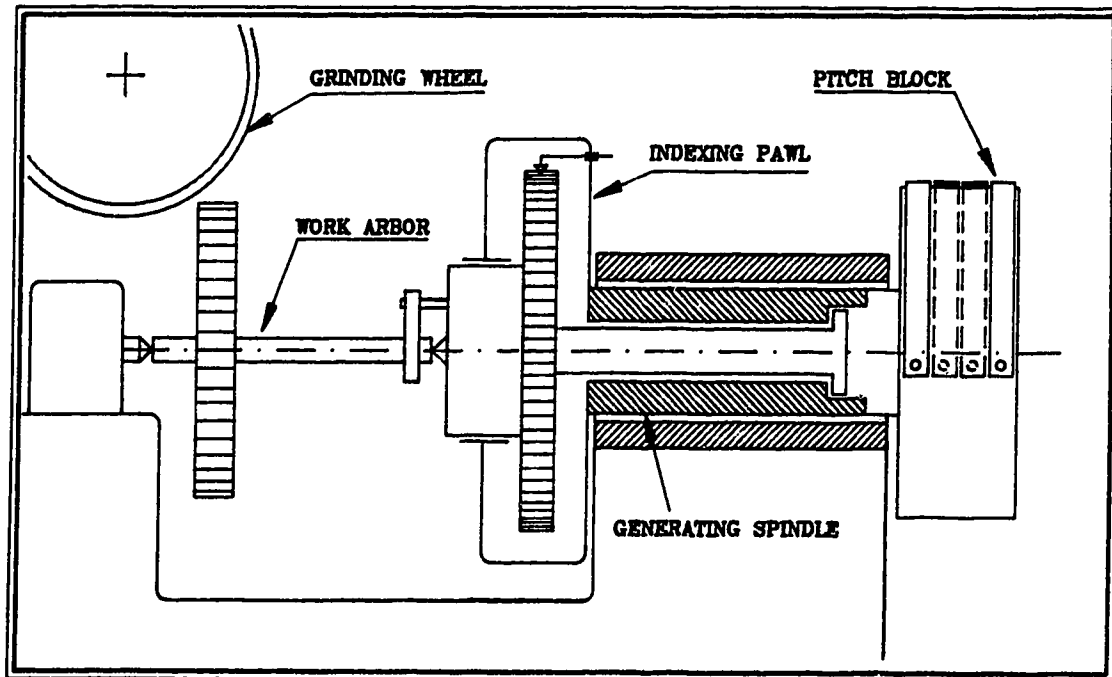


Figure 6.7: Section (diagrammatic) through generating head (conventional)

the slow reciprocating motion of the feed carriage (normally hydraulic feed) between two adjustable dogs, while the indexing arrangement (I) is housed inside (or adjacent to) the generating head. For grinding a helical gear, the guide plate (not shown) is set to the helix angle to laterally displace the tape stand proportional to the axial stroke, and the pitch block converts this translation to additional motion in the gear.

For generating the new design an advance unit (AU), with its accessory the adjusting piece (AP), has to be mounted to the pitch block and a few other changes have to be made to the generating head, indexing unit and centres.

6.7.1 Modification for rake advance group

Figure 6.7 shows a diagrammatic section through the generating head of a conventional small size size grinding machine. The indexing spindle is directly

connected to the work arbor while the generating spindle carrying the pitch block is connected to the indexing pawl. This permits the indexing spindle to be rotated independent of the generating spindle during the time of indexing. However, this conventional design has to be modified, as described below, to accommodate the motions imparted by the advance mechanism which is mounted behind the pitch block (Figure 6.8).

The cutter and the arbor are mounted between spring loaded centres and are attached to a splined shaft, which passes through the generating head and the pitch block and is connected to the advance unit, as shown in Figure 6.8. In this arrangement, without major changes to the existing roll motion kinematic structure, it will be possible to superimpose the motion of the advance group on that of the roll group and indexing group. This whole assembly of arbor, cutter, and indexing device floats between the two springs S_1 and S_2 which give it freedom of movement in the axial direction. The splined shaft F is connected through the advance spindle to the advance mechanism which displaces the cutter spindle assembly to its required axial position depending upon the grinding contact position the cutter. The mechanism by which an accurate axial displacement can be imparted to the work arbor is explained in the next section.

6.8 Rake advance kinematic group: Method I

Figure 6.9 shows the sectional view of a possible mechanism that relates the oscillatory motion of the cutter on its pitch circle to the required advance for modification of the ground surface. Zero pressure angle grinding is used so that radial distance of the grinding contact point from the centre of the grinding wheel remains unchanged during grinding. A rack R is mounted between the gear G and

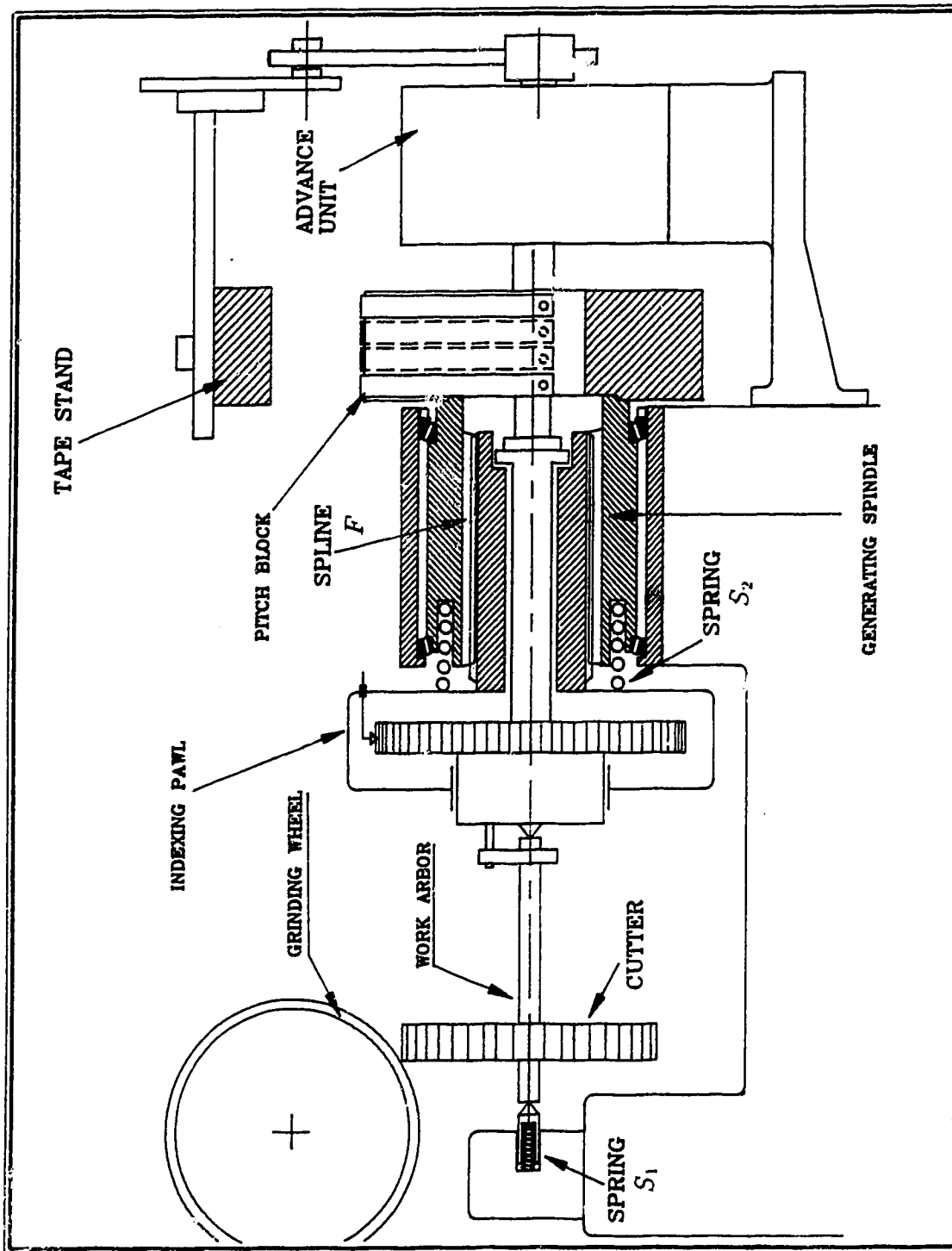


Figure 6.8: Section(diagrammatic) through generating head (modified)

roller O so that its pitch line always passes through the centre-line of the cutter spindle. The other end of the rack is pivoted to the tape stand of the rack through the adjusting piece.

6.9 Working principle of advance mechanism

Since the advance mechanism assembly shown in Figure 6.9 is mounted on the generating slide while the rack is pivoted to the stationary adjusting piece on the tape block, the oscillation of the generating slide will cause the gear (G) to rotate an amount proportional to the change in the radial distance of the cutter point of contact with the cutter profile. The sleeve (S) with the internal teeth ($S1$) meshes with gear (G) which in turn is driven by rack (R). This whole assembly can rotate freely within the casing (C) and thus allowing only the change in radial distance from the pitch point of the rack (R) and gear (G) to the pivot centre on the adjusting piece to be transmitted and not the change in rack inclination. This relative rotation of (S) with respect to carriage (CA) is converted to an axial advance by the internal screw arrangement which moves the nut (N) whose internal spline engages with the external spline of the carriage (CA). The bearing on the advance spindle (A) isolates the roll motion of the latter from the displacement of the nut (N) so that both these motion can be superimposed.

Let the radius of pitch circle of the gear (G) and that of the internal teeth in sleeve (S) be denoted by (R_G) and (R_S) respectively. Then if the change in rack distance is ΔR , the rotation of the gear (G) with respect to (CA) will be α_G where,

$$\alpha_G = \frac{\Delta R}{R_G} \quad (6.7)$$

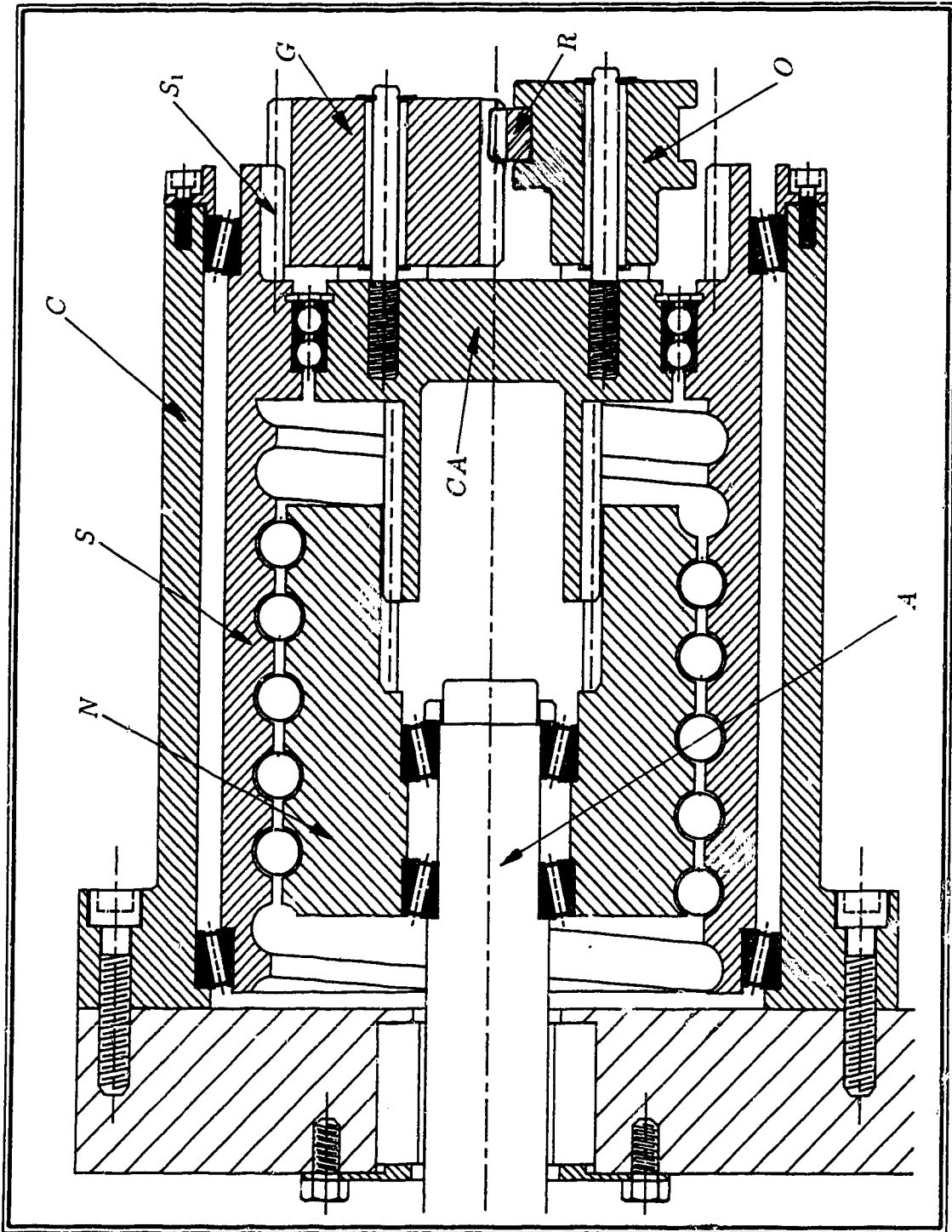


Figure 6.9: Sectional view of the advance mechanism

This will cause the sleeve (S) to rotate by an angle α_S where,

$$\begin{aligned}\alpha_S &= \alpha_G \cdot \frac{N_G}{N_S} \\ &= \Delta R \cdot \frac{N_G}{N_S R_G}\end{aligned}\quad (6.8)$$

Let the pitch circle radius of the helical screw on the sleeve (S) and nut (N) be R_N . Then the nut (N) having a helix angle ψ advances by Δd where,

$$\begin{aligned}\Delta d &= \alpha_S R_N \tan \psi \\ &= \Delta R \cdot \frac{N_G R_N}{N_S R_G} \cdot \tan \psi\end{aligned}\quad (6.9)$$

If the pitch circle radii of the internal gear (S_1), the nut (N), and the screw (S) are equal to the pitch diameter of the gear (G). and the helix angle of the screw (S) be equal to the rake angle γ i.e.,

$$\begin{aligned}\frac{N_S}{N_G} &= \frac{R_N}{R_G} \\ \psi &= \gamma\end{aligned}$$

or if

$$\psi = \tan^{-1} \left\{ \frac{N_S}{N_G} \cdot \frac{R_G}{R_N} \cdot \tan \gamma \right\}$$

then with the correct hand of helix in the screw (to take care of the sign) the advance will be proportional to the change in ΔR i.e.,

$$\Delta d = -\Delta R \tan \gamma$$

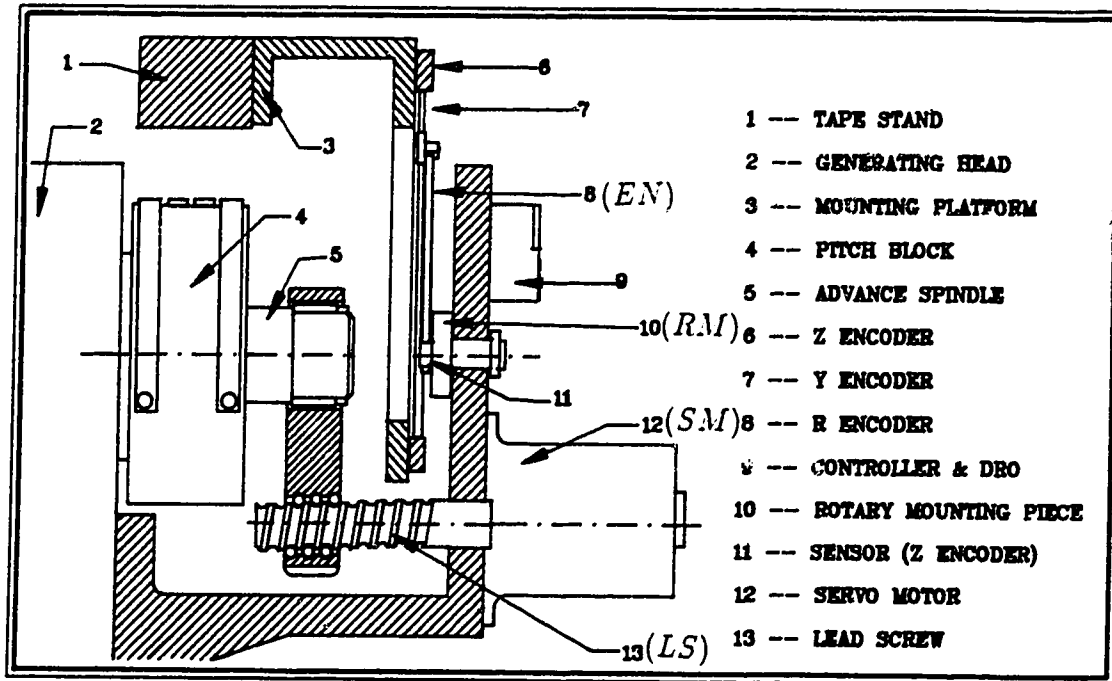


Figure 6.10: Alternative rake advance kinematic group: Method II

6.10 Alternative rake advance kinematic group: Method II

The wholly mechanical device shown in Figure 6.9 can be replaced by an alternative rake advance group where the external constraint is not the same as that of the roll motion group but is driven by an external servo-motor as shown in Figure 6.10. In this case the whole assembly of the rack (R), gear (G), roller (O), and their connecting elements can be replaced by a linear encoder (EN) instead of the rack, whose sensor is mounted on a rotary mounting piece (RM) whose axis is aligned with that of the spindle centre-line. The end of the linear encoder which is pivoted to the adjusting piece mounted on the tape-stand, and can have a double cross-hair so that it can be set up according to Method I (Section 6.11). If two more encoders

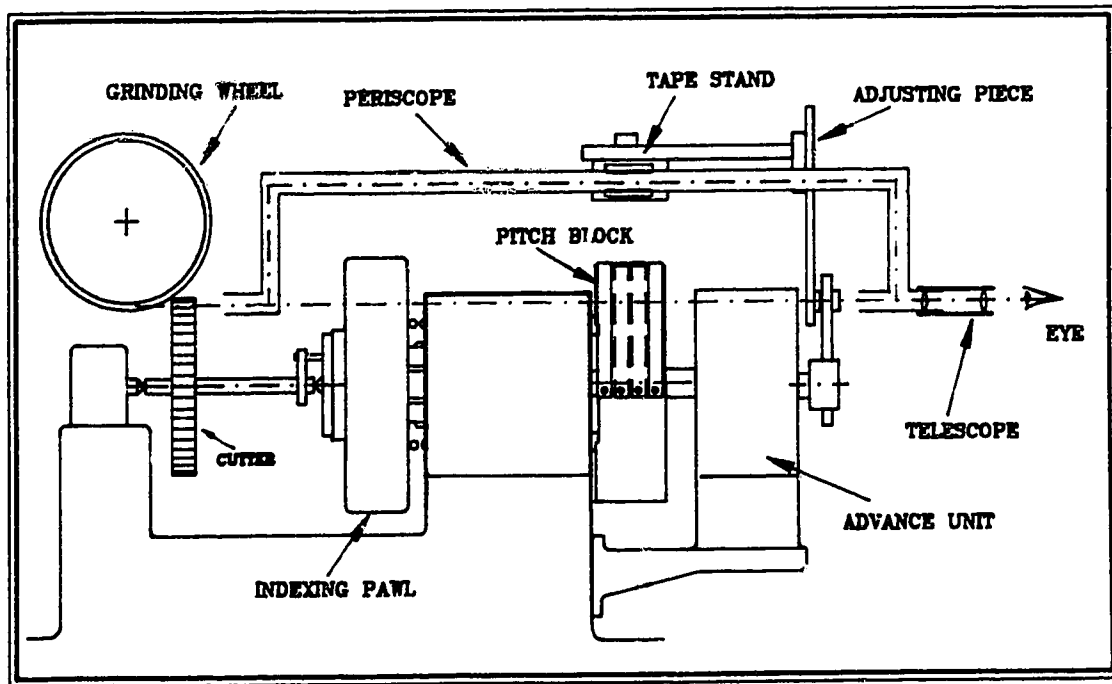


Figure 6.11: Setup of advance mechanism: Method I

(Y-encoder and Z-encoder) are fixed then the Method II (Section II) of initial setup procedure can be used.

The change in the radial distance of the contact point of the grinding wheel from the centre of the cutter is read directly by the encoder whose output is sent through a controller to a servo-motor (*SM*) which drives the ball-bearing lead screw (*LS*) arrangement, moving the advance spindle to the axial position required. Because of the inertia of motion and quick change of direction, a disk brake, governed by the controller, may be required to be attached to the lead screw.

6.11 Setup of advance mechanism: Method I

The initial setup position of the mechanism and cutter with respect to the grinding wheel is very important. A schematic layout of this method is shown in Figure 6.11. The rack has to be positioned in such a way that the distance between the centre of the spindle and the pivot point of the rack on the adjusting piece should be equal to the distance between the centre of the cutter and the point of contact of the grinding wheel and the cutter surface. This can be achieved by aligning the double cross-hair on the pivot with the contact point of the cutter surface. For this purpose a telescope can be placed in front of the cross-hair and a periscope behind it, in order to avoid the obstruction to the line of sight because of the presence of the tape-block, pitch-block, and the generating head. Once the advancing device has been correctly set up initially, then accurate indexing (with CNC control with feed back loop) will ensure a correct setting for all remaining teeth.

6.12 Setup of advance mechanism: Method II

Initially the cutter rake face and side on one tooth has to be marked at a radial distance of R_{set} and then the cutter placed on the arbor and with the grinding wheel touching the face the cutter is turned manually in a generating motion until the grinding wheel touches the marking. This ensures that contact is at the correct setting point and now one can proceed to set the rack or the encoder in its required position. The rack is positioned in such a way (Figure 6.12) that the position of its cross-hair relative to the pitch point of rack (R) and gear (G) is given by,

$$y_{set} = R_{bc} = \frac{1}{2} N'_c m \cos \phi_s \quad (6.10)$$

$$z_{set} = \frac{S}{2} = \frac{1}{2} \cos \phi_s \left[(N'_c - 1) \pi m + t_{sc}^T + N'_c m \operatorname{inv} \phi_s \right] \quad (6.11)$$

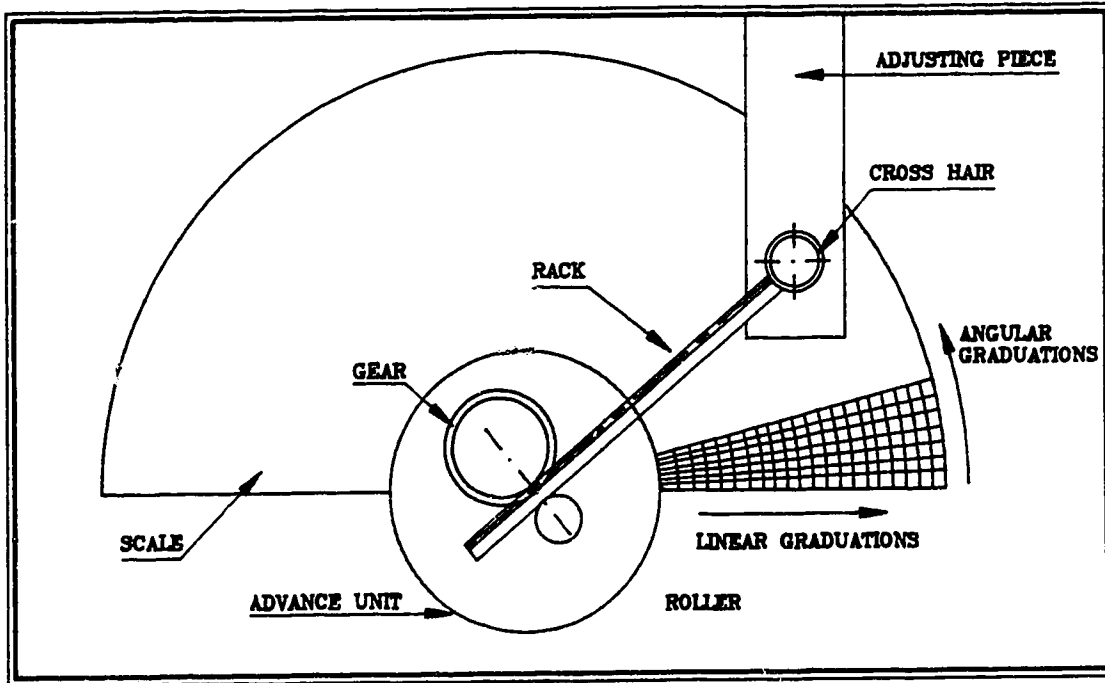


Figure 6.12: Setup of advance mechanism: Method II using scale

where S is the expression [4] for span measurement over N'_c teeth (Appendix A.6). In polar coordinates the setting position will be,

$$R_{set} = \sqrt{z_{set}^2 + y_{set}^2} \quad (6.12)$$

$$\theta_{set} = \tan^{-1} \left(\frac{y_{set}}{z_{set}} \right) \quad (6.13)$$

To facilitate this setup, a circular scale having angular as well as linear graduations may be attached to the advancing unit for positioning to the setup position (R_{set}, θ_{set}) as shown in Figure 6.12.

For an advance mechanism using encoders, the adjusting piece on which the scale is pivoted may itself be mounted on two perpendicular guide ways each having a linear encoder scale linked to the controller. The adjusting piece may be traversed (manual or motorised movement) in both directions to find the minimum reading which may be set to zero. Then the adjusting piece has to be positioned to the point

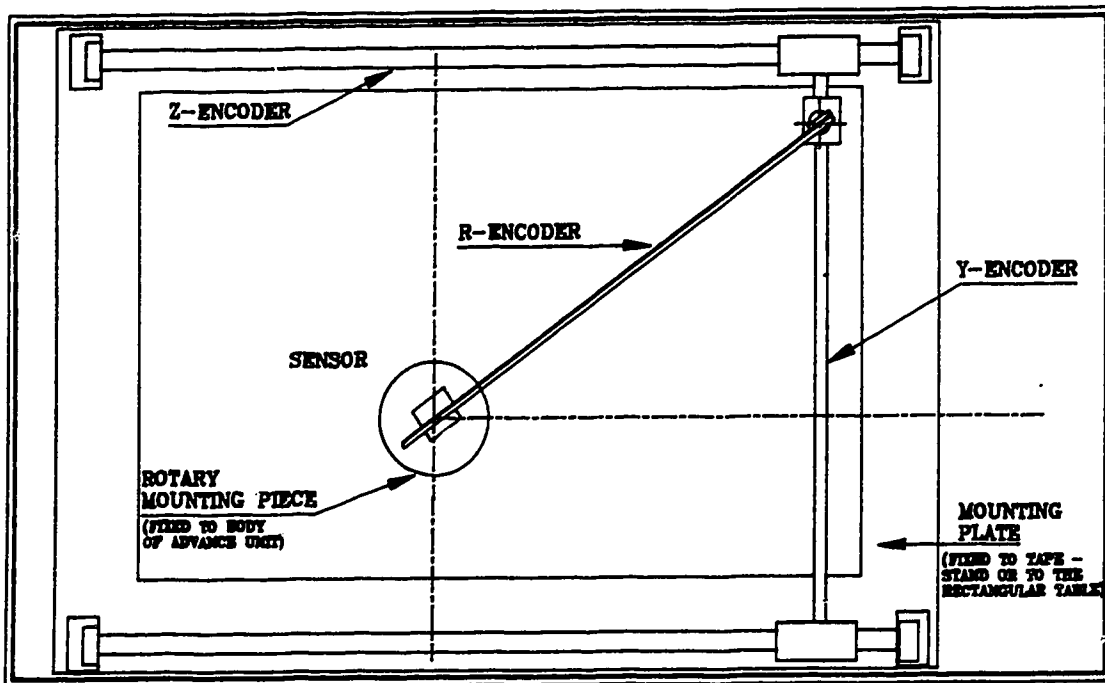


Figure 6.13: Setup of advance mechanism: Method II using Y & Z encoders

having the rectangular coordinates of (z_{set}, y_{set}) as shown in Figure 6.13. For a small size grinding machine, Figure 6.10 shows the location of the encoders and the mounting plate on the tape stand.

6.13 Medium size grinding machine

While the basic principle remains the same, the medium size grinding machine resembles a gear cutting machine. Figure 6.14 shows the kinematic structure of a medium size grinding machine also equipped with the modified group for rake advancing. The cutting motion group and the feed motion group are as explained in Sections 6.3, 6.4, 6.5.

The gear cutter is mounted with the vertical axis on the work-table which performs

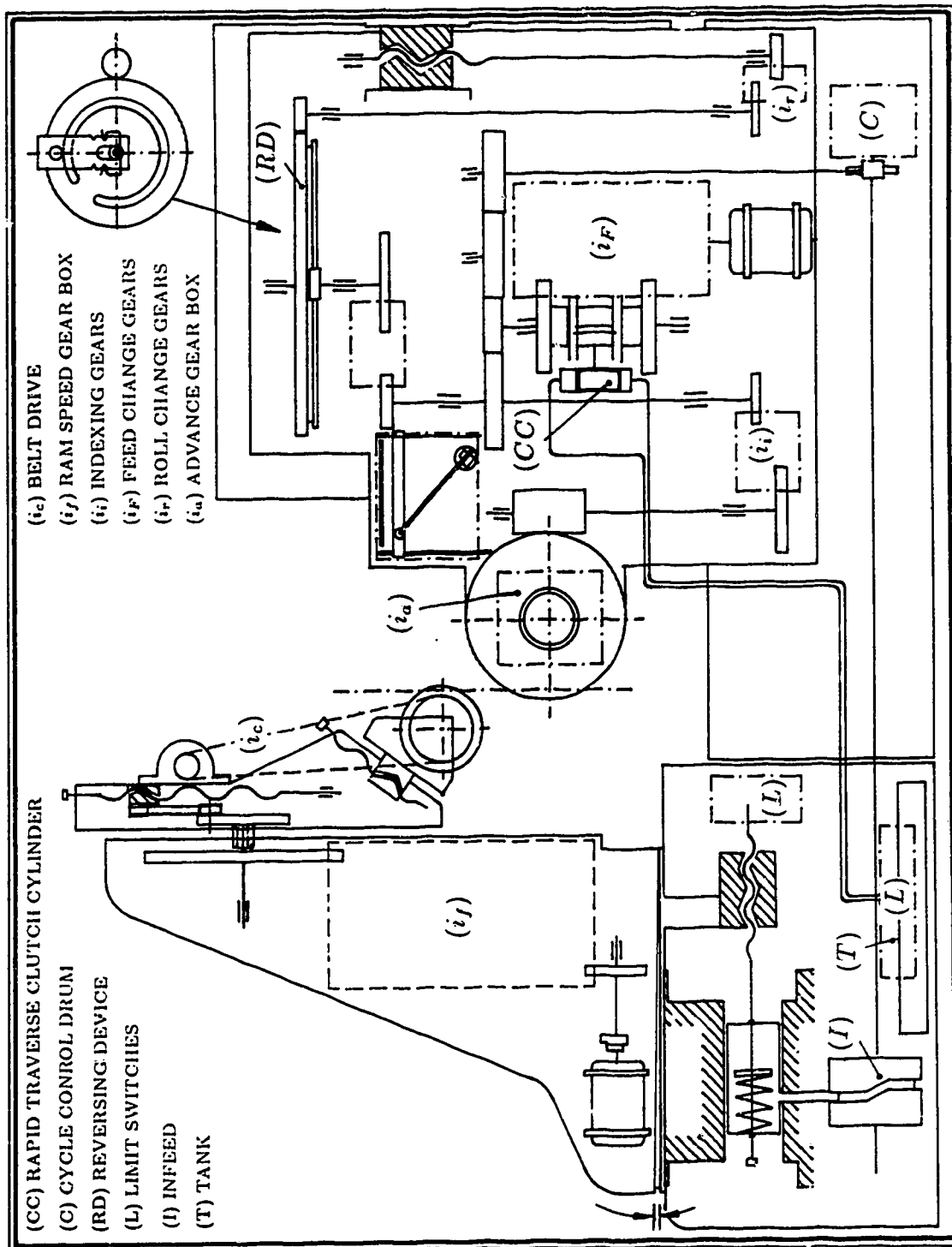


Figure 6.14: Medium size grinding machine

the generating motion only, while the feed motion along the tooth being ground is given by the vertical ram carrying the grinding wheel. Normally, the feed is fast and the transverse generated grinding motion is slow. The internal constraint of the roll motion group consists of a kinematic chain linking the round table and the rectangular table, interlinking their elementary motions R_r and V_r . As shown in Figure 6.14, this kinematic chain also has a mechanism for indexing, which is accomplished by a reversing device, which consists of a travelling pinion that meshes alternately with the external and internal teeth of the composite gear. When the grinding of a tooth is completed, the stanchion with the wheel is withdrawn by the in-feed drum, and the composite gear and travelling pinion reverse the direction of the rectangular table without reversing the rotation of the round table. Hence, while indexing, the roll motion (R_r, V_r) ceases and the motion R_r becomes the indexing motion R_i , while the motion V_r becomes the handling motion V_h .

For the advance motion group, it might be more convenient to install a linear encoder (Figure 6.15), similar to method II, which is housed between the round table and the rectangular table in such a way that the sensing piece is pivoted on a rotary mounting piece (5) that is fixed with a bracket to the round table, while the other end of the scale and the Y & Z encoders (3) are placed on the mounting plate that is fixed to the rectangular table (13). The output of the linear encoder is fed through a controller to the rotating ball lead screw that advances a nut supported inside the chuck by double thrust bearing so that the advance motion to the chuck can be superimposed on the roll motion of the same. The roll motion is transmitted to the chuck through a worm and a splined wormwheel arrangement to the external mating spline of the chuck (8), to allow freedom for axial movement of the latter, as shown in Figure 6.15. The initial set-up can be performed by following to the setup procedure outlined in method II (Section 6.12).

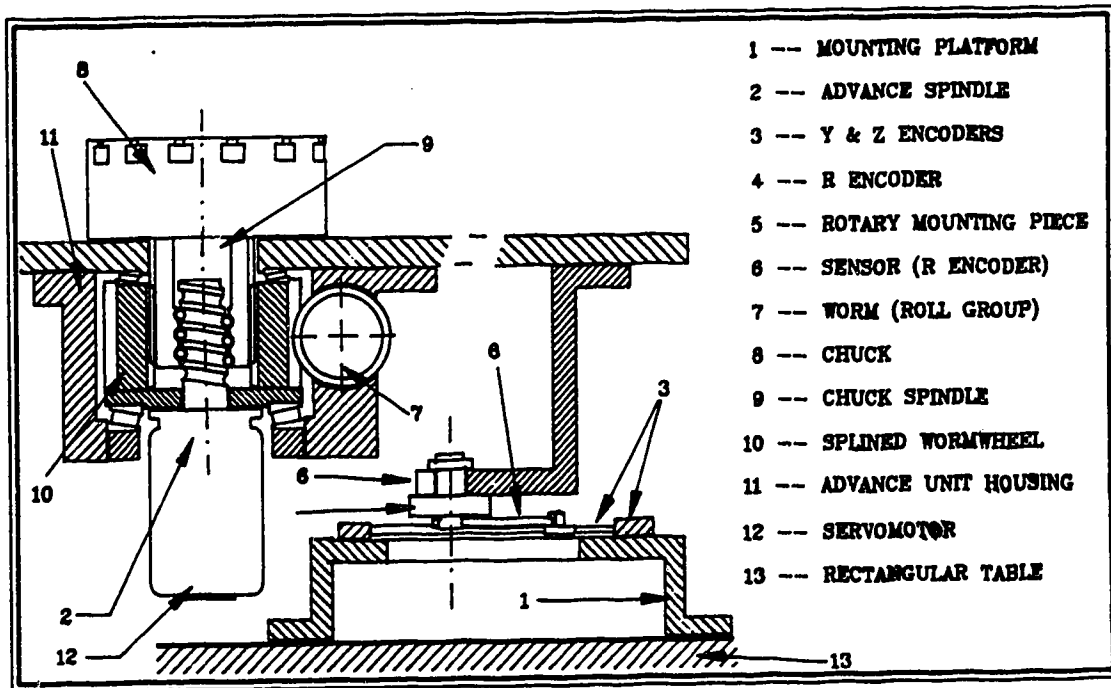


Figure 6.15: Placement of the linear encoder

6.14 Grinding procedure changes for new cutter

In grinding the new cutter design, sides of two adjacent teeth cannot be ground at the same time as in isoform grinding, since when one wheel side advances to grind the flank of one teeth the other side that grinds the face of the adjacent teeth should retreat back, which is not possible. For the same reason it not possible to have two grinding wheels grinding the opposite sides of two different teeth unless the separate advance motion is given to each of the grinding wheels rather than advancing the cutter assembly.

The isoform grinding method (Section 1.5.2) can not be used for grinding the new cutter, because in that method the grinding contact point varies along the grinding wheel thus making it difficult for the advance device to track the radial distance of the grinding contact point.

Hence, the zero pressure angle grinding method (Section 1.5.1) has to be used in this case. A dished grinding wheel has to be mounted and one face of each tooth has to be ground before the machine is stopped, the grinding wheel flipped over, and the direction of advance mechanism reversed, before the other face of each tooth is ground.

Chapter 7

Conclusion

The analysis of the present method of pinion shaper design shows that because of the presence of rake and relief angles the effective profile of the shaper cutter is not an exact involute. The deviation in effective profile increases with the increase of rake and relief angles which are as a result restricted to smaller values.

The profile deviations can be measured quantitatively by evaluating the normal deviation along the cutter profile which is numerically equal to half the difference in base tooth thickness (tooth thickness at the base circle) between the theoretical profile and the shifted involute profile passing through the point where deviation is to be found.

Variations in tooth thickness along the profile when compared with that of the theoretical profile show that the difference in tooth thickness is a quadratic in the radius vector R_c^A for a fixed tooth geometry ($\gamma, \delta, \phi_s = \text{constant}$).

These profile deviations in the conventional design can be reduced with help of certain correction methods. All the methods of profile correction aim to minimise the profile deviation in the vicinity of the cutter pitch point, so that the region near the

pitch point in the generated gear has a low profile error.

The profile correction methods comprise, firstly, the use of a greater corrected pressure angle of value $\phi^{corr} = \tan^{-1} \left\{ \frac{\tan \phi_s}{1 - \tan \delta \tan \gamma} \right\}$, and hence a smaller base circle that gives the required pressure angle at the pitch point upon grinding the rake face. Secondly a higher corrected value of tooth thickness is chosen so that after tooth thinning, which occurs on imparting the rake angle, the tooth thickness will diminish to near the required value.

In the cutter design, the value of the design distance "b" is important because both the possible number of resharpenings and the size of the tooth thickness at the tooth tip and its strength depend on it. The semi-analytical method, shown in chapter 2, is easier to use than the graphical method for determining the value of "b".

The new design of shaper cutter that is presented in this thesis is based on the reasoning that on knowing the required effective profile one can work backwards and determine the cutter surface required to generate it. The required surface is generated by the envelope of a family of shifted involute profiles lying on concentric axially shifted cones, where the cone angle determines the rake angle, and the amount of shift with axial displacement in the profiles determines the relief angle of the cutter.

The front and the side relief angles are decided on the basis of the practical requirement of providing clearance in the cutter tooth flank, in order to avoid rubbing with the blank during gear cutting. The front relief angle and the side relief angle depend on each other because their choice also depends on the criterion that, after regrinding, apart from the tooth thickness a constant whole depth should be achieved as far as possible. Regrinding of the cutter causes reduction of both cutter tooth thickness (related to the side relief angle) and the cutter addendum (related to the front relief angle) and with proper choice of these angles the infeed required by the cutter, to maintain constant gear tooth thickness can largely compensate for the

reduction in whole depth of the gear. It is also possible to impart cutter tooth modifications in the new design of the cutter so that the tooth tip relief can be obtained in the generated gear, if required.

Effects of resharpening on the active profile of both the conventional and the new design of cutter show that in the conventional design profile deviation varies after each resharpening while the new design always produces exact involutes throughout the cutter life.

The effect of resharpening on the cutter corner radius and subsequently on the generated gear fillet radius is investigated for both the cases of cylindrical and conical cutter corner surfaces. The results show that by choosing a proper oblique cutter corner surface, the changes in the gear fillet minimum radius generated after a number of resharpenings, can be minimised.

The shape of the side surface of the new cutter design can be produced by adding the rake advance kinematic group to the existing grinding machine that is used in the generated grinding of the cutter surface. The basic principle of the advance mechanism remains the same in both the medium and the smaller size grinding machine. The required change in the machine kinematic structure is not major, but the change in the grinding process and initial setup are important. To incorporate the rake advance motion "zero-pressure angle grinding of one side of one tooth at a time" has to be adopted, which will increase the grinding cycle time of the cutter when compared to isoform grinding, but the resulting cutter will be free of profile errors throughout the cutter life.

References

- [1] Acherkan, N. *Machine Tool Design, Vol 1-4*. Mir Publisher, 1973.
- [2] Arshinov, V. and Alekseev, G. *Metal cutting theory and cutting tool design* MIR Publisher, 1970.
- [3] Buckingham E. *Analytical Mechanics of Gears*. Dover Publications, 1949.
- [4] Colbourne J. R. *The Geometry of Involute Gears*. Springer Verlag Inc., 1987.
- [5] Crockett J. C. *Gear Cutting Practice, Machine and Tools*. Machinery Publishing Co. Ltd., 1971.
- [6] Derkach L. I. et al *Simplified calculation of gear cutting and gear measuring tools*. Machines and Toolings, 1965, Vol. XXXVI, No.2, pp 37-42.
- [7] Dudley D. W. *Gear Handbook*. McGraw Hill Book Company Inc., 1962.
- [8] Drago R.J. *Fundamentals of Gear Design*. Butterworth Publishers, 1988.
- [9] Evofeev A. F. *Grinding gear shaper end cutters*. Machines and Toolings, 1970, Vol. XLI, No. 2, pp 55-56.
- [10] Ivanov Yu. I. et al *Grinding gear-shaping cutters and broaches with CBN wheels*. Stanki i instruments, 1970, Vol. 46, Issue 3, pp 27-28.

- [11] Johnson S. J. *Controlling tooth fillet contours to increase finished gear strength*. AGMA 129.16, June 1965
- [12] Merrit H. E. *Gear Engineering*. Pitman 1971.
- [13] Patil J. S., Ramaswamy N. and Shunmugam M. S. *Analysis of interference in internal gear generation and the influence of shaping cutter regrindings*. Proceedings of 8th AIMTDR conference, IIT Bombay, 1978.
- [14] Petruklin S. S. and Erdokimov V. A. *Cutting force and metal removal when gear shaping*. Machines and Toolings, 1971, Vol. XLII, No. 2, pp 41-43.
- [15] Petruklin S. S. and Erdokimov V. A. *Increasing removal rates in gear shaping*. Machines and Toolings, 1970, Vol. XLI, No. 3, pp 35-36.
- [16] Polder, J. W. *Overcut interference in internal gears*. Proceedings of International Symposium on Gearing and Power Transmissions, Tokyo, 1981.
- [17] Rodin P. *Design and production of metal cutting tools*. MIR Publisher, pp 183-197.
- [18] Romanov V. F. *The optimum geometry of gear shaping cutters*. Machines and Toolings, 1963, Vol. XXXIV, No. 9, pp 2-5.
- [19] Romanov V. F. *Basic factors of gear shaper cutter design*. Machine and Toolings, 1964, Vol. XXXV, No. 8, pp 23-24.
- [20] Shankararajayanaswamy K. and Shunmugam M. S. *Minimum achievable quality of involute gears in generation process*. International Journal of Machine Tools and Manufacturing, 1988, Vol 28, No 1, pp 1-10.

- [21] Shunmugam M. S. Profile deviations in internal gear shaping. *International Journal of Tool Design and Research*, Vol. 22, No. 1, pp 33-39.
- [22] Srinivasan N. and Shunmugam M. S. *Effect of top relief and rake angles on the gear shaping cutter profile*. *Proceedings of Institution of Mechanical Engineers*, Vol 197C pp 249-254
- [23] Yakabson S. B. *Modified cutter for leaving a shaving allowance on gear teeth*. *Machine and Toolings*, 1963, Vol. XXXIV, No. 9, pp 6-7
- [24] Yastrebov V. M. *Checking shaping tools for internal gears*. *Machines and Toolings*, 1959, Vol. XXX, No. 6, pp 33-35.

Appendix A

Definitions and Derivations

A.1 Relation between pinion tooth thickness and rack space width

At time t_0 , let the rack and the pinion be meshed in the position shown in Figure A.1, where the contact point lies exactly at the pitch point. The x - axis of the pinion and the x_r - axis of the rack coincide with the respective tooth centrelines and point radially away from the respective centres, while the z axes point out of the paper. The positions of the rack and pinion with respect to the set of stationary axes (ξ, η) , with origin at the pitch point, are given by,

$$\beta_0 = -\frac{t_c}{2R_c} \quad (\text{A.1})$$

$$\text{and} \quad u_{r0} = \frac{1}{2}t_r \quad (\text{A.2})$$

After the pinion has rotated by an angle $\Delta\beta$ from the above position, displacing the rack by an amount Δu_r , the new positions at the new time t are given by the

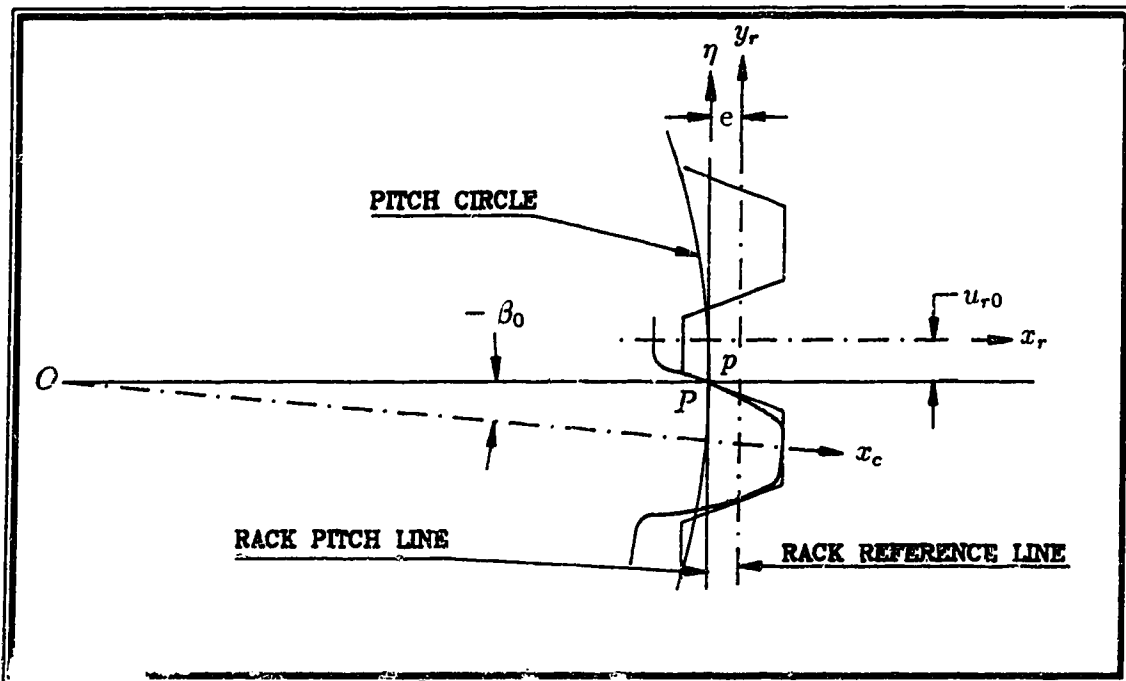


Figure A.1: Pinion and rack positions at time t_0

following expressions:

$$\beta = -\frac{t_c}{2R_c} + \Delta\beta \quad (\text{A.3})$$

$$u_r = \frac{1}{2}t_r + \Delta u_r \quad (\text{A.4})$$

Since we can consider the pinion pitch circle to be rolling on the rack pitch line without slipping, the relation between rack velocity V_r and the pinion angular velocity ω can be given by,

$$V_r = R_c\omega \quad (\text{A.5})$$

Multiplying both sides by dt and integrating from initial time t_0 to time t , we get

$$\Delta u_r = R_c\Delta\beta \quad (\text{A.6})$$

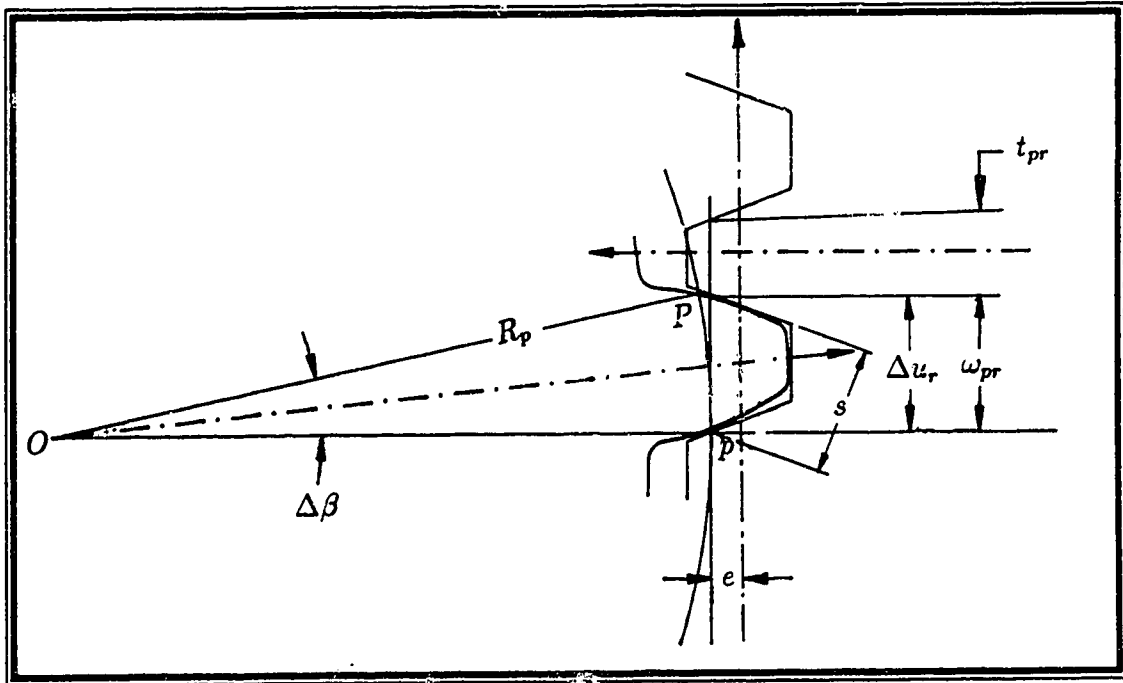


Figure A.2: Rack tooth position at t

Substituting from equations A.3 and A.4, the values of Δu_r and $\Delta\beta$, in equation A.6, gives the required relation between pinion angular position, β , and the rack position, u_r :

$$R_c\beta - u_r + \frac{1}{2}(t_c + t_r) = 0 \quad (\text{A.7})$$

Let the pinion rotate until the opposite face of the same tooth passes through the pitch point, in close mesh operation (no backlash), as shown in the Figure A.2. The rotation of the pinion by the amount $\Delta\beta$, between the position in Figures A.1 and A.2, can be expressed in terms of its tooth thickness at its pitch circle:

$$\Delta\beta = \frac{t_c}{R_c} \quad (\text{A.8})$$

The displacement, Δu_r , of the rack would be equal to the tooth space width w_r , measured at the pitch line,

$$\Delta u_r = w_r \quad (\text{A.9})$$

Feeding the values of $\Delta\beta$ and Δu_r in equation A-5 we have,

$$w_r = t_c \quad (\text{A.10})$$

Thus the space width of the rack at the cutting pitch line is equal to the tooth thickness of the pinion at the cutting pitch circle.

Let “ s ” be the distance of the point of contact from the pitch point. Since the rotation of the pinion by “ $\Delta\beta$ ” causes the rack to be displaced by a distance “ $R_c\Delta\beta$ ” (from equation A.6), the corresponding value of “ s ” will be (from Figure A.2):

$$\begin{aligned} s &= \Delta u_r \cos \phi_s \\ &= R_c \Delta\beta \cos \phi_s \\ &= R_{bc} \Delta\beta \end{aligned} \quad (\text{A.11})$$

A.2 Involute function and tooth thickness

An involute profile is generated by the locus of any point on a bar which rolls without slipping on a circle, called the base circle of the involute. For any typical point at a radius R (Figure A.3) on the involute the following three angles are frequently used in involutometry:

ϕ_R : The angle between the radius vector R and the tangent to the profile, at a radius R , is called the profile angle at a radius R , of the involute.

$$\phi_R = \angle AOC$$

ϵ_R : The angle between the radius vector at the start of the involute, on the base circle, and the tangent to the profile at a radius R , is called the roll angle at radius R of the involute.

$$\epsilon_R = \angle BOC$$

$inv\phi_R$: The angle subtended, at the centre of the base circle, by the arc between the start of the involute and the point on the profile at radius R , is called the involute function of ϕ_R , where ϕ_R is the profile angle of that point.

$$\begin{aligned} inv\phi_R &= \epsilon_R - \phi_R \\ &= \text{arc} \frac{\widehat{BC}}{R_b} - \phi_R \\ &= \frac{\overline{AC}}{R_b} - \phi_R \\ &= \tan \phi_R - \phi_R \end{aligned}$$

In this equation, the angles $inv\phi_R$ and ϕ_R must be expressed in radians.

The tooth thickness at any radius is defined as the arc length between opposite faces of a tooth, measured on the circumference of the circle of that radius (Figure A.4).

$$\begin{aligned}\theta_R &= \angle xOA_S + \angle A_SOB - \angle A_ROB \\ &= \frac{t_s}{2R_s} + \text{inv}\phi_s - \text{inv}\phi_R\end{aligned}\quad (\text{A.12})$$

The tooth thickness, at radius R , will be,

$$t_R = 2R \theta_R = 2R \left\{ \frac{t_s}{2R_s} + \text{inv}\phi_s - \text{inv}\phi_R \right\} \quad (\text{A.13})$$

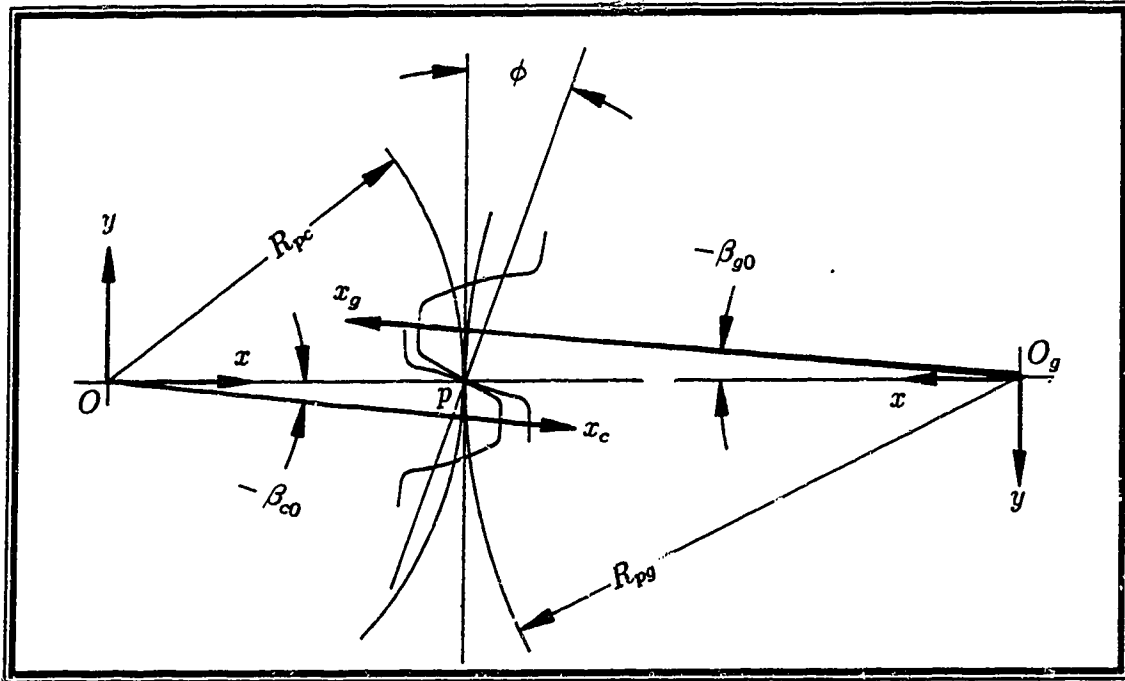


Figure A.5. Meshing position of gears with contact at the pitch point

A.3 Relation between the meshing gear and cutter positions

A relation can be derived between the angular position of the gear and the cutter, ϕ , measured from the line of centres, counter-clockwise, to their corresponding horizontal distances x and x_g passing through the centrelines of the meshing teeth, designated by x_c and x_g respectively, in Figure A.5. From the Figure A.5, when the contact point coincides with the pitch point, the angles, β_{co} and β_{g0} , can be written down by inspection,

$$\beta_{co} = -\frac{t_{pc}}{2R_{pc}} \quad (\text{A.14})$$

$$\beta_{g0} = -\frac{t_{pg}}{2R_{pg}} \quad (\text{A.15})$$

After rotation, $\Delta\beta_c$ and $\Delta\beta_g$, the angular position of the cutter and gear will be,

$$\beta_c = -\frac{t_{pc}}{2R_{pc}} + \Delta\beta_c \quad (\text{A.16})$$

$$\beta_g = -\frac{t_{pg}}{2R_{pg}} + \Delta\beta_g \quad (\text{A.17})$$

Since the pitch line velocity is the same for both the pitch circles in contact,

$$V_p = R_{pc}\omega_c = -R_{pg}\omega_g \quad (\text{A.18})$$

Multiplying both sides by dt and integrating we get,

$$R_{pc}\Delta\beta_c = -R_{pg}\Delta\beta_g \quad (\text{A.19})$$

Substituting equations A.15 and A.16 in equation A.18, the required relation is obtained, between the angular position of the pinion cutter and the generated gear, β_c and β_g respectively :

$$R_{pc}\beta_c + R_{pg}\beta_g + \frac{1}{2}(t_{pc} + t_{pg}) = 0 \quad (\text{A.20})$$

Since there is no backlash, equation A.19 can be simplified to:

$$N_c\beta_c + N_g\beta_g + \pi = 0 \quad (\text{A.21})$$

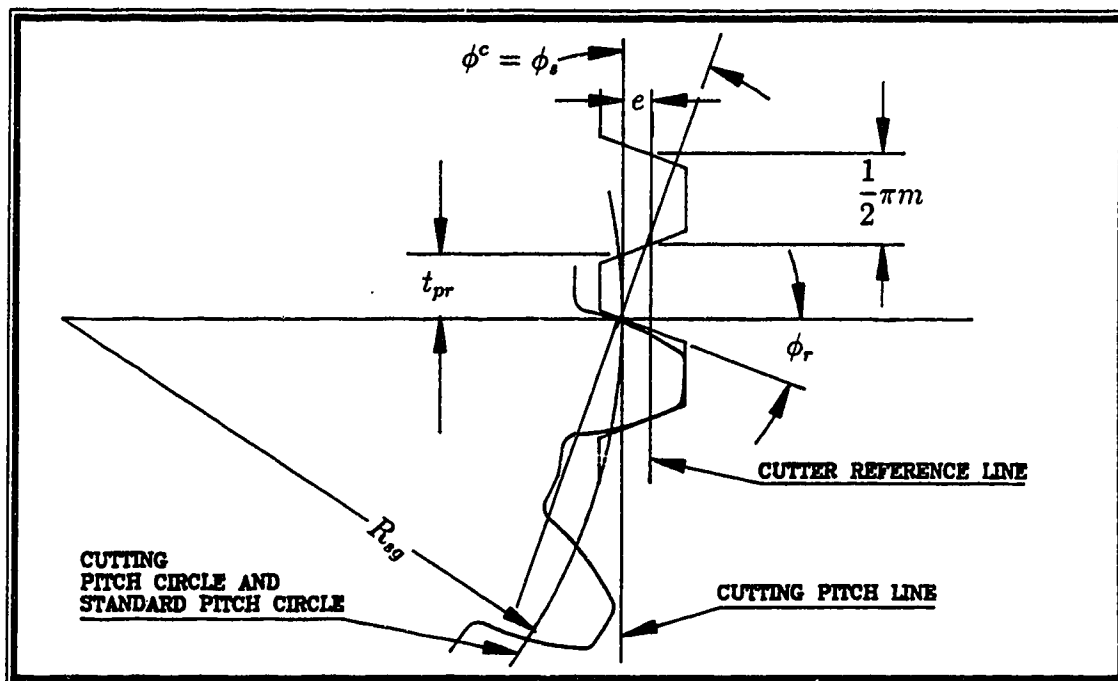


Figure A.6: Shift “ e ”, of the rack cutter, from standard cutting position

A.4 Standard cutting position

The standard cutting position is defined as the position of the rack cutter, when its reference line lies a distance R_{sg} from the centre of the gear blank, so that the cutter reference line coincides with the cutting pitch line. R_{sg} is the radius of the standard pitch circle, which is given in terms of the basic rack pitch p_r as,

$$\begin{aligned} R_{sg} &= \frac{N p_r}{2\pi} \\ &= \frac{1}{2} N m \end{aligned} \quad (\text{A.22})$$

where the module, m , is defined in terms of the basic rack pitch as,

$$m = \frac{p_r}{\pi} \quad (\text{A.23})$$

The reference line of the rack is the line, at which the tooth thickness is equal the the space width, so that each is equal to $\frac{\pi m}{2}$. Now, if the cutter is fed in the gear

blank, until its reference line lies at a distance $(R_{sg} + e)$, from the centre of the gear blank, as shown in figure A.6, the tooth thickness, t_{pr} , of the rack cutter, at cutting pitch line will be,

$$t_{pr} = \frac{1}{2}\pi m - 2e \tan \phi_s \quad (\text{A.24})$$

The tooth thickness generated in the gear, in this case, will be equal to the tooth space in the rack, as explained in Appendix A.1 :

$$\begin{aligned} t_g = w_r &= p_r - t_{pr} \\ &= \frac{1}{2}\pi m + 2e \tan \phi_s \end{aligned} \quad (\text{A.25})$$

A.5 Machine motions and constraints

Given below are some of the terminology (and their definitions) that are used in Chapter 6, in the description of the machine tool required for manufacturing the new design of shaper cutter.

A.5.1 Surfaces and elements

A real surface, corresponding to a geometrical (imaginary or ideal) surface, can be shaped on a material body by the aid of other auxiliary material bodies consisting of certain real surfaces, lines, and points which are referred to as auxiliary material elements, that are real approximations of corresponding geometrical (imaginary) elements.

A geometric surface is usually defined as the trace obtained during the motion of one geometric line called the generatrix along another line called the directrix.

The trace can be understood to be the shaped surface conceived as a continuum of consecutive geometrical positions of the generating line.

A.5.2 Operative motions

Each geometric line (generatrix and directrix), making up the geometrical surface, is produced by a definite number of shaping motions of certain geometrical elements. Shaping of real surfaces (corresponding to the above geometric surface) by machining requires a considerable number of kinematic links that are actively engaged in metal cutting and these are referred to as operative members or links whose motions are called operative motions.

The operative motion may be considered to be made up of several simpler motions called elementary motions, that have the following characteristics:

1. The elementary motions are basic motions like rotary or rectilinear motions obtained by means of rotary or rectilinear translational pairing elements.
2. The elementary motions are always simultaneous i.e. they begin at the same moment of time and are of identical duration.
3. The parameters of elementary motions comprising operative motion are always interconnected by a definite relationship.

Operative motions are of the following two types:

1. Simple: when the operative motion consists of a single elementary motion.
2. Complex: when the operative motions consists of several elementary motion.

According to the function, operative motions can be divided into two primary groups:

1. Formative or shaping motions
2. Indexing motions
3. Positioning motions (feed-in motions, setting-up motions).

If cutting occurs during a positioning motion it is called the feed-in motion (or in-feed motion). All positioning motions in which no cutting occurs are called setting-up motions.

The setting-up motions can be sub-divided into two more subgroups:

1. Controlling motions (compensating motions, adaptive motions etc.)
2. Handling motions

A.5.3 Kinematic group

A kinematic group is defined as the mechanism (device) which produces a simple operative motion (and is named after it) and is described by the path, path length, velocity and direction of motion, position at the beginning of motion and the relative geometrical position of the path of motion being followed. A kinematic group always consists of two kinematic constraints:

1. The internal constraint which provides the path of the given operative motion and,
2. The external constraint which provide the velocity, path length, direction, and the initial position.

A.5.4 Kinematic structure

A kinematic structure of a machine tool implies primarily the number and composition of its formative kinematic groups and their intergroup constraints. There are three classes of kinematic machine tool structure based on the presence of the following kinematic group that make up the structure:

1. Elementary structure: where the structure consists only of simple kinematic groups having elementary motions.

2. **Complex structure:** where the structure consists only of complex kinematic groups having complex operative motions each consisting of two or more elementary motions.
3. **Combined structure:** where the structure consists of both simplex and complex kinematic group.

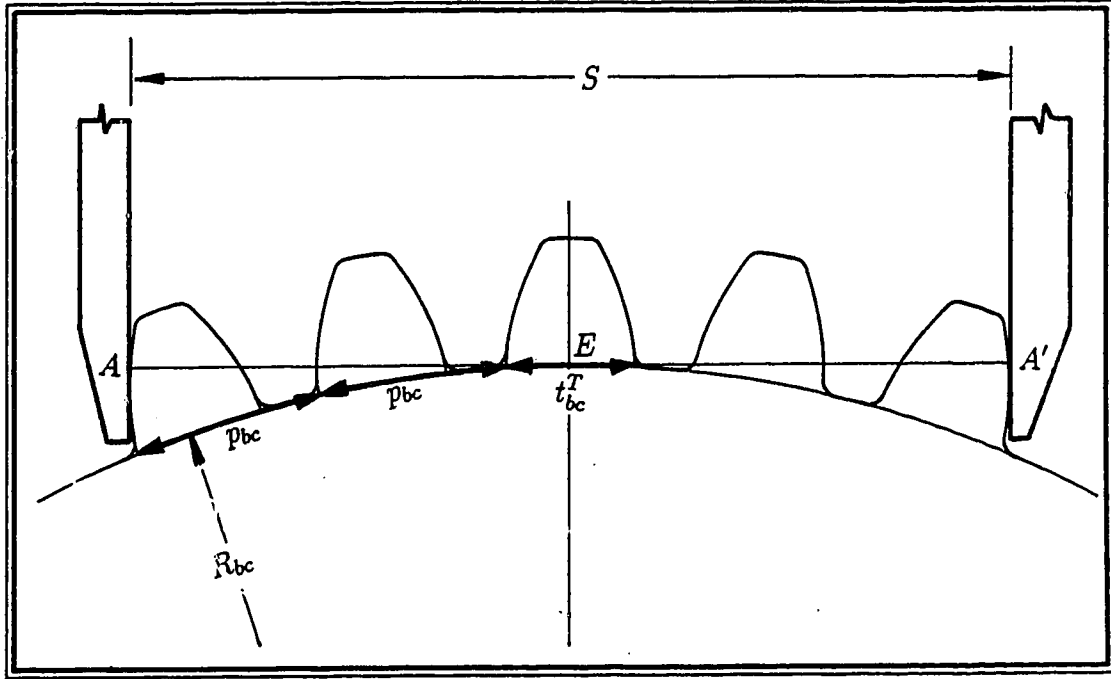


Figure A.7: Span measurement over N'_c teeth

A.6 Span measurement

The span measurement is made over N'_c number of teeth where N'_c is chosen such that the contact takes, ideally, at the middle of the tooth face ($R_{sc} + e^T$, for the case of the cutter)

Figure A.7 shows the span length over N'_c number of teeth. Assuming that the caliper is positioned over N'_c teeth, and noting that the span length $\overline{AA'}$ is equal to arc $\widehat{BB'}$, the span length can be written as:

$$S = \overline{AA'} = \widehat{BB'} = (N'_c - 1)p_{bc} + t^T_{bc} \quad (\text{A.26})$$

$$\text{where, } t^T_{bc} = R_{bc} \left(\frac{t^T_{sc}}{R_{sc}} + 2 \text{inv} \phi_s \right) \quad (\text{A.27})$$

$$R_{bc} = R_{sc} \cos \phi_s = \frac{1}{2} N'_c m \cos \phi_s \quad (\text{A.28})$$

$$p_{bc} = p_{sc} \cos \phi_s = \pi m \cos \phi_s \quad (\text{A.29})$$

Therefore, the expression for span length S over N'_c number of teeth becomes:

$$S = \cos \phi_s \left[(N'_c - 1) \pi m + t_{ac}^T + N'_c m \operatorname{inv} \phi_s \right] \quad (\text{A.30})$$

Appendix B

Case Studies Data

Input parameters for studies of different aspects of the conventional and the new cutter designs and the effect of cutter resharpenings are given here, for reference to various plotted figures in the thesis.

Essential results and parameters calculated by the simulator program are also given.

=====

FIGURE 1.9

INPUT DATA FOR SIMULATOR PROGRAM (GEAR):

INPUT=FILE : INPUT TO BE READ FROM FILE "INPUT" (UNIT=50)
 AM=10. : MODULE
 ANC=20. : NUMBER OF TEETH IN CUTTER
 ANG=40. : NUMBER OF TEETH IN GEAR
 PHIS=20. : STANDARD PRESSURE ANGLE
 DTG=420. : DIA. OF GEAR BLANK
 TSG=16. : STANDARD TOOTH THICKNESS OF GEAR
 FW=25. : USABLE FACE WIDTH OF CUTTER
 COND=2. : CUTTER IS CORRECTED(2) OR NOT(1)
 TSC=22. : STANDARD TOOTH THICKNESS OF CUTTER (READ IF COND=2)
 ADDC=14.0 : ADDENDUM OF CUTTER (READ IF COND=2)
 WDC=22.0 : WHOLE DEPTH OF CUTTER (READ IF COND=2)
 CLEAR=1. : IF CLEARANCE<0; THEN 1=STOP,2=NEW VALUES,3=CONTINUE
 CINV=1. : IF BCC<RCC; THEN 1=STOP, 2=NEW VALUES, 3=CONTINUE
 GINV=3. : IF BCG<RCG; THEN 1=STOP, 2=NEW VALUES, 3=CONTINUE
 TIP=1. : ERROR IN GEAR; THEN 1=STOP, 2=NEW VALUES, 3=CONTINUE
 E1=3. : DECREMENT IN STOCK IN EACH RUN
 RAKE=5. : RAKE ANGLE OF CUTTER
 RELIEF=20. : RELIEF ANGLE OF CUTTER
 CT=2. : RADIUS OF CIRCULAR TIP OF CUTTER
 DELTA=.5 : INCREMENTAL STEPS FOR PROFILE EVALUATION
 ROUT=1. : NEW DESIGN(1) OR CONVENTIONAL DESIGN(3)
 RUN=1. : NEW CUTTER(1) OR ALL RESHARPENINGS(2)
 B=20. : DESIGN DISTANCE
 PLNO=100. : NUMBER OF PLANES IN CONVENTIONAL DESIGN
 DES=CUTTER PROFILE IS INVOLUTE WITH ROUNDED TIP : CUTTER DESCRIPTION
 RNO=5. : NUMBER OF RESHARPENINGS IN EACH RUN

FIGURE 1.9 (CONTD.)

PROGRAM : CONJUGATE GEAR TOOTH PROFILE SHAPE GENERATED BY GENERAL PINION CUTTER

DEVELOPED BY : DEBKUMAR RAKSHIT
GRADUATE STUDENT (MECHANICAL)
UNIVERSITY OF ALBERTA

DATE : 18.5.88

NOTE : 1. The main program is in the file GEAR3
2. The output is file DATFL.
3. The output files DAT2 and DAT3 are used by the following programs for graphics output: PROFILE.GR2, 3DGEAR, 3DCUTTER.

FIXED PARAMETERS:

GEAR DATA:
NUMBER OF TEETH IN GEAR : 40
BLANK DIAMETER OF GEAR : 420.0000
TOOTH THICKNESS OF GEAR : 16.0000
RADIUS OF STANDARD PITCH CIRCLE OF GEAR : 200.0000
RADIUS OF BASE CIRCLE OF GEAR : 187.9385

CUTTER DATA:
NUMBER OF TEETH IN CUTTER : 20
RADIUS OF STANDARD PITCH CIRCLE OF CUTTER : 100.0000
RADIUS OF BASE CIRCLE OF CUTTER : 93.9693
FACE WIDTH OF CUTTER : 25.0000

GENERAL DATA:
MODULE OF GEAR AND CUTTER : 10.0000
STANDARD PRESSURE ANGLE : 20.0000
GEAR RATIO : 2.0000
STANDARD CUTTING CENTRE DISTANCE : 300.0000
STANDARD CIRCULAR PITCH : 31.4159

CUTTER PROFILE FUNCTION DESCRIPTION:

NEW DESIGN: EFFECTIVE CUTTER PROFILES ARE INVOLUTES
THE CUTTER TIP IS ROUNDED BY AN CIRCULAR ARC OF RADIUS 2.00 MM

TOOTH PROFILE PARAMETERS

CUTTER PARAMETERS										GEAR PARAMETER										MESHING VALUES																						
CUTTER PROFILE					CUTTER					TOOTH					GEARPROFILE					GEAR					RADIUS OF CURVATURE			TOOTH CENTRE ANGLE			GEAR THICKNESS			GEAR PROFIL ANGLE			OPT. PRESS ANGLE			PATH OF CONTACT		
X	Y	R	THETA	TOOTH THKNESS	CUTTER THKNESS	CUTTER PROFIL ANGLE	TOOTH CENTRE ANGLE	RADIUS OF CURVATURE (CUTTER)	R	THETA	GEARPROFILE	GEAR THKNESS	GEAR PROFIL ANGLE	TOOTH CENTRE ANGLE	RADIUS OF CURVATURE (GEAR)	OPT. PRESS ANGLE	PATH OF CONTACT	XI	ETA																							
121.28	0.00	121.2794	0.00	0.000	0.000	90.00	0.00	121.2794	192.8595	4.50	192.8593	30.294	90.00	-4.50	192.8593	90.00	-16.566		-0.000																							
121.27	1.10	121.2794	0.52	2.204	2.204	90.00	-0.52	121.2796	192.8595	4.24	192.8586	28.541	90.00	-4.24	192.8586	90.00	-16.566		-0.000																							
121.27	1.49	121.2786	0.71	2.988	2.988	88.41	-0.45	2.0000	192.8622	4.11	192.8622	27.701	88.00	-4.27	-4.5179	88.16	-16.564		-0.532																							
121.17	2.04	121.1866	0.97	4.087	4.087	72.62	1.88	2.0000	193.1952	3.66	193.1952	24.652	68.00	-5.44	-4.9300	69.78	-16.324		-6.013																							
121.07	2.29	121.0910	1.08	4.578	4.578	65.14	3.15	2.0000	193.5838	3.43	193.5838	23.171	58.26	-6.07	-5.4619	60.91	-16.048		-8.930																							
120.97	2.47	120.9946	1.17	4.940	4.940	59.29	4.28	2.0000	194.0330	3.24	194.0330	21.974	50.44	-6.64	-6.1412	53.84	-15.734		-11.499																							
120.87	2.62	120.8977	1.24	5.233	5.233	54.29	5.42	2.0000	194.5622	3.08	194.5622	20.902	43.50	-7.21	-7.0226	47.63	-15.369		-14.017																							
120.77	2.74	120.8004	1.30	5.478	5.478	49.82	6.62	2.0000	195.2020	2.92	195.2020	19.888	37.01	-7.81	-8.1911	41.90	-14.935		-16.646																							
120.67	2.84	120.7029	1.35	5.688	5.688	45.71	7.96	2.0000	196.0023	2.76	196.0023	18.898	30.68	-8.48	-9.7836	36.40	-14.399		-19.531																							
120.57	2.94	120.6051	1.39	5.871	5.871	41.87	9.53	2.0000	197.0497	2.60	197.0497	17.911	24.29	-9.27	-12.0357	30.95	-13.706		-22.857																							
UUUUUU	UUUUUU	120.5215	1.43	6.009	6.009	38.77	11.16	75.4666	198.2606	2.47	198.2606	17.073	18.57	-10.08	63.1388	26.18	-12.912		-26.262																							
UUUUUU	UUUUUU	120.0215	1.62	6.781	6.781	38.47	10.67	74.6656	198.5172	2.44	198.5172	16.921	18.79	-9.83	63.9396	26.18	-12.559		-25.543																							
UUUUUU	UUUUUU	119.5215	1.81	7.541	7.541	38.17	10.18	73.8592	198.7784	2.42	198.7784	16.764	19.01	-9.59	64.7459	26.18	-12.203		-24.820																							
UUUUUU	UUUUUU	119.0215	2.00	8.290	8.290	37.86	9.68	73.0473	199.0443	2.39	199.0443	16.602	19.23	-9.34	65.5575	26.18	-11.845		-24.091																							
UUUUUU	UUUUUU	118.5215	2.18	9.026	9.026	37.55	9.18	72.2298	199.3151	2.36	199.3151	16.435	19.45	-9.09	66.3752	26.18	-11.484		-23.357																							
UUUUUU	UUUUUU	118.0215	2.37	9.751	9.751	37.23	8.68	71.4064	199.5908	2.33	199.5908	16.261	19.67	-8.84	67.1954	26.18	-11.121		-22.619																							
UUUUUU	UUUUUU	117.5215	2.55	10.463	10.463	36.91	8.18	70.5768	199.8716	2.31	199.8716	16.082	19.90	-8.59	68.0286	26.18	-10.755		-21.874																							
UUUUUU	UUUUUU	117.0215	2.73	11.164	11.164	36.58	7.67	69.7410	200.1576	2.28	200.1576	15.897	20.12	-8.33	68.8644	26.18	-10.386		-21.124																							
UUUUUU	UUUUUU	116.5215	2.91	11.852	11.852	36.25	7.15	68.8987	200.4490	2.24	200.4490	15.705	20.35	-8.08	69.7070	26.18	-10.014		-20.368																							
UUUUUU	UUUUUU	116.0215	3.09	12.529	12.529	35.91	6.64	68.0498	200.7458	2.21	200.7458	15.506	20.58	-7.82	70.5559	26.18	-9.640		-19.606																							
UUUUUU	UUUUUU	115.5215	3.27	13.193	13.193	35.57	6.11	67.1937	201.0482	2.18	201.0482	15.301	20.81	-7.56	71.4121	26.18	-9.262		-18.838																							
UUUUUU	UUUUUU	115.0215	3.45	13.845	13.845	35.22	5.59	66.3304	201.3565	2.15	201.3565	15.089	21.04	-7.29	72.2752	26.18	-8.881		-18.064																							
UUUUUU	UUUUUU	114.5215	3.62	14.484	14.484	34.86	5.06	65.4595	201.6707	2.11	201.6707	14.869	21.27	-7.03	73.1460	26.18	-8.497		-17.282																							
UUUUUU	UUUUUU	114.0215	3.80	15.111	15.111	34.50	4.52	64.5809	201.9911	2.08	201.9911	14.641	21.50	-6.76	74.0243	26.18	-8.109		-16.493																							
UUUUUU	UUUUUU	113.5215	3.97	15.726	15.726	34.13	3.98	63.6940	202.3178	2.04	202.3178	14.406	21.73	-6.49	74.9114	26.18	-7.718		-15.697																							


```

=====
FIGURE 2.9 & 2.10
INPUT DATA SAME AS FIGURE 1.9 EXCEPT: DELTA=0.1, ROUT=1 & 3
=====
FIGURE 2.12, 2.13, 2.14, 2.15
INPUT DATA SAME AS FIGURE 1.9 EXCEPT: DELTA=0.1
ROUT=1
& ROUT=3, RAKE=0, 5, 8, 12, 15, 18, 20
=====
FIGURE 2.17, 2.18, 2.19, 2.20, 2.21 & 2.22
INPUT DATA SAME AS FIGURE 2.9 EXCEPT: DELTA=0.1
CORRECTION TO PHI AND TSC APPLIED AS FOLLOWS:
=====

```

	GAMMA	PHIC	METHOD I tsc	METHOD II tsc
	5.0000000	20.6033210	22.0000000	22.3351938
	8.0000000	20.9864139	22.0000000	22.5494094
	10.0000000	21.2525994	22.0000000	22.6989005
	12.0000000	21.5287207	22.0000000	22.8545435
	15.0000000	21.9643453	22.0000000	23.101304E
	18.0000000	22.4301925	22.0000000	23.3668660
	20.0000000	22.7604769	22.0000000	23.5562288

```

=====
FIGURE 3.4 & 3.5
INPUT DATA SAME AS FIGURE 1.9 EXCEPT: DELTA=0.1
=====

```

=====

FIGURE 4.5, 4.6, 4.7, 4.8, 4.9, 4.10, 4.11 & 4.12

INPUT DATA SAME AS FIGURE 1.9 EXCEPT:

ROUT=1, DELTA=0.1, TSC=23, ADDC=16

& ROUT=3, DELTA=0.1, TSC=23, ADDC=16

PARTIAL OUTPUT OF SIMULATOR PROGRAM:

DATAFILE NAME: DATFL (OUTPUT OF GEAR)

PROGRAM : CONJUGATE GEAR TOOTH PROFILE SHAPE GENERATED BY GENERAL PINION CUTTER

DEVELOPED BY : DEBKUMAR RAKSHIT
GRADUATE STUDENT (MECHANICAL)
UNIVERSITY OF ALBERTA

DATE : 18.5.88

NOTE : 1. The main program is in the file GEAR3
2. The output is file DATFL.
3. The output files DAT2 and DAT3 are used by the following programs for graphics output:
PROFILE.GR2, 3DGEAR, 3DCUTTER.

FIXED PARAMETERS:

GEAR DATA:

NUMBER OF TEETH IN GEAR : 40
BLANK DIAMETER OF GEAR : 420.0000
TOOTH THICKNESS OF GEAR : 16.0000
RADIUS OF STANDARD PITCH CIRCLE OF GEAR : 200.0000
RADIUS OF BASE CIRCLE OF GEAR : 187.9385

CUTTER DATA:

NUMBER OF TEETH IN CUTTER : 20
RADIUS OF STANDARD PITCH CIRCLE OF CUTTER : 100.0000
RADIUS OF BASE CIRCLE OF CUTTER : 93.9693
FACE WIDTH OF CUTTER : 25.0000

GENERAL DATA:

MODULE OF GEAR AND CUTTER : 10.0000
STANDARD PRESSURE ANGLE : 20.0000
GEAR RATIO : 2.0000
STANDARD CUTTING CENTRE DISTANCE : 300.0000
STANDARD CIRCULAR PITCH : 31.4159

CUTTER PROFILE FUNCTION DESCRIPTION:

NEW DESIGN: EFFECTIVE CUTTER PROFILES ARE INVOLUTES
THE CUTTER TIP IS ROUNDED BY AN CIRCULAR ARC OF RADIUS 2.00 MM

VARIABLE PARAMETERS:

GEAR DATA:
 RADIUS OF PITCH CIRCLE OF GEAR : 210.1310
 WHOLE DEPTH OF GEAR : 18.0829
 ADDENDUM OF GEAR : 10.0000
 DEDENDUM OF GEAR : 8.0829
 RADIUS OF ROOT CIRCLE OF GEAR : 191.9171
 RADIUS OF TIP CIRCLE OF GEAR : 210.0000

CUTTER DATA:
 TOOTH THICKNESS OF CUTTER : 28.2990
 RADIUS OF PITCH CIRCLE OF CUTTER : 105.0655
 WHOLE DEPTH OF CUTTER : 22.0000
 ADDENDUM OF CUTTER : 23.2794
 DEDENDUM OF CUTTER : -1.2794
 RADIUS OF TIP CIRCLE OF CUTTER : 123.2794
 RADIUS OF ROOT CIRCLE OF CUTTER : 101.2794

GENERAL DATA:
 ACTUAL CUTTING CENTRE DISTANCE : 315.1965
 CUTTING PRESSURE ANGLE : 26.5703
 CIRCULAR PITCH : 33.0073
 CLEARANCE BETWEEN CUTTER ROOT AND GEAR TIP : 3.9171

CUTTER TIP CORNER DATA

CASE I. ROUNDED TIP	CASE II. NON-ROUNDED TIP
RADIUS OF CIRCULAR ARC : 2.0000	X-COORDINATE OF CORNER : 123.2716
X-COORDINATE OF CIRCULAR ARC : 121.2786	Y-COORDINATE OF CORNER : 1.3850
Y-COORDINATE OF CIRCULAR ARC : 0.4329	

AFTER 5 REGRINDINGS OF CUTTER

CUTTER TOOL GEOMETRY:

AMOUNT OF STOCK REMOVED AFTER EACH REGRINDING : 0.6000
 TOTAL AMOUNT OF STOCK REMOVED IN CURRENT REGRINDING : 3.0000
 RAKE ANGLE OF CUTTER : 20.0000
 TOP CLEARANCE ANGLE OF CUTTER : 20.0000

VARIABLE PARAMETERS:

GEAR DATA:
 RADIUS OF PITCH CIRCLE OF GEAR : 209.4434
 WHOLE DEPTH OF GEAR : 17.7747
 ADDENDUM OF GEAR : 10.0000 | wrt S.P.C.
 DEDENDUM OF GEAR : 7.7747
 RADIUS OF ROOT CIRCLE OF GEAR : 192.2253
 RADIUS OF TIP CIRCLE OF GEAR : 210.0000

CUTTER DATA:

TOOTH THICKNESS OF CUTTER : 27.3239
 RADIUS OF PITCH CIRCLE OF CUTTER : 104.7217
 WHOLE DEPTH OF CUTTER : 22.0000 | wrt S.P.C.
 ADDENDUM OF CUTTER : 21.9400
 DEDENDUM OF CUTTER : 0.0600
 RADIUS OF TIP CIRCLE OF CUTTER : 121.9400
 RADIUS OF ROOT CIRCLE OF CUTTER : 99.9400

GENERAL DATA:

ACTUAL CUTTING CENTRE DISTANCE : 314.1653
 CUTTING PRESSURE ANGLE : 26.1917
 CIRCULAR PITCH : 32.8993
 CLEARANCE BETWEEN CUTTER ROOT AND GEAR TIP : 4.2253

CUTTER TIP CORNER DATA

CASE I. ROUNDED TIP	CASE II. NON-ROUNDED TIP
RADIUS OF CIRCULAR ARC : 2.0000	X-COORDINATE OF CORNER : 121.9253
X-COORDINATE OF CIRCULAR ARC : 119.9364	Y-COORDINATE OF CORNER : 1.8919
Y-COORDINATE OF CIRCULAR ARC : 0.9151	

AFTER 10 REGRINDINGS OF CUTTER

CUTTER TOOL GEOMETRY:

AMOUNT OF STOCK REMOVED AFTER EACH REGRINDING : 0.6000
 TOTAL AMOUNT OF STOCK REMOVED IN CURRENT REGRINDING : 6.0000
 RAKE ANGLE OF CUTTER : 20.0000
 TOP CLEARANCE ANGLE OF CUTTER : 20.0000

VARIABLE PARAMETERS:

GEAR DATA:
 RADIUS OF PITCH CIRCLE OF GEAR : 208.7471
 WHOLE DEPTH OF GEAR : 17.4797
 ADDENDUM OF GEAR : 10.0000 wrt S.P.C.
 DEDENDUM OF GEAR : 7.4797
 RADIUS OF ROOT CIRCLE OF GEAR : 192.5203
 RADIUS OF TIP CIRCLE OF GEAR : 210.0000

CUTTER DATA:

TOOTH THICKNESS OF CUTTER : 26.3489
 RADIUS OF PITCH CIRCLE OF CUTTER : 104.3736
 WHOLE DEPTH OF CUTTER : 22.0000
 ADDENDUM OF CUTTER : 20.6005 wrt S.P.C.
 DEDENDUM OF CUTTER : 1.3995
 RADIUS OF TIP CIRCLE OF CUTTER : 120.6005
 RADIUS OF ROOT CIRCLE OF CUTTER : 98.6005

GENERAL DATA:

ACTUAL CUTTING CENTRE DISTANCE : 313.1208
 CUTTING PRESSURE ANGLE : 25.8004
 CIRCULAR PITCH : 32.7899
 CLEARANCE BETWEEN CUTTER ROOT AND GEAR TIP : 4.5203

CUTTER TIP CORNER DATA

CASE I. ROUNDED TIP	CASE II. NON-ROUNDED TIP
RADIUS OF CIRCULAR ARC : 2.0000	X-COORDINATE OF CORNER : 120.5773
X-COORDINATE OF CIRCULAR ARC : 118.5926	Y-COORDINATE OF CORNER : 2.3697
Y-COORDINATE OF CIRCULAR ARC : 1.3677	

AFTER 15 REGRINDINGS OF CUTTER

CUTTER TOOL GEOMETRY:

AMOUNT OF STOCK REMOVED AFTER EACH REGRINDING : 0.6000
 TOTAL AMOUNT OF STOCK REMOVED IN CURRENT REGRINDING : 9.0000
 RAKE ANGLE OF CUTTER : 20.0000
 TOP CLEARANCE ANGLE OF CUTTER : 20.0000

VARIABLE PARAMETERS:

GEAR DATA:
 RADIUS OF PITCH CIRCLE OF GEAR : 208.0403
 WHOLE DEPTH OF GEAR : 17.2006
 ADDENDUM OF GEAR : 10.0000 | wrt S.P.C.
 DEDENDUM OF GEAR : 7.2006
 RADIUS OF ROOT CIRCLE OF GEAR : 192.7994
 RADIUS OF TIP CIRCLE OF GEAR : 210.0000

CUTTER DATA:
 TOOTH THICKNESS OF CUTTER : 25.3739
 RADIUS OF PITCH CIRCLE OF CUTTER : 104.0202
 WHOLE DEPTH OF CUTTER : 22.0000 | wrt S.P.C.
 ADDENDUM OF CUTTER : 19.2611
 DEDENDUM OF CUTTER : 2.7389
 RADIUS OF TIP CIRCLE OF CUTTER : 119.2611
 RADIUS OF ROOT CIRCLE OF CUTTER : 97.2611

GENERAL DATA:

ACTUAL CUTTING CENTRE DISTANCE : 312.0605
 CUTTING PRESSURE ANGLE : 25.3947
 CIRCULAR PITCH : 32.6789
 CLEARANCE BETWEEN CUTTER ROOT AND GEAR TIP : 4.7994

CUTTER TIP CORNER DATA

CASE I. ROUNDED TIP
 RADIUS OF CIRCULAR ARC : 2.0000
 X-COORDINATE OF CIRCULAR ARC : 117.2474
 Y-COORDINATE OF CIRCULAR ARC : 1.7904

CASE II. NON-ROUNDED TIP
 X-COORDINATE OF CORNER : 119.2278
 Y-COORDINATE OF CORNER : 2.8181

AFTER 20 REGRINDINGS OF CUTTER

CUTTER TOOL GEOMETRY:

AMOUNT OF STOCK REMOVED AFTER EACH REGRINDING : 0.6000
 TOTAL AMOUNT OF STOCK REMOVED IN CURRENT REGRINDING : 12.0000
 RAKE ANGLE OF CUTTER : 20.0000
 TOP CLEARANCE ANGLE OF CUTTER : 20.0000

VARIABLE PARAMETERS:

GEAR DATA:
 RADIUS OF PITCH CIRCLE OF GEAR : 207.3226
 WHOLE DEPTH OF GEAR : 16.9375
 ADDENDUM OF GEAR : 10.0000 | wrt S.P.C.
 DEPENDUM OF GEAR : 6.9375
 RADIUS OF ROOT CIRCLE OF GEAR : 193.0625
 RADIUS OF TIP CIRCLE OF GEAR : 210.0000

CUTTER DATA:

TOOTH THICKNESS OF CUTTER : 24.3988
 RADIUS OF PITCH CIRCLE OF CUTTER : 109.6613
 WHOLE DEPTH OF CUTTER : 22.0000 | wrt S.P.C.
 ADDENDUM OF CUTTER : 17.9217
 DEPENDUM OF CUTTER : 4.0783
 RADIUS OF TIP CIRCLE OF CUTTER : 117.9217
 RADIUS OF ROOT CIRCLE OF CUTTER : 95.9217

GENERAL DATA:

ACTUAL CUTTING CENTRE DISTANCE : 310.9841
 CUTTING PRESSURE ANGLE : 24.9737
 CIRCULAR PITCH : 32.5662
 CLEARANCE BETWEEN CUTTER ROOT AND GEAR TIP : 5.0625

CUTTER TIP CORNER DATA

CASE I. ROUNDED TIP	CASE II. NON-ROUNDED TIP
RADIUS OF CIRCULAR ARC : 2.0000	X-COORDINATE OF CORNER : 117.8772
X-COORDINATE OF CIRCULAR ARC : 115.9011	Y-COORDINATE OF CORNER : 3.2367
Y-COORDINATE OF CIRCULAR ARC : 2.1828	

AFTER 25 REGRINDINGS OF CUTTER

CUTTER TOOL GEOMETRY:

AMOUNT OF STOCK REMOVED AFTER EACH REGRINDING : 0.6000
 TOTAL AMOUNT OF STOCK REMOVED IN CURRENT REGRINDING : 15.0000
 RAKE ANGLE OF CUTTER : 20.0000
 TOP CLEARANCE ANGLE OF CUTTER : 20.0000

VARIABLE PARAMETERS:

GEAR DATA:
 RADIUS OF PITCH CIRCLE OF GEAR : 206.5932
 WHOLE DEPTH OF GEAR : 16.6924
 ADDENDUM OF GEAR : 10.0000
 DEPENDUM OF GEAR : 6.6924
 RADIUS OF ROOT CIRCLE OF GEAR : 193.3076
 RADIUS OF TIP CIRCLE OF GEAR : 210.0000

CUTTER DATA:

TOOTH THICKNESS OF CUTTER : 23.4238
 RADIUS OF PITCH CIRCLE OF CUTTER : 103.2966
 WHOLE DEPTH OF CUTTER : 22.0000
 ADDENDUM OF CUTTER : 16.5822
 DEPENDUM OF CUTTER : 5.4178
 RADIUS OF TIP CIRCLE OF CUTTER : 116.5822
 RADIUS OF ROOT CIRCLE OF CUTTER : 94.5822

GENERAL DATA:

ACTUAL CUTTING CENTRE DISTANCE : 309.8899
 CUTTING PRESSURE ANGLE : 24.5357
 CIRCULAR PITCH : 32.4516
 CLEARANCE BETWEEN CUTTER ROOT AND GEAR TIP : 5.3076

CUTTER TIP CORNER DATA

CASE I. ROUNDED TIP	CASE II. NON-ROUNDED TIP
RADIUS OF CIRCULAR ARC : 2.0000	X-COORDINATE OF CORNER : 116.5259
X-COORDINATE OF CIRCULAR ARC : 114.5540	Y-COORDINATE OF CORNER : 3.6252
Y-COORDINATE OF CIRCULAR ARC : 2.5445	


```
=====
FIGURE 5.1, 5.4, 5.5 & 5.6
INPUT DATA SAME FIGURE 1.9 EXCEPT DELTA=0.1
=====
FIGURE 5.8, 5.9 & 5.10
INPUT DATA SAME AS FIGURE 1.9 EXCEPT: DELTA=0.1
INPUT FOR EQ 5.24:
RDTC=116, RDPC=105, RDPG=210, RDCT=4,B=20
CALCULATED VALUES:
RF=4.77777, RTCT=2.47 => RACT = 4.0 - 0.0765*A
EQ 5.29 USED: RACT = 4.0 - 0.082*A
```

Appendix C

Gear Shaping Simulator Program Listing

The gear shaper simulator program is written in FORTRANVS and run on the University of Alberta's Amdahl 5870 mainframe computer, and the plots are generated on the Calcomp plotter linked to the mainframe.

The program takes input values both through interactive entry (for single runs) as well through file entry (for multiple runs - resharpenings). For both the designs (conventional and new), the program can evaluate the side and tip profiles of cutter and generated gear teeth for the case of a new cutter and for different stages of resharpening.

The program prints the results in tabular form for easy reference and also in form of a datafile to be read by the graphics programs for plotting.

```

*GEAR
CCCCCCCCCCCCCCCCCCCCCCCCCCCCCCCCCCCCCCCCCCCCCCCCCCCCCCCCCCCC
C      CONJUGATE GEAR TOOTH PROFILE SHAPE GENERATED
C      BY GENERAL PINION CUTTER(MAIN PROGRAM)
C
C      Developed by :  Debkumar Rakshit
C                   Graduate student (Mechanical) U. of A.
C
C      Date : May '88 - June '89
C
C      Note : 1. The main program is in the file -"GEAR"
C            2. The numerical output is in the file - "DATFL"
C            3. Plotter data are in DAT2 and DAT3
C            4. The input parameters are fed interactively.
C               or through file INPUT where there should
C               be a line INPUT=FILE. File entry is for batch run
C            5. To change cutter profile shape modify subroutine
C               CUT . The function  $y=f(x)$  has origin at the
C               center of cutter and can be piecewise continuous.
C            6. A number of different cutter shape function sub-
C               routines can be made in the file in an external
C               file. In this case name the external routine as
C               "EXT". Shape for convensional cutter is included
C               in subroutine "EFFECT". Shape for the new cutter
C               is included in subroutine "CUTTER".
C            7. The program automatically includes a circular
C               top land and a rounded tip in the cutter profile
C
CCCCCCCCCCCCCCCCCCCCCCCCCCCCCCCCCCCCCCCCCCCCCCCCCCCCCCCCCCCC

```

```

.....
*
          VARIABLES USED
.....

```

```

* X      X-COORDINATE OF CUTTER PROFILE
* -Y     Y-COORDINATE OF CUTTER PROFILE
* RC     R-COORDINATE OF CUTTER PROFILE
* THETAC THETA COORDINATE OF CUTTER PROFILE
* TC     THICKNESS OF CUTTER TOOTH AT RC,THETAC
* PHIC   PROFILE ANGLE OF CUTTER AT RC,THETAC
* BETAC  INCLINATION OF CUTTER TOOTH AT CONTACT PT OF RC,THETAC
* RHOC   RADIUS OF CURVATURE OF CUTTER TOOTH AT RC,THETAC
* NC     NUMBER OF TEETH IN CUTTER
* RSC    RADIUS OF THE STANDARD PITCH CIRCLE OF CUTTER
* RBC    RADIUS OF THE BASE CIRCLE OF CUTTER
* FW     FACE WIDTH OF THE CUTTER
* TSC    TOOTH THICKNESS OF CUTTER AT STANDARD PITCH CIRCLE
* RPC    RADIUS OF CUTTING PITCH CIRCLE OF CUTTER

```

- * WDC WHOLE DEPTH OF CUTTER
- * ADDC ADDENDUM OF CUTTER
- * RTCC RADIUS OF TIP CIRCLE OF CUTTER
- * RRCC RADIUS OF ROOT CIRCLE OF CUTTER
- * XC X-COORDINATE OF CENTRE OF TIP ROUNDING ARC
- * YC Y-COORDINATE OF CENTRE OF TIP ROUNDING ARC
- * XA X-COORDINATE OF LOWEST PT ON TIP CIRCLE OF CUTTER
- * XB X-COORDINATE OF HIGHEST PT ON INVOLUTE PROFILE
- * RAKE VALUE OF RAKE ANGLE OF CUTTER
- * RELIEF VALUE OF TOP RELIEF ANGLE
- * E1 AMOUNT OF STOCK REMOVED PER RESHARPENING
- * E PROFILE SHIFT
- * RTCAG RADIUS OF TIP CIRCLE OF CUTTER AFTER REGRINDING
-
- * NG NUMBER OF TOOTH IN GEAR
- * RG R-COORDINATE OF GEAR TOOTH
- * THETAG THETA COORDINATE OF GEAR TOOTH
- * TG THICKNESS OF GEAR TOOTH AT (R,THETA)
- * PHIG PROFILE ANGLE OF GEAR AT RG,THETAG
- * BETAG INCLINATION OF GEAR TOOTH AT CONTACT PT OF RG,THETAG
- * RHOG RADIUS OF CURVATURE OF GEAR TOOTH AT RG,THETAG
- * NG NUMBER OF TEETH IN GEAR
- * DTG DIAMETER OF THE GEAR BLANK
- * RPG RADIUS OF PITCH CIRCLE OF GEAR
- * RSG RADIUS OF STANDARD PITCH CIRCLE OF GEAR
- * RBG RADIUS OF BASE CIRCLE OF GEAR
- * RPG RADIUS OF THE CUTTING PITCH CIRCLE OF GEAR
- * WDG WHOLE DEPTH OF GEAR
- * ADDG ADDENDUM OF GEAR
- * RRCCG RADIUS OF THE ROOT CIRCLE OF GEAR
- * RTCCG RADIUS OF THE TIP CIRCLE OF GEAR
- * TSG TOOTH THICKNESS OF GEAR AT STANDARD PITCH CIRCLE
-
- * PHI CUTTING PRESSURE ANGLE FOR NEW CUTTER
- * XI ORDINATE OF AXIS AT PITCH POINT
- * ETA ABSCISSA OF AXIS AT PITCH POINT
- * PHIS STANDARD CUTTING PRESSURE ANGLE
- * CS STANDARD CUTTING CENTRE DISTANCE
- * PS CIRCULAR PITCH AT STANDARD PITCH CIRCLE
- * CC ACTUAL CUTTING CENTRE DISTANCE
- * PPC CIRCULAR PITCH AT CUTTING PITCH CIRCLES
- * C CLEARANCE BETWEEN CUTTER ROOT AND GEAR TIP
- * AM MODULE OF GEAR AND CUTTER
- * COND CONDITION PARAMETER FOR USER DEFINED/STANDARD CUTTER
- * ROUT SELECTION PARAMETER FOR PROFILE TYPE
- * S DISTANCE FROM PT OF CONTACT TO PITCH POINT
- * RUN SELECTION PARAMETER FOR NUMBER OF RUNS

```

*****
PARAMETER(RAD=3.1415927/180.)
CHARACTER*80 INPUT,CH
COMMON X,Y,RC,THETAC,TC,PHIC,BETAC,RHOC,RG,THETAG,
*TG,PHIG,BETAG,RHOG,PHI,XI,ETA,TOUCH
REAL INV
COMMON /F/NG,DTG,TSG,RSG,RGB,NC,RSC,RBC,FW,AM,PHIS,CS,PS,GR
COMMON /V/RPG,WDG,ADDG,RRCG,RTCG,TSC,RPC,WDC,ADDC,RTCC,
*RRCC,CC,PHIV,PPC,C,XC,YC
DONE=0
IRUN=0
ET=0
ITOUCH=0
XC=0.0
YC=0.0

```

C----- opens files-----

```

100 OPEN(UNIT=10,FILE='DAT3',STATUS='OLD')
OPEN(UNIT=20,FILE='DATFL',STATUS='OLD')
OPEN(UNIT=9,FILE='DAT2',STATUS='OLD')
OPEN(UNIT=55,FILE='RADIUS',STATUS='OLD')
CLOSE(UNIT=55,STATUS='DELETE')
CLOSE(UNIT=10,STATUS='DELETE')
CLOSE(UNIT=20,STATUS='DELETE')
CLOSE(UNIT=9,STATUS='DELETE')
OPEN(UNIT=20,FILE='DATFL',STATUS='NEW')
OPEN(UNIT=9,FILE='DAT2',STATUS='NEW')
OPEN(UNIT=10,FILE='DAT3',STATUS='NEW')
OPEN(UNIT=50,FILE='INPUT',STATUS='OLD')
OPEN(UNIT=55,FILE='RADIUS',STATUS='NEW')

```

C----- reads input parameters-----

```

CALL TITLE
E=0.0
INIT=0
NPAGE=1

CALL STAR
CALL PRGM(1)
CALL STUDY('INPUT',INPUT,RLNO)
IF(INPUT.EQ.'FILE')THEN
CALL STUDY('AM',CH,AM)
CALL STUDY('ANC',CH,ANC)

```

```

CALL STUDY('ANG',CH,ANG)
CALL STUDY('PHIS',CH,PHIS)
CALL STUDY('DTG',CH,DTG)
CALL STUDY('TSG',CH,TSG)
CALL STUDY('FW',CH,FW)
CALL STUDY('DELTA',CH,DELTA)
CALL STUDY('COND',CH,COND,*12)
END IF
CALL READER(' module of cutter and gear:',AM)
CALL READER(' no. of teeth in Cutter:',ANC)
CALL READER(' no of teeth in gear:',ANG)
CALL READER(' the standard pressure angle:',PHIS)
CALL READER(' the diameter of gear blank:',DTG)
CALL READER(' tooth thickness of gear to be cut:',TSG)
CALL READER(' usable face width:',FW)
CALL READER(' increment in X values:',DELTA)
CALL STAR
PRINT*,'Select cutter condition:'
PRINT*,'1. New cutter( $t_{sc} = P_s/2$ , radius of tip circle =  $WD/2 + R_s$ )'
PRINT*,'2. User supplied cutter dimensions'
PRINT*,'Type selection(1 or 2):'
READ*,COND

```

C-----calculates and writes fixed parameters-----

```

12  NC=INT(ANC)
    NG=INT(ANG)
    PHIS=PHIS*RAD
    RSC=0.5*NC*AM
    RSG=0.5*NG*AM
    GR=FLOAT(NG)/FLOAT(NC)
    RBG=RSG*COS(PHIS)
    RBC=RSC*COS(PHIS)
    CS=RSC+RSG
    PS=2*? 1415927*CS/(NC+NG)
    IF(COND.EQ.2)THEN
    IF(INPUT.EQ.'FILE')THEN
    CALL STUDY('TSC',CH,TSC)
    CALL STUDY('ADDC',CH,ADDC)
    CALL STUDY('WDC',CH,WDC,*3)
    END IF
    CALL READER(' Tooth thickness of cutter:',TSC)
    CALL READER(' Tooth addendum of cutter:',ADDC)
    CALL READER(' Whole depth of cutter:',WDC)
    ELSE
    TSC=PS/2.
    WDC=2.5*AM
    ADDC=1.25*AM

```

```

END IF
CALL LINE

3  IF(INPUT.EQ.'FILE')THEN

    IF(INIT.EQ.0)ADDCS=ADDC
    IF(INIT.EQ.0)TSCD=TSC
    INIT=1
      PRINT*,'ADDCS=',ADDCS
    CALL STUDY('E1',CH,E1)
    CALL STUDY('RAKE',CH,RAKE)
    CALL STUDY('PLNO',CH,PLNO)
    NOPLN=INT(PLNO)
    CALL STUDY('RNO',CH,RNO)
    CALL STUDY('B',CH,B)
    CALL STUDY('RELIEF',CH,RELIEF,*8)
    END IF
    CALL READER('Number of sharpenings per run:',RNO)
    CALL READER('decrement in stock after each run:',E1)
    CALL READER('rake angle of cutter:(degrees):',RAKE)
    CALL READER('top relief angle of cutter:(degrees):',RELIEF)
    CALL READER('no of plane sections:',NOPLN)
    CALL READER('design distance(B):',B)

8  E=E1*SIN(RELIEF*RAD)/COS(RELIEF*RAD+RAKE*RAD)
    E2=E1*COS(RELIEF*RAD)/COS(RELIEF*RAD+RAKE*RAD)
    TSC=TSC+2.*B*TAN(RELIEF*RAD)*TAN(PHIS)
    ADDC=ADDC+B*TAN(RELIEF*RAD)
    CALL WRITEF(NPAGE,RAD)
    CALL ROUTIN(ROUT,CT)

C-----calculates variable parameters-----
22  PINV=INV(PHIS)-(PS-TSG-TSC)/(2.*CS)
    Q=(PINV)**(2./3.)
    REC=1.0+1.04004*Q+0.32451*(Q**2)-0.00321*(Q**3)-0.00894*(Q**4)
    &+0.00319*(Q**5)-0.00048*(Q**6)
    PHI=ACOS(1./REC)
    PHIV=PHI
    CC=(RBG+RBC)*REC
    RPC=NC*CC/(NG+NC)
    PPC=2.*3.1415927*RPC/NC
    PPG=PPC
    RPG=NG*PPG/6.2831853
    RTCC=RSC+ADDC
    RRCC=RTCC-WDC

    RRCG=CC-RTCC

```

```

    IF(NPAGE.EQ.2)RORIG=RTCC
    BR=DTG/2.
    C=CC-RTCC+WDC-BR

    IF(RBC.GT.RRCC)THEN

    CALL STAR
    PRINT*,'RADIUS OF ROOT CIRCLE OF CUTTER IS: ',RRCC
    PRINT*,'RADIUS OF BASE CIRCLE OF CUTTER IS: ',RBC
    PRINT*,'INVOLUTE SECTION DOES NOT EXTEND TILL FULL DEPTH'
    CALL QUEST(INPUT,'CINV',*100)
    END IF
    IF(RBG.GT.RRCG)THEN
    CALL STAR
    PRINT*,'RADIUS OF BASE CIRCLE OF GEAR IS: ',RBG
    PRINT*,'RADIUS OF ROOT CIRCLE OF GEAR IS: ',RRCG
    PRINT*,'INVOLUTE SECTION DOES NOT EXTEND TILL FULL DEPTH'
    CALL QUEST(INPUT,'GINV',*100)
    END IF

    IF(C.LT.0)THEN
    CALL STAR
    PRINT*,'THE CLEARANCE BETWEEN THE CUTTER ROOT AND GEAR TIP '
    *,'IS: ',C
    CALL QUEST(INPUT,'CLEAR',*100)
    RTCG=CC-RRCC
    C=0.0
    ELSE
    RTCG=BR
    END IF

    ADDG=RTCG-RSG
    WDG=RTCG-RRCG
    IF(RTCG.LE.RRCG)THEN
    CALL STAR
    PRINT*,'RADIUS OF TIP CIRCLE OF GEAR IS: ',RTCG
    PRINT*,'RADIUS OF ROOT CIRCLE OF GEAR IS: ',RRCG
    PRINT*,'NON EXSISTENT WHOLE DEPTH: ERROR IN INPUT PARAMETERS'
    CALL QUEST(INPUT,'TIP',*100)
    END IF

```

C-----writes calculated values-----

```

IF(INPUT.EQ.'FILE')CALL STUDY('RUN',CH,RUN,*7)
CALL STAR
PRINT*,'SELECT TYPE OF RUN'
PRINT*,'1. Single run'

```



```

PRINT*, '2. Multiple run for all resharpenings'
PRINT*, ' Select (1 or 2):'
READ*, RUN
7  CALL WRITEV(NPAGE, IFLAG, RAD, ET, E1, RAKE, RELIEF, IRUN, RUN,
    *DONE, RNO, B)
    WRITE(10, *) NG, DTG, TSG, RSG, RBG, NC, RSC, RBC, FW, AM, PHIS, GR, CS, PS,
    TSG, RPG, WDG, ADDG, RRCG, RTCC, TSC, RPC, WDC, ADDC, RTCC, RRCC, XC, YC,
    CC, PHI, PPC, C, RAKE* RAD, RELIEF* RAD, B
    WRITE(9, *) PPC, RPC, RPG, WDC, WDG, TSC, TSG, NC, NG, RTCC, RTCC, ET,
    *INT(IRUN*RNO)

C-----starts loop-----
X = RTCC

C-----cutter profile-----

2  IF(ROUT.EQ.1) THEN
    CALL CUTTR(X, Y, DY, D2Y, RTCC, WDC, ROUT, CT, DELTA, RPC, NC, NG, CC,
    PHIS, RSC, RBC, TSC, XA, XB, *100, RHC, CS, XC, YC, AM, IFLAG)
    ELSE
    CALL CUTTER(X, Y, DY, D2Y, RTCC, WDC, ROUT, CT, DELTA, RPC, NC, NG, CC,
    PHIS, RSC, RBC, TSC, XA, XB, *100, RHC, CS, XC, YC, AM, IFLAG,
    RELIEF* RAD, RAKE* RAD, B, ADDCS, TSCD)
    END IF

    IF(X.LT.(RTCC-WDC)) THEN
    YROOT = SQRT((RTCC-WDC)**2 - X*X)
    IF(YROOT.GE.Y) GO TO 15
    END IF

C-----finds polar co-ordinates of cutter tooth-----
    CALL POLAR1(X, Y, RC, THETAC, TC, ROUT, TSC, RBC, DELTA, PHIS, RSC, PHIC,
    *XA, XB, RTCC, WDC, RHC, *15)

C-----finds point of contact and tooth inclinations----
    CALL CONTAC(X, Y, DY, RPC, RC, THETAC, GAMMA, PHIC, ALPHA, XB, ROUT)

C-----coordinates of contact point wrt pitch point-----
    CALL PITCH(RC, THETAC, ALPHA, RPG, PPC, XI, ETA, BETAC, BETAG, RPC)

C-----finds gear tooth profile coordinates-----
    CALL POLAR2(RPC, XI, ETA, RPG, BETAG, RG, THETAG,
    *ALPHA, PHIG, PHI, TG, S)

```

```
C-----calculates radius of curvatures-----
  CALL RADIUS(DY,D2Y,S,PHI,RPG,RPC,RHOC,RHOG,RTCC,XB,X,RC,RBC,
  *ROUT,CT)
```

```
  IF(X.LE.XA.AND.X.GE.XB)THEN
    WRITE(55,*)RC,RG,RHOC,RHOG
    SWITCH = 0.
  ELSE
    IF(SWITCH.EQ.0.)THEN
      WRITE(55, '(A3)')'END'
      SWITCH = 1.
    END IF
  END IF
```

```
C-----test contact conditions-----
```

```
  TOUCH = 1.
  IF(RG.GE.BR)THEN
    IF(ITOUCH.EQ.0)THEN
      RG = BR
      ITOUCH = 1
    ELSE
      TOUCH = 0.
    ENDIF
  END IF
```

```
C-----writes calculated values in outfile-----
```

```
  XTEMP = X
  IF(X.LT.XB.AND.ROUT.EQ.1)THEN
    X = UUUU
    Y = UUUU
  END IF
  CALL VALUES(NPAGE,IFLAG,E,RAD)
  X = XTEMP
```

```
C-----ends loop-----
```

```
  GO TO 2
```

```
15  WRITE(9,*)'END'
    IF(RUN.EQ.1.)THEN
      STOP
    ELSE
```

```
  NPAGE = NPAGE + 1
```

```
ITOUCH=0
```

```
B=B-E2
IF(B.LT.E2)STOP
TSC=TSC-2.*E*TAN(PHIS)
ADDC=ADDC-E
```

```
CALL STAR
PRINT*,' '
PRINT*,'          **** STATISTICS **** '
PRINT*,' '
PRINT*,'          NOW STARTING RUN NUMBER = ',IRUN+2
PRINT*,'          DESIGN DISTANCE, B = ',B
PRINT*,' CUTTER STD. TOOTH THICKNESS, TSC = ',TSC
PRINT*,'          ADDENDUM, ADDC = ',ADDC
PRINT*,' AMOUNT OF MATERIAL REMOVED, ET = ',ET+E1
PRINT*,' '

```

```
IF(RORIG-RTCC.LE.FW*TAN(RELIEF*RAD))GO TO 22
END IF
STOP
END
```

```
*****
```

```
SUBROUTINE CUT(X,Y,DY,D2Y,RTC,W)
```

```
C-----function description-----
Y=SQRT(729-(X-RTC+W+10)**2)-15
```

```
C-----
IF(Y.EQ.0)THEN
DY=-1.0E10
D2Y=-729.0E30
ELSE
```

```
C-----first derivative-----
DY=((RTC-W-10)-X)/(Y+15)
```

```
C-----second derivative-----
D2Y=-{(1+DY*DY)/(Y+15)}
END IF
```

```
RETURN
END
```

```

.....
SUBROUTINE POLAR1(X,Y,RC,THETAC,TC,ROUT,TS,RB,DELTA,PHIS,RS,
*PHIC,XA,XB,RTC,W,RHC,*)
REAL INV
SAVE START
DATA START/0./

IF(((X.LT.XB).OR.(X.LE.XA.AND.X.GE.XB.AND.CT.EQ.0))
*.AND.ROUT.EQ.1)THEN
RC = RC-DELTA*START
IF(START.EQ.0)RC = RHC
IF(RC.LT.RTC-W)RETURN 1
PHIC = ACOS(RB/RC)
THETAC = TS/(2.*RS) + INV(PHIS)-INV(PHIC)
TC = 2.*RC*THETAC
START = 1.
RETURN
ENDIF
THETAC = ATAN(Y/X)
RC = SQRT(Y*Y + X*X)
TC = 2.*RC*THETAC
RETURN
END

```

```

.....
SUBROUTINE CONTAC(X,Y,DY,RPC,RC,THETAC,GAMMA,PHIC,ALPHA,XB,
*ROUT)

```

```

C-----gamma-----
IF(ROUT.NE.1.OR.(X.GE.XB.AND.ROUT.EQ.1))THEN
IF(DY.LT.0)THEN
GAMMA = -ATAN(DY)
ELSE
GAMMA = ATAN(DY)
END IF
PHIC = GAMMA + THETAC
END IF
IF(RC-RPC)1,2,1
2 ALPHA = 0
RETURN
1 ALPHA = PHIC-ACOS(RC*COS(PHIC)/RPC)
RETURN
END

```

```

.....
SUBROUTINE PITCH(RC,THETAC,ALPHA,RPG,PPC,XI,ETA,BETAC,
*BETAG,RPC)
XI = RPC-RC*COS(ALPHA)
ETA = -RC*SIN(ALPHA)
BETAC = ALPHA-THETAC
BETAG = -(RPC*BETAC + PPC/2.)/RPG
RETURN
END

```

```

.....
SUBROUTINE POLAR2(RPC,XI,ETA,RPG,BETAG,RC,THETAG,
*ALPHA,PHIG,PHI,TG,S)
RG = SQRT((RPG + XI)**2 + ETA**2)
ALPHAG = ATAN(ETA/(RPG + XI))
THETAG = ALPHAG-BETAG
IF(ETA.EQ.0)THEN
PHI = 1.5707963
ELSE
PHI = ATAN(XI/ETA)
END IF
PHIG = ABS(PHI + ALPHAG)
S = SQRT(XI*XI + ETA*ETA)
IF(ETA.LT.0)S = -S
TG = 2.*RG*THETAG
RETURN
END

```

```

.....
SUBROUTINE RADIUS(DY,D2Y,S,PHI,RPG,RPC,RHOC,RHOG,RTC,
*XB,X,RC,RB,ROUT,CT)

IF(DY.LT.-1.0E10.OR.DY.GT.1.0E10)THEN
RHOC = RTC
ELSE
IF(X.LT.XB.AND.ROUT.EQ.1.)THEN
RHOC = SQRT(RC**2.-RB**2.)
GO TO 1
END IF
RHOC = -((1 + DY*DY)**1.5)/D2Y
END IF
1 RO = RPG*RPC/(RPG + RPC)
IF((RO*SIN(PHI)-(RHOC + S)).EQ.0)THEN
RHOG = -1.0E10

```

```

ELSE
RHOG = -RHOC - (RHOC + S)**2 / (RO * SIN(PHI) - (RHOC + S))
END IF
RETURN
END

```

```

.....

SUBROUTINE LINE
CHARACTER*1,L(132)
DATA L/132*' '/
WRITE(20,1)L
1  FORMAT(/T1,132A1/)
RETURN
END

```

```

.....

SUBROUTINE LINE1
CHARACTER*1,L(132)
DATA L/132*' '/
WRITE(20,1)L
1  FORMAT(T1,132A1)
RETURN
END

```

```

.....

SUBROUTINE LINE2(K)
CHARACTER*1,L(132)
DATA L/132*' '/
IF(K.EQ.2)THEN
WRITE(20,9)L
9  FORMAT(T1,132A1/' + ',T8,'|',T15,'|',T24,'|',T31,'|',T39,'|',
*T46,'|',T53,'|',T63,'|')
ELSE
WRITE(20,1)L
1  FORMAT(T1,132A1/' + ',T8,'|',T15,'|',T24,'|',T31,'|',T39,
*|',T46,'|',T53,'|',T63,'|',T72,'|',T79,'|',T87,'|',T94,
*|',T101,'|',T111,'|',T117,'|',T125,'|')
ENDIF
RETURN
END

```

```

.....

SUBROUTINE STAR

```

```

CHARACTER*1,S(132)
DATA S/132*'*/
WRITE(*,1)S
1  FORMAT(/T1,132A1/)
RETURN
END

```

```

.....

SUBROUTINE READER(XNAME,X)
CHARACTER*(*) XNAME
CALL STAR
PRINT*,' Give the value of ',XNAME(:LEN(XNAME))
READ*,X
RETURN
END

```

```

.....

SUBROUTINE WRITEF(NPAGE,RAD)
COMMON /F/NG,DTG,TSG,RSG,RBG,NC,RSC,RBC,FW,AM,PHIS,CS,PS,GR
NPAGE= 1
WRITE(20,1)NPAGE
PRINT*,'NOW WRITING PAGE NO. ',NPAGE
1  FORMAT('1',T120,'PAGE ',I2)
CALL LINE
CALL PRGM(2)
CALL LINE

WRITE(20,3)NG,DTG,TSG,RSG,RBG,NC,RSC,RBC,FW,AM,PHIS/RAD,
*GR,CS,PS
3  FORMAT(T50,'FIXED PARAMETERS: '//
*T5,'GEAR DATA: '//
*T5,'NUMBER OF TEETH IN GEAR',T50,': ',I5/
*T5,'BLANK DIAMETER OF GEAR',T50,': ',F9.4/
*T5,'TOOTH THICKNESS OF GEAR',T50,': ',F9.4/
*T5,'RADIUS OF STANDARD PITCH CIRCLE OF GEAR',T50,': ',F9.4/
*T5,'RADIUS OF BASE CIRCLE OF GEAR',T50,': ',F9.4//
*T5,'CUTTER DATA: '//
*T5,'NUMBER OF TEETH IN CUTTER',T50,': ',I5/
*T5,'RADIUS OF STANDARD PITCH CIRCLE OF CUTTER',T50,': ',F9.4/
*T5,'RADIUS OF BASE CIRCLE OF CUTTER',T50,': ',F9.4/
*T5,'FACE WIDTH OF CUTTER',T50,': ',F9.4//
*T5,'GENERAL DATA: '//
*T5,'MODULE OF GEAR AND CUTTER',T50,': ',F9.4/
*T5,'STANDARD PRESSURE ANGLE',T50,': ',F9.4/
*T5,'GEAR RATIO',T50,': ',F9.4/

```

```

*T5,'STANDARD CUTTING CENTRE DISTANCE',T50,': ',F9.4/
*T5,'STANDARD CIRCULAR PITCH',T50,': ',F9.4)
NPAGE=NPAGE+1
RETURN
END

```

```

.....

SUBROUTINE WRITEV(NPAGE,IFLAG,RAD,ET,E1,RAKE,RELIEF,
*IRUN,RUN,DONE,RNO,B)

COMMON //RPG,WDG,ADDG,RRCG,RTCC,TSC,RPC,WDC,ADDC,RTCC,
*RRCC,CC,PHIV,PPC,C,XC,YC
WRITE(20,1)NPAGE
PRINT*,'NOW WRITING PAGE NO. ',NPAGE
1  FORMAT('1',T120,'PAGE ',I2)
CALL LINE

DDNC=WDC-ADDC
DDNG=WDG-ADDG

IF(RUN.EQ.2.AND.DONE.EQ.1.)THEN
IRUN=IRUN+1
ET=ET+E1
WRITE(20,222)INT(IRUN*RNO)
222 FORMAT(/T50,'AFTER ',I2,' REGRINDINGS OF CUTTER')
WRITE(20,225)
225 FORMAT('1+',T50,'_____')//
WRITE(20,333)E1/RNO,ET,RAKE,RELIEF
333 FORMAT(T50,'CUTTER TOOL GEOMETRY: '//
*T5,'AMOUNT OF STOCK REMOVED AFTER EACH REGRINDING',
*T60,': ',F9.4/
*T5,'TOTAL AMOUNT OF STOCK REMOVED IN CURRENT REGRINDING',
*T60,': ',F9.4/
*T5,'RAKE ANGLE OF CUTTER',T60,': ',F9.4/
*T5,'TOP CLEARANCE ANGLE OF CUTTER',T60,': ',F9.4)
CALL LINE
END IF

WRITE(20,3)RPG,WDG,ADDG,DDNG,RRCG,RTCC,TSC,RPC,WDC,ADDC,DDNC,
*RTCC,RRCC,CC,PHIV/RAD,PPC,C
3  FORMAT(/T50,'VARIABLE PARAMETERS: '//
*T5,'GEAR DATA: '//
*T5,'RADIUS OF PITCH CIRCLE OF GEAR',T50,': ',F9.4/
*T5,'WHOLE DEPTH OF GEAR',T50,': ',F9.4/
*T5,'ADDENDUM OF GEAR',T50,': ',F9.4,' | wrt S.P.C. /'
*T5,'DEDENDUM OF GEAR',T50,': ',F9.4,' | /'

```



```

*T5,'RADIUS OF ROOT CIRCLE OF GEAR',T50,': ',F9.4/
*T5,'RADIUS OF TIP CIRCLE OF GEAR',T50,': ',F9.4//
*T5,'CUTTER DATA:/'//T5,'TOOTH THICKNESS OF CUTTER'
*,T50,': ',F9.4/T5,'RADIUS OF PITCH CIRCLE OF CUTTER',
*T50,': ',F9.4/T5,'WHOLE DEPTH OF CUTTER',T50,': ',F9.4/
*T5,'ADDENDUM OF CUTTER',T50,': ',F9.4,' | wrt S.P.C.!'
*T5,'DEDENDUM OF CUTTER',T50,': ',F9.4,' |!'
*T5,'RADIUS OF TIP CIRCLE OF CUTTER',T50,': ',F9.4/
*T5,'RADIUS OF ROOT CIRCLE OF CUTTER',T50,': ',F9.4//
*T5,'GENERAL DATA:/'//T5,'ACTUAL CUTTING CENTRE DISTANCE'
*,T50,': ',F9.4/T5,'CUTTING PRESSURE ANGLE',T50,': ',F9.4/
*T5,'CIRCULAR PITCH',T50,': ',F9.4/
*T5,'CLEARANCE BETWEEN CUTTER ROOT AND GEAR TIP',T50,': ',
*T5,F9.4)
WRITE(20,334)B
334 FORMAT(T5,'DESIGN DISTANCE',T50,': ',F9.4)
NPAGE=NPAGE + 1
DONE = 1.
IFLAG = 1
RETURN
END

```

```

.....

SUBROUTINE HEADNG
CALL LINE1
WRITE(20,1)
1 FORMAT(T2,'<----- CUTTER PARAMETERS '
*,'-> | <----- GEAR PARAMETER'
*,'-----> | <---MESHING VALUES--->')
CALL LINE1
WRITE(20,3)
3 FORMAT(' + ',T63,'|',T111,'|')
WRITE(20,2)
2 FORMAT(T12,'CUTTER PROFILE',T31,'|CUTTER',T39,
*'|CUTTER',T46,'|TOOTH',T53,'|RADIUS OF',T63,'| GEAR',
*'|PROFILE',T79,'| GEAR',T87,'| GEAR',T94,'|TOOTH',T101,
*'|RADIUS OF',T111,'|OPT.',T117,'|PATH OF CONTACT'/T1,
*'|_____',T30,'|TOOTH',T38,
*'|PROFIL',T45,'|CENTRE',T52,'|CURVATURE',T62,'|__'
*,'_',T78,'|TOOTH',T86,'|PROFIL',T93,
*'|CENTRE',T100,'|CURVATURE',T110,'|PRESS',T116,
*'|_____',/
*'| X',T8,'| Y',T15,'| R',T24,'| THETA',
*T31,'|THKNNESS',T39,'|ANGLE',T46,'|ANGLE',T53,
*'| (CUTTER)',T63,'| R',T72,'| THETA',
*T79,'|THKNNESS',T87,'|ANGLE',T94,'|ANGLE',T101,'| (GEAR)',

```

```

*T111,'|ANGLE',T117,'| XI',T125,'| ETA')
CALL LINE2(1)
RETURN
END

```

```

.....

SUBROUTINE VALUES(NPAGE,IFLAG,E,RAD)
COMMON X,Y,RC,THETAC,TC,PHIC,BETAC,RHOC,RG,THETAG,
*TG,PHIG,BETAG,RHOG,PHI,XI,ETA,TOUCH
DATA J/1
IF(J.EQ.1.OR.IFLAG.EQ.1)THEN
WRITE(20,1)NPAGE
PRINT*,'NOW WRITING PAGE NO. ',NPAGE
1  FORMAT('1',T10,'TOOTH PROFILE PARAMETERS',T120).
*PAGE ',I2/)
CALL HEADNG
J= 1
END IF
J=J+ 1
IF(J.EQ.26)THEN
NPAGE= NPAGE+ 1
J= 1
END IF
IFLAG= 0

```

```

C-----touch = 1-----

```

```

IF(TOUCH.EQ.1)THEN
IF(ABS(RHOC).LE.999.9999.AND.ABS(RHOG).LE.999.9999)THEN
WRITE(20,3)X,Y,RC,THETAC/RAD,TC,PHIC/RAD,BETAC/RAD,RHOC,RG,
*THETAG/RAD,TG,PHIG/RAD,BETAG/RAD,RHOG,PHI/RAD,XI,ETA
3  FORMAT(T2,F6.2,'|',F6.2,'|',F8.4,'|',F6.2,'|',F7.3,'|',
*F6.2,'|',F6.2,'|',F9.4,'|',F8.4,'|',F6.2,'|',
*F7.3,'|',F6.2,'|',F6.2,'|',F9.4,'|',F5.2,'|',
*F7.3,'|',F7.3)

ELSE IF(ABS(RHOC).GT.999.9999.AND.ABS(RHOG).LE.999.9999)THEN
WRITE(20,4)X,Y,RC,THETAC/RAD,TC,PHIC/RAD,BETAC/RAD,RHOC,RG,
*THETAG/RAD,TG,PHIG/RAD,BETAG/RAD,RHOG,PHI/RAD,XI,ETA
4  FORMAT(T2,F6.2,'|',F6.2,'|',F8.4,'|',F6.2,'|',F7.3,'|',
*F6.2,'|',F6.2,'|',E9.2,'|',F8.4,'|',F6.2,'|',
*F7.3,'|',F6.2,'|',F6.2,'|',F9.4,'|',F5.2,'|',
*F7.3,'|',F7.3)

ELSE IF(ABS(RHOC).LE.999.9999.AND.ABS(RHOG).GT.999.9999)THEN
WRITE(20,5)X,Y,RC,THETAC/RAD,TC,PHIC/RAD,BETAC/RAD,RHOC,RG,

```

```

*THETAG/RAD, TG, PHIG/RAD, BETAG/RAD, RHOG, PHI/RAD, XI, ETA
5  FORMAT(T2, F6.2, '|', F6.2, '|', F8.4, '|', F6.2, '|', F7.3, '|',
   *F6.2, '|', F6.2, '|', F9.4, '|', F8.4, '|', F6.2, '|',
   *F7.3, '|', F6.2, '|', F6.2, '|', E9.2, '|', F5.2, '|',
   *F7.3, '|', F7.3)

ELSE IF(ABS(RHOC).GT.999.9999.AND.ABS(RHOG).GT.999.9999)THEN
WRITE(20,6)X,Y,RC,THETAC/RAD,TC,PHIC/RAD,BETAC/RAD,RHOC, RG,
*THETAG/RAD, TG, PHIG/RAD, BETAG/RAD, RHOG, PHI/RAD, XI, ETA
6  FORMAT(T2, F6.2, '|', F6.2, '|', F8.4, '|', F6.2, '|', F7.3, '|',
   *F6.2, '|', F6.2, '|', E9.2, '|', F8.4, '|', F6.2, '|',
   *F7.3, '|', F6.2, '|', F6.2, '|', E9.2, '|', F5.2, '|',
   *F7.3, '|', F7.3)
END IF
CALL LINE2(1)
WRITE(9,20)RC,THETAC, RG, THETAG
20  FORMAT(4(F15.8,5X))

C-----touch = 0-----
ELSE IF( TOUCH.EQ.0)THEN

IF(ABS(RHOC).LE.999.9999)THEN
WRITE(20,7)X,Y,RC,THETAC/RAD,TC,PHIC/RAD,BETAC/RAD,RHOC
7  FORMAT(T2, F6.2, '|', F6.2, '|', F8.4, '|', F6.2, '|', F7.3, '|',
   *F6.2, '|', F6.2, '|', F9.4, '|', T80, 'N O   C O N T A C T')

ELSE IF(ABS(RHOC).GT.999.9999)THEN
WRITE(20,8)X,Y,RC,THETAC/RAD,TC,PHIC/RAD,BETAC/RAD,RHOC
8  FORMAT(T2, F6.2, '|', F6.2, '|', F8.4, '|', F6.2, '|', F7.3, '|',
   *F6.2, '|', F6.2, '|', E9.2, '|', T80, 'N O   C O N T A C T')

END IF
WRITE(9,21)RC,THETAC
21  FORMAT(2(F15.8,5X))
CALL LINE2(2)
END IF
RETURN
END

```

```

SUBROUTINE PRGM(K)
IF(K.EQ.1)WRITE(*,2)
IF(K.EQ.2)WRITE(20,2)
2  FORMAT(T5,'PROGRAM',T22,':  CONJUGATE GEAR TOOTH '
   *, 'PROFILE SHAPE GENERATED BY GENERAL PINION CUTTER'//
   *T5,'DEVELOPED BY',T22,':  DEBKUMAR RAKSHIT')

```

```

*T27,'GRADUATE STUDENT (MECHANICAL)'/
*T27,'UNIVERSITY OF ALBERTA'//
*T5,'DATE',T22,': 18/05/88 (LAST REVISED: 10/04/89)'
//T5,'NOTE',T22,
': 1. The main program is in the file GEAR3'/T24,
'2. The output is file DATFL.'/T24,
'3. The output files DAT2 and DAT3 are'/T24,
'used by ',
'the following programs for graphics output:'/T24,
'GR3.PLOT, GR3.FILLET, GPLOT.')
```

```

RETURN
END
```

.....

```

SUBROUTINE TITLE
CHARACTER*132 L
OPEN(UNIT = 12,FILE = 'TITLE3',STATUS = 'OLD')
WRITE(20,6)
6  FORMAT('1','FILE NAME: DATAFILE (OUTPUT OF GEAR2)'
*/////////)
DO 1 I = 1,100
READ(12,2,END = 5)L
2  FORMAT(T1,A132)
1  WRITE(20,3)L
3  FORMAT(T1,A132)
5  RETURN
END
```

.....

```

SUBROUTINE CUTTER(X,Y,DY,D2Y,RTC,W,ROUT,CT,DELTA,RPC,NC,NG,CC,
*PHIS,RS,RB,TS,XA,XB,*,RHC,CS,XC,YC,AM,IFLAG,RELIEF,RAKE,B,
*ADDCS,TSCD)
IMPLICIT DOUBLEPRECISION(A-H,O-Z)
DOUBLE PRECISION ALLOT(100),INV,AAM(18)
REAL ROUT,START,FACTOR,DELTA
CHARACTER*10, ANS
SAVE START,FACTOR
DATA START,FACTOR/0.,1./
IF(IFLAG.EQ.1)START = 0.
IF(START.EQ.0)THEN

IF(ROUT.EQ.1)THEN
PRINT*, 'INVOLUTE CASE: EVALUATING A,B,C'
RDASHC = RTC - CT
PHIHC = DATAN((SQRT(RDASHC**2 - RB**2) + CT)/RB)
```

```

RHC = RB/DCOS(PHIHC)
THETAH = TS/(2.*RS) + INV(PHIS) - INV(PHIHC)
GAMMAH = PHIHC - THETAH
XC = RHC*DCOS(THETAH) - CT*DSIN(GAMMAH)
YC = RHC*DSIN(THETAH) - CT*DCOS(GAMMAH)
C
C NO CIRCULAR TOOTH TIP
C
PHIM = DACOS(RB/RTC)
THETAM = TS/(2.*RS) + INV(PHIS) - INV(PHIM)
XM = RTC*DCOS(THETAM)
YM = RTC*DSIN(THETAM)

WRITE(20,10)CT,XM,XC,YM,YC
10 FORMAT(/T50,'CUTTER TIP CORNER DATA'//
* T5,'CASE I. ROUNDED TIP ',
* T70,'CASE II. NON-ROUNDED TIP'//
* T5,'RADIUS OF CIRCULAR ARC',T50,' ',F9.4,
* T70,'X-COORDINATE OF CORNER',T115,' ',F9.4/
* T5,'X-COORDINATE OF CIRCULAR ARC',T50,' ',F9.4,
* T70,'Y-COORDINATE OF CORNER',T115,' ',F9.4/
* T5,'Y-COORDINATE OF CIRCULAR ARC',T50,' ',F9.4)

CALL TIPDAT(CT,XM,XC,YM,YC)

WRITE(10,*)CT,XC,YC,XM,YM
THETAD = DATAN(YC/XC)
XB = RHC*DCOS(THETAH)
XA = RTC*DCOS(THETAD)
YA = RTC*DSIN(THETAD)
CALL LINE
PRINT*,'EVALUATION OF A,B,C COMPLETE *****'
GO TO 2
ELSE

C----- gauss seidal method to find centre of tip radius circle---
C PRINT*,'NON-INVOLUTE CASE: EVALUATING A,B,C'
A = B - W*DTAN(RAKE)/2.DO
WEIGHT = .8

DO 1 I = 1,50
IF(ROUT.EQ.3)THEN
CALL EFFECT(PHIS,RELIEF,RAKE,
*TSCD,RB,RS,ADDCS,B,XX,Y,DY,D2Y,A)
ELSE
CALL CUT(XX,Y,DY,D2Y,RTC,W)
END IF

```

```

X1=((RTC-CT)**2-(Y-CT/DSQRT(1+DY*DY))**2)/(XX-CT*DSQRT(
*DY*DY/(1+DY*DY))) + CT*DSQRT(DY*DY/(1+DY*DY))
A1=(DSQRT(X1*X1+Y*Y)-RTC)*DTAN(RAKE)+B
IF(DABS(X1-XX).LT.0.0001D0)THEN
XB=X1
TEMP=XB
YB=Y
XC=XB-CT*DSQRT(DY*DY/(1+DY*DY))
YC=YB-CT/DSQRT(1+DY*DY)
XA=XC*RTC/(RTC-CT)
YA=YC*RTC/(RTC-CT)
XB=TEMP
CALL TIPDAT(CT,XM,XC,YM,YC)
PRINT*,'EVALUATION OF A, B, C COMPLETE *****'
GO TO 2
END IF
1 A=A+(A1-A)*WEIGHT
PRINT*,'NO CONVERGENCE IN "GAUSS SEIDAL" FOR ',I,' ITERATIONS'
END IF
2 IF(YA.LE.0.D0)THEN

IF(YC.EQ.0.D0) THEN
PRINT*,'THE CUTTER TIP CONSISTS OF CIRCULAR ARC '
PRINT*,'OF RADIUS ',CT,' MM.'
PRINT*,'Do you wish to change parameters ? (Y/N)'
READ*,'(A10)')ANS
CALL LINE
IF(ANS.EQ.'Y'.OR.ANS.EQ.'YES'.OR.ANS.EQ.'y'.OR.ANS.EQ.'yes')
* RETURN 1
ELSE IF(YA.LT.0.D0)THEN
PRINT*,'VALUE OF YA IS ',YA
PRINT*,'VALUE OF XM IS ',XM
PRINT*,'VALUE OF YM IS ',YM
PRINT*,'THE CUTTER TIP IS POINTED. REDIFINE PARAMETERS AGAIN'
CALL LINE
RETURN 1
END IF
END IF

END IF
IF(X.LT.XB.AND.ROUT.EQ.1)RETURN

X=X-DELTA*START/FACTOR
IF(X.GT.XA)THEN
C PRINT*,'EVALUATING POINTS ON CIRCULAR TIP *****'
CALL ARC(X,Y,DY,D2Y,RTC)
FACTOR=100.

```

```

ELSE IF(X.LE.XA.AND.X.GE.XB.AND.CT.NE.0)THEN
C   PRINT*, 'EVALUATING POINTS ON CORNER RADIUS'
   Y=DSQRT(CT*CT-(X-XC)**2) + YC
   IF(Y.EQ.YC)THEN
     DY = -2.D10
     D2Y = -2.D10
   ELSE
     DY = (XC-X)/(Y-YC)
     D2Y = -(1 + DY*DY)/(Y-YC)
   ENDIF
   FACTOR = 5.

ELSE IF(X.LT.XB)THEN
C   PRINT*, 'EVALUATING POINTS ON ACTIVE SIDE PROFILE'
   FACTOR = 0.2
   IF(ROUT.EQ.1)RETURN
   IF(ROUT.EQ.3)THEN

C     A1 = B - (RTC - DSQRT(X*X + Y*Y)) * DTAN(RAKE)
     WEIGHT = 1.D0

     DO 222 II = 1,50
     CALL EFFECT(PHIS,RELIEF,RAKE,
     *TSCD,RB,RS,ADDCS,B,XP,YY,DY,D2Y,A1 + .00001D0)
     CALL EFFECT(PHIS,RELIEF,RAKE,
     *TSCD,RB,RS,ADDCS,B,XN,YY,DY,D2Y,A1 - .00001D0)
     CALL EFFECT(PHIS,RELIEF,RAKE,
     *TSCD,RB,RS,ADDCS,B,XX,YY,DY,D2Y,A1)
     DX = (XP-XN)/(2*.00001D0)
     IF(DABS(X-XX).LT.0.0001D0)GO TO 223
     A = A1 - (XX-X)/DX
222   A1 = A1 + (A-A1) * WEIGHT
     PRINT*, 'NO CONVERGENCE AFTER ',II, ' ITERATIONS.'
223   A = A1
     CALL EFFECT(PHIS,RELIEF,RAKE,
     *TSCD,RB,RS,ADDCS,B,X,Y,DY,D2Y,A)
     ELSE
     CALL CUT(X,Y,DY,D2Y,RTC,W)
     END IF
     END IF

START = 1.
RETURN
END

```

C*****

```

SUBROUTINE CUTTR(X,Y,DY,D2Y,RTC,W,ROUT,CT,DELTA,RPC,NC,NG,CC,
*PHIS,RS,RB,TS,XA,XB,*RHC,CS,XC,YC,AM,IFLAG)
CHARACTER*10, ANS
REAL INV,AAM(18)
C   SAVE XA,XB,XC,YC,START,FACTOR,RHC,TS,RS,PHIS,RB
DATA START,FACTOR/0.,1./
IF(IFLAG.EQ.1)START = 0
      IF(START.EQ.0)THEN
        IF(ROUT.EQ.1)THEN
          RDASHC = RTC - CT
          PHIHC = ATAN((SQRT(RDASHC**2 - RB**2) + CT)/RB)
          RHC = RB/COS(PHIHC)
          THETAH = TS/(2.*RS) + INV(PHIS) - INV(PHIHC)
          GAMMAH = PHIHC - THETAH
          XC = RHC * COS(THETAH) - CT * SIN(GAMMAH)
          YC = RHC * SIN(THETAH) - CT * COS(GAMMAH)
        C
        C   NO CIRCULAR TOOTH TIP
        C
          PHIM = ACOS(RB/RTC)
          THETAM = TS/(2.*RS) + INV(PHIS) - INV(PHIM)
          XM = RTC * COS(THETAM)
          YM = RTC * SIN(THETAM)
          CALL LINE
          WRITE(20,10)CT,XM,XC,YM,YC
10    FORMAT(/T50,'CUTTER TIP CORNER DATA'//
* T5,'CASE I.  ROUNDED TIP ',
* T70,'CASE II.  NON-ROUNDED TIP'//
* T5,'RADIUS OF CIRCULAR ARC',T50,':',F9.4,
* T70,'X-COORDINATE OF CORNER',T115,':',F9.4/
* T5,'X-COORDINATE OF CIRCULAR ARC',T50,':',F9.4,
* T70,'Y-COORDINATE OF CORNER',T115,':',F9.4/
* T5,'Y-COORDINATE OF CIRCULAR ARC',T50,':',F9.4)
          WRITE(10,*)CT,XC,YC,XM,YM
          THETAD = ATAN(YC/XC)
          XB = RHC * COS(THETAH)
          XA = RTC * COS(THETAD)
          YA = RTC * SIN(THETAD)
          CALL LINE
          GO TO 2
          ELSE
C----- gauss seidal method to find centre of tip radius circle---
          XX = RTC - W
          WEIGHT = 0.8
          DO 1 I = 1,50
            IF(ROUT.EQ.3)THEN

```



```

CALL EXT(XX,Y,DY,D2Y,RTC,W)
ELSE
CALL CUT(XX,Y,DY,D2Y,RTC,W)
END IF
X1=SQRT((RTC-CT)**2-(Y-CT/SQRT(1+DY*DY))**2)+CT*SQRT(
*DY*DY/(1+DY*DY))
IF(ABS(X1-XX).LT.0.0001)THEN
XB=XX
YB=Y
XC=XB-CT*SQRT(DY*DY/(1+DY*DY))
YC=YB-CT/SQRT(1+DY*DY)
XA=XC*RTC/(RTC-CT)
YA=YC*RTC/(RTC-CT)
GO TO 2
END IF
1 XX=XX+(X1-XX)*WEIGHT
END IF
2 IF(YA.LE.0)THEN
IF(YC.EQ.0) THEN
PRINT*,'THE CUTTER TIP CONSISTS OF CIRCULAR ARC '
PRINT*,'OF RADIUS ',CT,' MM.'
PRINT*,'Do you wish to change parameters ? (Y/N)'
READ(*,'(A10)')ANS
CALL LINE
IF(ANS.EQ.'Y'.OR.ANS.EQ.'YES'.OR.ANS.EQ.'y'.OR.ANS.EQ.'yes')
RETURN 1
ELSE IF(YA.LT.0)THEN
PRINT*,'VALUE OF YA IS ',YA
PRINT*,'VALUE OF XM IS ',XM
PRINT*,'VALUE OF YM IS ',YM
PRINT*,'THE CUTTER TIP IS POINTED. REDIFINE PARAMETERS AGAIN'
CALL LINE
RETURN 1
END IF
END IF
END IF
IF(X.LT.XB.AND.ROUT.EQ.1)RETURN
X=X-DELTA*START/FACTOR
IF(X.GT.XA)THEN
CALL ARC(X,Y,DY,D2Y,RTC)
FACTOR=100.
ELSE IF(X.LE.XA.AND.X.GE.XB.AND.CT.NE.0)THEN
Y=SQRT(CT*CT-(X-XC)**2)+YC
IF(Y.EQ.YC)THEN
DY=-2.E10
D2Y=-2.E10
ELSE

```

```

DY=(XC-X)/(Y-YC)
D2Y=-(-1+DY*DY)/(Y-YC)
ENDIF
FACTOR=5.
  ELSE IF(X.LT.XB)THEN
    FACTOR=0.2
  IF(ROUT.EQ.1)RETURN
    IF(ROUT.EQ.3)THEN
CALL EXT(X,Y,DY,D2Y,RTC,W)
    ELSE
CALL CUT(X,Y,DY,D2Y,RTC,W)
    END IF
  END IF
START = 1
RETURN
END

```

```

.....
SUBROUTINE ARC(X,YA,DYA,D2YA,RTC)
YA = SQRT((RTC)**2-X*X)
IF(YA.EQ.0)THEN
DYA = -1.0E15
D2YA = -1.0E40
ELSE

```

```

C-----derivatives-----
DYA = -X/YA
D2YA = -(1+DYA*DYA)/YA
END IF
RETURN
END

```

```

.....
SUBROUTINE ROUTIN(ROUT,CT)
CHARACTER*80,ANS,DES
CALL LINE
CALL STAR
CALL STUDY('INPUT',ANS,RLNO)
IF(ANS.EQ.'FILE')THEN
CALL STUDY('ROUT',DES,ROUT)
CALL STUDY('CT',DES,CT,*5)
END IF
PRINT*,' Select profile to be used :!'
PRINT*,' 1. Rounded tip involute profile(NEW DESIGN)'
PRINT*,' 2. Circular arc'

```

```

PRINT*,' 3. Non-involute profile(OLD DESIGN)'
PRINT*,' Type (1,2 or 3) :'
```

READ*,ROUT
CALL READER(' radius of circular tip (in mm):',CT)

5 IF(ROUT.EQ.2)THEN
WRITE(20,1)

1 FORMAT(T5,'CUTTER PROFILE FUNCTION DESCRIPTION:///
*T5,'THE CUTTER FUNCTION IS AN ARC OF A CIRCLE OF EQUATION///
*T5,' 2 2 2 /'
*T5,' (X-Rtc-w-10) + (Y-15) = (25) /'
*T5,' where Rtc-w < X < Rtc')

WRITE(20,4)CT

4 FORMAT(T5,'THE CUTTER TIP IS ROUNDED BY AN CIRCULAR ARC '
*,'OF RADIUS ',F5.2,' MM')
ELSE IF(ROUT.EQ.1)THEN
WRITE(20,2)

2 FORMAT(T5,'CUTTER PROFILE FUNCTION DESCRIPTION:///
*T5,'NEW DESIGN: EFFECTIVE CUTTER PROFILES ARE INVOLUTES')
WRITE(20,4)CT
ELSE
CALL STAR
PRINT*,'NOTE:'
PRINT*,'THE EXTERNAL ROUTINE SHOULD BE NAMED "EXT" '
PRINT*,'AND MUST BE CONTAINED IN FILE "PROFILE"
PRINT*
PRINT*,'Give the function description in rectangular'
PRINT*,'coordinates:(MAX 1 LINE)'
IF(ANS.EQ.'FILE')CALL STUDY('DES',DES,RLNO,*6)
READ(*,'(A80)')DES

6 WRITE(20,3)DES

3 FORMAT(T5,'CUTTER PROFILE FUNCTION DESCRIPTION:///
*T5,A80)
WRITE(20,4)CT
END IF
RETURN
END

```

FUNCTION INV(ANGLE)
DOUBLEPRECISION INV,ANGLE
INV=TAN(ANGLE)-ANGLE
RETURN
END
```

```

SUBROUTINE STUDY(VAR,CHAR,REALNO,*)
CHARACTER*(*) VAR,CHAR,VALUE*80
REWIND 50
5  READ(50,'(A80)',END = 60)VALUE

      K = INDEX(VALUE,'=')

15  IF(VAR.EQ.VALUE(:K-1))THEN
      READ(VALUE(K + 1:),*,ERR = 50)REALNO
50  CHAR = VALUE(K + 1:)
      RETURN 1
      END IF
      GO TO 5
60  RETURN
      END

```

```

.....

SUBROUTINE QUEST(INPUT,LEAR,*)
CHARACTER*(*),INPUT,LEAR,CH*80
IF(INPUT.EQ.'FILE')CALL STUDY(LEAR,CH,ANS,*4)
PRINT*,'1. To stop program'
PRINT*,'2. To restart program with modified parameters'
PRINT*,'3. To continue'
PRINT*,' Type selection (1,2 or 3):'
READ*,ANS
4  IF(ANS.EQ.1)STO?
   IF(ANS.EQ.2)RETURN 1
   RETURN
   END

```

```

.....

SUBROUTINE EXT(X,Y,DY,D2Y,RTC,W)
RETURN
END
.....

```

```

SUBROUTINE THEORY(PHI,RTC,RSC,RBC,TSC,PART,DELR)

CHARACTER*(*) PART

INV(X) = TAN(X)-X
THETA(R) = TSC/(2.*RSC) + INV(PHI)-INV(ACOS(RBC/R))
L = 7
IF(PART.EQ.'CUTTER')L = 8
OPEN(UNIT = L,FILE = PART,STATUS = 'NEW',IOSTAT = IERR)
IF(IERR.NE.0)THEN

```

```

CLOSE(UNIT=L,STATUS='DELETE')
OPEN(UNIT=L,FILE=PART,STATUS='NEW')
END IF

R=RBC-DELR
DO 10 I=1,2000
R=R+DELR
IF(R.GE.RTC)GO TO 20
WRITE(L,*)R,THETA(R)
10 CONTINUE
20 DO 30 I=0,15
30 WRITE(L,*)RTC,THETA(R)*((15-I)/15)
RETURN
END
.....

SUBROUTINE EFFECT(PHI,DELTA,GAMMA,TSC,RBC,RSC,
* ADDC,B,X,Y,DY,D2Y,A)

IMPLICIT DOUBLEPRECISION(A-H,O-Z)

RAC(A)=RSC+ADDC+B*DTAN(DELTA)-(B-A)/DTAN(GAMMA)

THETA(A)=(TSC+2.D0*A*DTAN(DELTA)*DTAN(PHI))/(2.D0*RSC
* +DTAN(PHI)-PHI
*-DTAN(DACOS(RBC/(RSC+ADDC+B*DTAN(DELTA)-(B-A)/DTAN(GAMMA))))
* +DACOS(RBC/(RSC+ADDC+B*DTAN(DELTA)-(B-A)/DTAN(GAMMA)))

XX(A)=RAC(A)*DCOS(THETA(A))
YY(A)=RAC(A)*DSIN(THETA(A))
D1(A)=(YY(A+.000001D0)-YY(A-0.000001D0))/
*(XX(A+.000001D0)-XX(A-0.000001D0))
D2(A)=(YY(A+.000001D0)-2.D0*YY(A)+YY(A-0.000001D0))/
*(XX(A+.000001D0)-XX(A-0.000001D0))*2

C.....END OF FUNCTION DEFINATIONS.....

X=XX(A)
Y=YY(A)
DY=D1(A)
D2Y=D2(A)
RETURN
END
.....

```

```
SUBROUTINE TIPDAT(CT,XM,XC,YM,YC)
CALL LINE
WRITE(20,10)CT,XM,XC,YM,YC
10  FORMAT(/T50,'CUTTER TIP CORNER DATA'//
      * T5,'CASE I.  ROUNDED TIP ',
      * T70,'CASE II.  NON-ROUNDED TIP'//
      * T5,'RADIUS OF CIRCULAR ARC',T50,': ',F9.4,
      * T70,'X-COORDINATE OF CORNER',T115,': ',F9.4/
      * T5,'X-COORDINATE OF CIRCULAR ARC',T50,': ',F9.4,
      * T70,'Y-COORDINATE OF CORNER',T115,': ',F9.4/
      * T5,'Y-COORDINATE OF CIRCULAR ARC',T50,': ',F9.4)
RETURN
END
```